

**New York City Department of Environmental Protection  
Bureau of Water Supply**

**Stream Management Program  
Upper Esopus Creek Watershed Turbidity/Suspended Sediment  
Monitoring Study: Mid-Term Report**

**November 2022**

**Revised March 2023**

*Prepared in accordance with Section 4.6 of the NYSDOH  
2017 Filtration Avoidance Determination*



Prepared by: DEP, Bureau of Water Supply



# Table of Contents

List of Acronyms .....	ii
<b>1. Introduction.....</b>	<b>1</b>
1.1 Background .....	1
1.2 Report Purpose.....	2
1.3 Study Goals and Objectives .....	3
1.4 Study Area .....	4
<b>2. Study Conceptual Model .....</b>	<b>8</b>
<b>3. Study Methods, Assumptions and Limitations .....</b>	<b>14</b>
3.1 Streamflow and Water Quality Monitoring Stations .....	14
3.2 Suspended Sediment Source Characterization .....	19
3.3 Study Assumptions.....	24
3.4 Study Limitations.....	24
<b>4. Study Mid-Term Results .....</b>	<b>27</b>
4.1 Metric Development.....	27
4.2 Streamflow Monitoring .....	28
4.3 Turbidity Monitoring .....	37
4.4 Suspended Sediment Monitoring.....	51
4.5 Turbidity and Suspended Sediment Source Characterization .....	59
4.6 Sediment and Turbidity Reduction Projects Monitoring.....	82
<b>5. Discussion.....</b>	<b>96</b>
5.1 Turbidity and Suspended Sediment Production in the UEC .....	96
5.2 Turbidity and SS Production in the Stony Clove Sub-basin.....	100
5.3 Turbidity Reduction Through STRPs.....	101
5.4 Conceptual Framework Suitability .....	102
5.5 Next Steps .....	103
<b>6. Study Mid-Term Conclusions.....</b>	<b>105</b>
<b>7. References .....</b>	<b>106</b>
<b>Appendix A.....</b>	<b>111</b>

## List of Acronyms

ACM	Active channel margin
AEP	Annual exceedance probability
AL	Alluvium
ANCOVA	Analysis of covariance
ANOVA	Analysis of variance
AWSMP	Ashokan Watershed Stream Management Program
BEMS	Bank erosion monitoring study
CL	Colluvium
DEM	Digital Elevation Model
DEP	New York City Department of Environmental Protection
DLM	Dynamic linear modeling
EI	Erosional index
FAD	Filtration Avoidance Determination
FFA	Flood frequency analysis
FNU	Formazin nephelometric units
GLS	Glacial legacy sediment
GT	Glacial till
LS	Lacustrine sediment; glacial lacustrine sediment
MAR	Mean annual runoff
MBS	Mean basin slope
PQR	Peak streamflow runoff
Q	Streamflow
REM	River erosion model
RI	Recurrence interval
SCI	Sediment connectivity index
SFI	Stream feature inventory
SfM	Structure-from-motion
SS	Suspended sediment

SSC	Suspended sediment concentration
SSL	Suspended sediment load
SSY	Suspended sediment yield
STRP	Stream turbidity reduction project
Tn	Turbidity
UAS	Uncrewed aerial system (AKA drone)
UEC	Upper Esopus Creek
USGS	United States Geological Survey

# 1. Introduction

## 1.1 Background

The New York City Department of Environmental Protection (DEP) and the U.S. Geological Survey (USGS) initiated a 10-year study in October 2016 to characterize stream turbidity source conditions in the Esopus Creek watershed upstream of the Ashokan Reservoir and to evaluate the turbidity reduction efficacy of stream turbidity reduction projects (STRPs) in the Stony Clove sub-basin. The study and STRPs are mandated by the 2017 Filtration Avoidance Determination (FAD). Several reports document the initial study design and preliminary study status on a recurring biennial basis (DEP, 2017; DEP, 2019a; DEP, 2021). The 2017 FAD requires DEP to submit a report documenting the preliminary findings of the first five years by November 30, 2022; this mid-term report meets that FAD requirement.

In Catskill streams, turbidity ( $T_n$ ) is generally a function of the suspended sediment (SS) concentration (SSC) in streamflow ( $Q$ ) – as SSC increases, so does  $T_n$  (Siemion et al., 2021). Upper Esopus Creek (UEC) serves as a representative Catskill fluvial system to investigate turbidity and SS production and source dynamics at the basin to sub-basin scale (Figure 1.1). It has a documented history of chronic and acute elevated turbidity levels during and following large floods (Effler et al., 1998; Mukundan et al., 2013; McHale and Siemion, 2014). Stony Clove Creek is the largest tributary to UEC and serves in this research as an experimental sub-basin fluvial system for enhanced turbidity source and production investigation as well as evaluating STRP turbidity reduction efficacy from the reach to sub-basin and reservoir basin scales. The study began in water year 2017 (October 1, 2016) and will continue through water year 2026 (September 30, 2026). Per the FAD, DEP will submit a final study report in November 2027.

The study is a collaborative effort led by USGS and DEP with support from the Ashokan Watershed Stream Management Program (AWSMP). USGS is responsible for: (1) monitoring and analyzing  $Q$ ,  $T_n$ , SSC, SS load (SSL) and SS yield (SSY); (2) evaluating STRP impacts on monitored  $T_n$  and SS metrics; (3) using SS fingerprinting as a source sediment characterization technique in the study area; and (4) publishing peer-reviewed scientific literature documenting research findings. DEP is responsible for: (1) research project funding, coordination, and FAD reporting; (2) geologic and geomorphologic investigations; (3) developing an interpretive conceptual model of turbidity production and reduction; and (4) funding design, construction, and monitoring of STRPs in the Stony Clove sub-basin through an agreement with Ulster County Soil and Water Conservation District. The AWSMP further supports this study through research grants administered by Cornell Cooperative Extension of Ulster County. Such grants have expanded the  $Q$ , SSC and  $T_n$  monitoring in Woodland Valley (not covered in this report).

A quantitative understanding of turbidity or SS production is requisite for achieving some measure of success in turbidity reduction management practices. Research by Mukundan et al. (2013) demonstrated that  $T_n$  and SSC scale with increasing streamflow in the study area and that big floods account for most of the load of turbid streamflow to the Ashokan Reservoir. For an 8-

year monitoring period, 80% of the estimated SS load delivered to Ashokan Reservoir by Esopus Creek occurred during large runoff events that represented less than 4% of the monitored streamflow over the same period. They found the spatial and temporal variability in turbidity and SSC can be largely explained by catchment runoff variability, antecedent hydrologic conditions, and seasonal conditions. Hydraulic conditions such as stream power and geologic sources were assumed to be other important controlling factors but were not directly examined.

This DEP-USGS study is intended to further investigate the driving conditions and other factors that generate turbid streamflow in the UEC watershed through a more expansive stream monitoring network operating over a longer period and coupling the stream monitoring with SS source investigations. An assumption in the past and current studies is that turbidity production is controlled not only by streamflow sediment transport capacity but also by sediment supply. This study aims to collect the data needed to evaluate that assumption. The watershed management objective of this study is to evaluate whether stream management practices (STRPs in this case) can measurably reduce stream turbidity delivered to the Ashokan Reservoir through reducing sediment entrainment and to identify the limits of measurable reduction.

## 1.2 Report Purpose

This mid-term report provides an update on the study framework, objectives, methods, and mid-term results, with a discussion of the findings' relevance to turbidity reduction efforts and scope of continued study. The stream monitoring data analyzed is from the first five water years (October 2016 to September 2021). Data acquisition status and presentation are included as needed to support the results and discussion.

**Section 1** provides the basic information to set the context for the research results and discussion. **Section 2** presents the current conceptual framework for investigating the study area turbidity and SS production conditions and the approach to turbidity reduction through source treatment. **Section 3** briefly describes the methods used in the research and details revisions to the methods made through the course of the study. This section also includes a presentation of the study limitations and assumptions that define the study conceptual boundaries with implications for management. A more comprehensive documentation of original methods is provided in DEP's 2017 FAD study design report (DEP, 2017). **Section 4** presents the streamflow, turbidity and suspended sediment monitoring, turbidity source investigation and STRP turbidity reduction monitoring results. **Section 5** presents a brief interpretive account of study findings covering applicability and limitations of the research at the mid-term phase of the study period. **Section 6** presents a summary of the key points made throughout the report. **Section 7** lists the cited research resources informing the study mid-term report.

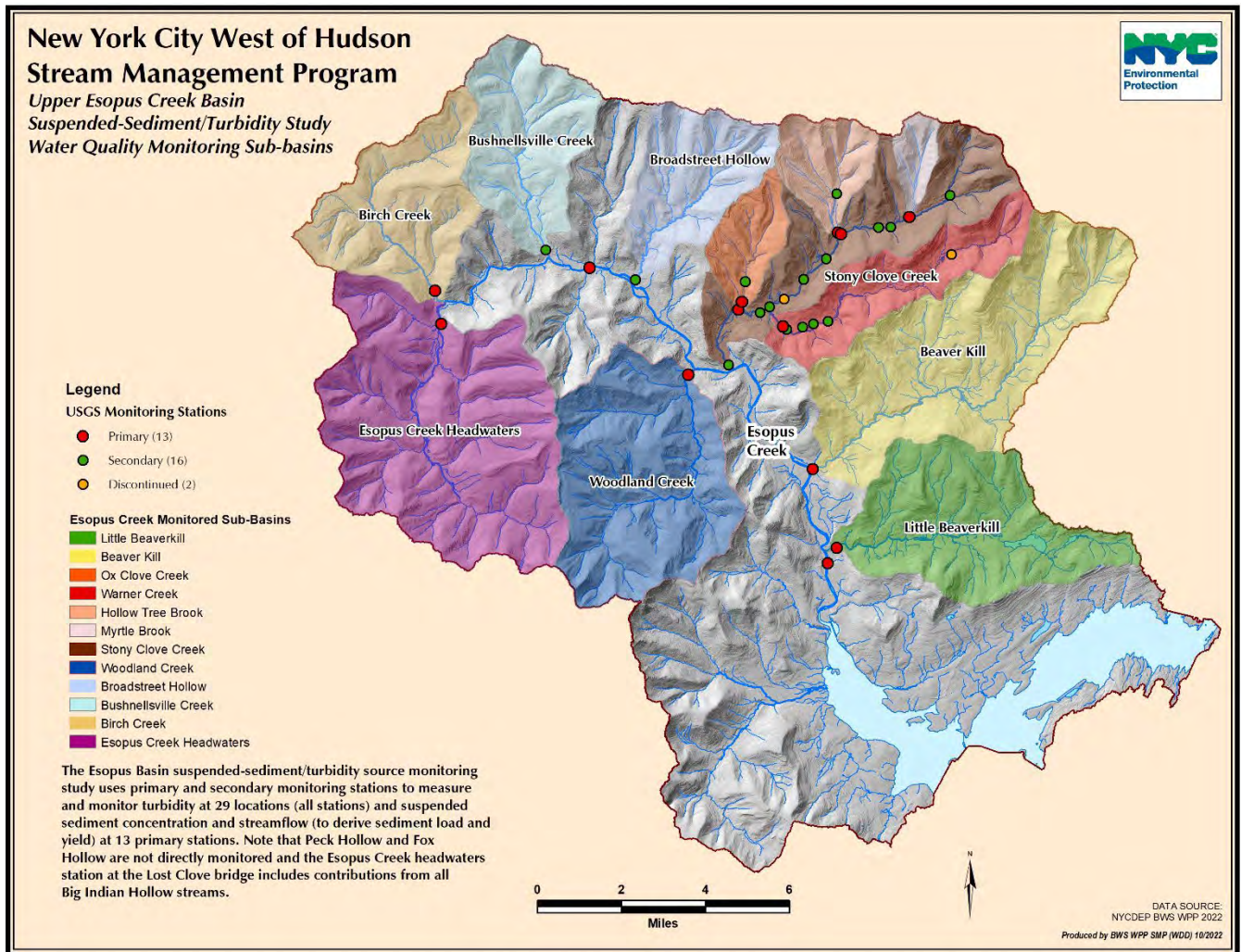


Figure 1.1 UEC watershed study area with USGS water quality monitoring stations.

### 1.3 Study Goals and Objectives

DEP is collaborating with USGS on this 10-year research project to potentially answer the following New York City water supply resource management questions:

- What are the primary sub-basin sources and causal factors influencing turbidity delivered to the Ashokan Reservoir?
- Can stream management practices reduce stream turbidity and suspended sediment delivered to the Ashokan Reservoir?

The study addresses three research goals that will inform DEP’s efforts to protect and improve source water quality through stream turbidity reduction. The study goals and objectives

have been streamlined for this report to focus the results presentation on ranking sub-basin Tn and SS production, source conditions, and evaluating STRP efficacy. The report provides provisional mid-term results for the objectives posed for each study goal.

- A. UEC watershed investigation: Characterize how turbidity and SS production dynamics vary among the monitored UEC sub-basins and identify their relative ranking.
  - 1. Quantitatively rank UEC sub-basin turbidity production and SS load and yield in streamflow to the Ashokan Reservoir for the first five years.
  - 2. Document how these rankings change over the course of the study period.
  - 3. Identify driving conditions and source factors that influence measured differences in turbidity and SS in the monitored UEC sub-basins through the course of the study period.
  - 4. Characterize how the mid-term study results can inform stream management turbidity reduction strategies within the UEC watershed.
- B. Stony Clove sub-basin investigation: Using the Stony Clove as a model sub-basin, characterize how different stream segments (turbidity monitoring reaches) and tributary sub-basins vary in terms of turbidity and SS condition metrics within the same sub-basin.
  - 1. Quantitatively rank Stony Clove Creek and tributary sub-basin turbidity production and SS load and yield for the first five years.
  - 2. Using the data from the 20 turbidity monitoring stations in the Stony Clove sub-basin identify the highest turbidity production reaches for each monitored stream.
  - 3. Identify driving conditions and source factors that influence observed spatial and temporal heterogeneity in turbidity and SS production within the Stony Clove sub-basin.
- C. STRP evaluation: Using the Stony Clove Creek sub-basin and Esopus Creek basin Q, SS, and turbidity monitoring data, evaluate the effectiveness of existing and future STRPs on reducing turbidity and SS for the monitoring reach scale, the sub-basin scale and the reservoir basin scale across a range of flows.
  - 1. Using monitored turbidity and SSC quantify impacts of extant STRPs across a range of spatial, temporal, and hydrologic scales at measurably reducing turbidity and SS.
  - 2. Identify any observed limits of STRP efficacy or limits on detecting efficacy.
  - 3. Characterize how the study results can inform future STRP siting and design.

## 1.4 Study Area

The UEC watershed drains 192 mi<sup>2</sup> of mostly forested mountainous terrain, ranging in elevation from 585 ft at the Ashokan Reservoir to 4,180 ft at Slide Mountain with 21 peaks exceeding 3,000 ft, creating a high topographic relief catchment basin (Figures 1.1 and 1.2). The

National Hydrography Dataset available for the study area includes more than 330 miles of streams draining the UEC watershed. The high gradient fluvial system is a heterogeneous network of alluvial channels, bedrock channels, and non-alluvial channels incised into glacial and colluvial deposits.



Figure 1.2 The UEC watershed looking north from the Esopus Headwaters and Woodland Valley Creek drainage divide toward the Stony Clove sub-basin.

The stream network includes 10 primary tributaries that contribute to UEC (Table 1.1; Figure 1.1). The USGS monitors eight UEC tributaries and two additional locations along Esopus Creek for Q, SSC and/or Tn. Additional enhanced sub-basin and reach scale monitoring occurs in the Stony Clove Creek sub-basin. USGS monitoring stations are described in Section 3.

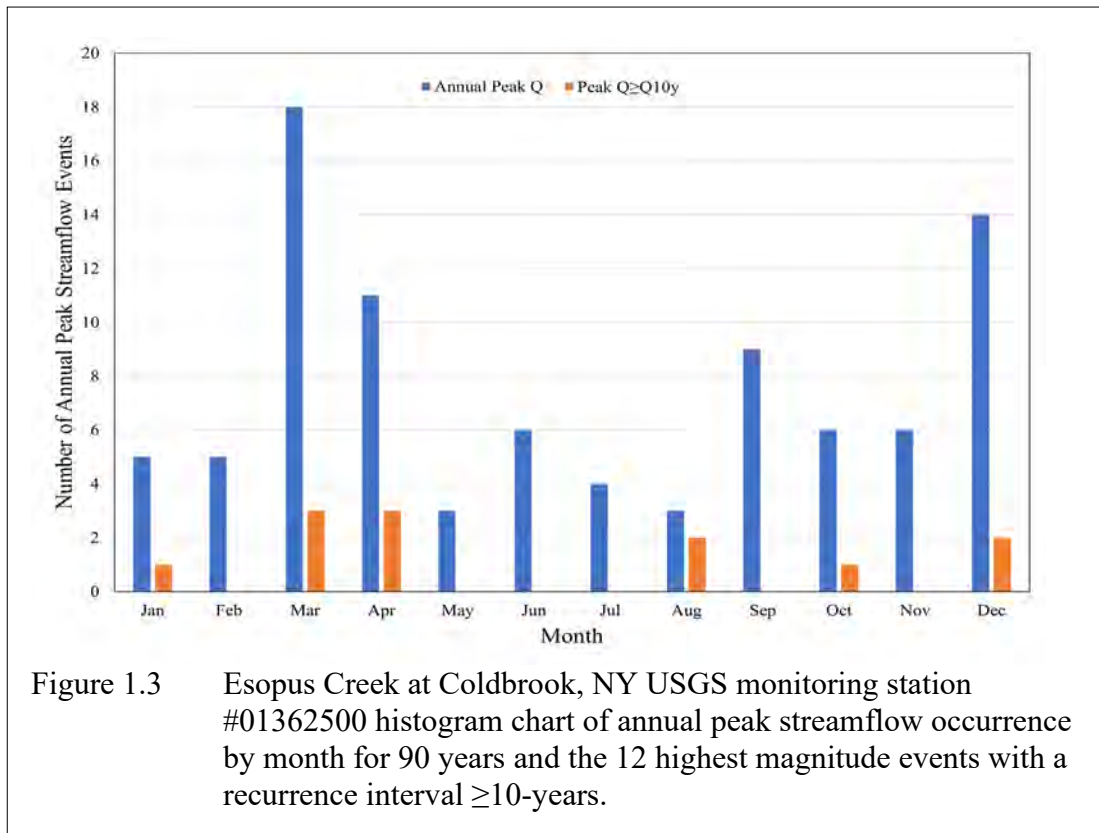
Large floods are the primary disturbance events producing turbidity in UEC watershed streams (Mukundan et al., 2013; McHale and Siemion, 2014; Wang et al., 2021). Historical annual precipitation rates in the Catskill Mountain region range between 39 and 63 inches (Frei and Kelly-Voicu, 2017). The higher range is associated with the study area in the southeastern Catskills due to orographic effects and the track of many high precipitation storms. The mountainous terrain can magnify flooding from heavy precipitation events, maximizing runoff volume and potential stream power forcing stream channel geomorphic adjustment (Matonse and Frei, 2013). Rainfall intensity, duration and sequencing has a strong seasonal influence on streamflow with many of the highest magnitude precipitation events associated with late summer/early fall tropical storms (Frei and Kelly-Voicu, 2017). Historically, the high magnitude tropical storm events don't necessarily yield the highest runoff events, however. On a seasonal

basis, rainfall-induced snowmelt events have produced nearly 60% of the annual peak streamflow events and most of the biggest floods in the 90 years of monitored streamflow at the Esopus Creek monitoring station upstream of Ashokan Reservoir (Figure 1.3).

Table 1.1 UEC and primary contributing streams listed from upstream to downstream.

Stream name	Drainage area (mi <sup>2</sup> )	Stream length (mi)
Esopus Creek Headwaters (above Big Indian, NY) <sup>1</sup>	30	42
Birch Creek	13	16
Bushnellsville Creek	11	14
Fox Hollow Creek	4	6
Peck Hollow Creek	5	7
Broadstreet Hollow Creek	9	12
Woodland Creek	21	25
Stony Clove Creek	32	39
Beaver Kill	25	29
Little Beaver Kill	17	21
Esopus Creek (above the Ashokan Reservoir)	192	330

<sup>1</sup> Esopus Creek headwaters include streams ranging in drainage area from <2 mi<sup>2</sup> to 5 mi<sup>2</sup>.



Catskill Mountain geology influences the fluvial valley geometry, substrate erosional resistance, spatial heterogeneity in fluvial sediment sources and entrainment, and composition of bedload and suspended sediment. Bedrock consists of Devonian fluvial sedimentary repeating sequences of sandstones, mudstones, and conglomerates (Ver Straeten, 2013). The fluvial drainage network is strongly influenced by the bedrock layering and fracture orientations, lithologic variations, and lack of structural deformation (Haskins et al., 2010). Surficial geology is primarily a complex distribution of Pleistocene continental glacial and proglacial deposits variably covered or replaced in stream valleys by Holocene alluvium and colluvium (Rich, 1935; Cadwell, 1986; Rayburn et al., 2015). Glacial legacy sediment (GLS) is enriched in fine sediment (silt and clay) and channel erosion into these deposits can account for acute and chronic sources of turbidity. Past research in the Esopus Creek basin found that silica and clay minerals (generally originally sourced in GLS) accounted for greater than 87% of suspended sediment composition (Effler et al., 1998).

Valley bottom margins are a complex configuration of mountain slopes, glacially constructed features, pro-glacial lake deltas and glaciofluvial terraces at higher elevations and Holocene fluvial terraces at lower valley elevations. Stream planform geometry is variably confined to unconfined based on proximity to these valley bottom features and anthropogenic confining boundaries (roads and revetment).

Most of the human population in the UEC watershed resides in the valley bottoms and lower slopes of the mountains. This centuries-long co-existence between streams and people (and associated infrastructure) in the limited area of the valley bottoms imposes limitations on the streams' ability to adjust in response to high runoff events. Most streams in the UEC watershed are not pristine wild streams; they have instead been shaped by historic and ongoing land use/land cover conditions as well as direct and indirect stream management practices. Many valley bottoms hosted sawmill dams and modified channels. Extensive deforestation in the 18<sup>th</sup> and 19<sup>th</sup> centuries very likely impacted sediment delivery to streams and floodplains. These human legacy impacts on the streams in the study area are not included in the scope of this study. The AWSMP has produced several stream management plans for UEC watershed streams that include more detail on the human impacts to the stream system and on study area physiography, hydrology, geology and geomorphology ([www.ashokanstreams.org](http://www.ashokanstreams.org)).

## 2. Study Conceptual Model

A geomorphic connectivity framework (Fryirs and Brierley, 2013; Wohl et al., 2019), and more specifically, sediment connectivity concepts (Heckmann et al., 2018) are used to build a simplified conceptual model of turbidity production dynamics in the study area and to examine the individual and cumulative turbidity reduction efficacy of STRPs across a range of spatial, temporal, and hydrologic scales. Figure 2.1 presents the basic components of a simplified conceptual model of turbidity production in the UEC watershed.

Turbidity production is defined in this report as the generation of turbid streamflow (or suspended sediment in streamflow) through hydraulic energy applied in the landscape; and the delivery of that turbid streamflow to any reference point (e.g., monitoring station, catchment outlet, or a reservoir). Since turbidity is not a mass-based property, standard quantification terms such as load (mass of sediment transported by a stream) or yield (the mass transported from a source area over time) are not readily applied to turbidity. Thus, production in this usage is a descriptive term that can be more appropriately quantified using SS data and metrics such as SSC, SSL and SSY.

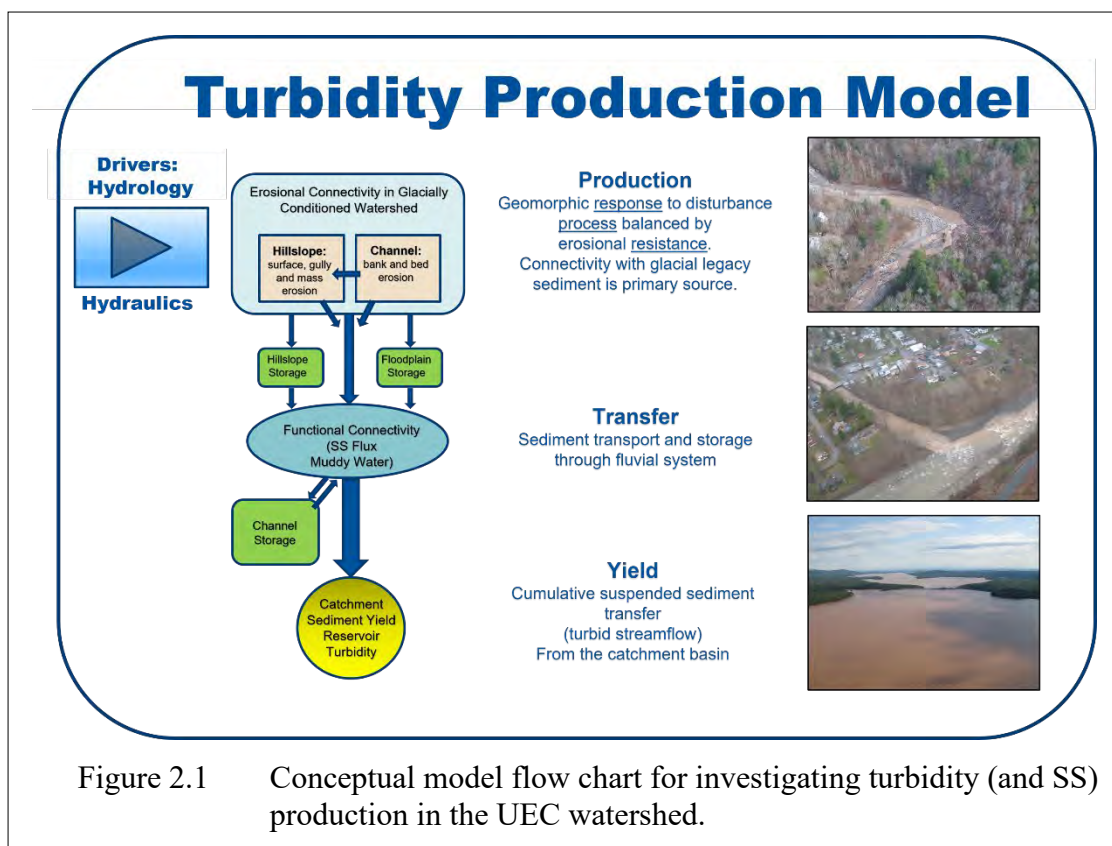
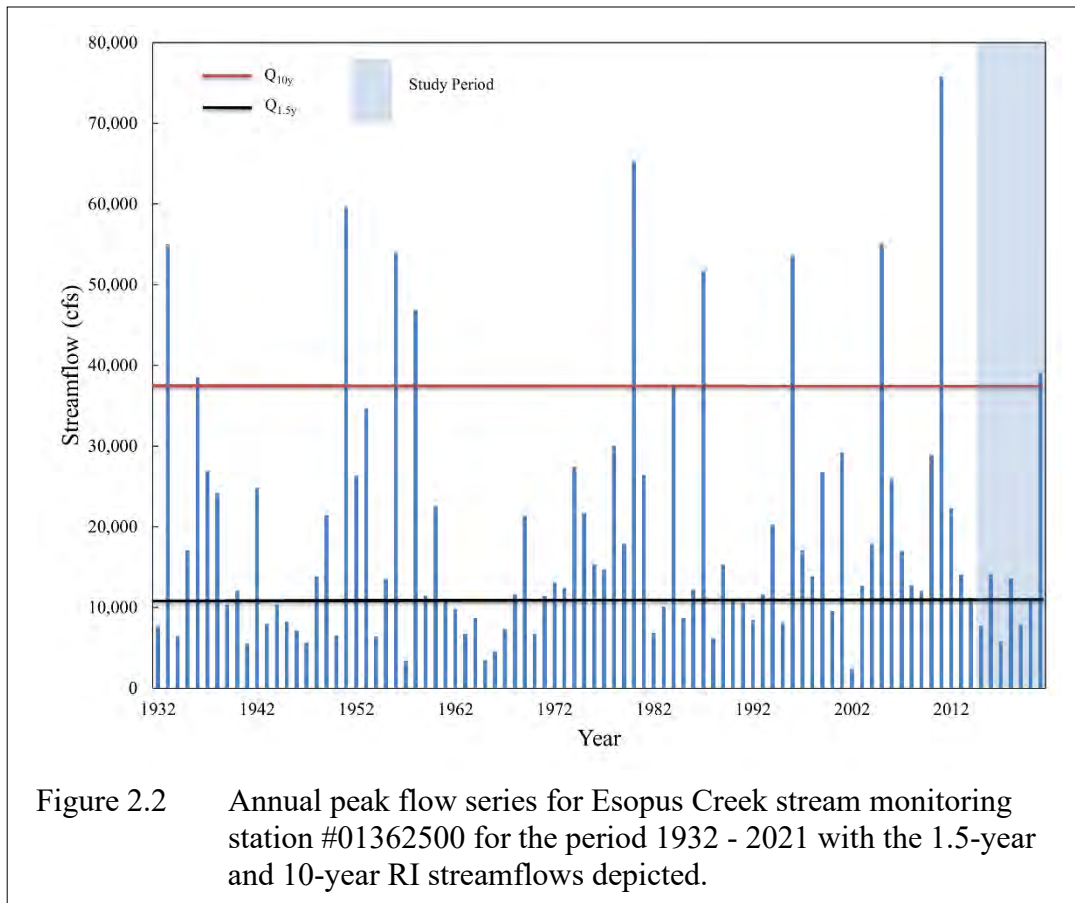


Figure 2.1 Conceptual model flow chart for investigating turbidity (and SS) production in the UEC watershed.

In this simplified conceptual model, the Ashokan Reservoir can fill with turbid streamflow during and following very large floods capable of entraining and transferring fine sediment throughout the UEC stream network. The process is largely driven by precipitation and resulting runoff hydrology (hydro-meteorology) and hydraulics influenced by the intrinsic terrain properties of channel slope, confinement, and roughness. Past research finds that seasonal and antecedent hydrologic conditions influence the hydrological role (Mukundan et al., 2013). The stream monitoring network in this study is designed to help quantify hydrology, turbidity, and SS flux through the stream channel network necessary to answer most of the posed research questions on spatial and temporal variability and trends in turbidity production and measured turbidity reduction response to STRPs.

The working assumption in the study is that turbidity production scales with hydrologic conditions capable of entraining and transferring fine sediment through the fluvial system (Mukundan et al., 2013; Siemion et al., 2016). The scaling is assumed to not be entirely linear, in that there are hydrologic thresholds that once exceeded result in localized reach scale geomorphic adjustment (erosion and deposition) at the lower threshold to basin-wide reach scale geomorphic adjustment at a higher threshold. The basin-wide geomorphic adjustment can consequently lower the hydrologic threshold for elevated turbidity production if the adjustment significantly increases connectivity with turbidity sources.

In this study, streamflow thresholds that trigger a geomorphic response are referred to as hydrogeomorphic thresholds. Figure 2.2 presents the annual peak flow series for Esopus Creek at Coldbrook stream monitoring station that has been continuously operating since 1932. Two *hypothetical* hydrogeomorphic thresholds proposed in this study are depicted as horizontal lines on the hydrograph: the lower threshold is the bankfull streamflow (assumed proximal to the 1.5-year recurrence interval,  $Q_{1.5y}$ ) and a higher threshold is represented by a decadal scale flow magnitude, currently set at the 10-year recurrence interval,  $Q_{10y}$ . To date, there has been no analysis of long-term SS or Tn monitoring data to test these hypothetical thresholds. As the study progresses and reaches ten years of streamflow and turbidity monitoring, these reference flows can be adjusted or calibrated to match the observed conditions. This concept is discussed further in Section 4.2.



The conceptual model assumes that turbidity sediment **input** (new production) originates at discrete erosional connections between the stream and sediment sources (e.g., eroding banks, beds and hillslopes). Stream turbidity is also systemically supplied during streamflow capable of mobilizing stored channel alluvium and re-suspending fine sediment (Figure 2.1). The conceptual model also assumes that a primary control on turbidity production is the geologic composition of the landscape. The study area has a complex Pleistocene glacial history that has resulted in a heterogeneous distribution of GLS that influences the total (fine and coarse fraction) sediment supply. These basic assumptions are based on more than 20 years of geomorphic assessments and observations supporting stream management planning as well as measurements of SSC and turbidity throughout the Ashokan Reservoir watershed (Effler et al., 1998; Davis et al., 2009; Baldigo et al., 2010; McHale and Siemion, 2014; Siemion et al., 2016; DEP, 2021; Wang et al., 2021). There are other factors that influence turbidity production. Riparian buffer composition and integrity influence stream channel stability thresholds, and past and ongoing stream management and land use practices can attenuate or exacerbate channel erosion. The current study scope includes acquiring data for some of these factors (e.g., riparian buffer width and adjacent land use, and stream bank revetment are recorded during stream channel mapping); however, these data are not currently factored into development of explanatory metrics presented in this report. Some of the assumptions in this conceptual model about turbidity production

source conditions may be modified as data are obtained and analyzed, and/or as other researchers use the available data to pursue other lines of investigation.

The geomorphic investigations inform the characterization and quantification of the turbidity and SS sources from the channel network (Figure 2.3). The study currently assumes terrestrial sources (floodplains and other upland terrain, roadways) are generally a smaller fraction of the SS supply in the study area. This is consistent with past research in the area and in other mostly forested, formerly glaciated terrains (Nagle et al., 2006; Yellen et al., 2015; Cienciala et al., 2020). Stream channel erosional connectivity with fine sediment is the assumed principal source of SS input transferred through the fluvial system. Erosional sediment connectivity is lateral (stream banks and connected hillslopes) and vertical (streambed incision). Erosional processes include hydraulic entrainment, mass wasting, and wet and dry ravel. Channel adjustment processes such as channel enlargement, avulsions and headcut migration also influence sediment connectivity. Figure 2.4 lists the four assumed principal SS source geologic categories currently used in this study: alluvium (AL), glacial lacustrine sediment (LS), glacial till (GT), and colluvium (CL). DEP’s previous FAD status reports describe these geologic or sedimentologic units in detail (DEP, 2019; DEP, 2021). Preliminary sediment fingerprinting investigations by USGS tested for and found different geochemical signatures for AL, LS and GT (Staub et al., 2022).

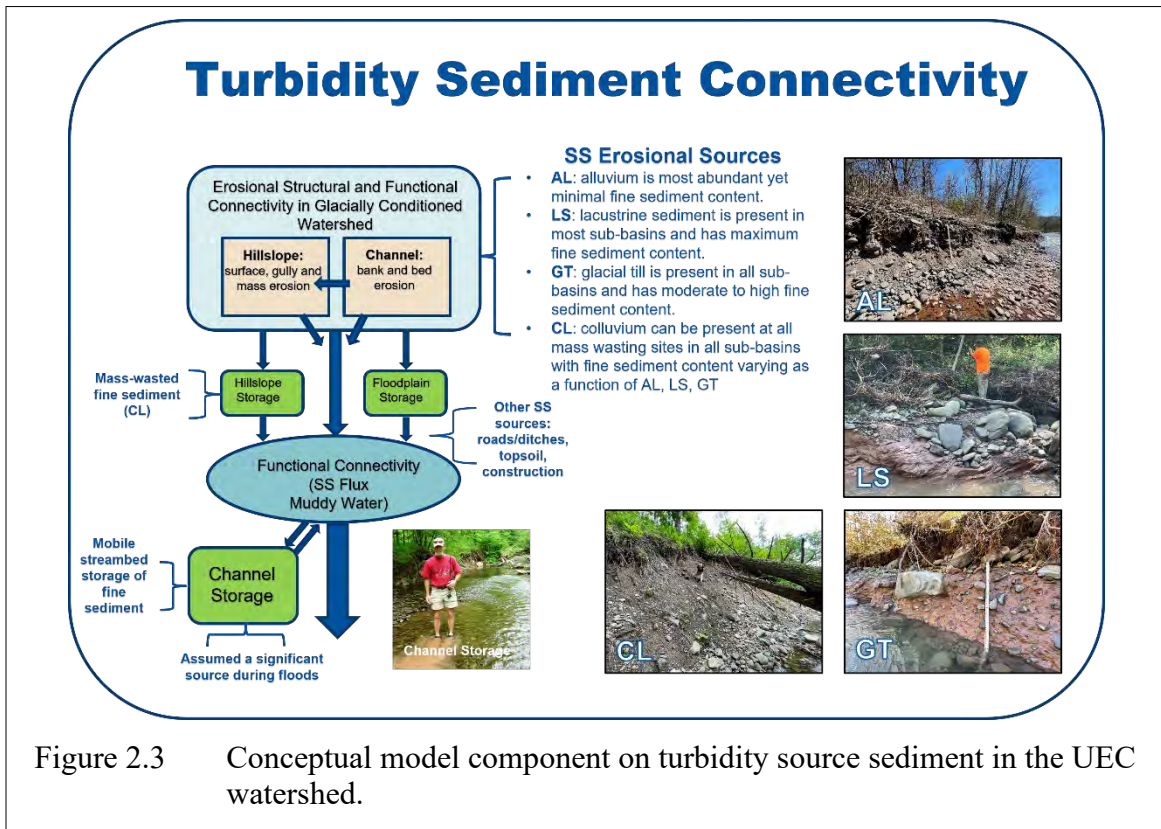


Figure 2.3 Conceptual model component on turbidity source sediment in the UEC watershed.

AL is the mixed grain size deposits of streams that predominantly are composed of sand up to boulder-sized sediment yet also have some small percentage of finer sediment in the mix. AL can be parsed into two sub-categories: (“older” AL in stream banks and fluvial terraces, and “recent” AL in the mobile streambed and associated depositional features like gravel bars). By area and volume, AL is the most ubiquitous and largest SS source in the channels. AL is entrained from erosion into alluvial banks and from mobilization of stored AL in the channel. Previous sampling of streambed AL in Esopus Creek was conducted to support the UEC Management Plan and found fine sediment content ranged from <1% up to ~3% with an increasing content from upstream to downstream. (Cornell Cooperative Extension of Ulster County, 2007). Preliminary calculations in the UEC Management Plan found that considering just Esopus Creek, the re-suspended fine sediment could account for ~17% of the measured SS yield (excluding major floods) at the Esopus Creek at Coldbrook station. Its contribution during major floods would be expected to be potentially higher.

LS is a predominantly silt/clay cohesive sediment (with varying amounts of sand) deposited in pro-glacial Pleistocene lakes that inundated much of the UEC terrain as glacial ice meltwater drained into the blocked valleys. Geologic investigations in the first decades of the 20<sup>th</sup> century mapped glacial lake deposits depicting the potential areas of inundation in the study area (Rich 1935). Large UEC watershed scale glacial lakes and smaller localized lakes are hypothesized to have inundated much of the study area terrain below at least an elevation of around 1800 feet based on mapped deltas and likely spillways. The result is a complex distribution of LS throughout the study area.

GT is an abundant glacial deposit in the study area terrain composed of the mixed grain size deposits from the base and margins of glacial ice. GT is a “catchall” term for unsorted glacially produced sediment that was either lodged in place at the base of glacial ice or pushed or carried into place along glacial margins. GT exposed in channel margins in valley bottoms tends to be a very consolidated sediment (difficult to erode) with a fine sediment matrix that contains the coarser clasts. GT fine sediment content can vary depending on mode of deposition and source terrain.

CL is the typically unconsolidated to semi-consolidated mixed grain size deposit from mass-wasting in stream banks and connected hillslopes. It is a complex mix in grain size and consolidation that varies as a function of the mass-wasting process, slope hydrology, and geologic composition. Fine sediment content in CL is a function of the mass-wasted source sediment and is assumed to range from the low of AL to the high of LS.

The discrete stream bank and hillslope erosion and bed incision connections with the GLS sources are considered “point” or reach sources; resuspended streambed AL is considered a “non-point” or systemic areal source in this conceptual model. The goal of the STRPs implemented in this study is to reduce T<sub>n</sub> production. This is pursued through the design objective of disconnecting reach scale T<sub>n</sub> sources from the stream channel to measurably reduce stream sediment input (Figure 2.4). The areal “conveyor belt” of AL-sourced resuspended fine sediment in the stream network is not the direct target for STRP treatment, although reach scale

STRPs at disproportionately large GLS sources may, over time, reduce the amount of fine sediment stored downstream of these projects in the stream network available for resuspension.

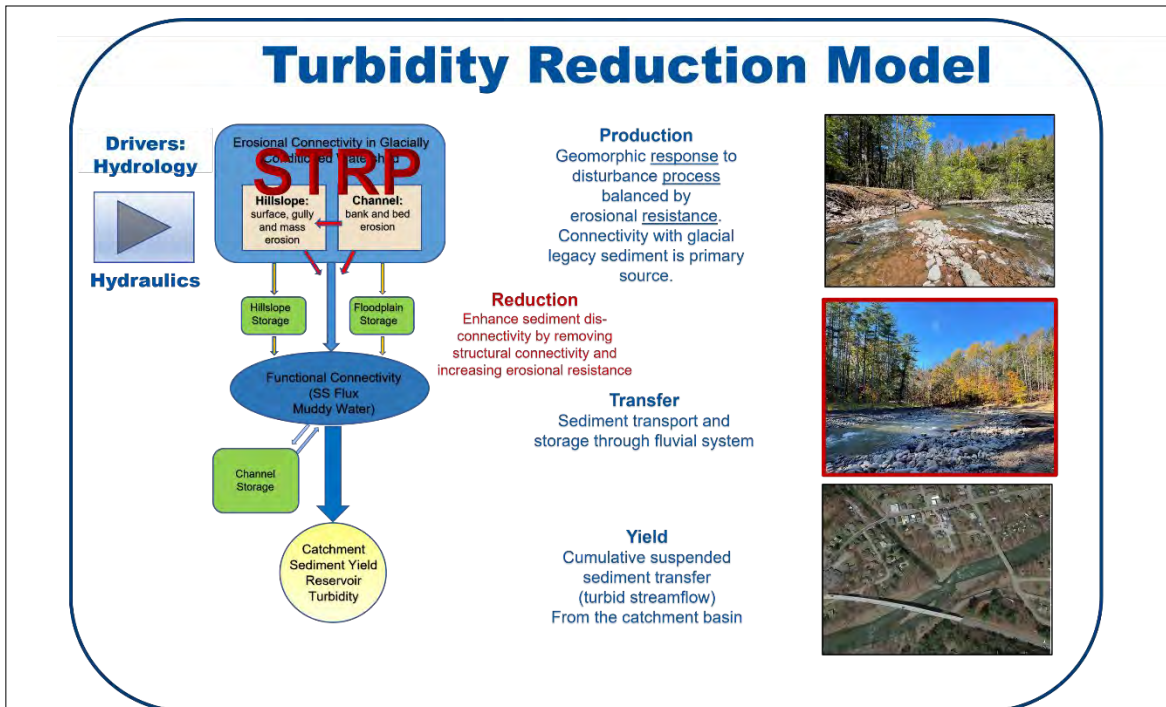


Figure 2.4 Flow chart of how the turbidity production conceptual model incorporates potential turbidity reduction through STRP modification of the sediment connectivity component.

### **3. Study Methods, Assumptions and Limitations**

The study has progressed since fall 2016 using a range of empirical, analytical, geospatial and computer modeling methods. DEP’s FAD study design report used to initiate this investigation presented the overall research goals, specific objectives, and the planned methods to achieve those objectives. Several assumptions informing the study have been made based on past research, assessment and monitoring efforts in the study area. Similarly, there are several limitations to the study that constrain the results findings. The assumptions and limitations are detailed in this section.

The methods have not remained static as the researchers learn more about what is important and what is not so important to help answer the primary questions regarding UEC watershed turbidity production and reduction potential through stream management. The overall approach of spatially extensive stream monitoring of Q, SSC and Tn for a minimum 10-year period coupled with turbidity source characterization through geomorphic investigations remains essentially the same. Through the course of the study, some methods have changed, some have been dropped, and others have been added to this adaptive research project. In some cases, monitoring or survey equipment changes were made to improve the data quality. In other cases, data collection efforts expanded and/or protocols were revised for data quality improvement. The following sub-sections briefly describe the methods used and highlight key changes since DEP submitted the initial 2017 FAD study design report.

When the study was initially designed, it was clear that a successful research project needed to capture temporal variability in hydrology and turbidity conditions in the study area. A ten-year period was established as the minimum needed to provide enough data for robust statistical analysis. Further, the initial design assumed that monitoring stations and source investigations needed to be broadly distributed (UEC watershed) yet also intensively focused in a sample area (Stony Clove sub-basin) to help understand how stream reach to segment scale source conditions and dynamics can influence reservoir watershed scale conditions and dynamics. This “telescopic” focus has so far proven to be well-suited to the need for investigating complex conditions, while maintaining a practical feasibility for implementation.

#### **3.1 Streamflow and Water Quality Monitoring Stations**

USGS uses a network of 29 stream monitoring stations distributed across the UEC watershed to measure and monitor Q, SSC and Tn to support the statistical analyses detailed in the study design report. Additional short-term stations have been added using funding from the AWSMP. Primary monitoring stations are those where Q and Tn are continuously monitored in 15-minute increments and SSC is measured across most of the range of observable Q conditions. SSC-Tn regression relationships are developed for each primary station to estimate continuous SSC and SSL. Secondary stations are those where only turbidity is measured and monitored every 15-minutes. Tables 3.1 and 3.2 provide details on the primary and secondary monitoring stations established for the study area and in operation for most of the study period. The three additional monitoring stations funded by the AWSMP are also listed in Table 3.1, and changes in monitoring locations within the Stony Clove sub-basin are listed in Table 3.2. Results from the

first five water years suggest the monitoring design has been mostly successful in measuring SSC and turbidity for the flows observed during that period, with the exception of some stations impacted by a high magnitude flood in December 2020 and, as described below in Table 3.3, some limits on turbidity probe detection range. Details on the equipment and methods used at the monitoring sites are available in Siemion and others (2021).

The 20 Stony Clove sub-basin monitoring stations include six primary stations measuring Q, Tn and SSC for four tributary sub-basins and two locations on Stony Clove Creek, and 14 secondary stations to delineate water quality monitoring sections (“reaches”) across the five streams: Stony Clove Creek, Ox Clove Creek, Warner Creek, Hollow Tree Brook, and Myrtle Brook (Figure 1.1). The water quality monitoring reaches segment the monitored streams into discrete SS loading and turbidity production sections. Two of the monitoring stations were discontinued, and two new locations were activated based on discussions between DEP and USGS. Warner Creek headwater monitoring station #01362354 was discontinued because the stream reach went dry for long periods and Stony Clove Creek station #01362350 was discontinued because of poor mixing of suspended sediment from an upstream hillslope source into the streamflow. Monitoring station #0136235585 was established at a location between two nearly adjacent STRPs in Warner Creek, and station #01362352 was established in a well-mixed stream reach of Stony Clove Creek downstream of the discontinued station #01362350.

Since the inception of the study, USGS has monitored turbidity using DTS-12 probes, which were the stand-alone turbidity probe supported by the USGS Hydrologic Instrumentation Facility. However, the DTS-12 had a limited range of 1,600 FNU which was exceeded during the December 2020 flood at some locations. In 2020, USGS recommended switching the turbidity monitoring probes from DTS-12 probes to Analite NEP-5000 probes for the remainder of the study period because the Analite NEP-5000 probes measure a greater range of values and can be calibrated on site. The Analite NEP-5000 are the stand-alone turbidity probe currently supported by the USGS Hydrologic Instrumentation Facility. The output from the two turbidity probes are not equivalent, and so new turbidity-SSC regression equations will need to be developed. This also precludes using turbidity as a long-term continuous measure of changes in sediment transport at these monitoring stations. SSC will continue to be comparable for long-term monitoring. Additionally, two locations will be instrumented with both turbidity probes to develop a comparative relation. Turbidity probes at 3 monitoring stations were upgraded from DTS-12 probes to Analite NEP-5000 probes when the DTS-12 were damaged. The probes were changed at Myrtle Brook (#01362322) on January 10, 2020, Hollow Tree Brook (#01362345) on January 31, 2020, and Birch Creek (#013621955) on February 3, 2021.

Table 3.1 UEC watershed USGS monitoring stations listed from upstream to downstream.  
Source: USGS.

Station Name	USGS Station ID	Drainage Area (mi <sup>2</sup> )	Station Type	Measurements
Esopus Cr blw Lost Clove @ Big Indian	0136219503	29.6	Primary	Q, SSC, Tn
Birch Cr @ Big Indian <sup>1</sup>	013621955	12.5	Primary	Q, SSC, Tn
Bushnellsville Creek @ Shandaken	0136219702	11.1	Secondary	Est. Q, Tn
Esopus Cr @ Allaben <sup>1</sup>	01362200	63.7	Primary	Q, SSC, Tn
Broadstreet Hollow Brook at Allaben	01362232	9.2	Secondary	Est. Q, Tn
Woodland Cr at Wilmot Way nr Woodland <sup>2</sup>	01362286	5.2	Secondary	Est. Q, SSC, Tn
Panther Kill at Panther Kill Rd nr Phonecia <sup>2</sup>	01362295	3.0	Secondary	Est. Q, SSC, Tn
Panther Kill at Woodland Valley Rd nr Phonecia <sup>2</sup>	01362297	3.5	Primary	Q, SSC, Tn
Woodland Cr abv mouth @ Phonecia <sup>1</sup>	0136230002	20.6	Primary	Q, SSC, Tn
Stony Clove Cr blw Ox Clove @ Chichester <sup>1</sup>	01362370	30.9	Primary	Q, SSC, Tn
Beaver Kill @ Mt Tremper	01362487	25.0	Primary	Q, SSC, Tn
Little Beaver Kill at Beechford nr Mt Tremper <sup>1</sup>	01362497	16.5	Primary	Q, SSC, Tn
Esopus Cr at Coldbrook <sup>1</sup>	01362500	192	Primary	Q, SSC, Tn

<sup>1</sup>Existing monitoring station funded through a separate DEP-USGS agreement. Note that Stony Clove Creek blw Ox Clove @ Chichester (01362370) is included in both the UEC watershed monitoring count and the Stony Clove sub-basin monitoring count.

<sup>2</sup>Short-term site funded by the AWSMP.

Table 3.2 Stony Clove sub-basin USGS monitoring stations listed from upstream to downstream. Source: USGS

Station Name	USGS Station ID	Drainage Area (mi <sup>2</sup> )	Station Type	Measurements
Stony Clove Cr @ Edgewood	01362312	2.3	Secondary	Est. Q, Tn
Myrtle Br @ SR 214 @ Edgewood	01362322	1.8	Primary	Q, SSC, Tn
Stony Clove Cr nr Lanesville	01362330	7.5	Secondary	Est. Q, Tn
Stony Clove Cr @ Wright Rd nr Lanesville	01362332	8.1	Secondary	Est. Q, Tn
Stony Clove Cr @ Jansen Rd @ Lanesville	01362336	9.3	Primary	Q, SSC, Tn
Hollow Tree Br @ SR 214 @ Lanesville	01362345	4.6	Primary	Est. Q, SSC, Tn
Hollow Tree Br @ Lanesville <sup>1</sup>	01362342	2.0	Secondary	Q, Tn
Stony Clove Cr @ Lanesville	01362347	15.4	Secondary	Est. Q, Tn
Stony Clove Cr abv Moggre Rd nr Chichester	01362349	16.4	Secondary	Est. Q, Tn
<i>Stony Clove Cr @ Chichester<sup>2</sup></i>	<i>01362350</i>	<i>17.5</i>	<i>Secondary</i>	<i>Est. Q, Tn; Discontinued Mar 2021</i>
Stony Clove Cr abv Warner Cr at Chichester <sup>3</sup>	01362352	17.5	Secondary	Est. Q, Tn Established Jul 2021
<i>Warner Cr blw Silver Hollow Notch nr Edgewood<sup>2</sup></i>	<i>01362354</i>	<i>2.3</i>	<i>Secondary</i>	<i>Est. Q, Tn; Discontinued Nov 2018</i>
Warner Cr nr Carl Mountain nr Chichester	0136235575	7.1	Secondary	Est. Q, Tn
Warner Cr in Silver Hollow nr Chichester	0136235580	7.3	Secondary	Est. Q, Tn
Warner Cr in Silver Hollow nr Phoenicia <sup>3</sup>	0136235585	7.4	Secondary	Est. Q, Tn; Established Dec 2018
Warner Cr @ Silver Hollow Rd nr Chichester	01362356	8.6	Secondary	Est. Q, Tn
Warner Cr nr Chichester	01362357	8.9	Primary	Q, SSC, Tn
Stony Clove Cr @ Silver Hollow Rd, Chichester	01362359	26.6	Secondary	Est. Q, Tn
Ox Clove @ Chichester	01362365	3.1	Secondary	Est. Q, Tn
Ox Clove nr mouth @ Chichester	01362368	3.8	Primary	Q, SSC, Tn
Stony Clove Cr blw Ox Clove @ Chichester <sup>1</sup>	01362370	30.9	Primary	Q, SSC, Tn
Stony Clove Cr abv SR 214 @ Phoenicia	01362398	32.4	Secondary	Est. Q, Tn

<sup>1</sup>Existing monitoring station funded through a separate DEP-USGS agreement.

<sup>2</sup>Site discontinued.

<sup>3</sup>Site installed during 3<sup>rd</sup> or 4<sup>th</sup> year of study.

### 3.1.1 Streamflow Monitoring

Streamflow at primary monitoring stations is monitored through use of a stage-discharge rating curve that is developed and maintained, or revised as needed, through repeat measurements of stream stage and streamflow, as per standard USGS methods (Sauer and Turnipseed, 2010; Turnipseed and Sauer, 2010). USGS also measures streamflow at three of the secondary stations (#01362312, #01362345, and #01362365) to calibrate estimates at these stations. Streamflow was not measured at the Broadstreet Hollow Brook (#01362232) and Bushnellsville Creek (#0136219702) sub-basins. Daily mean streamflow at these two stations was estimated based on daily mean streamflow from West Kill Creek (#01349810) and methods used in Gazoorian (2015). Fifteen-minute streamflow was estimated for Hollow Tree Brook (#01362345) based on 15-minute streamflow from station #01362342 approximately 0.9 miles upstream and equation 5 in Lumia and others (2006). The estimated streamflows are available from Siemion (2022). Daily mean streamflow at secondary stations in the Stony Clove sub-basin was estimated by drainage area weighting daily mean streamflow from the nearest downstream primary station. The December 2020 flood in the Stony Clove sub-basin caused significant damage to several monitoring stations infrastructure and stream stage-discharge controls, requiring repairs, replaced equipment, and new stage-discharge ratings. Table 3.3 identifies primary stations impacted by the flood and measures taken to recover the stations.

Table 3.3 USGS primary monitoring stations damaged during the December 2020 flood.  
Source: USGS.

Station Name	USGS Station ID	Description of problem and solution
Esopus Cr blw Lost Clove @ Big Indian	0136219503	Q exceeded rating; indirect Q measurement was conducted and new rating developed.
Myrtle Br @ SR 214 @ Edgewood	01362322	Q exceeded rating and equipment damaged; indirect Q measurement was conducted, new rating developed, and equipment replaced.
Stony Clove Cr @ Jansen Rd @ Lanesville	01362336	Q exceeded rating; indirect Q measurement was conducted and new rating developed.
Hollow Tree Br @ SR 214 @ Lanesville	01362345	Equipment damaged and replaced.
Warner Cr nr Chichester	01362357	Q exceeded rating; indirect Q measurement was conducted and new rating developed.
Ox Clove nr mouth @ Chichester	01362368	Q exceeded rating and equipment damaged; indirect Q measurement was conducted, new rating developed and equipment replaced.
Beaver Kill @ Mt Tremper	01362487	Q exceeded rating; indirect Q measurement was conducted and new rating developed.

### **3.1.2 Turbidity Monitoring**

Turbidity has been measured through use of Forest Technology Systems DTS-12 turbidity probes following standard methods (Wagner et al., 2006). Starting in 2020, USGS determined that observed limitations of the original DTS turbidity probes – long calibration times, measurement range limited to 0-1,600 FNU – merited replacement at all primary stations with Analyte probes that can be more efficiently calibrated and have a greater measurement range (0-4,000 FNU). One impact of the lower FNU limits of the DTS probes is that during some high streamflow magnitude-high turbidity events, turbidity exceeded the upper limit of the DTS, resulting in peak turbidity values not being measured for some runoff events. DEP and USGS recognize that the switch in turbidity measurement technology can impact continuity in data comparability if there are significant differences between the measurement results. To determine the differences in results, USGS will measure turbidity with side-by-side deployments of DTS and Analite probes at Stony Clove at Chichester (#01362370) and Little Beaver Kill (#01362497). New turbidity-SSC regression equations will be developed for the monitoring stations where the Analite probes are deployed. The resulting SSC dataset will be compatible with the SSC derived from the DTS probe regression equations, though the long-term turbidity datasets will not be directly comparable without adjustment.

### **3.1.3 Suspended Sediment Monitoring**

Water samples are collected for analysis of SSC throughout the range in streamflow and turbidity following standard methods (Edwards and Glysson, 1999). An automated sampler was used to collect discrete point samples during storms at predetermined changes in stream stage. Cross-section samples were collected using the equal-width depth-integrated method by either wading at the measurement section or from a nearby bridge using isokinetic samplers. Cross-section and point samples were analyzed for SSC at either the USGS Ohio Kentucky Indiana Water Science Center or the Cascade Volcano Observatory sediment laboratories using methods described in Guy (1969). The cross-section samples were used to calibrate and ensure the representativeness of the point samples. Periods of high streamflow and turbidity were targeted for more frequent sampling because this was when most suspended sediment was transported. More than 120-point samples and 9-12 cross section samples were collected at each primary station during the first five years of the study. The SSC samples and continuous turbidity data were used to develop turbidity-SSC regression equations (Siemion et al., 2021). The equations were then used to estimate SSC at a 15-minute timestep. Particle size was measured on a subset of suspended sediment samples from each primary station, generally when turbidity exceeded 200 FNU.

## **3.2 Suspended Sediment Source Characterization**

The original study design relied on a combination of stream feature inventory mapping (SFI) methods for synoptic measurements of stream channel erosional sources of SS and topographic monitoring cross-sections at several potential high turbidity producing reaches to measure stream channel erosion. Additional potential methods described available remote-sensing data to obtain estimates of stream power and complete historic channel alignment delineations. The intent of these methods was to obtain data that could help explain the

geomorphologic and geologic components that influence turbidity production in the study area. As with the Q, SSC and turbidity monitoring, the Stony Clove sub-basin was selected for most of the sediment source characterization.

DEP made several improvements to the proposed methods within the first year of the study. Some of the proposed GIS-based methods were either modified, discontinued, or replaced as needed to improve the study quality and efficiency. DEP modified the SFI methods and the stream bank erosion monitoring survey methods described in the study design report. The primary change to the stream bank sediment characterization was to integrate this method into the bank erosion monitoring surveys (BEMS) and to add streambed sediment sampling for grain size distribution analysis. The changes for each of these source characterization components are presented below.

### **3.2.1 GIS Analysis of Watershed and Stream Channel Characteristics**

One objective in the original study design was to obtain watershed characteristics in monitored sub-basins and reaches utilizing remote-sensed data. Most methods were to be applied to the Stony Clove sub-basin only. Many of the original methods described in the study design were completed as part of past stream management planning (e.g., historic channel alignment analysis using digitized stream centerlines, computing drainage areas, delineating stream geomorphic management reaches).

In 2018, DEP added digitizing active channel margins (ACM) using available time series of orthophotography (principally 2009 and 2016) to increase the potential value of the historic channel alignment analysis. This was reported in detail in DEP's 2021 biennial FAD status report (DEP, 2021). DEP is still developing this method and exploring metric potential; thus it will have limited presentation and discussion in this report.

The proposed stream power assessment using digital elevation model (DEM) slopes and reference streamflow magnitudes has been deferred until an optimized stream power modeling method can be added. Stream power or specific stream power (normalized by channel width) is a demonstrated driver forcing stream channel adjustment through erosion and deposition (Magilligan et al., 2015). A variation of the utility of stream power was explored with the use of the River Erosion Model (Lammers and Bledsoe 2018; Wang et al., 2021) to simulate stream channel adjustment to streamflow; however, this is a very labor-intensive method to apply across the UEC monitored sub-basins and is not advised for general application. As a first-cut estimate of slope values influencing hydraulics in a monitored sub-basin, DEP used the mean basin slope values for drainages upstream of the sub-basin USGS monitoring stations provide by the USGS online application StreamStats Version 4 ([StreamStats \(usgs.gov\)](https://www.usgs.gov/streamstats)). DEP plans to continue exploring optimal ways to compute distributed stream power in the study area using available remote-sensed data.

DEP investigated stream channel-hillslope connectivity through the application of techniques described in Fryirs et al. (2015). This method uses available DEM and orthophotography to delineate channel confinement margins (valley margins, valley bottom feature margins, anthropogenic margins) and measures the connection of the stream to these

margins to produce spatial distribution of confined, partly confined, and unconfined stream reaches. The pilot application of this method in 2018 indicated that it was useful for detecting potential for channel-hillslope connectivity, yet field observations during SFI mapping found that the dated 1-meter DEM (2009) did not always represent the observed 2018 conditions. DEP will continue to explore this method but has used the first five years of the research to focus on the field methods detailed in sections 3.2.2 and 3.2.3 below.

As reported in prior FAD reports, DEP has investigated GIS-based DEM differencing techniques to measure geomorphic changes in the stream channel corridor by using raster math to subtract the elevation values of one temporal DEM from another. The available DEM for the entire study area is a 2009 1-meter DEM based on April 2009 LiDAR-derived data (RACNE 2012). An additional 2014 1-m DEM for the Ulster County portion of the study area (~75%) based on November 2013 to June 2014 LiDAR-derived data is available for computing changes between the two periods (Dewberry, 2015). This DEM differencing technique was successfully used in a recent study in the nearby Biscuit Brook drainage in the Neversink basin (Hinshaw et al., 2020). Unfortunately, ~84% of the Stony Clove sub-basin is in Greene County and thus the DEM differencing has very limited application in the intensively researched sub-basin. Additional challenges to this task are differences in resolution and noise-reduction quality between the two DEMs, with the 2009 DEM providing higher quality data; it is not always clear in the 2014 DEM if differences are attributable to flood impacts or post-flood management actions. DEP will continue to explore how to best use the available basin scale DEM data. DEM differencing is used at the reach scale in the BEMS site investigations, as detailed below.

### **3.2.2 Stream Feature Inventory Mapping**

Suspended sediment source connectivity in the study area is largely measured and characterized using SFI methodology. SFIs in the monitored UEC sub-basins conducted by DEP and Ulster County and Greene County Soil and Water Conservation Districts between 2001-2021 are used to estimate the potential SS source conditions in those sub-basins. Suspended sediment source characterization investigations in the Stony Clove sub-basin use a modified SFI protocol to facilitate explaining variations in water quality monitoring reach and tributary sub-basin turbidity dynamics. DEP determined that the standard SFI features, attributes and protocol used for general stream management planning purposes identified in the original study design were insufficient for the more detailed suspended sediment source characterization investigations needed for the Stony Clove sub-basin. DEP created a new SFI protocol and data attribute dictionary specifically for the study prior to collection of any study SFI data.

SFI features (e.g., bank erosion) are mapped using high resolution, hand-held GPS units (Trimble Geo-XH) that are H-Star enabled and claim mapping accuracy to well under 1 foot. In practice, mapping accuracy and precision varies from inches to many feet and is partially a function of satellite availability, terrain and vegetation obscuration, and antenna models. Field experience also finds that waning battery power can negatively influence accuracy. This constrains the use of the SFI data to developing erosional connectivity metrics based on a minimum 3-feet (~1-meter) scale of accuracy. This presumed level of accuracy has not been fully tested yet is considered by DEP to be sufficient for computing a sub-basin scale to reach

scale erosion connectivity index – ratio of total mapped bank erosion length to total assessed channel length – since computed total bank erosion and assessed channel lengths are hundreds to thousands of feet.

The Trimble Geo-XH uses a data dictionary to define the features that can be mapped and the various attributes for those features. The existing data dictionary in 2017 was sufficient for the broader objectives for reconnaissance mapping to inform stream management plans yet did not include the level of detailed feature attributes (and some features) that increased the potential for this methodology to yield useful explanatory metrics for interpreting or predicting turbidity production. DEP revised the bank erosion feature to include more detailed information on stream confinement, erosional status, bank composition, SS production potential, and several diagnostic attributes. Since streambed erosion into GLS is also a primary turbidity input source, a bed erosion feature and a headcut feature were added.

User bias is an additional source of uncertainty in mapping erosional connectivity and selecting feature attribute values. Determining whether a section of apparent eroding stream bank is active (i.e., sediment can be entrained during bankfull flows), dormant or recovering requires experienced observation. Similarly, identifying the geologic composition of the eroding bank requires experienced familiarity with the fluvial and glacial legacy sediment in the study area. SFI mapping quality assurance and control measures used in this study included requiring that all data collection and processing is supervised by an experienced fluvial geomorphologist leading a team trained in the research SFI protocol. This was achieved for the 2018-2021 data by having a DEP geomorphologist supervise all training and data collection. The SFI mapping teams included a DEP geomorphologist and other experienced field staff, SUNY Ulster interns, and a consulting geologist in 2021. For 2018, 2019 and 2021 mapping, the SFI team included the same three SUNY Ulster intern members in addition to the DEP science team. In 2020, all data was collected by DEP. User bias was limited by having a small set of the same trained and experienced individuals collect the data. DEP performed all post-processing of data.

### **3.2.3 Stream Bank Erosion Monitoring Surveys**

DEP contracted with Milone & MacBroom, Inc. (now SLR Consulting) to collect the data for the BEMS sites. The original intent of the BEMS analysis was to obtain recurring topographic surveys at monumented channel cross sections and along the channel longitudinal profile that can be used to determine time-averaged bank erosion at up to 10 sites that exhibited erosional connectivity with GLS. In the study design, the BEMS data was not intended to provide predictive metrics for turbidity production analysis but could be used to help prioritize BEMS sites for possible STRP implementation and to monitor untreated sites for evolutionary trajectory. DEP initially proposed surveying previously established BEMS sites initiated in 2001, using laser level survey technology that provides data for two-dimensional topographic profiling and does not locate the survey in a geographic coordinate system. This is the standard technology and approach for many channel morphology surveys necessary for stream channel classification and two-dimensional channel adjustment monitoring. The original study design assumed recurring surveys every two years, with optional post-flood surveys. Many of the former

monumented BEMS sites were no longer monumented, replaced with STRPs, or had stabilized. DEP opted to select new sites based on SFIs completed between 2010-2015.

In 2017, DEP decided to increase the value of the topographic survey monitoring by having SLR Consulting perform reach scale three-dimensional topographic surveys using ground-based total station technology and uncrewed aerial system (UAS) technology to obtain high resolution orthophotography that can be converted to high resolution topography through Structure from Motion (SfM) techniques. This change in methods allows for the development of digital terrain or elevation models (DTM/DEM) that can be used for (1) measuring differences in reach scale channel morphology (erosion/deposition), (2) constructing hydraulic models to simulate varying hydrology and associated shear stress on channel boundaries, and (3) potentially computing sediment input/output budgets. The limitations of the UAS-based approach are that surveys must be performed during leaf-off and snow-free conditions, thus limiting the surveys to late fall/early winter and late winter/early spring. Also, not all sites are suitable for SfM topographic modeling due to obscuring presence of coniferous trees that mask the underlying terrain. DEP and SLR Consulting increased the frequency of surveys for active sites and/or sites selected for STRPs, while other sites that were either less active or more remote received surveys every 2-3 years.

In addition to increased topographic monitoring spatial and temporal resolution, DEP included funding for SLR Consulting to develop hydraulic models for monitored reaches and to integrate stream bank sediment sampling (a separate task in the original study design) into the BEMS scope of work. Streambed sediment sampling is currently also included through use of Modified Wolman Pebble Counts to obtain grain-size distribution data for the streambed surface susceptible to hydraulic shear stress. Bulk sediment sampling of streambed deposits was tested in 2021 at one of the BEMS sites converted to an STRP. DEP plans to expand streambed sampling to other locations in 2023.

### **3.2.4 Suspended Sediment Fingerprinting**

Sediment fingerprinting is a technique that apportions the sources of fine-grained sediment in a watershed using diagnostic tracers or “fingerprints”. Sources are classed into geologic units where each unit because of its geologic history has a unique geochemical signature (Gellis and Walling, 2011). This technique was piloted in the Stony Clove and Woodland Creek watersheds from 2017 through 2020. The pilot study demonstrated the potential to develop a source sample library and use storm samples to identify the relative contributions of each source class as they vary through the storm hydrograph (Staub et al., 2022). Sediment fingerprinting will be expanded to the upper Esopus Creek watershed during the second 5 years of the study. Based on the pilot study, the sources of sediment have been identified as either originating from the stream corridor: (1) LS, (2) GT, (3) AL, and (4) forested upland soil. The source sample library will be expanded to include the Esopus Creek mainstem and the monitored tributaries. Storm samples for fingerprinting analysis will be collected at Stony Clove at Chichester (#01362370), Woodland Creek at Phoenicia (#0136230002), and Esopus Creek at Coldbrook (#01362500). The storm samples will be used to identify the proportion of different geologic sources of suspended sediment at different points on the hydrograph.

### 3.3 Study Assumptions

Based on past research, assessment and monitoring efforts, DEP has made some assumptions to inform methodology development and interpretation that are restated below.

- Turbidity production and related suspended sediment flux in the study area is primarily sourced in the channel network and connected hillslopes and not from other terrestrial sources. The study acknowledges there are other sources (unpaved road runoff, roadside ditch erosion, construction site runoff, fine sediment from forested overland flow) but that these sources are sufficiently small contributions during runoff events that deliver turbid streamflow to the Ashokan Reservoir.
- There are hydrologic thresholds that function as hydrogeomorphic thresholds that scale the level of geomorphic response contributing to sediment flux or turbidity production. This assumption is complicated by the condition that big floods frequently alter the erosion resistance threshold – variably, reach to reach – for subsequent lower magnitude flows for an extended period of time.
- There are two primary categories of suspended sediment generation: (1) input of new sources through channel margin and connected hillslope erosion and sediment entrainment and (2) resuspension of stored fine sediment in mobilized streambed alluvium. The study currently only directly accounts for the input of new sources through erosion. Future sampling efforts of stored fine sediment in channel AL may help extend the accounting to the resuspension source.
- Glacial legacy sediment stored in the watershed is the principal erosional source of suspended sediment and the glacial lake sediment (LS) is the primary source for recruited input of suspended sediment in the fluvial system. Eroding stream channel boundaries composed only of AL contribute much less sediment per dimensional unit than those that include LS and/or GT, based on the fine sediment content.
- Turbidity production is heterogeneously distributed at the sub-basin to reach scale in the upper Esopus Creek watershed and varies spatially and temporally as a direct function of hydrologic and hydraulic forcing and suspended sediment source connectivity. The study aims to quantify that distribution to the extent feasible.
- A small fraction of a stream channel length can account for significant turbidity/SS production, therefore strategic treatment placement can yield a significant reduction in turbidity/SS. STRPs that disrupt reach-scale stream channel-fine sediment source connectivity can produce a measurable reduction in suspended-sediment concentration and turbidity at the sub-basin scale, and potentially at the reservoir basin scale.

### 3.4 Study Limitations

There are several limitations to the study scope, methods and ultimately the findings. This section briefly describes each critical limitation that should be factored into evaluating the study findings to date.

1. The study currently does not investigate the following factors that influence turbidity in the UEC watershed:
  - The Schoharie Diversion is a notable source of turbidity and SS to Esopus Creek and the Ashokan Reservoir. However, it is outside the scope of this study, which is investigating the UEC contributions to identify which sub-basins may disproportionately yield turbid streamflow and would be targeted for STRP implementation. The measured turbidity and SSC at the Esopus Creek at Coldbrook station includes potential contributions from the Schoharie Diversion during non-flood flows. The Schoharie Diversion is typically shutdown during flood flows.
  - The sediment source investigations mapped static erosional connectivity conditions observed during a field season and primarily focused on fluvial erosion and adjacent geotechnical erosion. Seasonal and episodic erosional events not directly linked to streamflow (e.g. freeze-thaw processes and other mass-wasting processes not evident during field inspection such as saturated debris flow) are not explicitly addressed in metric development.
  - Historic and recent human modifications to the landscape and stream corridor do influence streamflow runoff, hydraulics, and sediment connectivity. The current study does not investigate the role of these human legacy effects, as distinct from non-anthropogenic influences on streamflow runoff, hydraulics, and sediment connectivity.
  - The role of riparian vegetation condition on influencing channel stability thresholds and turbidity production is recognized but not investigated in the current study scope. Data is collected during SFI mapping that can be available for other studies to investigate this potential important explanatory variable.
2. There are some limitations to the methods and measuring equipment used in the study:
  - Section 3.1.2 describes the upper limits of turbidity measurements in the Forest Technology System DTS probes as 1,600 FNU. This limit was met/exceeded during the December 2020 flood, thus limiting the quantification of the turbidity for portions of the event (and potentially other events). This is being addressed through targeted probe replacement with Analite models that reportedly have an upper limit of 4,000 FNU.
  - Big floods damage monitoring equipment, especially in the smaller high-energy, high-sediment load streams. USGS optimizes sampling/monitoring locations to sample well-mixed streamflow, with infrastructure attached to stable natural features (large streamside boulders) or constructed features (bridge abutments). Site access and health and safety standards also influence monitoring station placement. It is understood that floods capable of generating sub-basin to basin scale turbidity production have the capacity to damage equipment.
  - Field investigations of turbidity source conditions did not cover the entire stream network in a monitored sub-basin. The SFI mapping in Stony Clove sub-basin could not

investigate every unit of channel length, in part due to a lack of landowner permission. Most headwater reaches and tributaries to tributaries were not assessed. This means probable connections with turbidity sources were not accounted for in the study. Section 4.3 discusses this limitation further.

- SFI mapping has limited accuracy and precision. Inconsistency in GPS accuracy limits the ability to rely on mapped features for detailed position analysis (e.g., time series bank retreat). The accuracy may be sufficient to show >3-feet (~1-meter) differences in feature position and dimension that can be compared across time and space; however, the study currently only uses the data to compute dimensionless erosional sediment connectivity indices as described in Section 3.2.2. Further investigation into data accuracy may extend further use of the data in subsequent studies by other researchers.
- Finally, it is important to clearly state that not all contributing areas and sub-basins to UEC are monitored. The current stream monitoring network upstream of the Esopus Creek at Coldbrook gage accounts for 82% of the contributing area.

## 4. Study Mid-Term Results

This section presents research results for streamflow, turbidity and SS monitoring, sediment source characterization, and STRP evaluation through water year 2021. Rather than presenting all the data collected thus far, this mid-term report presents the first five years of findings that most pertinently address the research goal and objectives. All streamflow, turbidity and SSC data collected through the monitoring period is available through the [USGS National Water Information System](#).

Section 4.1 describes the metrics developed so far based on the monitoring and source characterization data. Section 4.2 presents streamflow monitoring results for the reporting period. Sections 4.3 and 4.4 present turbidity and SS monitoring results, respectively, for the reporting period. Section 4.5 reports on the limited turbidity and SS source investigations at the UEC watershed scale and the deeper dive into source characterization for Stony Clove sub-basin. Section 4.6 provides an updated provisional evaluation of STRP efficacy.

### 4.1 Metric Development

Streamflow metrics that help explain observed turbidity and SS production include mean annual streamflow and mean annual runoff (MAR), dimensionless relative water yield for flood peak flows or flood frequency computed flows (PQR), occurrence and magnitude of runoff events exceeding hypothetical hydrogeomorphic thresholds. Additionally, daily mean streamflow is used as an explanatory variable in measured daily mean turbidity and estimated daily mean SSC, and as a component variable in calculation of SS loads and yields. Related hydraulic metrics including sub-basin scale streamflow and runoff power for all monitored sub-basins and reach scale stream power in the Stony Clove sub-basin are potentially powerful metrics that are not yet developed in the study.

Turbidity metrics examined at the mid-term stage of the research to help identify a sub-basin's relative role in Ashokan Reservoir turbidity levels include statistical metrics of turbidity values derived by USGS: daily mean turbidity summed for storm to annual time scales used in Q-Tn regression relationships and percent exceedance values for a range of flow conditions.

SS metrics examined in this research include SSC-Q, SS load (SSC\*Q) and SS yield (SSC\*Q/DA). Continuous estimates of SSC and SSL are derived from Tn-SSC regression relationships developed by USGS using the first three years of SSC point and cross-section sampling and continuous turbidity measurements (Siemion et al., 2021). The regression equations are developed for each monitored sub-basin representing the unique relationships between the SS sources and concentrations and turbidity.

SS and turbidity source geomorphic metrics are derived from the available SFI data through 2021. For the UEC sub-basin analysis, the pre-study and more recent SFI data is used to compute basic erosional and sediment connectivity indices. The stream bank erosion index ( $EI_{Bnk}$ ) is a measure of the mapped bank erosion length divided by the total length of assessed stream channel. This index was presented as percent bank erosion in Table 4.1 in the 2021 biennial status report (DEP, 2021) and was computed as mapped bank erosion length divided by

twice the length of assessed channel, to account for both banks. The change made for this report is to improve consistency with recent scientific literature investigating bank erosion connectivity (Cienciala et al., 2020). Bank erosion is further categorized into two sediment connectivity indices (SCI) to represent whether the mapped bank erosion includes connectivity with GLS ( $SCI_{GLS}$ ) or only AL ( $SCI_{AL}$ ). These two indices are lengths normalized by the total length of mapped bank erosion used to compute  $EI_{Bnk}$ . The dominant source of GLS (LS or GT) in a mapped stream is also identified based on review of the SFI data. It is important to re-emphasize that this UEC watershed data spans 20 years, had multiple different observers, and used three different SFI data schema. Given that significant quality control limitation, these data are used to represent potential for connectivity conditions during the study period, not actual contemporaneous connectivity. Stony Clove index values presented at the UEC scale are for the pre-study 2013 data. The results used to compute study metrics for Stony Clove, reported separately, are based on different SFI methods and represent data coincident with the reporting period.

Erosional and sediment connectivity metrics for Stony Clove sub-basin can be more numerous and refined owing to the additional detail in the SFI data dictionary used for that component of the study. As a result, erosional sediment connectivity can include bed erosion and both bank and bed erosional connectivity can be further explored through more specific geologic composition and inclusion of confinement conditions. In this report, bank and bed erosional connectivity indices ( $EI_{Bnk}$ ,  $EI_{Bed}$ ) are investigated and sediment connectivity indices include the previous  $SCI_{GLS}$  and  $SCI_{AL}$ , along with  $SCI_{LS}$  and  $SCI_{GT}$  to quantify the relative proportions of the respective GLS component of connectivity.

## 4.2 Streamflow Monitoring

The USGS streamflow monitoring network successfully monitored continuous streamflow at 15-minute intervals for all UEC sub-basins and the two mainstem EC monitoring stations through the duration of the reporting period. Streamflow data (continuous, daily and annual means, annual peak) for the reporting period are available from the [USGS National Water Information System](#).

Streamflow represents energy applied to the landscape that powers fluvial processes (Castro and Thorne 2019; Figure 4.1). The magnitude, timing, duration, and flow energy of discrete flood events directly influence the geomorphic process-response relationship that produces stream turbidity and SS load. Figures 4.2 and 4.3 show the continuous streamflow hydrographs for Esopus Creek and Stony Clove Creek, covering a 23-year period from water year 2000 through water year 2022. The water year 2022 data is considered provisional and subject to change. The Study monitoring period is marked on the hydrographs. The depicted 23-year record places the monitoring period in a temporal and hydrologic context.



(a)

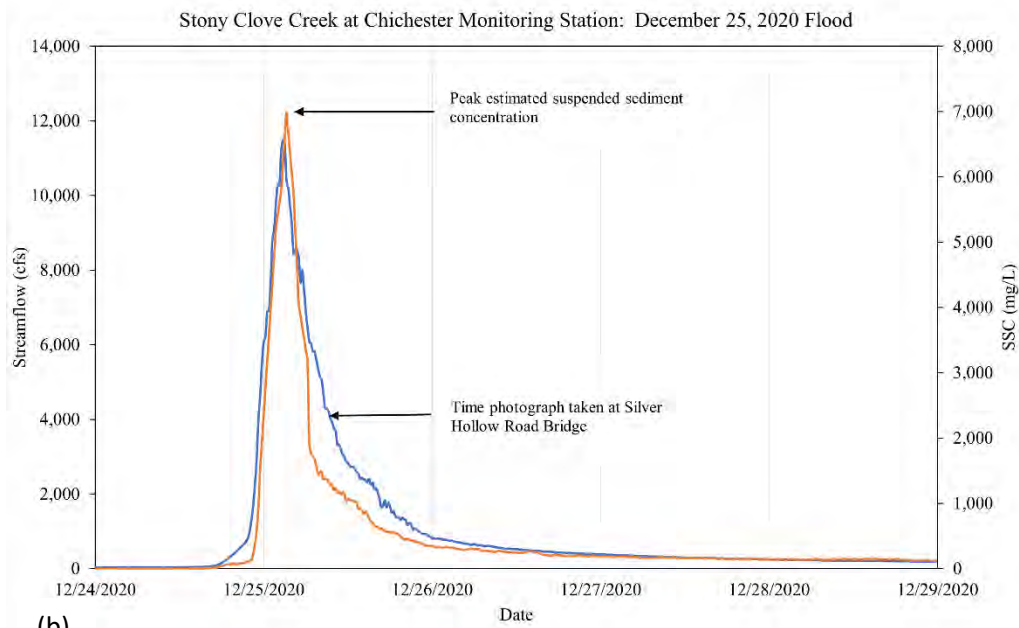


Figure 4.1 (a) Very turbid flood runoff in Stony Clove Creek at Silver Hollow Rd bridge on December 25, 2020. (b) storm hydro-sedigraph depicting the cumulative suspended sediment transported during the flood.

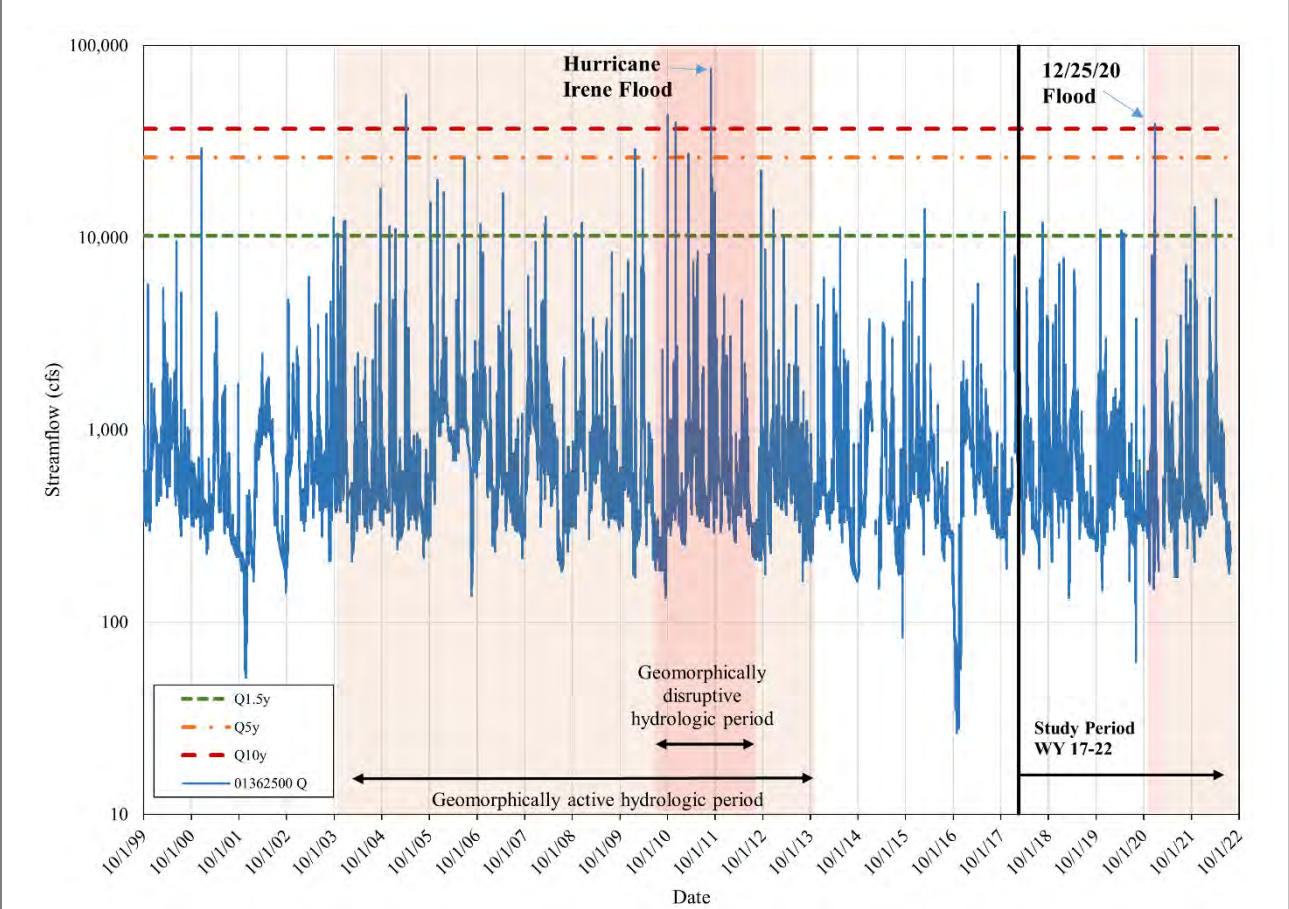


Figure 4.2 Continuous streamflow hydrograph for Esopus Creek monitoring station #01362500 with reference recurrence interval streamflows using the full period of record for FFA. Water year 2022 data is provisional and subject to change.

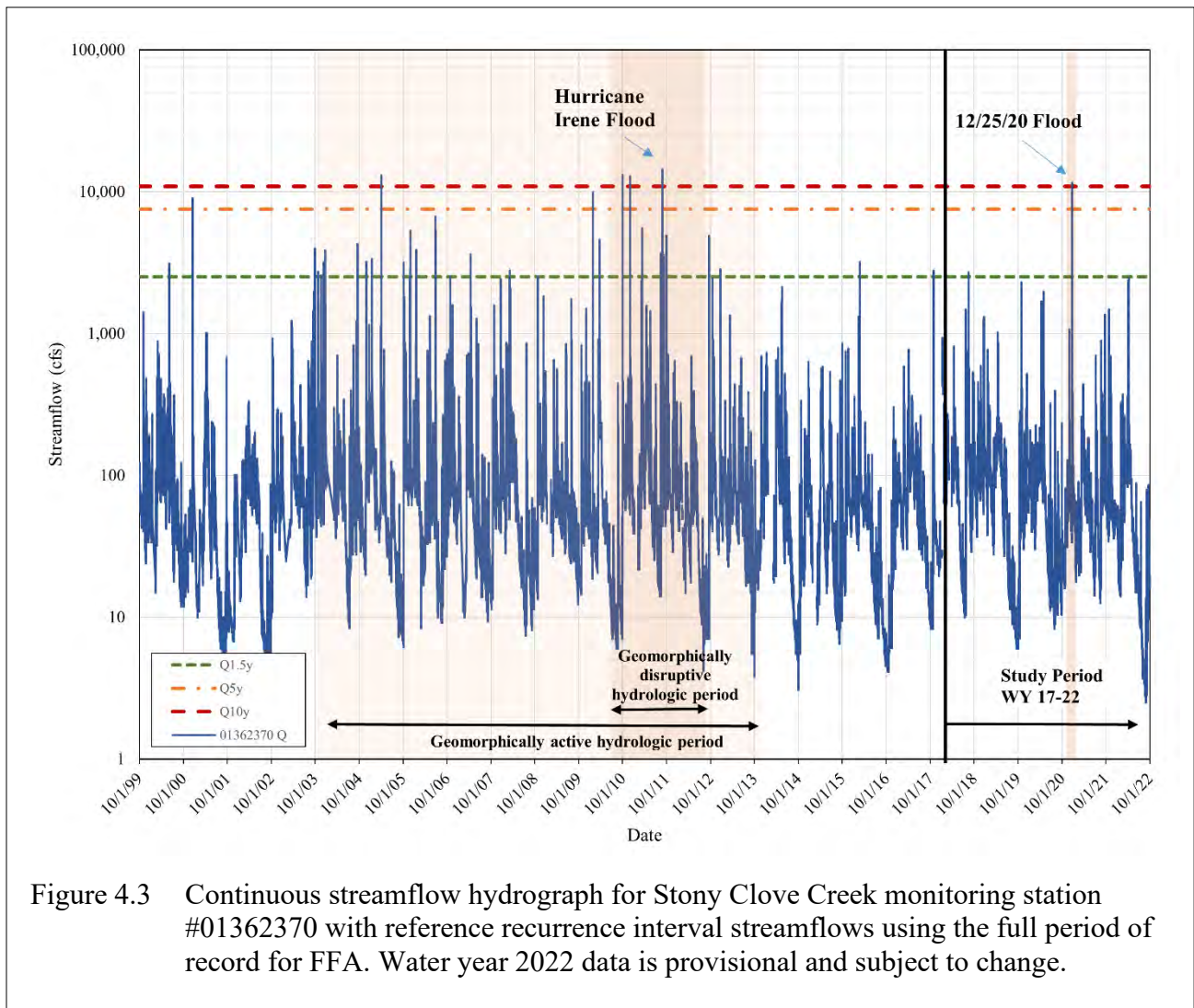


Figure 4.3 Continuous streamflow hydrograph for Stony Clove Creek monitoring station #01362370 with reference recurrence interval streamflows using the full period of record for FFA. Water year 2022 data is provisional and subject to change.

#### 4.2.1 Annual Streamflow and Runoff Results

The daily mean streamflow reported by USGS for each primary monitoring station is used in this study to compute some basic streamflow metrics that can be used to consider the relative contributing streamflow volume from each monitored sub-basin to the total flow measured at the Esopus Creek at Coldbrook station just upstream of the Ashokan Reservoir. The study assumes most turbidity production takes place during big floods capable of forcing a lot of geomorphic work and sediment transport through the fluvial system; however, an examination of the mean streamflow runoff conditions could provide some insight into each sub-basin’s unique hydrology. Table 4.1 presents the mean annual streamflow for each primary station in the study for each water year. Mean annual streamflow is obtained by dividing the sum of all the individual daily flows by the number of daily flows recorded for a year. As expected, streamflow magnitude scales with drainage area, and the two highest contributing streamflows (not counting

the two Esopus Creek monitoring stations that include monitored sub-basins) are Stony Clove Creek and the Esopus Creek headwaters. Woodland Creek and Beaver Kill are third and fourth, respectively, though Woodland Creek has a smaller drainage area. Little Beaver Kill and Birch Creek have the lowest annual streamflow, respectively. This table does not include the other primary stations within Stony Clove Creek. Water year 2018 had the highest monitored streamflows for all sub-basins, except for Stony Clove Creek and Beaver Kill, which were slightly higher in 2019.

Annual runoff is a measure of the streamflow normalized by the contributing drainage area. It can be considered a streamflow yield and serves for comparison of the hydrologic load among basins with varying drainage area, e.g., which sub-basins produce the most streamflow per unit area, which may in turn influence turbidity production potential. Annual runoff magnitude is known to influence channel dimensions in the study area (Miller and Davis 2003), though its relationship to turbidity production is not known. Mean annual runoff (MAR) is computed by normalizing the annual sum of daily mean streamflow (Q) by the monitored drainage area (DA). MAR supports comparison of streamflow availability among the monitored sub-basins. MAR values are presented for each study period water year through 2021 in flow per drainage area units (cfs/mi<sup>2</sup>) in Table 4.2, though runoff is also often computed as a depth of water on the landscape in length units. It is clear in Table 4.2 that some sub-basins have a higher flow yield than other sub-basins. The highest MAR sub-basins are Woodland Creek and Stony Clove Creek, respectively, while Little Beaver Kill has the lowest MAR. Factors that are known to influence MAR variability include, precipitation, basin slope, landcover, geology, and storage).

Table 4.1 Mean annual streamflow reported in ft<sup>3</sup>/s for each UEC sub-basin streamflow monitoring station for water years 2017-2021. Values for UEC sub-basins excluding #01362200 and #01362500 are color-coded to represent relative ranking, with green to red scaling depicting lowest to highest values.

Stream (USGS Station ID)	2017	2018	2019	2020	2021	Mean
Esopus Creek (0136219503)	69	81	82	75	77	79
Birch Creek (013621955)	29	38	35	29	28	33
Esopus Creek (01362200)	140	205	204	163	167	185
Woodland Creek (0136230002)	54	75	74	60	65	69
Stony Clove Creek (01362370)	73	99	102	79	95	93
Beaver Kill (01362487)	39	75	79	58	61	68
Little Beaver Kill (01362497)	30	41	44	35	37	39
Esopus Creek (01362500)	638	752	681	598	646	669

Table 4.2 Mean annual runoff (MAR) reported in cfs/mi<sup>2</sup> for each streamflow monitoring station for water years 2017-2021. Values for UEC sub-basins excluding #01362200 and #01362500 are color-coded to represent relative ranking, with green to red scaling depicting lowest to highest values. Note MAR for #01362500 is influenced by contributions from the Schoharie Diversion.

Stream (USGS Station ID)	2017	2018	2019	2020	2021	Mean
Esopus Creek (0136219503)	2.34	2.73	2.77	2.53	2.60	2.66
Birch Creek (013621955)	2.32	3.05	2.80	2.33	2.27	2.61
Esopus Creek (01362200)	2.20	3.22	3.20	2.56	2.62	2.90
Woodland Creek (0136230002)	2.60	3.64	3.61	2.93	3.18	3.34
Stony Clove Creek (01362370)	2.38	3.21	3.29	2.54	3.06	3.02
Beaver Kill (01362487)	1.55	2.99	3.18	2.31	2.45	2.73
Little Beaver Kill (01362497)	1.80	2.46	2.67	2.10	2.24	2.37
Esopus Creek (01362500)	3.32	3.92	3.55	3.11	3.36	3.48

## 4.2.2 Flood Hydrology

The scale of a flood’s “geomorphic effectiveness” is relative to the flood magnitude-frequency, the geomorphic resistance of the stream channel, and the recovery process period (Fryirs and Brierley, 2013; Dethier et al., 2016). Flood magnitude-frequency is readily estimated using the available USGS streamflow monitoring stations in the study area. Estimates of geomorphic resistance and recovery period in the study area are much more complicated and beyond the scope of the current study. As described in Section 2, DEP assumes there are streamflow event magnitudes (or more aptly, magnitude ranges) that represent lower and upper geomorphic effectiveness thresholds. The lower threshold represents a frequently recurring flood capable of geomorphic work and the upper threshold represents a less frequently recurring flood that is capable of “excess” geomorphic work resulting in a more widely distributed disturbance to reaches in the stream network. Disturbance in this context refers to a process resulting in an adjustment that requires a period of recovery or initiating a new geomorphic condition (Wohl, 2019). Floods capable of geomorphic disturbance can lead to the acute and chronic turbidity conditions observed in the disturbed area. Geomorphic disturbances typically do not destabilize the entire stream network, but rather specific reaches, with specific geomorphic conditions, and other reaches, with different, more stable geomorphologies, may remain undisturbed. The same goes for reach level variability in geomorphic resilience: the time it takes a newly disturbed reach to adjust and evolve to a more stable form.

Three reference streamflow magnitudes are depicted in Figures 4.2 and 4.3. The streamflow values are flood frequency recurrence interval (RI) streamflows and were computed using the available period of record for each station in a Log-pearson Type III (LPT3) flood frequency analysis. The 1.5-year RI streamflow ( $Q_{1.5y}$ ) approximately represents the bankfull flow, which over decadal time scales performs most of the fluvial geomorphic work in shaping the stream channel and conveying sediment. This frequently recurring event is set as the lower threshold, as it is generally not associated with a stream network scale channel “disturbance” event but can perform geomorphic work. The 10-year RI streamflow ( $Q_{10y}$ ) is an event capable of geomorphic work that has the potential to cause disruptive channel reach disturbance at the stream network scale. Flood events at or exceeding this threshold may result in potential reach-level or systemic geomorphic responses including chronic elevated turbidity triggered by reach-to-network scale bank erosion, headcut initiation and migration, channel avulsions, planform changes, and mass wasting at channel-hillslope coupled reaches. Not all  $Q_{10y}$  floods will have this effect in all reaches of a stream system, though observations of similar magnitude events in the study area demonstrate its potential for geomorphic response in several reaches. An intermediate 5-year RI streamflow ( $Q_{5y}$ ) is also depicted.

These reference streamflows represent hypothetical hydrogeomorphic thresholds and are used in this report as indicators for potential geomorphic response in the monitored UEC watershed. Table 4.3 presents flood frequency flow values and corresponding runoff values (PQR) for the  $Q_{1.5y}$  and  $Q_{10y}$  for those primary monitoring stations with a sufficient period of record. The flood frequency flows in Table 4.3 were computed using (1) the period of record through water year 2021 for each station, and (2) the LPT3 frequency distribution method and regionalized skew coefficients. These include the reference flows used in Figures 4.2 and 4.3. Given the range in periods of record (11-90 years), the uncertainty for each probabilistic flow varies considerably. Table 4.4 presents alternate LPT3 flood frequency results for streams with a shared minimum 19-year record (2003-2021) to test for uncertainties associated with differing periods of record and potential non-stationarity in the long-term flow record. The Woodland Creek station period of record is 19 years so there is no difference between the tables. The differences in the  $Q_{1.5y}$  flow were all small to moderate increases except for Esopus Creek at Coldbrook with a 17% increase. Results were mixed for the higher magnitude  $Q_{10y}$  flows, with Birch Creek, Stony Clove Creek, and Little Beaver Kill having small decreases, while the two Esopus Creek longer term stations had an 8% increase for the Coldbrook station and a 15% increase for the Allaben station. This analysis was conducted by DEP and did not use the regional regression weighting method and PeakFQ software that USGS uses, so the results would also differ based on computational methods.

While there are differences in results depending on flood frequency distribution methods and different periods of record, the values in Tables 4.3 and 4.4 do provide a reasonable range estimate of what scale of runoff event may influence turbidity production in these streams. The highest PQR values for these reference flows are in Stony Clove Creek, Woodland Creek and Beaver Kill; the lowest by a significant amount is in Birch Creek. Birch Creek is on the western margin of the UEC and is partially influenced by lower precipitation amounts (Miller and Davis, 2003).

Table 4.3 Hydrogeomorphic threshold streamflow and PQR (Q/DA) metrics ( $Q_{1.5y}$ ,  $Q_{10y}$ ) for each streamflow monitoring station with records  $\geq 10$  years. Flood frequency flows are computed by DEP using log-Pearson Type III methods without regional regression weighting and may differ from USGS computed values.

Stream (USGS Station ID)	Period of Record (yrs)	$Q_{1.5y}$ (cfs)	$PQR_{1.5y}$ (cfs/mi <sup>2</sup> )	$Q_{10y}$ (cfs)	$PQR_{10y}$ (cfs/mi <sup>2</sup> )
Birch Creek (013621955)	22	341	27.3	1,019	81.5
Esopus Creek (01362200)	59	2,485	39.0	10,761	168.9
Woodland Creek (0136230002)	19	1,569	76.2	5,473	265.7
Stony Clove Creek (01362370)	28	2,611	84.5	11,529	373.1
Beaver Kill (01362487)	11	2,220	88.8	5,842	233.7
Little Beaver Kill (01362497)	24	915	55.5	2,245	136.1
Esopus Creek (01362500)	90	10,318	53.7	37,570	195.7

Table 4.4 Hydrogeomorphic threshold streamflow and PQR (Q/DA) metrics ( $Q_{1.5y}$ ,  $Q_{10y}$ ) for streamflow monitoring stations with a coincident 19-year period of record (2003 – 2021). Flood frequency flows are computed by DEP using log-Pearson Type III methods without regional regression weighting and may differ from USGS computed values.

Stream (USGS Station ID)	Period of Record (yrs)	$Q_{1.5y}$ (cfs)	$PQR_{1.5y}$ (cfs/mi <sup>2</sup> )	$Q_{10y}$ (cfs)	$PQR_{10y}$ (cfs/mi <sup>2</sup> )
Birch Creek (013621955)	19	367	29.4	1,012	81.0
Esopus Creek (01362200)	19	2,529	39.7	12,388	194.5
Woodland Creek (0136230002)	19	1,569	76.2	5,473	265.7
Stony Clove Creek (01362370)	19	2,681	86.8	10,837	350.7
Little Beaver Kill (01362497)	19	990	60.0	2,164	131.1
Esopus Creek (01362500)	19	12,076	62.9	40,560	211.3

Table 4.5 summarizes the number of recorded peak streamflows that occur in three categories:  $Q_{1.5} < Q_5$ ,  $Q_5 < Q_{10}$  and  $\geq Q_{10}$  for Esopus Creek (#01362500) and Stony Clove Creek

(#01362370) using the results in Table 4.3. The frequency distribution of flood events in these three categories is similar for both stations. For a 23-year period there were 26 and 29 events between  $Q_{1.5y}$  and  $Q_{5y}$  for Stony Clove Creek and Esopus Creek, respectively. The events in this category are not evenly distributed through the 23-year period. In both streams, 21 of the events occur in a 10-year period from 2003 to 2012, representing a geomorphically active decade. Between water years 2013 to 2020, there are only three events in this category in Stony Clove Creek and six similar magnitude events at the Esopus Creek station. The first four years of the study period correspond to a less geomorphically active period. The December 25, 2020 flood magnitude exceeded the  $Q_{10y}$  threshold for both Esopus Creek at Coldbrook and Stony Clove Creek at Chichester stations marking the end of the “recovery” period.

Table 4.5 Number of peak streamflows in magnitude-frequency categories for Stony Clove Creek and Esopus Creek monitoring stations for a 23-year period of record from October 1, 1999 to September 30, 2021. This does not include provisional streamflows for water year 2022.

Stream (USGS Station ID)	$Q_{1.5} - Q_5$	$Q_5 - Q_{10}$	$\geq Q_{10}$
Stony Clove Creek (01362370)	26	2	5
Esopus Creek (01362500)	29	3	5

The flood events that meet or exceed the upper magnitude-frequency threshold are similarly clustered. At both stream stations there are five events (counting the December 2020 flood) that exceed the  $Q_{10y}$  threshold during the 23-year period. Three of the five events occur within an 11-month period (October 2010 to August 2011). This would correspond to a period of geomorphic disturbance. The prolonged elevated monitored turbidity levels in the UEC watershed during this period support this point (McHale and Siemion 2014). DEP’s 2021 biennial FAD status report includes a more detailed discussion on the hydrology and geomorphic response for the period depicted in the hydrographs (DEP 2021).

Between December 24-25, 2020, five inches of rain fell on a large snowpack in the UEC watershed. The resulting flood had an annual exceedance probability (AEP) of 4-20% (recurrence intervals of 25 to five years) in streams across the basin (Table 4.6) and resulted in substantial geomorphic changes in some stream channels. The effects of the flood were heterogeneous across and within the sub-basins of the UEC watershed. The greatest runoff was observed in the Stony Clove Creek sub-basin and the lowest observed in the Birch Creek and Little Beaver Kill sub-basins. The AEP and RI values in Table 4.6 are based on a LPT3 flood frequency analysis (FFA) conducted by USGS (Graziano and Siemion, 2022) and may differ from other reported FFA results because of differences in methodology. The preliminary observed geomorphic response to that flood through changes in channel morphology (e.g., channel erosion) and monitored turbidity and SS flux confirm that a flood of this magnitude ( $>Q_{10y}$ ) yields a system-scale geomorphic disturbance that can substantively alter geomorphic connectivity with SS sources in the study area. However, as presented in Section 4.3 and 4.4, a

lower magnitude-frequency flood was recorded for Woodland Creek ( $Q_{5y}$ ) yet it experienced a notable increase in turbidity and SS production during and following the event. This would seem to challenge the hypothesis that it would take a runoff event at or above the  $Q_{10y}$  threshold to trigger the measured change in turbidity production following the flood.

Table 4.6 Peak streamflow, annual exceedance percentage (AEP), return interval (RI), and PQR (Q/DA) for the December 25, 2020 storm at primary monitoring sites. Source: USGS

Stream (USGS Station ID)	Peak Streamflow (cfs)	AEP (%)	RI range (years)	PQR (cfs/mi <sup>2</sup> )
Esopus Creek below Lost Clove near Big Indian (0136219503)	5,540 <sup>1</sup>	na	na	187
Birch Creek at Big Indian (013621955)	936	20	5	75
Esopus Creek at Allaben (01362200)	8,580	10-20	10-5	135
Woodland Creek at Phoenicia (0136230002)	3,620	20	5	176
Myrtle Brook near Edgewood (01362322)	na	na	na	na
Stony Clove at Jansen Rd at Lanesville (01362336)	1,700 <sup>1</sup>	na	na	183
Hollow Tree Brook at Lanesville (01362342)	456	4-10	25-10	228
Warner Creek near Chichester (01362357)	2,900 <sup>1</sup>	na	na	326
Ox Clove at Chichester (01362368)	916 <sup>1</sup>	na	na	241
Stony Clove at Chichester (01362370)	11,500	4	25	369
Beaver Kill at Mt Tremper (01362487)	4,440 <sup>1</sup>	na	na	178
Little Beaver Kill (01362497)	1,430	50-20	2-5	87
Esopus Creek (01362500)	39,100	10-4	10-25	204

<sup>1</sup>Peak streamflow estimated by indirect method.

## 4.3 Turbidity Monitoring

### 4.3.1 UEC Results

Comparison of SSC or turbidity between monitoring stations may be complicated by differences in monitoring periods between stations, missing data at some stations, and differences in the magnitude of storms across the Esopus Creek basin. Use of the daily mean streamflow-daily mean SSC and daily mean streamflow-daily mean turbidity relations for comparisons between stations can minimize these concerns. The daily mean streamflow-daily mean turbidity relations for the sub-basin stations for the reporting period are shown in Figure

4.4 and regression equation information given in Table 4.7. Daily mean turbidity was used in place of daily mean SSC because SSC was not monitored at two of the sub-basin stations. It should be noted that turbidity is a point measurement and is not necessarily representative of the true cross-section concentration, though most streams in this study can be considered well-mixed at the highest streamflows. The sub-basins generally fell into two groups: those that produced greater turbidity per unit streamflow (Stony Clove Creek, Woodland Creek, Broad Street Hollow Brook, and Birch Creek) and those that produced less (Little Beaver Kill, Bushnellsville Creek, and Esopus Creek below Lost Clove Rd). Beaver Kill was similar to the lower production group at low streamflows but crossed into the greater producing group at higher streamflows. Broadstreet Hollow Brook had the greatest “base level” turbidity of all sub-basins. The mainstem Esopus Creek stations at Allaben and Coldbrook had similar streamflow-turbidity relations to the lower producing group.

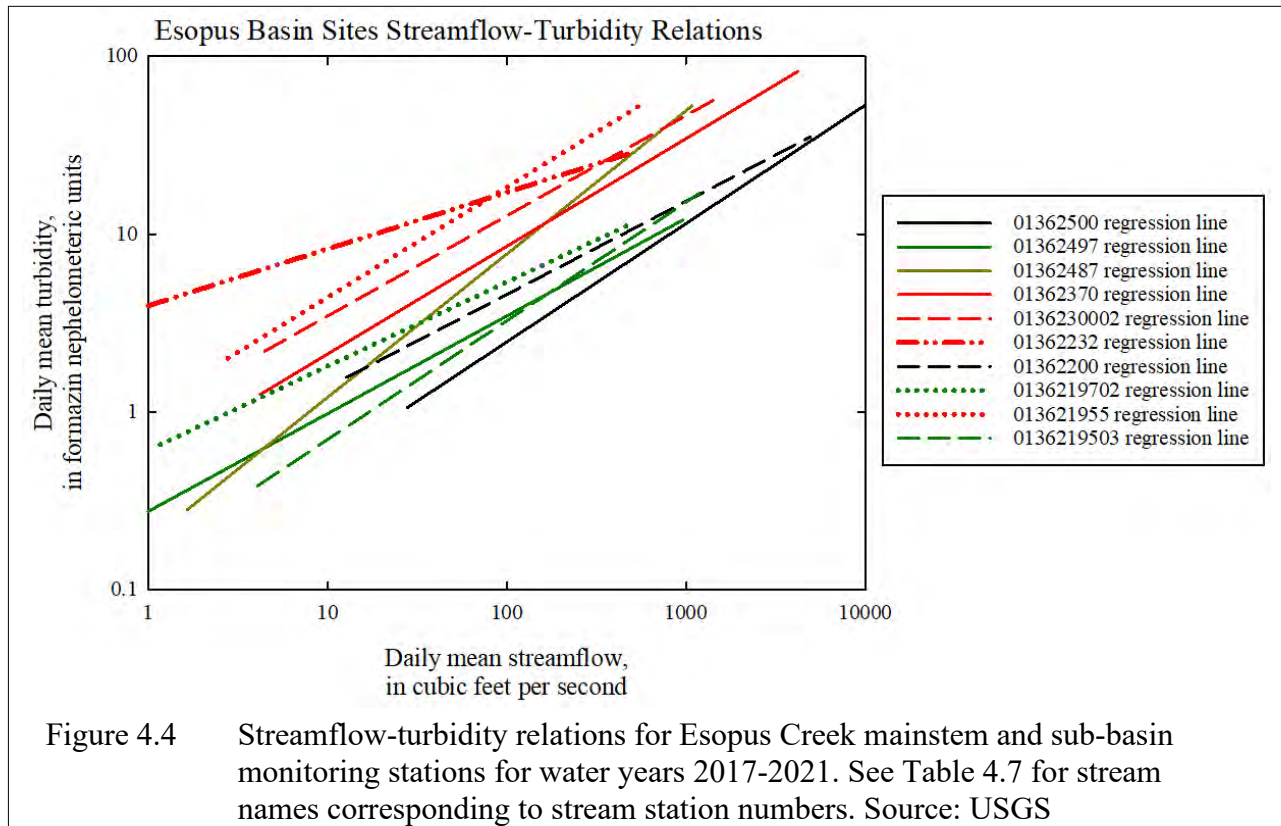


Table 4.7 Summary information for daily mean streamflow-daily mean turbidity regression equations (in log form) shown in Figure 4.4. Source: USGS

Stream (USGS Station ID)	Slope	Intercept	Coefficient of determination
Esopus Creek below Lost Clove near Big Indian (0136219503)	0.67	-0.82	0.47
Birch Creek at Big Indian (013621955)	0.62	0.03	0.40
Bushnellsville Creek (0136219702)	0.47	-0.21	0.28
Esopus Creek at Allaben (01362200)	0.52	-0.38	0.31
Broadstreet Hollow Brook (01362232)	0.32	0.60	0.19
Woodland Creek at Phoenicia (0136230002)	0.56	-0.02	0.26
Stony Clove at Chichester (01362370)	0.61	-0.28	0.35
Beaver Kill at Mt Tremper (01362487)	0.81	-0.72	0.56
Little Beaver Kill (01362497)	0.55	-0.56	0.55
Esopus Creek (01362500)	0.67	-0.93	0.27

Turbidity exceedance percentage is the percent of time a certain turbidity is equaled or exceeded. For example,  $T_1$  is the turbidity that is equaled or exceeded 1 percent of the time.  $T_1$  would generally be associated with high streamflows and  $T_{50}$  with moderate to low streamflows. The monitoring stations grouped in a similar manner to the streamflow-turbidity relation groupings, except for Esopus at Coldbrook which was more similar to the higher producing stations. The monitoring sites with the greatest turbidity at  $T_1$  were Woodland Creek and Stony Clove at Chichester. They were also the stations with the greatest turbidity at  $T_{50}$ , along with Birch Creek, Broadstreet Hollow Brook and Esopus Creek at Coldbrook.

These results are similar to the earlier monitoring research conducted by USGS and DEP between 2009-2014 (McHale & Siemion, 2014; Siemion et al., 2016). There are significant differences worth noting however that are detected by this research monitoring data. Previously, Stony Clove Creek had, by far, the highest turbidity-streamflow relationship in the UEC watershed followed by Woodland Creek. Stony Clove Creek during water years 2017-2021 had substantially lower daily mean turbidity values for a given range of daily mean streamflow, relative to three other sub-basins, and four if Beaver Kill is included for higher flows. Published (Wang et al., 2021) and pending published research by USGS and DEP demonstrates that much of this shift is due to successful application of STRPs on strategically disconnecting the stream channel from erosional contact with glacial legacy sediment. This is tempered by the fact that these are regressions for the full record so the impacts of the geomorphically disruptive flood in December 2020 on Stony Clove Creek turbidity-streamflow is diminished by more than four years of pre-flood data.

Table 4.8 Turbidity exceedance values for Esopus Creek mainstem and sub-basin tributary monitoring stations for water years 2017 through 2021 [T<sub>1</sub>, turbidity exceeded 1% of the time; T<sub>5</sub>, turbidity exceeded 5% of the time; T<sub>10</sub>, turbidity exceeded 10% of the time; T<sub>25</sub>, turbidity exceeded 25% of the time; T<sub>50</sub>, turbidity exceeded 50% of the time]. Source: USGS

Stream (USGS Station ID)	T <sub>1</sub>	T <sub>5</sub>	T <sub>10</sub>	T <sub>25</sub>	T <sub>50</sub>
Esopus Creek below Lost Clove near Big Indian (0136219503)	45.6	11.7	6.90	2.80	1.50
Birch Creek at Big Indian (013621955)	110	39.1	21.6	10.1	5.60
Bushnellsville Creek (0136219702)	69.4	14.2	7.10	2.80	1.60
Esopus Creek at Allaben (01362200)	84.5	25.5	15.3	6.90	4.10
Broadstreet Hollow Brook (01362232)	119	42.3	23.6	11.8	6.80
Woodland Creek at Phoenicia (0136230002)	156	62.3	32.2	13.8	5.60
Stony Clove at Chichester (01362370)	133	48.8	24.0	8.70	4.50
Beaver Kill at Mt Tremper (01362487)	115	36.2	16.7	5.00	2.00
Little Beaver Kill (01362497)	23.9	5.80	3.60	2.20	1.40
Esopus Creek (01362500)	113	33.7	21.0	10.3	5.90

### 4.3.2 Stony Clove Sub-basin Results

The daily mean streamflow-daily mean turbidity relations for the Stony Clove sub-basin stations up to the December 2020 flood are shown in Figure 4.5. Daily mean turbidity is used in place of daily mean SSC because SSC was not available for all monitoring stations for the complete time period. Turbidity per unit streamflow was greater at the Ox Clove monitoring station than at the other Stony Clove Creek sub-basin monitoring stations. The Stony Clove Creek monitoring stations had lower turbidity per unit streamflow than the sub-basin stations in the Stony Clove basin. Warner Creek had lower turbidity and was more similar to the Stony Clove stations at low streamflow but had higher turbidity and was more similar to Ox Clove at higher streamflow. The Hollow Tree Brook station had a small increase in turbidity per unit streamflow prior to the December 2020 flood. The coefficient of determination for the streamflow-turbidity relation at the Hollow Tree Brook station was very low (Table 4.9), suggesting the relation should be interpreted with caution.

The daily mean streamflow-daily mean turbidity relations for most Stony Clove sub-basin stations increased after the December 2020 flood (Figure 4.6). The relations for Ox Clove and Hollow Tree Brook increased by an order of magnitude through the range in streamflow. Small changes were observed for Stony Clove Creek at Jansen Road and increases at Stony Clove Creek at Chichester were most pronounced at higher streamflow. The relation for Warner Creek decreased at higher streamflow.

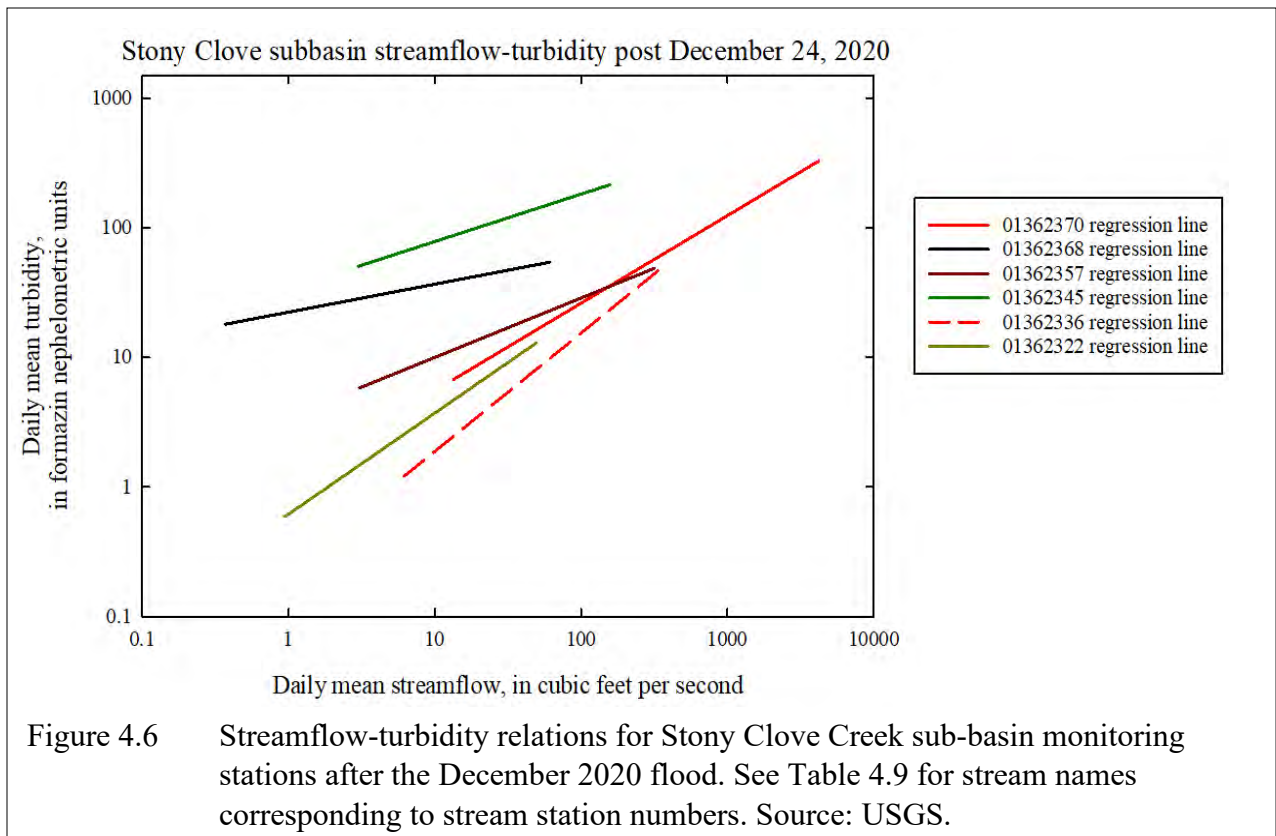
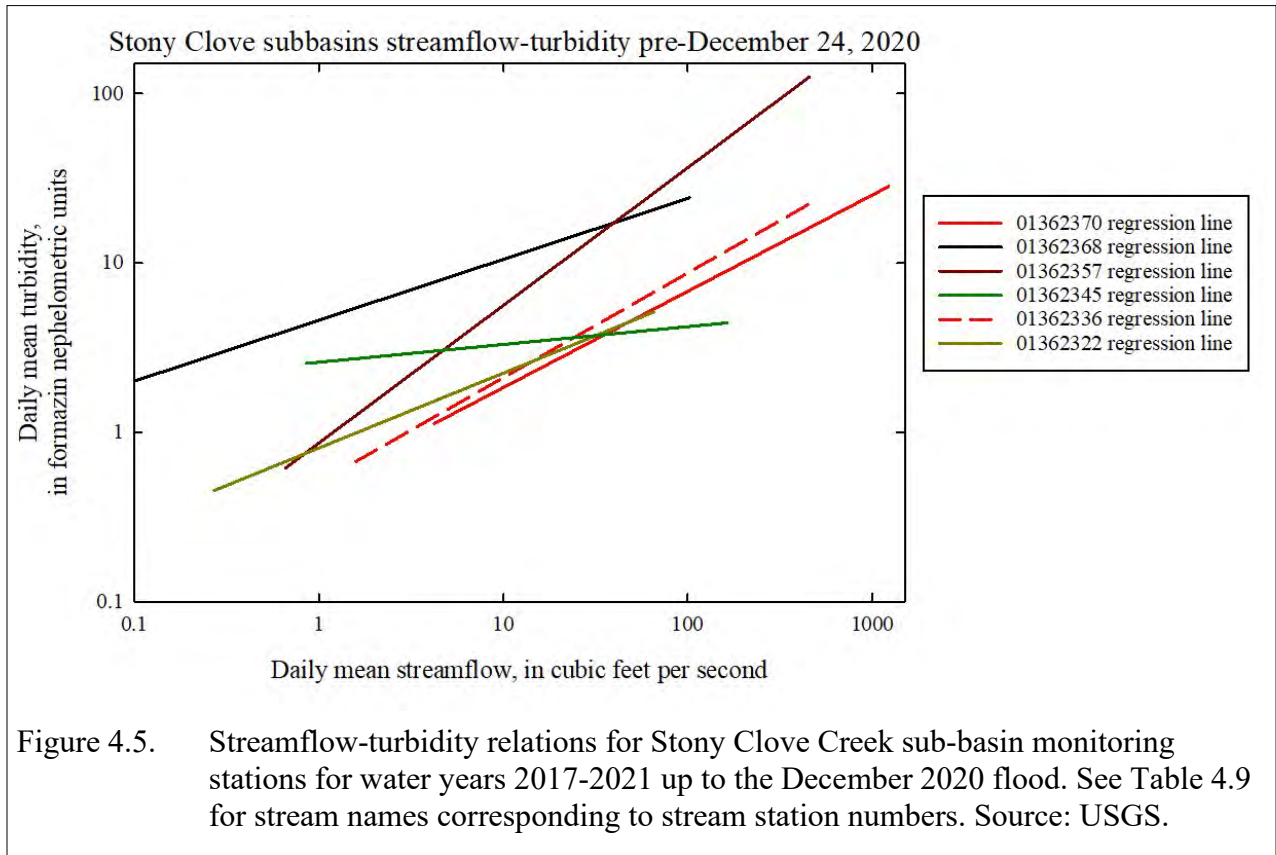
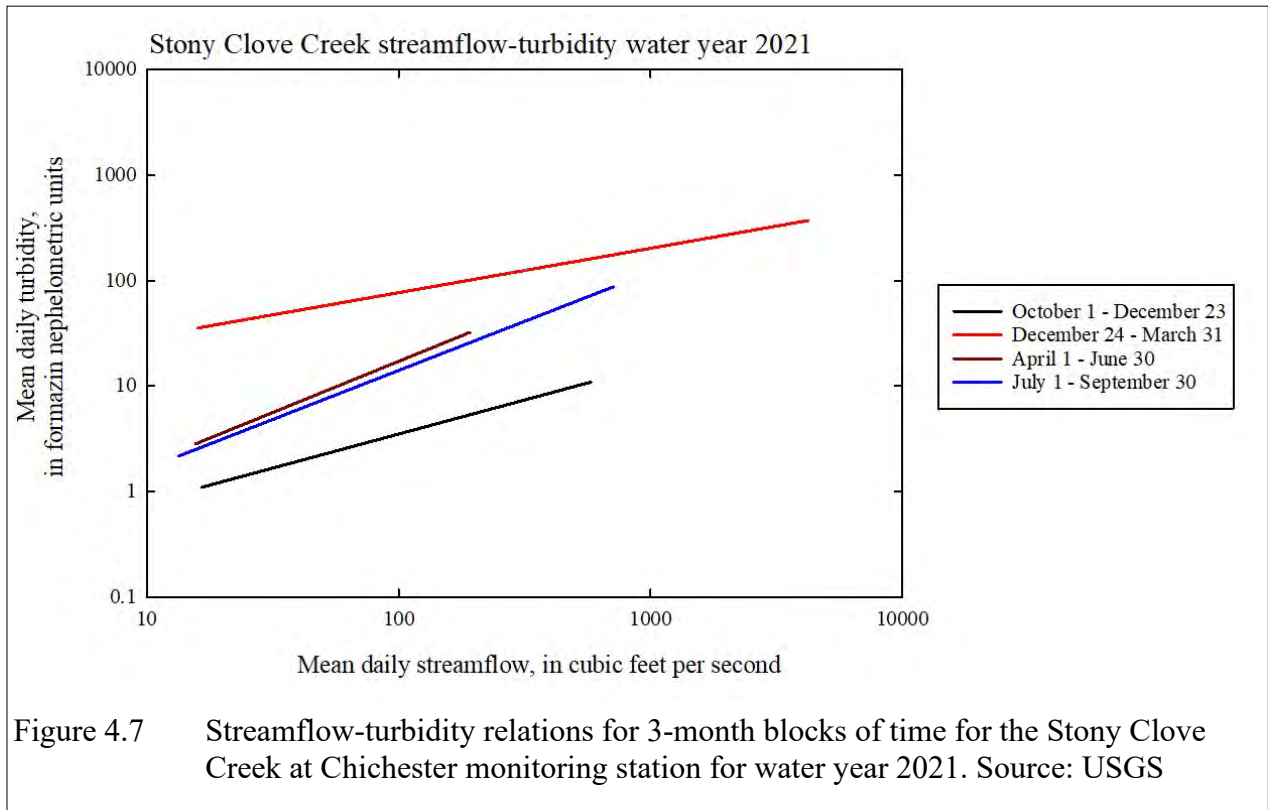


Table 4.9 Summary information (in log form) for daily mean streamflow-daily mean turbidity regression equations pre- and post-December 25, 2020 flood shown in Figures 4.5 and 4.6. Source: USGS

Stream	USGS Station ID	Pre-December 25, 2020 flood			Post-December 25, 2020 flood		
		Slope	Intercept	Coefficient of determination	Slope	Intercept	Coefficient of determination
Myrtle Brook	01362322	0.44	-0.09	0.35	0.78	-0.2	0.40
Stony Clove Creek (upper)	01362336	0.62	-0.30	0.45	0.91	-0.64	0.41
Hollow Tree Brook	01362345	0.11	0.41	0.04	0.37	1.53	0.07
Warner Creek	01362357	0.81	-0.06	0.64	0.46	0.54	0.17
Ox Clove Creek	01362368	0.36	0.66	0.44	0.22	1.35	0.08
Stony Clove Creek (lower)	01362370	0.57	-0.30	0.50	0.67	0.07	0.24



The daily mean streamflow-daily mean turbidity relation for the Stony Clove at Chichester monitoring station increased by an order of magnitude through the range in streamflow for three months after the December 2020 flood (red line) compared to the three months prior to the flood (black line; Figure 4.7). The increase diminished after approximately three months, especially at lower streamflow, but had not returned to pre-storm levels by September 30, 2021.

### Reach Monitoring Results

Table 4.10 presents the turbidity exceedance results for the 14 secondary and six primary monitoring stations in the Stony Clove sub-basin. Stony Clove Creek at State Route 214 at Phoenicia (#01362398) is the sub-basin outlet monitoring station and had the greatest turbidity at the 1% exceedance. Warner Creek had the greatest turbidity at 50% exceedance (Table 4.10), excluding monitoring station 01362352 which was only in operation for a short time. Upstream, Hollow Tree Brook (#01362342) had the lowest 1% exceedance turbidity. Downstream, Hollow Tree Brook (#01362345) had more than an order of magnitude increase in turbidity through the range in turbidity exceedance levels after the December 2020 flood. A substantial increase in turbidity through the range in turbidity exceedance levels at both upstream (#01362365) and downstream (#01362368) Ox Clove stations was measured after the December 2020 flood. These results suggest significant increases in erosional sediment connectivity with turbidity source sediment.

Table 4.10 Turbidity exceedance values for Stony Clove Creek mainstem and sub-basin tributary monitoring stations for water years 2017-2021 [T<sub>1</sub>, turbidity exceeded 1% of the time; T<sub>5</sub>, turbidity exceeded 5% of the time; T<sub>10</sub>, turbidity exceeded 10% of the time; T<sub>25</sub>, turbidity exceeded 25% of the time; T<sub>50</sub>, turbidity exceeded 50% of the time]. Note Hollow Tree Brook and Ox Clove Creek stations have multiple entries based on equipment changes either before or after the December 2020 flood. Source: USGS

USGS Station ID	T <sub>1</sub>	T <sub>5</sub>	T <sub>10</sub>	T <sub>25</sub>	T <sub>50</sub>
Stony Clove Creek stations (upstream to downstream)					
01362312	6.3	1.6	1.0	0.5	0.3
01362330	26.2	5.6	3.3	1.9	1.2
01362332	24.8	7.5	5.3	3.4	2.2
01362336	57.1	16.6	9.4	4.3	2.8
01362347	82.1	25.5	15.2	6.7	3.7
01362349	63.6	20.2	10.9	5.0	3.3
01362350	136	45.3	23.9	9.1	5.0

01362352	193	51.6	29.3	13.6	7.2
01362359	90.1	33.7	20.7	8.8	4.5
01362370	133	48.8	24.0	8.70	4.50
01362398	146	50.7	28.0	9.3	4.7
Warner Creek stations (upstream to downstream)					
0136235575	27.3	10.8	5.5	3.3	1.4
0136235580	54.6	21.3	12.5	6.2	3.7
0136235585	77.4	41.6	25.1	7.9	4.1
01362356	87.0	41.2	26.6	11.6	5.6
01362357	89.4	44.4	30.7	15.6	7.1
Hollow Tree Brook stations (upstream to downstream)					
01362342	4.6	1.9	1.7	1.3	1.0
01362342	4.4	1.6	1.4	1.3	0.7
01362342	8.1	2.2	1.5	0.6	0.3
01362345	20.4	8.6	6.0	4.1	2.9
01362345	35.0	20.0	17.1	12.6	8.0
01362345	666	389	307	185	67.5
Myrtle Brook station					
01362322	17.5	4.5	3.0	2.2	1.5
Ox Clove Creek stations (upstream to downstream)					
01362365	18.7	5.6	4.2	3.1	2.3
01362365	257	139	90.2	60.2	17.5
01362368	70.4	23.3	16.9	9.5	6.2
01362368	253	113	88.1	59.1	23.8

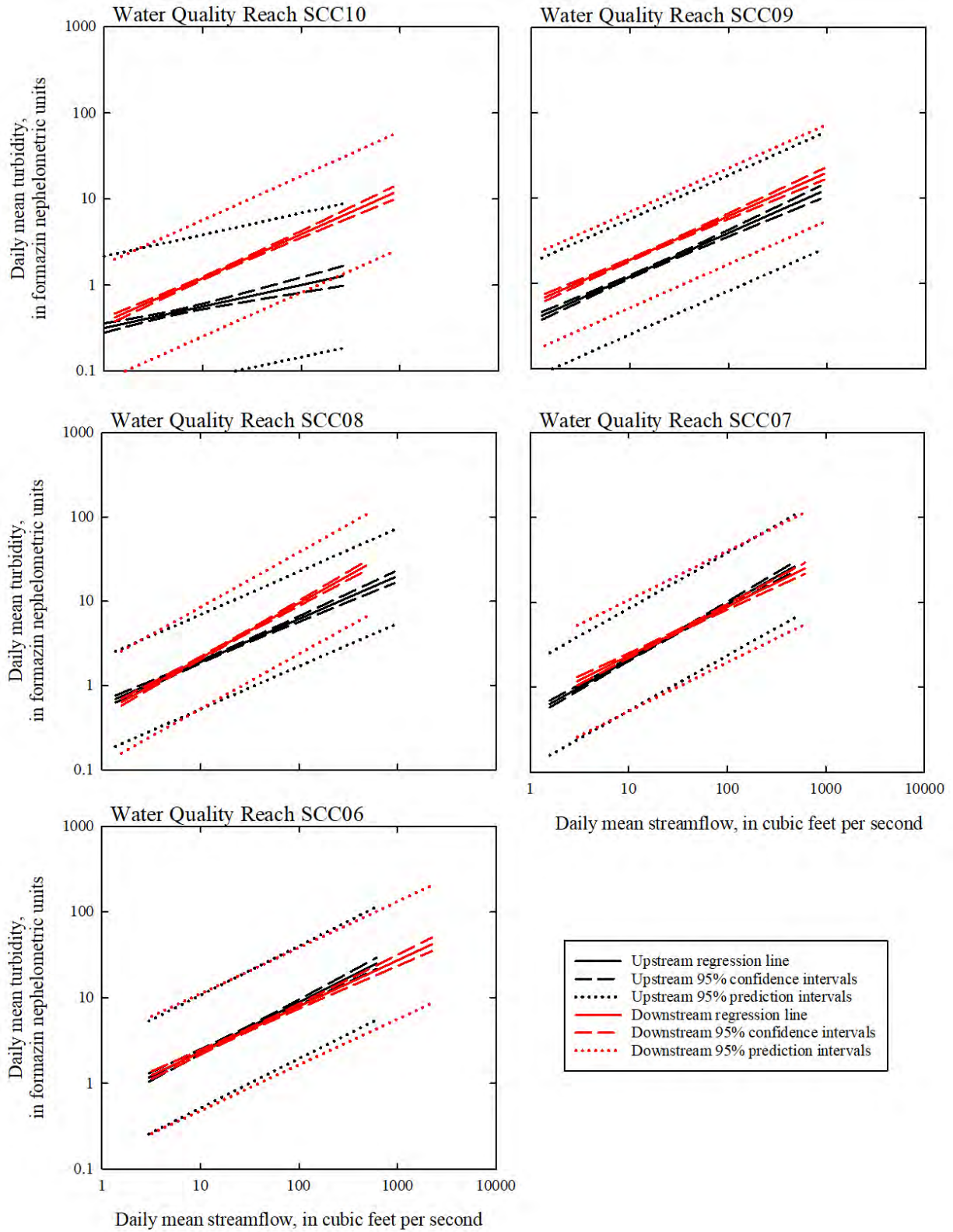
Figure 4.8 (which spans multiple pages) and Table 4.11 present the reach scale monitoring results through September 30, 2021. Daily mean turbidity at the Stony Clove Creek reach scale monitoring stations generally increased in a downstream direction from monitoring station #01362312 to #01362350 (Figure 4.8). The results for #01362350 were likely biased high by the positioning of the monitoring equipment a short distance downstream of a hillslope sediment source. Daily mean turbidity then decreased downstream to #01362359, and then increased again to the most downstream monitoring station #01362398. Turbidity was lowest at the most upstream Stony Clove Creek monitoring station (#01362312). The Stony Clove Creek monitoring stations with the greatest increases in turbidity per increase in streamflow (i.e., slope

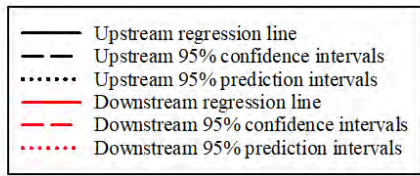
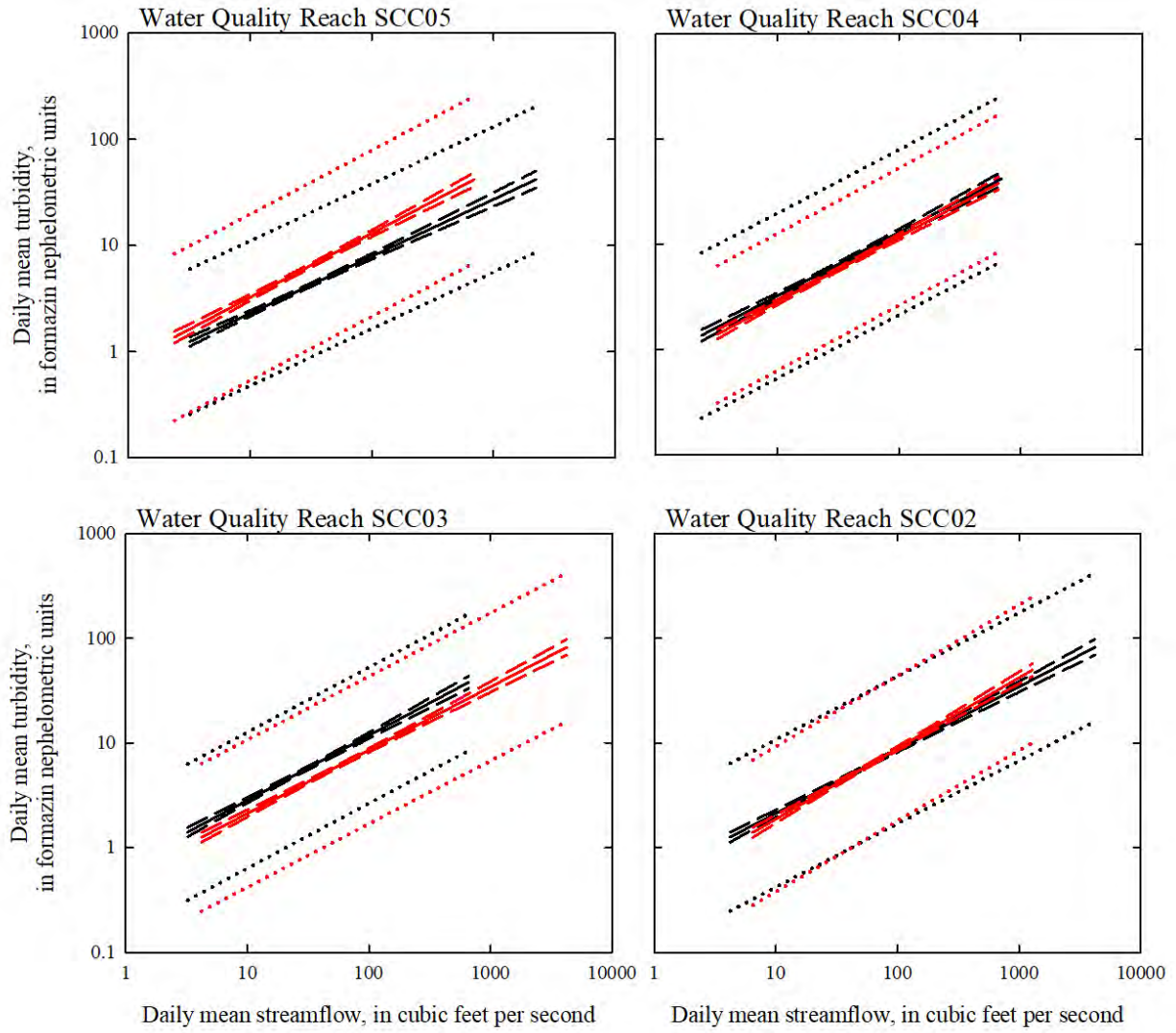
of the streamflow-turbidity regression equation) were #01362336 and #01362398, while the station with the greatest base level turbidity (intercept of the streamflow-turbidity regression equation) was #01362350 (Table 4.11).

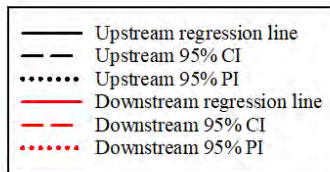
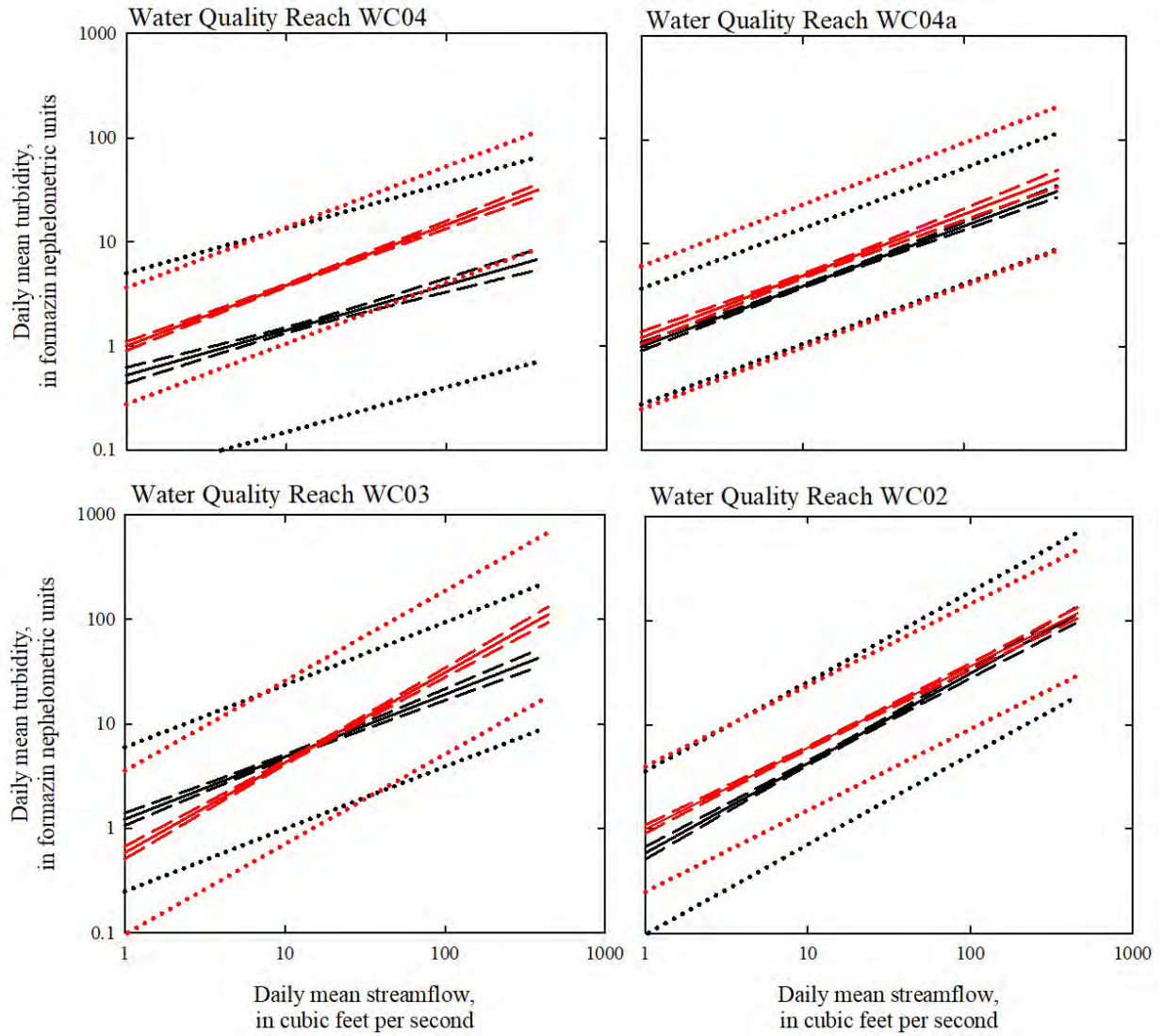
Daily mean turbidity at the Warner Creek reach scale monitoring stations increased in a downstream direction from monitoring station #0136235575 to monitoring station #01362357. Monitoring station #01362356 had the greatest increases in turbidity per increase in streamflow (slope of the streamflow-turbidity regression equation). This station is located downstream of the two BEMS monitoring sites converted to STRPs in 2021. Station #0136235585 had the greatest base level turbidity (greatest streamflow-turbidity regression equation intercept) and is located between the two BEMS/STRP reaches.

The daily mean turbidity records at the Hollow Tree Brook stations were separated into three periods: (1) when a DTS12 turbidity probe was in place at #01362345 (10/1/2016 to 1/31/2020), (2) after changing to an Analite NEP5000 turbidity probe at #01362345, but before the flood of December 2020 (2/2/2020 to 12/23/2020), and (3) after the flood (12/24/2020 to 9/30/2021). Turbidity data during the second monitoring period was excluded to simplify the analysis. There was a small increase in turbidity between monitoring stations # 01362342 and #01362345 prior to the December 2020 flood. The turbidity probe at #01362342 was destroyed during the December 2020 flood and was not replaced until March 17, 2021 due to supply chain issues. The turbidity probe at #01362345 was also destroyed during the December 2020 flood and not replaced until December 30, 2020. Regardless of the differences in turbidity probes and periods when the equipment was damaged, there was a large increase in turbidity caused by the December 2020 flood. There were also substantial increases in turbidity per increase in streamflow (slope of the streamflow-turbidity regression equation) and base level turbidity (intercept of the turbidity-streamflow regression equation), from 0.11 to 0.37 and from 0.42 to 1.53, respectively. The substantial increases in turbidity production in Hollow Tree Brook after the flood originate in the lower section of the valley with a deeply incised channel reach that increased connectivity with LS for at least 600 feet. This reach has been incorporated into the BEMS set of sites.

The daily mean turbidity records at the Ox Clove Creek stations were separated into two periods: (1) before the flood of December 2020 (11/22/2016 to 12/24/2020), and (2) after the flood when station #01362368 was moved 80 feet downstream after being damaged in the flood (1/7/2021 to 9/30/2021). There was an increase in turbidity between monitoring stations #01362365 and #01362368 prior to the December 2020 flood. Turbidity increased by more than an order of magnitude at #01362365 through the range in streamflow after the flood. A lesser, though still four-fold, increase in turbidity was observed at #01362368 through the range in streamflow after the flood. There were substantial increases in turbidity per unit streamflow (slope of the streamflow-turbidity regression line) and base level turbidity (intercept of the streamflow-turbidity regression equation) at #01362365 after the flood. The slope decreased while the intercept increased at #01362368 after the flood. As with Hollow Tree Brook, the increases in turbidity are seemingly attributable to substantial new and enhanced connectivity with LS in the channel.







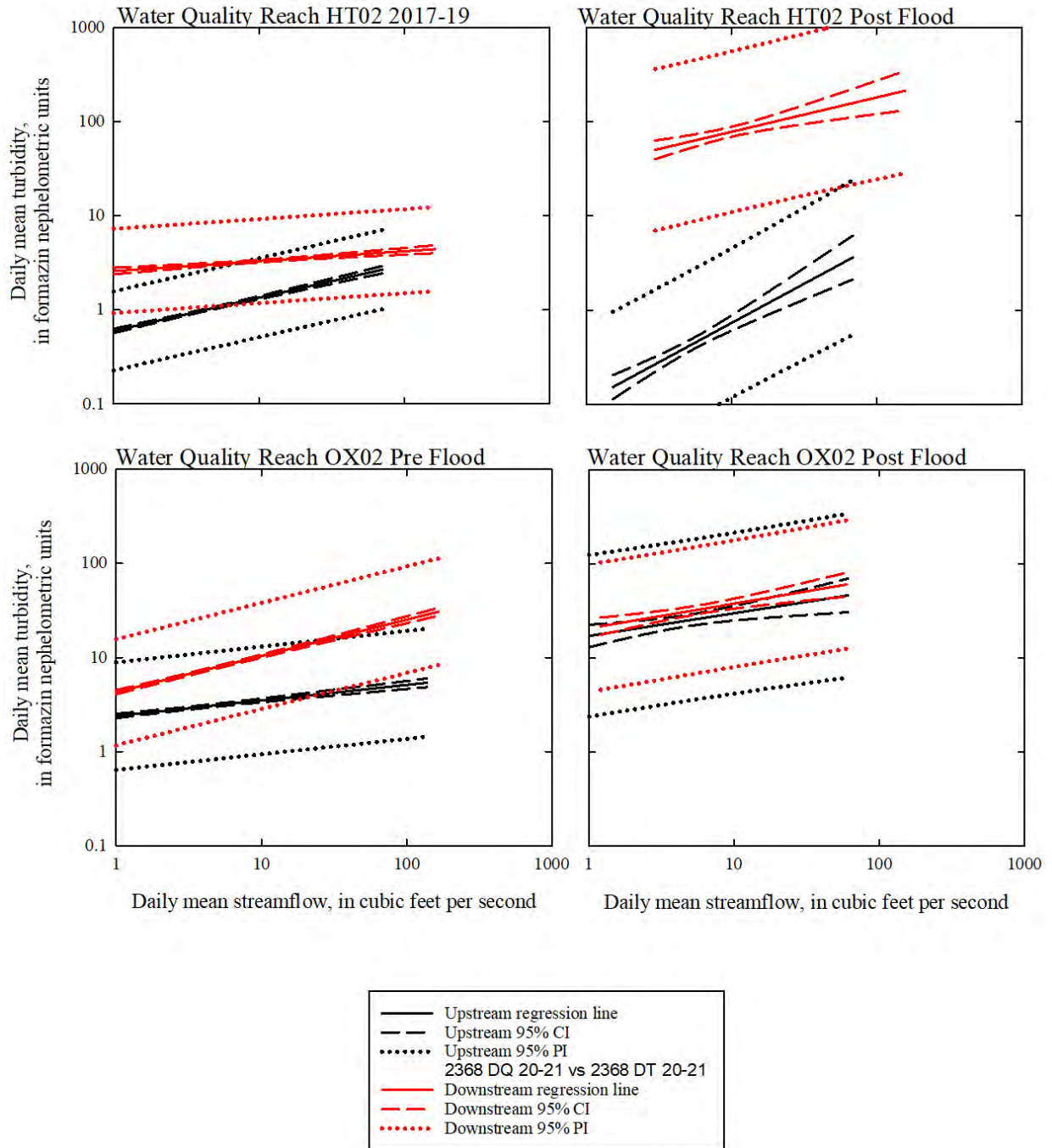


Figure 4.8 Turbidity generally increased through the water quality reaches in Stony Clove basin. Substantial increases were measured after the December 2020 flood in Ox Clove and Hollow Tree Brook. Source: USGS

Table 4.11 Slope and intercept of log transformed daily mean streamflow-daily mean turbidity relation at Stony Clove basin monitoring stations listed in upstream to downstream order for each stream. Hollow Tree Brook and Ox Clove Creek stations have multiple lines to account for changes in monitoring equipment. Source: USGS.

Stream	USGS Station ID	Analysis period	Slope	Intercept
Stony Clove Creek	01362312	10/1/2016 to 9/30/2021	0.28	-0.58
Stony Clove Creek	01362330	10/1/2016 to 9/30/2021	0.51	-0.43
Stony Clove Creek	01362332	10/1/2016 to 9/30/2021	0.51	-0.23
Stony Clove Creek	01362336	10/1/2016 to 9/30/2021	0.66	-0.33
Stony Clove Creek	01362347	10/1/2016 to 9/30/2021	0.58	-0.20
Stony Clove Creek	01362349	10/1/2016 to 9/30/2021	0.54	-0.19
Stony Clove Creek	01362350	10/1/2016 to 3/17/2021	0.60	-0.10
Stony Clove Creek	01362359	10/1/2016 to 9/30/2021	0.62	-0.29
Stony Clove Creek	01362370	10/1/2016 to 9/30/2021	0.61	-0.28
Stony Clove Creek	01362398	10/1/2016 to 9/30/2021	0.67	-0.40
Warner Creek	0136235575	10/1/2016 to 9/30/2021	0.46	-0.30
Warner Creek	0136235580	10/1/2016 to 9/30/2021	0.61	-0.03
Warner Creek	0136235585	12/19/2018 to 9/30/2021	0.60	0.08
Warner Creek	01362356	10/1/2016 to 9/30/2021	0.85	-0.22
Warner Creek	01362357	10/1/2016 to 9/30/2021	0.78	0.00
Hollow Tree Brook	01362342	10/1/2016 to 1/31/2020	0.35	-0.22
Hollow Tree Brook	01362342	2/2/2020 to 12/23/2020	0.70	-0.52
Hollow Tree Brook	01362342	12/24/2020 to 9/30/2021	0.83	-0.97
Hollow Tree Brook	01362345	10/1/2016 to 1/31/2020	0.11	0.42
Hollow Tree Brook	01362345	2/2/2020 to 12/23/2020	na	na
Hollow Tree Brook	01362345	12/24/2020 to 9/30/2021	0.37	1.53
Myrtle Brook	01362322	10/1/2016 to 9/30/2021	0.48	-0.10
Ox Clove Creek	01362365	10/1/2016 to 12/23/2020	0.14	0.34
Ox Clove Creek	01362365	12/24/2020 to 9/30/2021	0.24	1.23
Ox Clove Creek	01362368	10/1/2016 to 12/23/2020	0.37	0.60
Ox Clove Creek	01362368	12/24/2020 to 9/30/2021	0.26	1.31

## 4.4 Suspended Sediment Monitoring

### 4.4.1 UEC Results

Table 4.12 summarizes the point sample SSC for each sub-basin monitoring station for water years 2017 through 2020 and partial water year 2021 data. Minimum SSC measured in point samples ranged from below detection limits (<1) to 2 mg/L. Maximum SSC in point samples ranged from 4,280 to 9,570 mg/L and were measured during the December 25, 2020 flood event. The highest median values were measured at Beaver Kill, Woodland Creek, and Birch Creek. It is important to note that the point samples may not be representative of the true cross-section concentrations. However, most point samples are collected during moderate to high streamflow conditions when the streams are considered to be well-mixed and cross-section adjustments to concentrations minimized.

Table 4.12 Summary of SSC in point samples for each sub-basin monitoring station for the period October 1, 2016 through September 30, 2021. Source: USGS.

Station Name	USGS Station ID	Number of Samples	Minimum (mg/L)	Median (mg/L)	Maximum (mg/L)
Esopus Cr blw Lost Clove @ Big Indian	0136219503	132	<1	54	4,680
Birch Cr @ Big Indian	013621955	142	1	107	4,280
Esopus Cr @ Allaben	01362200	138	<1	69	9,570
Woodland Cr abv mouth @ Phoenicia	0136230002	137	<1	128	7,340
Stony Clove Cr blw Ox Clove @ Chichester	01362370	127	2	80	6,990
Beaver Kill @ Mt Tremper	01362487	145	<1	178	5,290
Little Beaver Kill at Beechford nr Mt Tremper	01362497	131	1	77	5,320
Esopus Cr at Coldbrook	01362500	126	2	89	9,440

Suspended sediment loads are the product of SSC and streamflow at the monitoring stations. Periods of missing 15-minute SSC data were estimated using linear interpolation during periods of stable sediment transport conditions, using a streamflow-SSC relation during storms, and by linear interpolation between point sample SSC during the December 25, 2020 flood. Thus, any estimated 15-minute SSC resulted in estimated SSL. Beaver Kill consistently had the greatest SS loads of the sub-basins, with the exception of water year 2021 (Table 4.13). Little Beaver Kill had lower SS loads than the other sub-basins. SSL varied between years and amongst the monitoring stations. Of note are the loads at Esopus below Lost Clove at Big Indian. Though this station produced less suspended sediment per unit streamflow than most of the sub-basins and had relatively low concentrations, the greater streamflow resulted in greater loads than at other monitoring stations.

The SSLs during water year 2021 were greatly affected by the December 2020 flood. It is important to consider that the peak streamflow during this flood exceeded the limits of the stage-streamflow ratings at some stations, necessitating an indirect measurement of streamflow. The indirect measurements have a much greater uncertainty (20% or greater) than standard streamflow measurements. It is also important to consider that the concentrations during the flood were estimated using the point samples rather than the turbidity-SSC regression because the range of the turbidity probes was exceeded. This resulted in a high level of uncertainty in the estimates of SSL during the flood. The flood accounted for 62-93% of the annual load in water year 2021 at the sub-basin and mainstem stations. Far more suspended sediment was estimated to have been exported from the watershed during the flood than the previous four years combined. For comparison, the 2021 water year SSL at the Esopus Creek at Coldbrook monitoring station was approximately half that reported for the 2011 water year, which included Hurricane Irene and Tropical Storm Lee. The greatest sub-basin loads during the flood were from Stony Clove Creek. This is not unexpected given the greater recurrence interval streamflows measured in the Stony Clove during the flood. The 2021 water year SSL at the Stony Clove at Chichester monitoring station was approximately five times less than that reported for the 2011 water year (Siemion et al., 2016). SSC, and thus SSL, for Little Beaver Kill are based on the regression equation developed using only point samples because a cross-section correction was not available. Therefore, the SSL are not necessarily representative of the true cross-section.

A previous study estimated that 80% of the SSL to the Ashokan Reservoir was transported during less than 4% of the time (Mukundan et al., 2013). During the first five years of this study, 89% of the SSL at the Esopus at Coldbrook monitoring station was transported in less than 5% of the time. The percentage drops to 67% of the SSL when the December 2020 flood is excluded from the analysis. These results highlight the importance of the highest streamflows in transport of SSL to the Ashokan Reservoir.

Table 4.13 Suspended sediment loads for Esopus Creek mainstem and sub-basin monitoring stations (t, short tons) for water years 2017-2020. Water year 2021 data vary depending on last day of regression equation validation. Source: USGS.

Station Name	USGS Station ID	2017 (t)	2018 (t)	2019 (t)	2020 (t)	2021 <sup>1</sup> (t)	12/25/2020 flood (t)
Esopus Cr blw Lost Clove @ Big Indian	0136219503	555	4,970	2,230	3,440	11,300	9,750
Birch Cr @ Big Indian	013621955	377	1,530	1,450	582	1,970	1,620
Esopus Cr @ Allaben	013622200	1,840	10,400	5,890	4,880	82,700	77,300
Woodland Cr abv mouth @ Phoenicia	0136230002	511	4,660	1,230	1,110	9,740	6,050
Stony Clove Cr blw Ox Clove @ Chichester	01362370	886	5,760	1,260	2,660	47,200	41,200

Beaver Kill @ Mt Tremper	01362487	2,540	10,860	5,000	3,900	22,300	15,300
Little Beaver Kill at Beechford nr Mt Tremper	01362497	179	544	890	617	818	345
Esopus Cr at Coldbrook	01362500	14,300	46,800	18,700	18,200	285,000	255,000

<sup>1</sup>2021 water year data includes provisional, estimated data for the December 2020 flood.

Suspended sediment yield (SSY) represents the SSL per unit drainage area. The SSY results suggest Beaver Kill produced the most sediment per unit drainage area and Little Beaver Kill the least during the first four years of the study, similar to the SSL results (Table 4.14). Also similar, the relative importance of the other sub-basins shifted from year to year. The SSYs during the December 25, 2020 flood were up to seven times greater than the greatest annual SSY during water years 2017-2020 at Esopus Creek at Allaben and Stony Clove Creek at Chichester.

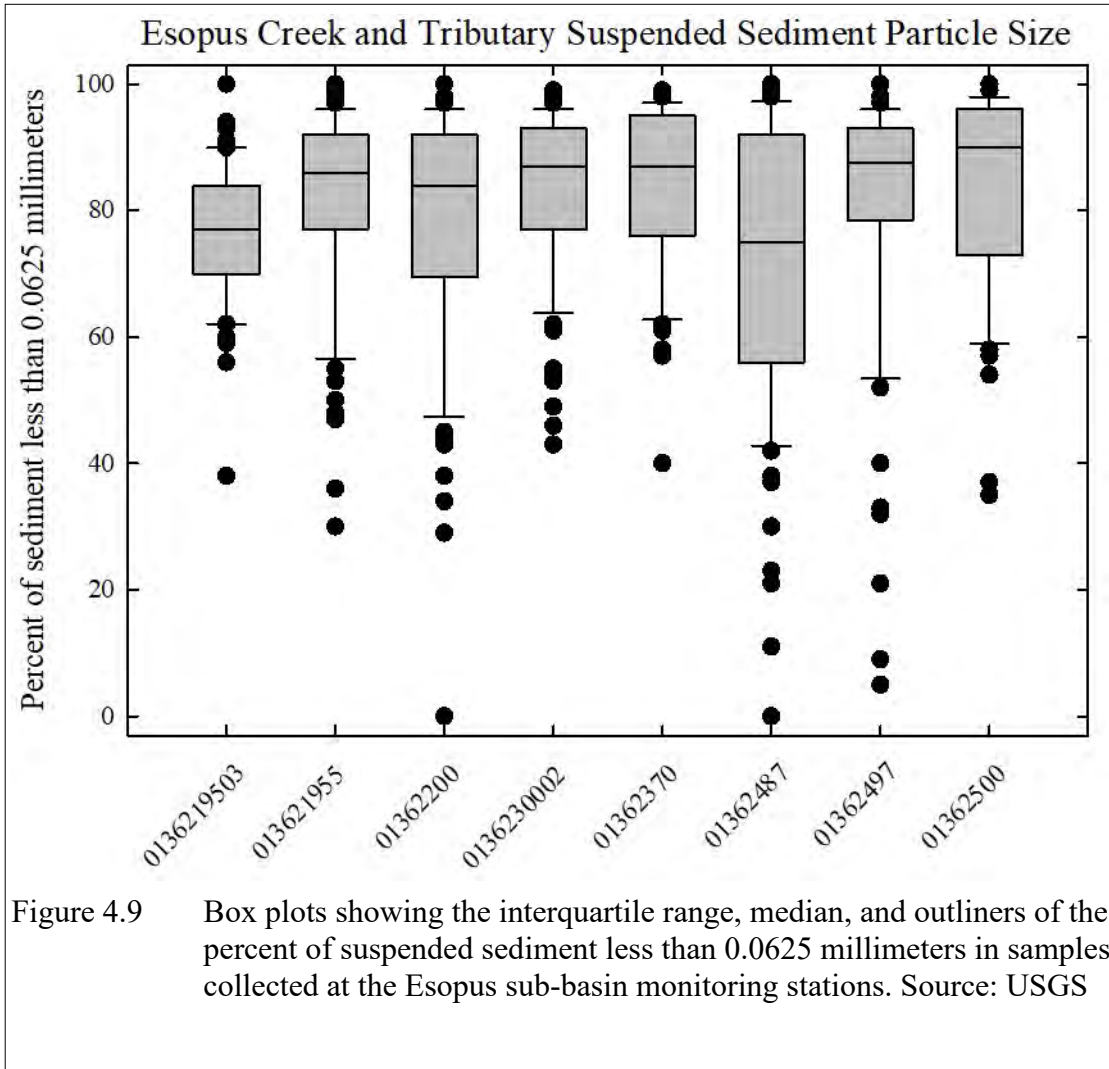
Table 4.14 Suspended sediment yields for Esopus Creek mainstem and sub-basin monitoring stations (t, short tons) for water years 2017-2020. Water year 2021 data vary depending on last day of regression equation validation.

Station Name	USGS Station ID	2017 (t/mi <sup>2</sup> )	2018 (t/mi <sup>2</sup> )	2019 (t/mi <sup>2</sup> )	2020 (t/mi <sup>2</sup> )	2021 <sup>1</sup> (t/mi <sup>2</sup> )	12/25/2020 flood (t/mi <sup>2</sup> )
Esopus Cr blw Lost Clove @ Big Indian	0136219503	18.7	168	75.5	116	380	329
Birch Cr @ Big Indian	013621955	30.1	122	116	46.6	158	130
Esopus Cr @ Allaben	01362200	28.9	164	92.5	76.5	1,300	1,210
Woodland Cr abv mouth @ Phoenicia	0136230002	24.8	226	59.7	54.0	473	294
Stony Clove Cr blw Ox Clove @ Chichester	01362370	28.7	186	40.9	86.0	1,530	1,330
Beaver Kill @ Mt Tremper	01362487	102	434	200	156	891	612
Little Beaver Kill at Beechford nr Mt Tremper	01362497	10.8	33.0	54.0	37.4	49.5	20.9
Esopus Cr at Coldbrook	01362500	74.3	244	97.3	94.7	1,480	1,330

<sup>1</sup>2021 water year data includes provisional, estimated data for the December 2020 flood.

The percent of suspended sediment less than 0.0625 mm (threshold between silt/clay and fine sand particle sizes) was measured for most cross-section samples and for storm samples collected by automated samplers when turbidity exceeded 200 FNU. The Esopus Creek at Allaben and Esopus Creek at Coldbrook had similar interquartile ranges and median particle size (Figure 4.9). Birch Creek, Woodland Creek, Stony Clove Creek at Chichester, and Little Beaver Kill had similar interquartile ranges and median particle size. The interquartile ranges at these

stations were smaller than at Esopus Creek at Allaben and Esopus Creek at Coldbrook. Esopus Creek below Lost Clove and Beaver Kill had median values that were outside the interquartile ranges of the other sub-basins. Beaver Kill also had the largest interquartile range of all the sub-basins. Both streams had a higher percentage of suspended sediment greater than 0.0625 mm. The percent of suspended sediment less than 0.0625 mm generally decreased with increasing streamflow at Esopus Creek at Coldbrook (Figure 4.10) up to approximately 15,000 cfs. The percent of suspended sediment less than 0.0625 mm remained at approximately 55-60% as streamflow increased beyond 15,000 cfs.



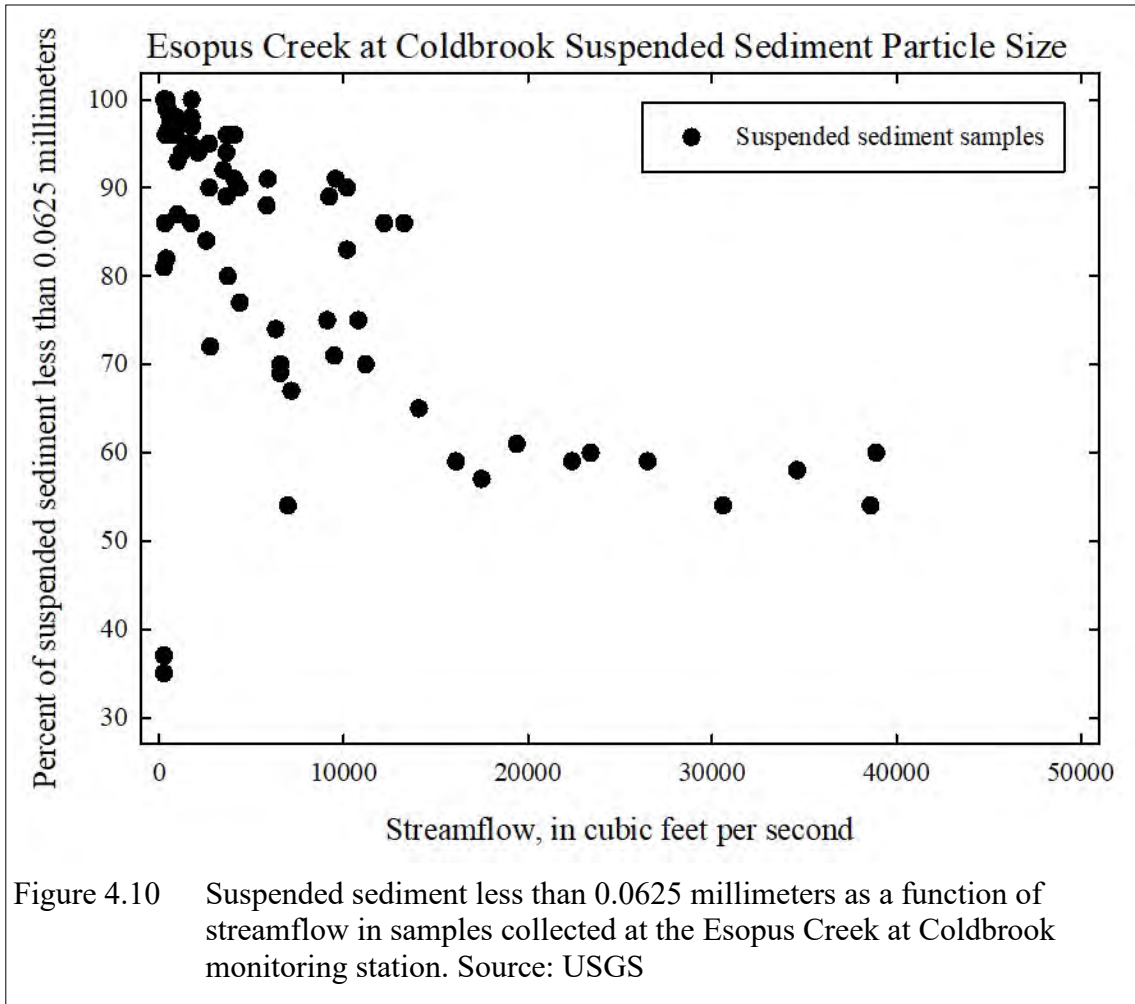


Figure 4.10 Suspended sediment less than 0.0625 millimeters as a function of streamflow in samples collected at the Esopus Creek at Coldbrook monitoring station. Source: USGS

#### 4.4.2 Stony Clove Sub-basin Results

Point sample SSC ranged between below detection limits to 2 mg/L at the Stony Clove Creek sub-basin monitoring stations (Table 4.15). Median SSC was greatest at Stony Clove Creek at Jansen Rd and smallest at Myrtle Brook. The greatest maximum SSC was measured at Hollow Tree Brook while the smallest at Myrtle Brook. Maximum SSC in point samples was measured during the December 2020 flood at all monitoring stations in Stony Clove except for Myrtle Brook and Ox Clove, which were measured on October 29, 2017 and September 23, 2021, respectively. The Myrtle Brook monitoring station was severely damaged during the December 2020 flood and no point samples were collected during the storm as a result. The Ox Clove monitoring station was damaged near the peak of the December 2020 flood and so the maximum SSC may not have been sampled.

Table 4.15 Summary of SSC in point samples for each Stony Clove Creek sub-basin monitoring station. Source: USGS

Station Name	USGS Station ID	Number of Samples	Minimum (mg/L)	Median (mg/L)	Maximum (mg/L)
Myrtle Br @ SR 214 @ Edgewood	01362322	124	<1	16	920
Stony Clove Cr @ Jansen Rd @ Lanesville	01362336	143	<1	100	19,400
Hollow Tree Br @ SR 214 @ Lanesville	01362345	127	1	34	34,700
Warner Cr nr Chichester	01362357	131	<1	72	4,300
Ox Clove nr mouth @ Chichester	01362368	134	1	80	6,620
Stony Clove Cr blw Ox Clove @ Chichester	01362370	127	2	80	6,990

Table 4.16 Suspended sediment loads for Stony Clove Creek sub-basin monitoring stations (t, short tons) for water years 2017-2020. Water year 2021 data vary depending on last day of regression equation validation. Source: USGS

Station Name	USGS Station ID	2017 (t)	2018 (t)	2019 (t)	2020 (t)	2021 <sup>1</sup> (t)	12/25/2020 flood (t)
Myrtle Br @ SR 214 @ Edgewood	01362322	24.8	134	56.5	NA	NA	NA
Stony Clove Cr @ Jansen Rd @ Lanesville	01362336	244	3,040	484	953	11,600	10,100
Hollow Tree Br @ SR 214 @ Lanesville	01362345	31.9	183	99.1	NA	NA	NA
Warner Cr nr Chichester	01362357	273	1,030	569	572	6,030	5,170
Ox Clove nr mouth @ Chichester	01362368	98.7	201	197	146	1,860	1,520
Stony Clove Cr blw Ox Clove @ Chichester	01362370	886	5,760	1,260	2,660	47,200	41,200

<sup>1</sup>2021 water year data includes provisional, estimated data for the December 2020 flood.

Warner Creek was the Stony Clove sub-basin with the greatest SSL each year; the sub-basin with the smallest SSL was Myrtle Brook (Table 4.16). The greatest SSY varied between Ox Clove and Warner Creek (Table 4.17). SSL and SSY were not available for Hollow Tree Brook or Myrtle Brook for water years 2020 and 2021 because new regression equations were required to calculate SSC after the change from DTS-12 to NEP-5000 turbidity probes. Three

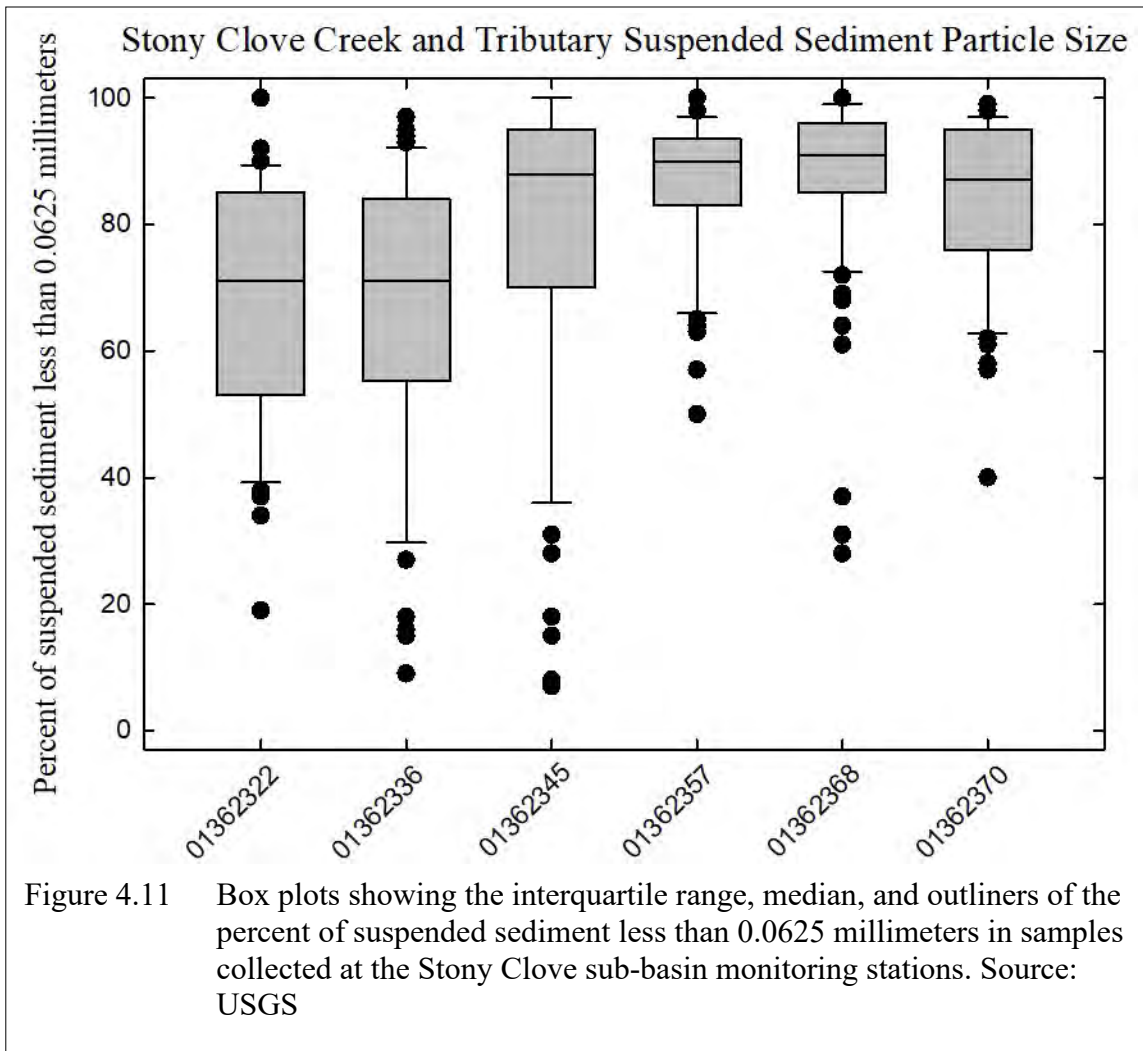
years of data are required before new regression equations can be developed. The Hollow Tree Brook and Myrtle Brook monitoring stations were severely damaged during the December 2020 flood. Thus SSC, SSL and SSY could not be estimated for the flood in the same manner as the other monitoring sites.

Table 4.17 Suspended sediment yields for Stony Clove Creek sub-basin monitoring stations (t, short tons) for water years 2017-2020. Water year 2021 data vary depending on last day of regression equation validation. Source: USGS

Station Name	USGS Station ID	2017 (t/mi <sup>2</sup> )	2018 (t/mi <sup>2</sup> )	2019 (t/mi <sup>2</sup> )	2020 (t/mi <sup>2</sup> )	2021 <sup>1</sup> (t/mi <sup>2</sup> )	12/25/2020 flood (t/mi <sup>2</sup> )
Myrtle Br @ SR 214 @ Edgewood	01362322	13.7	74.0	31.2	NA	NA	NA
Stony Clove Cr @ Jansen Rd @ Lanesville	01362336	26.4	329	52.3	103	1,250	1,090
Hollow Tree Br @ SR 214 @ Lanesville	01362345	6.93	39.7	21.5	NA	NA	NA
Warner Cr nr Chichester	01362357	31.3	118	65.3	65.7	692	594
Ox Clove nr mouth @ Chichester	01362368	25.8	52.4	197	146	486	397
Stony Clove Cr blw Ox Clove @ Chichester	01362370	28.7	186	40.9	86.0	1,530	1,330

<sup>1</sup>2021 water year data includes provisional, estimated data for the December 2020 flood.

The percent of suspended sediment less than 0.0625 mm in samples collected at the Ox Clove and Warner Creek had similar interquartile ranges and median values (Figure 4.11). Stony Clove Creek at Chichester and Hollow Tree Brook had similar median values to Ox Clove and Warner Creek but had larger interquartile ranges. Myrtle Brook and Stony Clove at Jansen Rd both had median values that were outside the interquartile ranges of most of the other stations. There was a greater percentage of suspended sediment larger than 0.0625 mm at both Myrtle Brook (#01362322) and Stony Clove Creek at Jansen Rd (#01362336).



## 4.5 Turbidity and Suspended Sediment Source Characterization

The conceptual framework for this study is founded in the science of geomorphology, specifically employing the concept of connectivity in fluvial geomorphology (Yellen, 2014; Wohl et al., 2019; Cienciala et al., 2020). Connectivity in this context can refer to structural connections between SS/turbidity sources in the fluvial system (e.g., linkages between channels and valley bottom features such as hillslopes, or erosional linkages with different sediment sources and functional connections such as SS flux. The USGS monitoring network measures the functional connectivity in this study. DEP measures and investigates the structural connectivity, primarily in the Stony Clove sub-basin. DEP reviews and uses available non-study SFI connectivity data for the other UEC sub-basins and Esopus Creek as appropriate.

The turbidity and SS flux regime in the UEC watershed is driven by hydrology and hydraulics and sourced by three primary types of fine sediment input: fine sediment stored in streambed alluvium during bed mobilizing streamflows, lateral fine sediment inputs from channel margins and connected terrain, and channel incision into and entrainment of fine sediment in glacial legacy deposits exposed in the streambed (Figure 2.3; Figure 4.12). The study assumes that an important part of the observed variability in turbidity and SS flux and yield in the UEC watershed is associated with spatially variable stream erosional contact with GLS enriched in fine sediment content. The SS source characterization part of the study aims to qualify and quantify these controlling source conditions through use of a range of field and GIS investigations.

The study currently uses multiple methods to investigate the primary SS recruitment source conditions and processes. These methods include (1) baseline and repeat mapping of spatial and temporal erosional connectivity with sediment sources using SFI methods; (2) repeat geomorphic assessment, topographic monitoring, sediment sampling, and hydraulic modeling at select stream erosion sites; (3) geologic sediment source investigation and interpretation (including grain size distribution analysis and sediment fingerprinting techniques); and (4) terrain and process interpretation using remote-sensing data in GIS. During the 10-year study, DEP and USGS (and other researchers) will use these methods to derive and test potential predictive geomorphic metrics to help explain monitored turbidity and SS production and the potential for reduction through STRP implementation. This section is organized to present the limited characterization work in the UEC sub-basins first (4.5.1) and the more extensive characterization in the Stony Clove sub-basin (4.5.2). Prior DEP reports presented the details on several GIS-based investigations (DEP, 2019a; DEP, 2021). Many of those investigations have not been advanced due largely to the December 2020 flood that presented a unique opportunity to re-map erosional connectivity in the Stony Clove sub-basin to test the hypothesis that a flood >10-year RI could produce a system scale geomorphic response in structural and functional sediment connectivity. Therefore, this section primarily reports on the SFI mapping that took place between 2018 and 2021, followed by data analysis in 2022.



Figure 4.12 SS input conditions: (a) stored in streambed alluvium, (b) bank erosion, (c) mass wasting, (d) channel incision.

#### 4.5.1 UEC Watershed Turbidity and SS Source Characterization

DEP's original study design did not include in-depth investigations into UEC watershed source conditions. Source conditions are broadly characterized using previous and ongoing SFI mapping conducted by Greene and Ulster County Soil and Water Conservation Districts and DEP from 2001-2021, along with some remote-sensed data GIS analysis.

## Mapping Sediment Source Distribution

DEP used the SFI methodology to compute erosional sediment connectivity indices. Figure 4.13 depicts the extent of SFI data for the UEC watershed spanning over 20 years covering a period that includes three different data dictionaries (pre-2008, 2008-2018, and 2019 to present), different SFI teams, different levels of QA/QC, and changes in GPS technology. An additional limitation with the pre-2008 data is that the data dictionary did not include a geology field for bank erosion so use of that data requires some interpretation of the available data to deduce the probable SS source geology. Given these quality control issues, DEP used the non-study SFI data to report a simple bank erosion connectivity index ( $EI_{Bnk}$ ) and sediment connectivity indices (SCI) stratified by erosional contact with and without GLS (Table 4.18). The indices are computed as follows:

Bank Length  $EI_{Bnk}$  = bank erosion length/SFI-assessed channel length

Bank Length  $SCI_{AL}$  = bank erosion length without GLS connectivity/bank erosion length

Bank Length  $SCI_{GLS}$  = bank erosion length with GLS connectivity/bank erosion length.

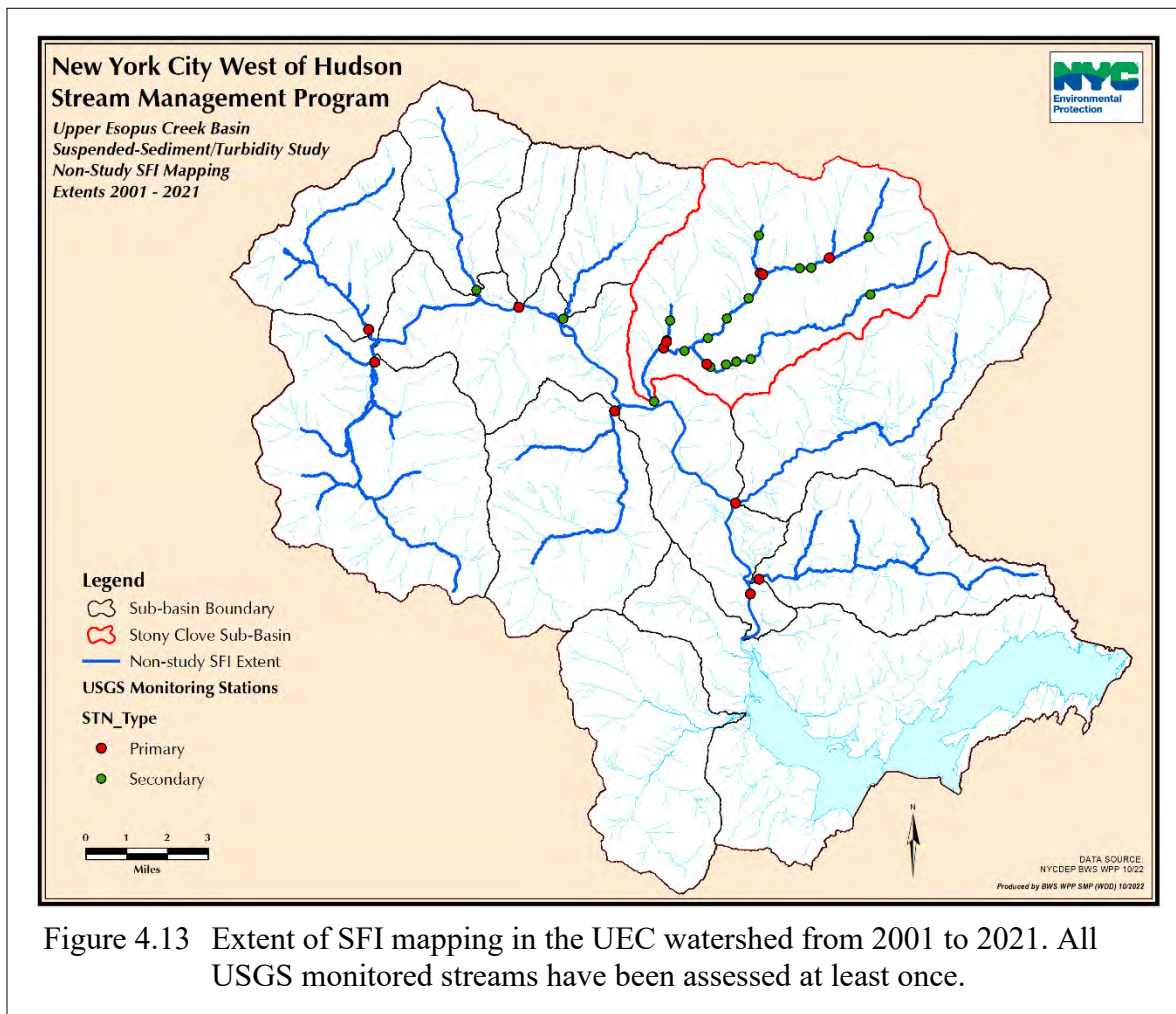


Figure 4.13 Extent of SFI mapping in the UEC watershed from 2001 to 2021. All USGS monitored streams have been assessed at least once.

Table 4.18 UEC watershed and Stony Clove sub-basin non-study SFI stream bank erosional connectivity data (2001-2021). GLS comprises two primary sources: glacial till (GT) and lacustrine sediment (LS).  $SCI_{AL}$  and  $SCI_{GLS}$  are computed by dividing the length of eroding bank with GLS or AL-only connectivity by the total bank erosion length. The dominant GLS source is determined by reviewing the relative lengths of each recorded in the SFI data.

Stream Name	SFI Year	SFI Stream Length (ft)	Bank Erosion Length (ft)	Bank Length $EI_{Bnk}$ (ft/ft)	Bank Length $SCI_{AL}$ (ft/ft)	Bank Length $SCI_{GLS}$ (ft/ft)	GLS Source (1 <sup>st</sup> /2 <sup>nd</sup> )
UEC and Sub-basin SFI Results (2001–2019)							
Esopus Creek (all)	2005-06	144,974	25,003	0.17	0.78	0.22	GT/LS
Esopus Creek: Lost Clove to Bushnellsville Creek	2019	21,019	5,897	0.28	0.79	0.21	LS/GT
Birch Creek	2011	49,662	8,940	0.18	0.91	0.09	LS/GT
Bushnellsville	2013	28,858	8,658	0.30	0.75	0.25	LS/GT
Broadstreet Hollow	2001	17,992	4,678	0.26	0.86	0.14	LS/GT
Beaver Kill	2009	50,338	26,175	0.52	0.71	0.29	GT/LS
Little Beaver Kill	2017	59,307	4,229	0.07	0.85	0.15	GT/LS
Woodland Valley (2015, 2021)							
Woodland Creek	2015	33,099	9,508	0.29	0.66	0.34	GT/LS
Panther Kill	2021	16,140	2,903	0.18	0.53	0.47	LS/GT
Total		49,239	12,411	0.25	0.63	0.37	LS/GT
Esopus Headwaters (2018-2020)							
Esopus Creek upstream of Lost Clove	2019	77,353	15,446	0.20	0.79	0.21	GT/LS
Lost Clove	2018	8,424	2,112	0.25	0.93	0.07	LS/GT
Hatchery Hollow	2018	9,105	4,520	0.50	0.85	0.15	GT/LS
McKenley Hollow	2020	9,215	1,881	0.20	1.00	0.00	None
Elk Bushkill	2020	14,144	4,289	0.30	0.62	0.38	GT/LS
Little Peck Hollow	2020	8,051	1,111	0.14	0.89	0.11	GT
Total		126,292	29,359	0.23	0.80	0.20	GT/LS
Stony Clove Sub-basin SFI Results (2012–2015)							
Stony Clove Creek	2013	54,459	12,129	0.22	0.45	0.55	LS/GT
Ox Clove Creek	2015	6,696	1,161	0.17	0.70	0.30	GT/LS
Warner Creek	2012	16,721	4,266	0.26	0.70	0.30	LS/GT
Hollow Tree Brook	2015	7,684	1,529	0.20	0.89	0.11	GT/LS
Myrtle Brook	2015	4,281	1,070	0.25	1.00	0.00	None
Total		89,841	20,155	0.22	0.58	0.42	LS~GT

All data in Table 4.18, including Stony Clove (2012-2015), is either pre-study data or coincident with the study period but uses a non-study SFI data schema and protocol. Table 4.18 separates sub-basins that had multiple streams assessed to provide individual index values and summed index values for the sub-basins (Woodland Valley, Esopus Headwaters, and Stony Clove). There are other features in this non-study SFI data, such as the “fine sediment” feature which includes bank erosion as well as some bed erosion. However, this SFI feature is used inconsistently through the years and throughout the study area and is therefore not investigated as a potential metric for UEC at this time.

The data presented in Table 4.18 is modified from past reports (DEP, 2019a; DEP, 2021) as described in Section 3.2.3. Recent review of available non-study SFI data attributes resulted in some changes in previously reported feature lengths and noting that some of the geology classification may be open to interpretation. All mapped eroding bank lengths were used whether they were classified as active or dormant. This can result in some streams having potentially erroneously high bank length EI values (e.g., 2009 Beaver Kill with 0.52).

An additional significant limitation of the SFI data for geomorphic metric development is that SFIs are seasonal “snapshots” of channel condition and reflect the occurrence or absence of geomorphic disturbance events such as high magnitude floods and management actions. For example, the conditions mapped in Broadstreet Hollow in 2001 reflect the hydrology and management intervention of the previous years; it is reasonable to assume they do not reflect the current conditions. This is so for all the SFI results prior to the start of the Study in 2016. Given these limitations, DEP is not relying on the broader UEC sub-basin SFI mapping for source attribution in the study, although the data will be considered when interpreting the turbidity and SS flux monitoring.

Keeping the above constraints in mind, the monitored sub-basin streams can be categorized into the following EI categories:

Bank Length  $EI_{Bnk} \geq 0.3$ : Bushnellsville Creek (0.3), Beaver Kill (0.52)

Bank Length  $EI_{Bnk} = 0.2 - 0.29$ : Broadstreet Hollow (0.26), Woodland Valley (0.25), Esopus Headwaters (0.23), Stony Clove Creek (0.22), Esopus Creek between Lost Clove and Bushnellsville Creek (0.28)

Bank Length  $EI_{Bnk} = 0.1 - 0.19$ : Esopus Creek (0.17), Birch Creek (0.18)

Bank Length  $EI_{Bnk} < 0.1$ : Little Beaver Kill (0.07)

The monitored sub-basin streams can also be categorized by SCI *potential* for connectivity with GLS. Stony Clove and Woodland Valley streams tended to have the highest percentage of mapped erosional sediment connectivity with GLS, and Little Beaver Kill had the lowest percentage. This is generally coincident with the monitored turbidity conditions. Beaver Kill and Birch Creek had relatively low mapped erosional sediment connectivity with GLS yet can have high turbidity production during portions of the study period, indicating that turbidity production is not only influenced by magnitude of connectivity but also potentially by other

factors such as distribution of occurrence (e.g., concentration near monitoring station), LS versus GT dominance, and modes of entrainment (bank failure, mass wasting, bed failure).

### Basin Characterization: Mean Basin Slope

Using the online USGS application [StreamStats](#), DEP obtained estimates of mean basin slope (MBS) for each monitored UEC watershed stream, to get a rough estimate of the potential energy influencing runoff hydraulics as represented by MBS (Table 4.19) that can increase potential source connectivity. StreamStats computes MBS by summing lengths of all contours in a basin, multiplying by contour interval and dividing the product by drainage area. The MBS value is for the whole catchment area so it is not equivalent to channel slope, which would be significantly less. Computing mean channel slope for all monitored streams and associated tributaries is planned but not completed within the reporting period.

The UEC sub-basins with the highest MBS (Woodland Creek and Stony Clove Creek) also have the highest total streamflow and runoff, as well as being top turbidity producers. The Little Beaver Kill sub-basin has the lowest MBS, MAR, and turbidity and SS production. Exceptions to this pattern are Beaver Kill and Birch Creek, which both have moderate MBS values. Both streams can exhibit high turbidity and/or SS production, but on average their MAR tends to be moderate with the notable exception of 2018, which was the wettest year in the five-year study period. MBS, and/or mean channel slope when combined with streamflow metrics, is expected to be among the potential multiple variables influencing turbidity production. Future work will include obtaining estimates of mean channel slope for all monitored sub-basins to further explore this for multi-variate analysis.

Table 4.19 MBS for each streamflow monitoring station obtained from USGS StreamStats.

Stream (USGS Station ID)	MBS (ft/ft)
Esopus Creek (0136219503)	0.326
Birch Creek (013621955)	0.256
Esopus Creek (01362200)	0.316
Woodland Creek (0136230002)	0.367
Stony Clove Creek (01362370)	0.379
Beaver Kill (01362487)	0.273
Little Beaver Kill (01362497)	0.195
Esopus Creek (01362500)	0.195

### Channel Planform and Confinement Analyses

DEP paused all remote-sensed data GIS analyses in 2021 to take advantage of measuring and analyzing the changed connectivity conditions attributable to the December 2020 flood. The

one advancement in GIS analysis since 2021 is that DEP completed digitizing 2009 active channel margins (ACMs) using the 1-ft orthoimagery for all monitored UEC and Stony Clove sub-basins (Figure 4.14), and 2016 ACMs using the 2016 0.5-ft orthoimagery for Esopus Creek, Woodland Creek (and tributary streams), Beaver Kill, and Broadstreet Hollow. In early 2022, New York State released 1-ft orthoimagery captured in April 2021. Since this was taken following the December 2020 flood it can be used with the 2016 imagery to provide two time steps within the study period. No channel centerlines or ACMs have been developed using the 2021 imagery. All remote-sensed data investigations have been on hold through 2022 to advance the higher priority Stony Clove sub-basin SFI investigations.

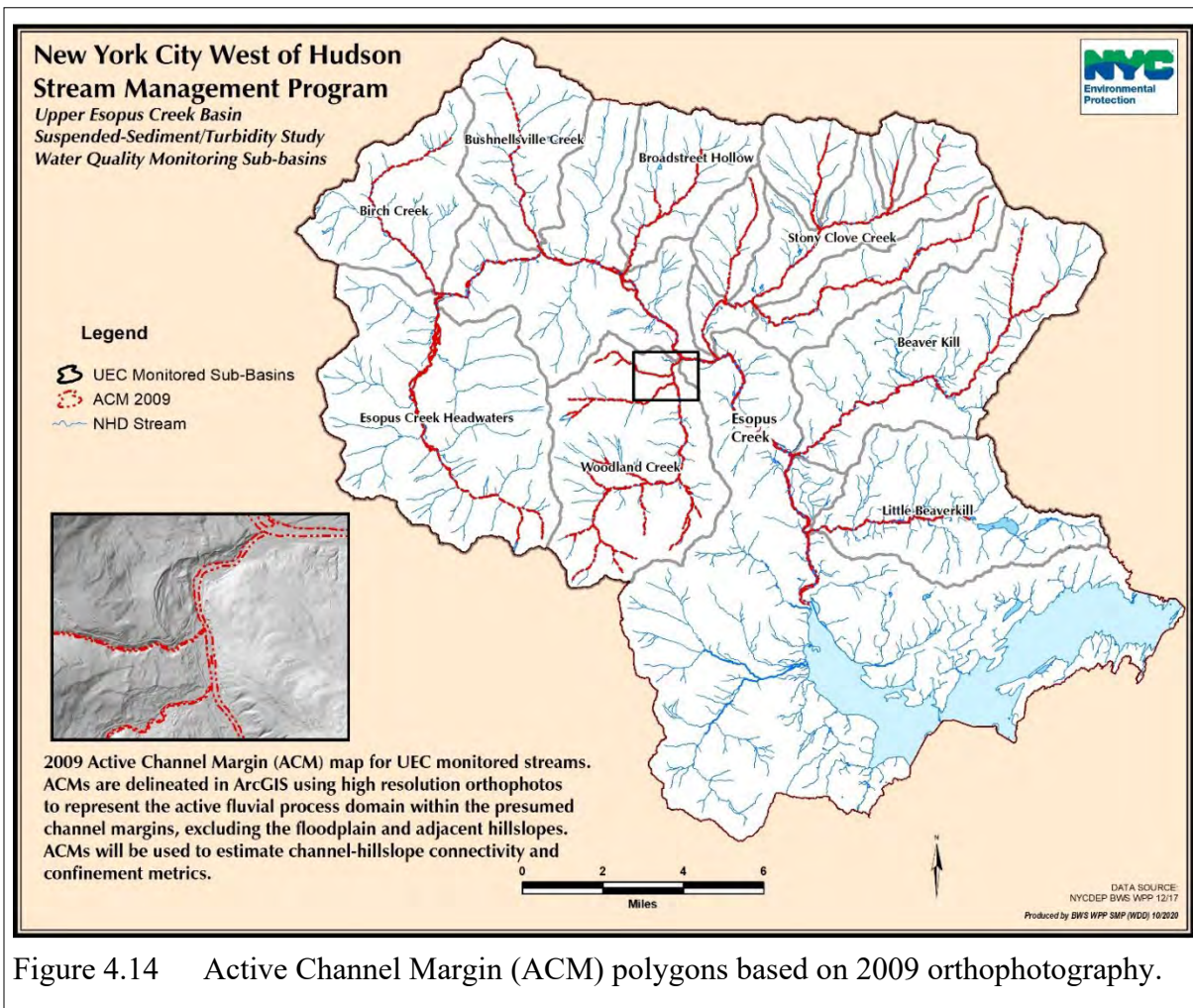


Figure 4.14 Active Channel Margin (ACM) polygons based on 2009 orthophotography.

#### 4.5.2 Stony Clove Sub-basin Turbidity and SS Source Characterization

The Stony Clove sub-basin serves as the experimental research area to investigate SS source conditions through intensive SFI mapping, reach-scale channel morphologic monitoring and hydraulic modeling, sediment source sampling investigations, and remote-sensed data

analysis. The primary focus in this section is demonstrating the value of SFI mapping to help explain the measured turbidity and sediment flux. Thus far, this method has provided the most substantive contribution to help explain the source conditions influencing turbidity production in the Stony Clove sub-basin. The report presents representative results for considering the roles of channel margin geology in turbidity production. DEP is still in the early stages of analyzing these results, with plans to examine the roles of channel and valley confinement observed in the field, along with other attributes collected for each erosional connectivity feature. The data exists for investigating several attributes, as needed to meet the study objective. DEP is also working to make this data available to university researchers to expand its utility.

The study also includes measuring and monitoring reach scale stream morphology at representative sites of high erosional sediment connectivity with GLS that can measurably contribute to turbidity and suspended sediment flux – the BEMS sites. This work is performed under a DEP contract with SLR Consulting. DEP is currently reviewing a draft six-year summary report submitted by SLR Consulting in October 2022 for the BEMS analysis, which limits the coverage of the BEMS results in this report. Multiple rounds of topographic monitoring using ground-based and UAS-based methods are also not included pending further internal review. However, the latest BEMS sediment sampling results have been reviewed and are presented.

### Mapping Sediment Source Distribution

Stony Clove streams are the most SFI-assessed in the UEC watershed. Stony Clove Creek was first mapped in 2002 by DEP and Greene County Soil and Water Conservation District as part of the Stony Clove Stream Management Plan process. It was subsequently remapped by the AWSMP in 2013. DEP collaborated with SUNY New Paltz from 2010-2012 to map all of Warner Creek in 2010 and the lower 2.5 miles in 2011 and 2012. In 2015, DEP hired an engineering firm to complete rapid SFI mapping of portions of the primary Stony Clove tributary streams: Ox Clove Creek, Warner Creek, Hollow Tree Brook, and Myrtle Brook. While these SFI data sets are not used to generate study metrics, they were very useful in scoping the extents of study mapping for each stream and selecting BEMS sites.

For this study, the first SFI covered 44,449 feet on Stony Clove Creek in 2018 from the headwater reaches to Esopus Creek. By the end of 2020, DEP supervised SFI mapping for 13,987 feet of Warner Creek, 6,696 feet for Ox Clove Creek, and 4,280 feet for Myrtle Brook (Table 4.21). Hollow Tree Brook was not mapped prior to 2021, due to the pandemic and limited landowner access permission. In April 2021, DEP initiated SFI mapping to repeat map as much Stony Clove sub-basin erosional connectivity as feasible following the December 2020 flood to measure change in the primary geomorphic metrics used in this study – bank and bed erosional connectivity indices. The field mapping continued through early November 2021 without any geomorphically significant streamflow to modify the erosional connectivity that could be attributed to the December 2020 flood. The final effort accounted for 86% of previously mapped channel, plus a 2,165-foot section of Hollow Tree Brook with extensive erosional sediment connectivity with LS.

The December 2020 flood breached stabilizing geomorphic thresholds along the channels and forced geomorphic adjustment and increased SS flux throughout the Stony Clove sub-basin. Since flood magnitude was at or above the study assumed hydrogeomorphic threshold that would force big changes in stability and water quality in the study area, it presented an opportunity to evaluate the conceptual model assumptions and utility for explaining turbidity production.

DEP’s previous FAD status reports covered the comparison of the Stony Clove Creek 2018 SFI data with the SFI conducted by the AWSMP in 2013, demonstrating that there was a measured geomorphic recovery response through the years following the disruptive hydrology of 2010-2011 (DEP, 2021; Wang et al., 2021). The initial state (2013) for the comparison represented a very destabilized stream system with high turbidity production. By 2018, Stony Clove Creek was demonstrably stabilizing. The 2012-2016 STRPs also effectively disconnected most of the biggest turbidity producing reaches from source sediment in Stony Clove Creek and Warner Creek and significantly increased the erosion resistant threshold in those reaches. As presented in past reports and covered in Section 4.6, turbidity and SS production diminished markedly following STRP implementation.

Table 4.21 Stony Clove sub-basin study SFI periods and associated reach lengths

Stream	Pre-Flood Year	Pre-Flood Length (ft)	% Total Stream	Post-Flood Year	Post-Flood Length (ft)	% Total Stream	Comparison Length (ft)
Stony Clove Creek	2018	44,449	82	2021	34,934	64%	34,934
Ox Clove Creek	2019, 2020	6,696	35%	2021	6,696	35%	6,696
Warner Creek	2019	13,987	28%	2021	13,987	28%	13,987
Hollow Tree Brook	-	-	0%	2021	2,165	14%	-
Myrtle Brook	2020	4,280	34%	2021	4,280	34%	4280
Totals		69,412			62,062		59,897

Figures 4.15 and 4.16 present results of mapped stream bank erosional connectivity classified by primary and secondary SS sources for pre- and post-flood conditions. Figures 4.17 and 4.18 depict the pre- and post-flood mapping results of stream bed connectivity classified by GLS source. The mapped results demonstrate the impact of the December 2020 flood on increasing the amount of bank and bed erosional connectivity in the mapped Stony Clove streams and significantly increasing connectivity with GLS. Figure 4.16 shows that the 2021 effort was not able to cover most of Stony Clove Creek’s downstream of Ox Clove Creek to the confluence with Esopus Creek and a segment of the upper reaches mapped in 2018. A proximal bankfull flow event in late fall 2021 precluded further mapping to make sure mapped features were associated with the December 2020 flood.

In the maps, SS stream bank sources are stratified by primary and secondary geologic units exposed in an eroding bank. If a mapped length of stream bank included at least 25% of the bank height as a GLS unit, then it was classified as the primary SS source. If the bank contained a GLS unit, but the content was less than 25% of the bank height it was classified as a secondary source and AL was classified as the primary SS source. In all instances, the GLS unit was stratigraphically beneath the AL unit. CL was a less common occurrence and when present was more often a secondary SS source. If there was no GLS present, then the eroding bank length was classified solely as AL – the most frequent occurrence by far in both periods.

The 2021 bank erosion mapping also produced an increased number of primary and secondary SS source configurations. Some of this is due to the fresh exposures being much easier to interpret. An example of this was the creation of a new category, CL-LS, a mass-wasted glacial lacustrine sediment likely from prehistoric mass wasting of glacial lake sediment on mountain slopes following lake dewatering. The CL-LS is predominantly silt and clay, yet has some coarse sediment incorporated during mass wasting, has very deformed relic depositional layers, and tends to be more consolidated than LS. It is most prevalent in Ox Clove Creek (in bank and bed) and in some instances was previously interpreted as GT based on the mixed sediment size. Due to its high fine sediment content and origin, it can be appropriately lumped with LS.

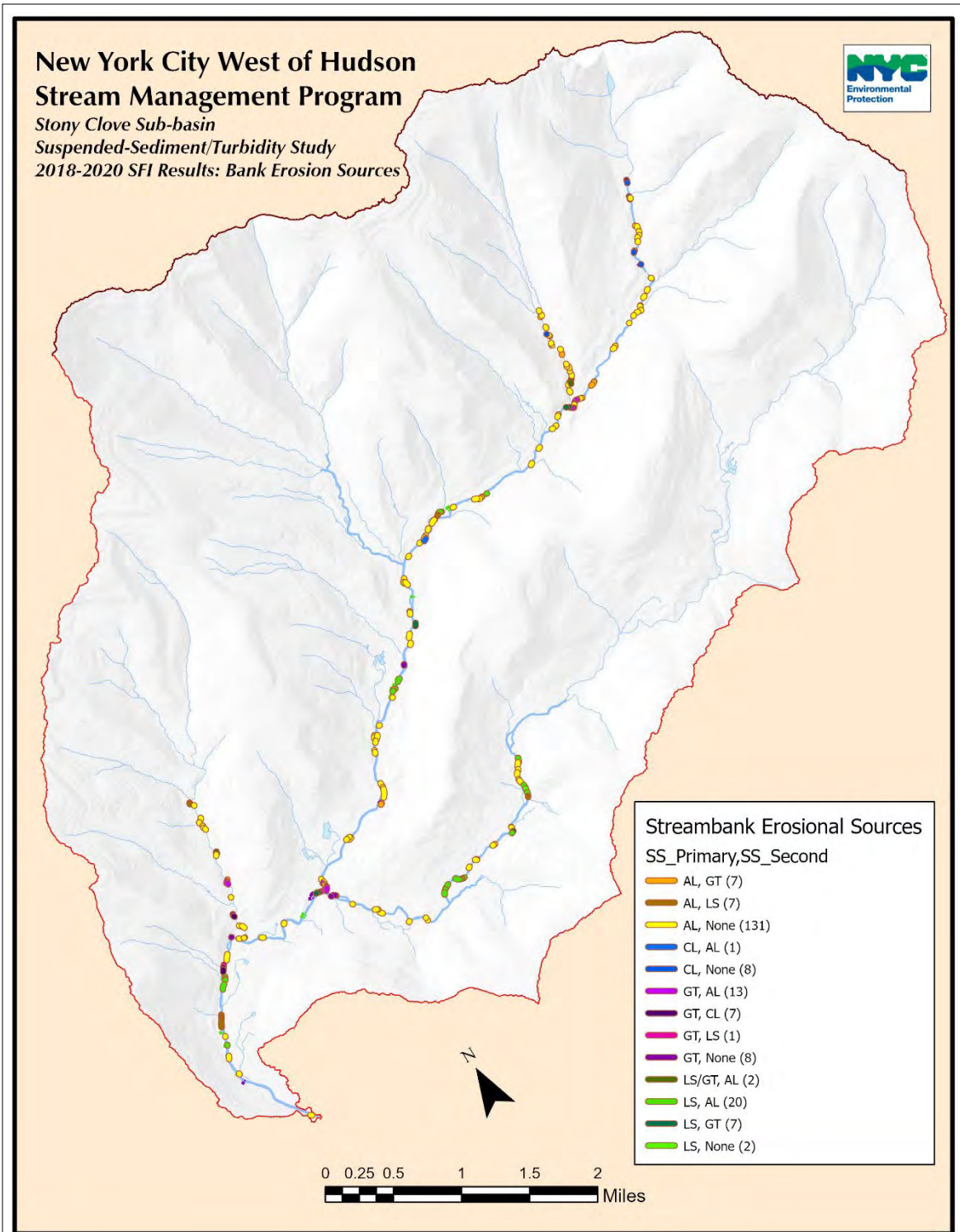


Figure 4.15 2018-2020 SFI mapping results depicting stream bank erosional connectivity with primary and secondary SS source sediment configurations. Mapped active and dormant stream bank erosion are combined in this map.

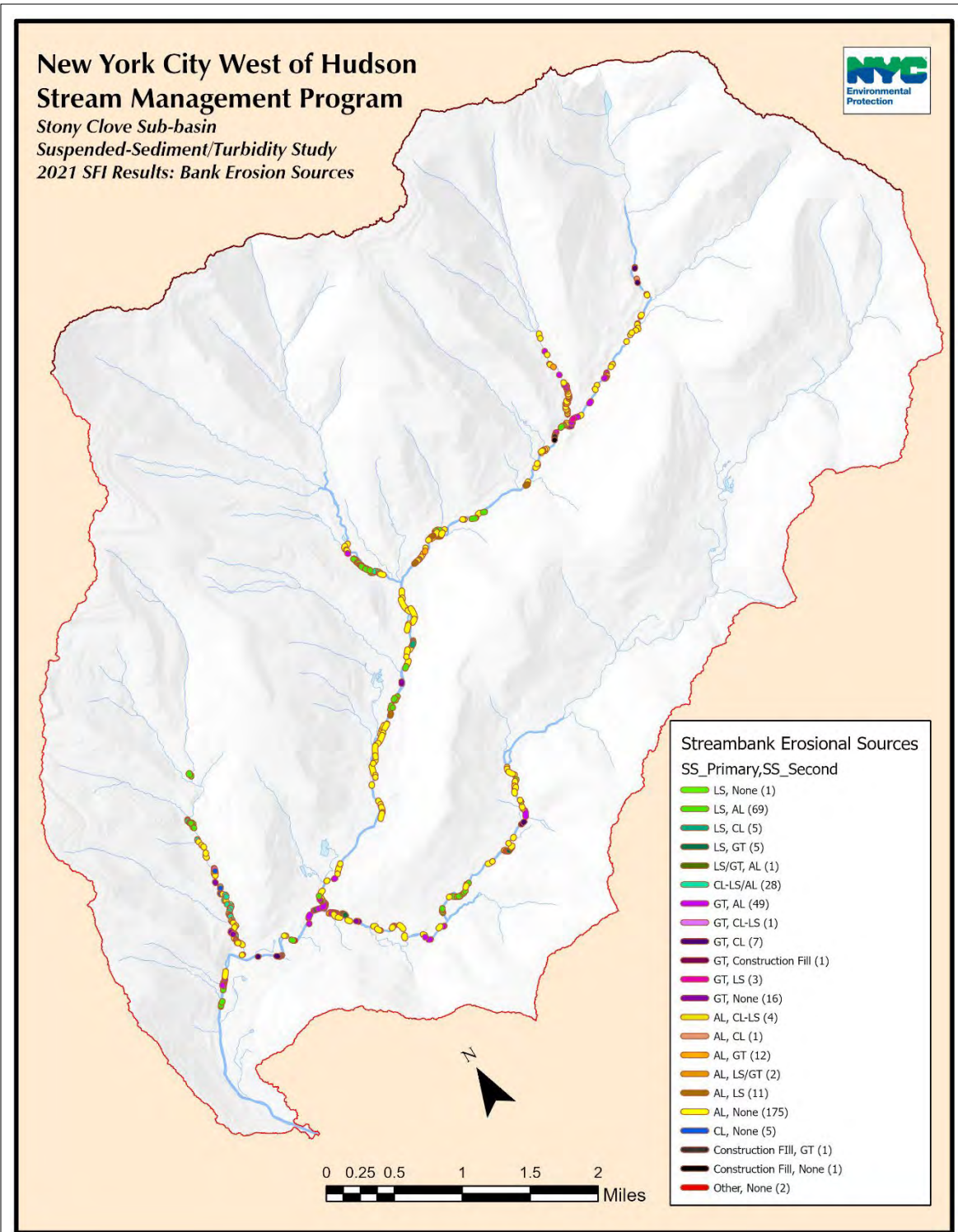


Figure 4.16. 2021 SFI mapping results depicting stream bank erosional connectivity with primary and secondary SS source sediment configurations. Mapped active and dormant stream bank erosion are combined in this map.

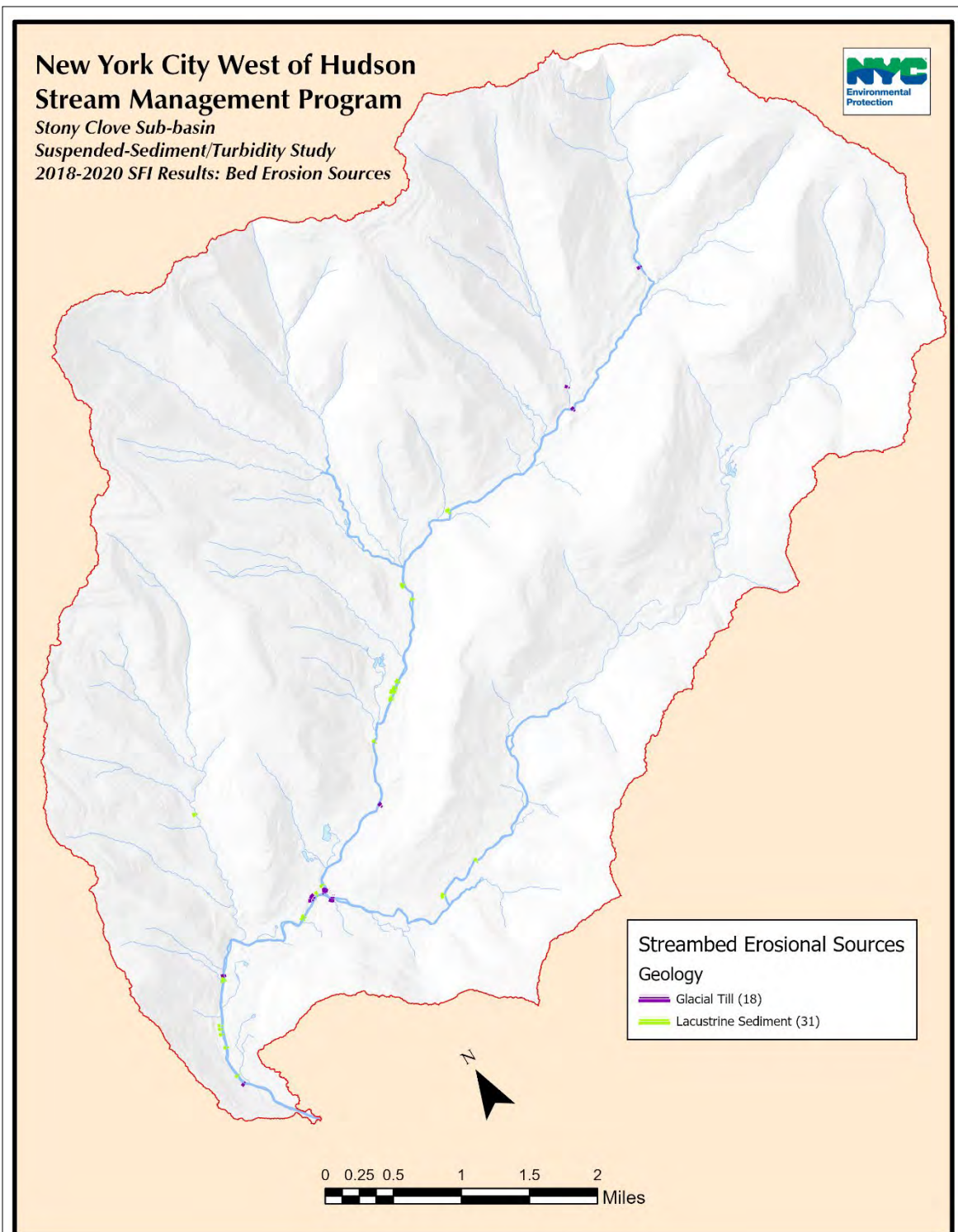


Figure 4.17 2018 – 2020 SFI mapping results depicting streambed erosional connectivity with glacial till and glacial lacustrine sediment.

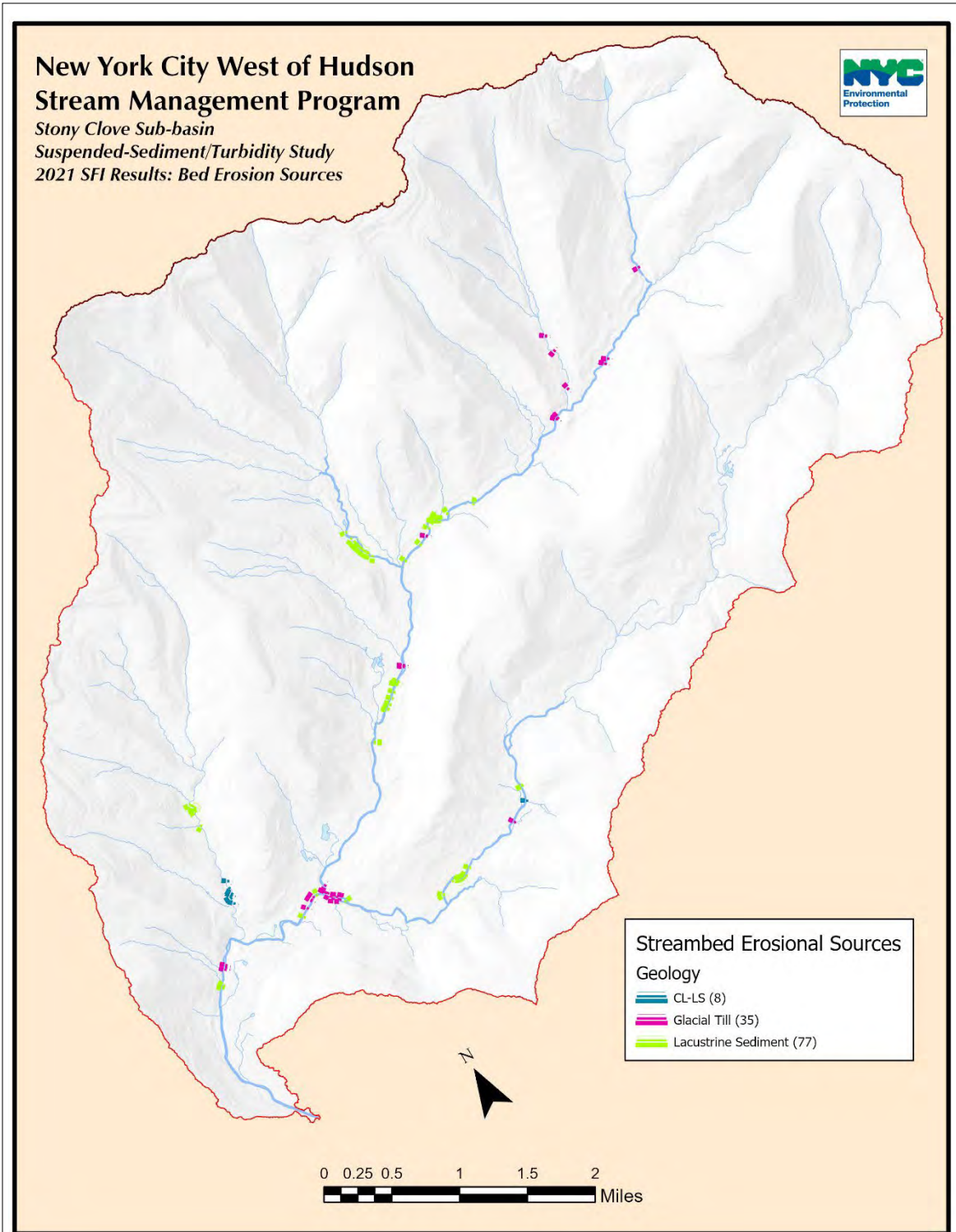


Figure 4.18 2021 SFI mapping results depicting streambed erosional connectivity with glacial till (GT) and glacial lacustrine sediment (LS). CL-LS is a mass-wasted variant of LS.

The SFI erosional connectivity data for the full 2018-2021 period is far too extensive to cover in this report. There are over 1,000 features (points and derived lines) representing stream bank and streambed erosional connectivity occurrence, lengths and areas. Erosional feature area is computed by combining the feature length with the average feature height (banks) or width (beds). The erosional feature data is then categorized by the various connectivity attributes recorded in the field:

- bank erosion status (active, dormant/recovering);
- bank connectivity with or without GLS;
- bank/bed connectivity with the different geologic units (AL, LS, CL-LS, GT, CL);
- bank connectivity by primary and secondary SS source geology (used to produce Figures 4.15 and 4.16);
- bank connectivity by erosion mechanics (hydraulic erosion, mass wasting and surficial wasting);
- bank/bed connectivity by reach confinement (unconfined reach, confined reach);
- bank/bed connectivity by confining margin type (valley bottom feature (e.g., high terrace or glacial moraine), valley margin, anthropogenic margin (e.g., road or revetment), and absence of confining margin); and
- other potential recorded attributes that might influence erosional connectivity include riparian woody buffer width and adjacent land use classification.

In addition to the bed and bank erosional features, DEP mapped the presence of potential and actual headcuts (upstream points of channel incision), large wood (individual pieces and accumulations), bank revetment, bedrock and constructed grade and planform controls, and hundreds of photo points that each include numerous photos to visually document stream channel conditions for future reference. There is a lot of data to explore for further analysis and future discussion in DEP's final FAD study report due in November 2027.

Table 4.22 presents pre- and post-flood results for bank erosion length data for Stony Clove Creek, Ox Clove Creek, Warner Creek, and Myrtle Brook considering only bank erosion mapped as active (expected to yield sediment in a bankfull scale runoff) and further segregated by connectivity with only AL or connectivity with GLS. The GLS is further segregated by LS and GT. Many mapped eroding banks in 2018-2020 were classified as dormant or recovering and those features are not included in the metrics presented in the table. The 2018 pre-flood data for Stony Clove Creek excludes sections of stream that were not mapped in 2021 to ensure accurate comparison. Hollow Tree Brook is not included since there is no pre-flood data and the SFI mapping was only for the section that became the biggest turbidity production source in the sub-basin (based on downstream turbidity monitoring). The table includes the same bank length

erosional connectivity indices ( $EI_{Bnk}$ ,  $SCI_{AL}$ ,  $SCI_{GLS}$ ) in the UEC SFI table (Table 4.19) plus  $SCI_{LS}$  and  $SCI_{GT}$ , computed as:

$SCI_{LS}$  = bank erosion length with LS connectivity/active bank erosion length

$SCI_{GT}$  = bank erosion length with GT connectivity/active bank erosion length

Table 4.23 presents results for bed erosion area connectivity data for the assessed streams excluding Hollow Tree Brook, stratified by general confinement condition ( $EI_{UR}$ ,  $EI_{CR}$ ) and bed area erosional sediment connectivity indices for LS and GT ( $SCI_{LS}$ ,  $SCI_{GT}$ ). Bed erosion features were mapped by collecting lengths and widths of exposed GLS in the streambed, as indicators of channel incision into primary SS source sediment. The mapped features indicate that in these reaches the channel is eroding into the underlying GLS and bed scour can be a locally significant source of turbidity production. The bed area confinement condition erosional index and erosional sediment connectivity index values are computed as follows:

Bed Area  $EI_{Bed}$  = bed erosion area in all mapped reaches/SFI-assessed channel length

Bed Area  $EI_{UR}$  = bed erosion area in unconfined reaches/SFI-assessed channel length

Bed Area  $EI_{CR}$  = bed erosion area in confined, partly confined, constricted (confined on both sides) reaches/SFI-assessed channel length

$SCI_{LS}$  = bed erosion area with LS connectivity/total bed erosion area

$SCI_{GT}$  = bed erosion area with GT connectivity/total bed erosion area

DEP will continue working to associate the mapped erosional sediment connectivity data with the USGS monitoring station delineated water quality monitoring reaches and monitored reach scale turbidity and SS production. Additional future work will explore multi-variable analytical approaches to investigate use of the various SFI potential erosional attribute metrics to help further explain turbidity production at the reach to sub-basin scale.

Table 4.22 Stony Clove SFI active bank erosion length results for pre- and post-flood conditions.  $EI_{Bnk}$  equals bank erosion length divided by assessed channel length. SCI values stratified by geology are eroding bank lengths per category divided by total active bank erosion length. LS and CL-LS are combined.

Stream Name	Active Bank Erosion Length (ft)	Bank Length $EI_{Bnk}$ (ft/ft)	Bank Length $SCI_{AL}$ (ft/ft)	Bank Length $SCI_{GLS}$ (ft/ft)	Bank Length $SCI_{LS}$ (ft/ft)	Bank Length $SCI_{GT}$ (ft/ft)
Pre-Flood Data (2018-2020)						
Stony Clove Creek	3,543	0.10	0.68	0.32	0.14	0.18
Ox Clove Creek	437	0.07	0.60	0.40	0.17	0.23
Warner Creek	958	0.07	0.45	0.55	0.40	0.16
Myrtle Brook	178	0.04	1.0	0.0	0.0	0.0
Post-Flood Data (2021)						
Stony Clove Creek	12,336	0.35	0.63	0.37	0.19	0.19
Ox Clove Creek	2,322	0.35	0.35	0.65	0.52	0.13
Warner Creek	4,409	0.32	0.51	0.49	0.25	0.30
Myrtle Brook	1,002	0.23	0.61	0.39	0.00	0.39

Table 4.23 Stony Clove SFI bed erosional connectivity area results for pre- and post-flood conditions. Bed erosion area  $EI_{Bed}$  equals the bed erosion area divided by assessed channel length. EI values stratified by confinement are  $EI_{UR}$  for unconfined reaches and  $EI_{CR}$  for confined reaches. SCI values stratified by LS and GT geology are eroding bed areas per category divided by total bed erosion area.

Stream Name	Bed Erosion Area (ft <sup>2</sup> )	Bed Area $EI_{Bed}$ (ft <sup>2</sup> /ft)	Bed Area $EI_{UR}$ (ft <sup>2</sup> /ft)	Bed Area $EI_{CR}$ (ft <sup>2</sup> /ft)	Bed Area $SCI_{LS}$ (ft <sup>2</sup> /ft)	Bed Area $SCI_{GT}$ (ft <sup>2</sup> /ft)
Pre-Flood Data (2018-2020)						
Stony Clove Creek	523	0.015	0.001	0.014	0.57	0.43
Ox Clove Creek	98	0.015	0.015	0.00	1.00	0.00
Warner Creek	464	0.010	0.002	0.008	0.66	0.34
Myrtle Brook	2.5	0.0006	0.000	0.0006	0.00	1.00
Post-Flood Data (2021)						
Stony Clove Creek	827	0.024	0.005	0.019	0.60	0.40
Ox Clove Creek	942	0.141	0.35	0.65	0.00	1.00
Warner Creek	2,659	0.058	0.002	0.056	0.59	0.41
Myrtle Brook	85.5	0.020	0.000	0.020	0.00	1.00

There were large increases in bank and bed erosion and GLS sediment connectivity in all monitored streams (including Hollow Tree Brook not represented in the tables) as a result of the December 2020 flood. Bank length  $EI_{Bnk}$  increased by factors of 3.5 in Stony Clove Creek and up to 5.6 in Myrtle Brook.

The biggest measured percent increase in erosional sediment connectivity with GLS (especially LS) occurred in Ox Clove Creek in both bank and bed erosion. The change in GLS connectivity in Ox Clove Creek reversed the dominant SS source from AL to GLS. The LS component of the GLS connectivity increased from 0.17 in 2019 to 0.52 in 2021. This is reflected in the monitored turbidity and SS presented in Sections 4.3 and 4.4. Some of the increased LS connectivity is attributable to changing some banks GT classification in 2021 to CL-LS; however, it is mostly attributable to the extensive new exposures of LS and CL-LS not present before the December 2020 flood.

Warner Creek bed connectivity with GLS increased by a factor of 5.7 and much of this was into GT in the lower reaches above the Stony Clove Creek confluence where the channel incised up to three feet into GT in the reach between the Stony Clove Creek confluence and a bifurcated reach on Warner Creek.

Myrtle Brook remains the stream with the least erosional sediment connectivity with GLS (only GT), yet its relative increases in erosional connectivity were the greatest of all the streams mapped before and after the December 2020 flood. If Hollow Tree Brook had been mapped prior to the flood, it is very likely that there would be a similar reversal in AL versus GLS SS source dominance, based on field observations and monitored turbidity and SS flux.

It is important to remember the limitation in this preliminary presentation of the SFI data that these SFI assessments do not cover the full length of the streams, nor any of the tributary streams. Past SFIs helped define the upper reach extents for each stream that were both feasible to map in a season and were in the zone that would have increased probability of encountering LS, based on the highest elevation mapped Pleistocene glacial lake delta in the Stony Clove sub-basin (Figure 4.19; Rich, 1935).

The results support assumptions in the conceptual model of study area turbidity production: (1) the potential presence of LS in a channel margin is a primary turbidity production factor, and (2) big floods can significantly increase erosional connectivity with SS sources that can create a prolonged period of turbidity production, altering the Q-Tn and Q-SS relationship across a range of flows. Further Q, Tn, and SS monitoring in Stony Clove sub-basin through the remainder of the study will help quantify the legacy impact of a big flood on turbidity production in the UEC watershed.

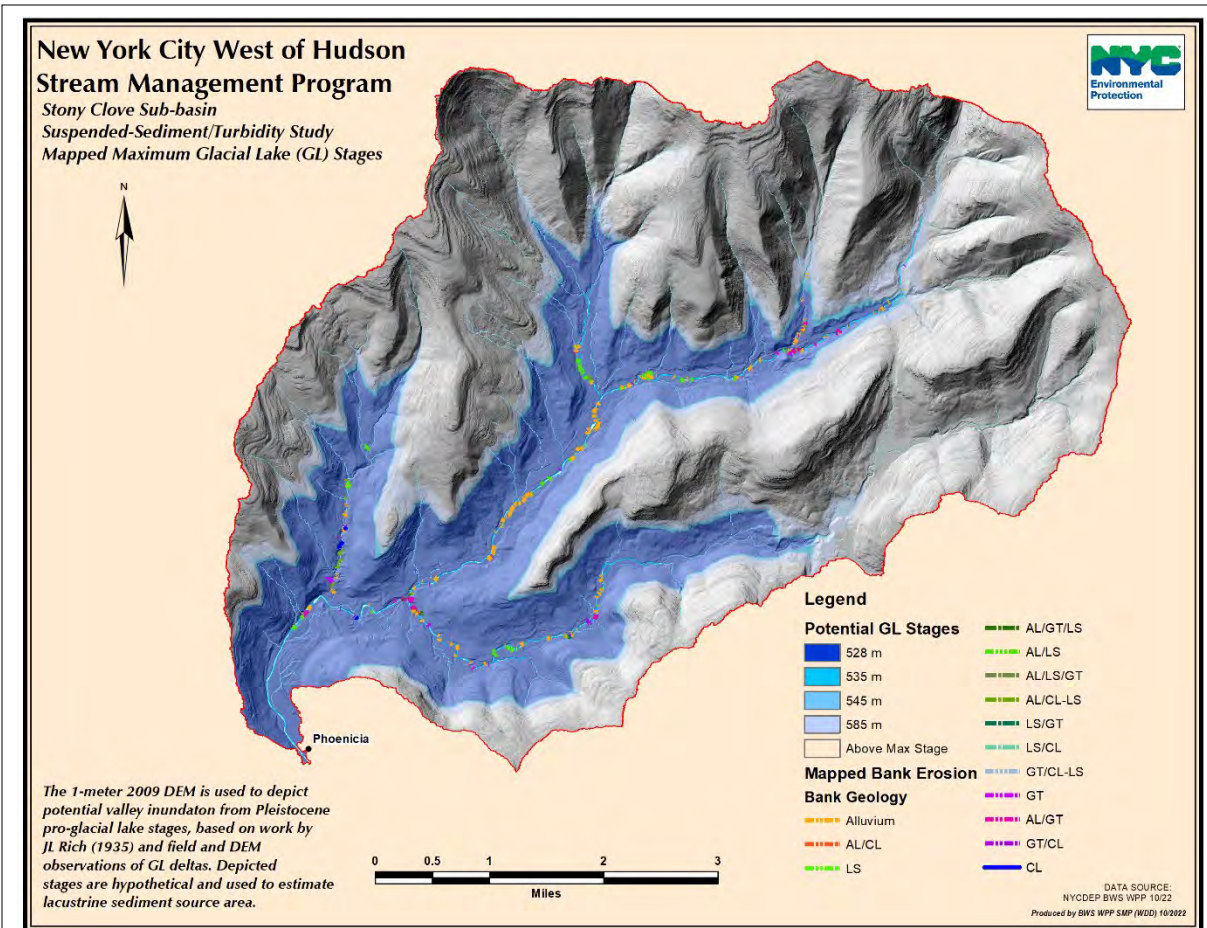


Figure 4.19 Map depicting the highest mapped glacial lake stage based on delta features in the Warner Creek sub-basin (Rich, 1935) and the 2021 mapped occurrence of glacial lake sediment (LS) and glacial till (GT) exposed in the stream channel.

### Stream Erosion Monitoring

The study includes monitoring of reach-scale channel erosion at a set of sites in the Stony Clove sub-basin (Figure 4.20). DEP established eight BEMS sites during the period 2016 to 2018, selected from previously mapped SS sources. DEP added two sites in 2021, and SLR Consulting performed monitoring under contract to DEP. A draft report prepared by SLR Consulting in 2019 was expected to be completed in early 2022, following completion of the first five years of monitoring and for inclusion in this report. The final BEMS report is now expected to be discussed in DEP’s next FAD status report due in March 2024.

The BEMS sites have four valuable roles in advancing this study so far. The selected sites presented an opportunity to test methodology for optimizing topographic monitoring methods (as discussed in Section 3), sample and analyze stream bank and streambed sediment sources for fine sediment content, track several representative reaches that could give quantitative insight

into reach scale dynamics that influence watershed scale turbidity production, and serve as a pool of candidate STRP sites. The sediment sampling and STRP site selection have been the most useful results so far. The sediment sampling has helped to quantify the fine sediment content of the SS source sediment units in stream banks categorized in this study. Three new STRPs constructed in 2021 and 2022 were former BEMS sites.

Table 4.24 presents the current status of BEMS site topographic monitoring through spring 2022. Two new sites were added since DEP’s 2021 FAD status report, one on Stony Clove Creek and one on Hollow Tree Brook. Both sites were selected based on the field reconnaissance following the December 2020 flood. The Hollow Tree Brook site is currently the largest turbidity production site in the Stony Clove sub-basin. SLR Consulting surveyed the new BEMS sites in 2021 and 2022, for two rounds each. The three BEMS sites that were converted to STRPs (WC-01, WC-02, and SCC-03) received the most monitoring surveys prior to STRP construction: seven for WC-01 and WC-02 and six for SCC-03. WC-01 and WC-02 also have two post-construction surveys for comparison with pre-construction status. SCC-03 will also receive at least two surveys.

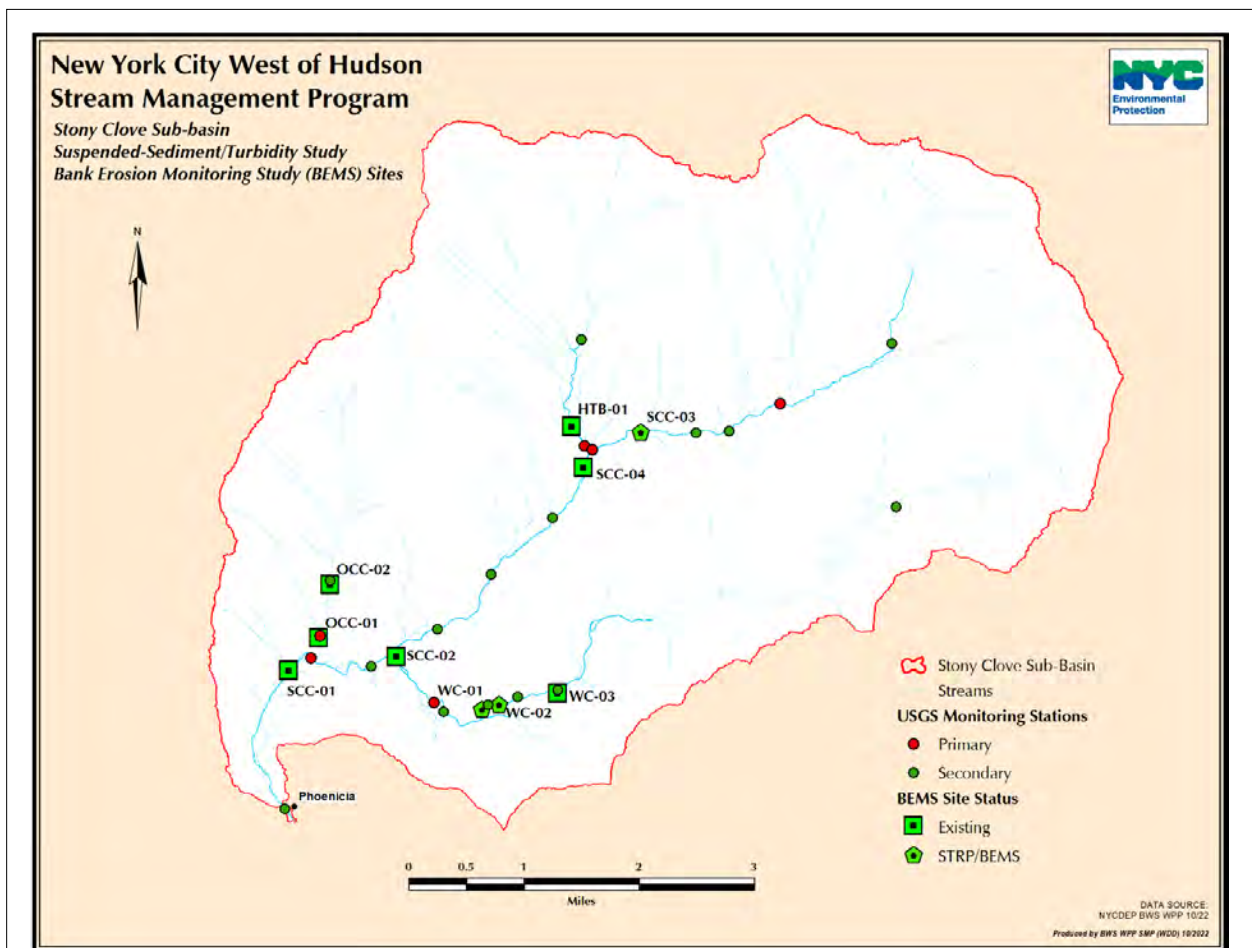


Figure 4.20 Stony Clove sub-basin BEMS locations and USGS monitoring stations.

Table 4.24 Stony Clove sub-basin BEMS status table.

Site	Length (ft)	Survey Dates	Survey Method <sup>1</sup>	Sediment Analysis <sup>2</sup>	Description <sup>3</sup>
SCC-01	700	12/2017 04/2021 03/2022	TS UAS UAS	Yes	Mass wasting of AL/GT in right VM; Bank erosion in LS and GT on left ACM.
SCC-02	750	12/2017 01/2021 12/2021	TS UAS UAS	Yes	Mass wasting of GT in left VBM (moraine); Channel incision in GT.
SCC-03	1,700	04/2018 01/2019 04/2020 11/2020 01/2021 12/2021	UAS UAS UAS UAS UAS UAS	Yes	Mass wasting of AL/LS in right VBM (delta terrace); Channel incision in LS. Bank erosion in AL/LS in left ACM.
SCC-04	1,800	04/2021 12/2021	UAS UAS	No	Aggrading and degrading reach with bank erosion into AL and history of incision into LS.
WC-01	500	11/2016 07/2017 04/2018 12/2018 04/2020 11/2020 01/2021 11/2021 <sup>4</sup> 05/2022 <sup>4</sup>	TS UAS UAS UAS UAS UAS UAS UAS UAS	Yes	Mass wasting of AL/LS in right VBM (terrace); Channel incision in LS.
WC-02	650	11/2016 07/2017 11/2017 12/2018 04/2020 11/2020 01/2021 11/2021 <sup>4</sup> 05/2022 <sup>4</sup>	TS UAS UAS UAS UAS UAS UAS UAS UAS	Yes	Mass wasting of AL/LS in left VBM (terraces); Channel incision in LS; Former avulsion
WC-03	450	07/2017 05/2018 04/2020 11/2020 11/2021	TS UAS UAS UAS UAS	Yes	Mass wasting of AL/GT/LS in left VM; Channel incision in LS.
OCC-01	500	11/2016 11/2017 04/2021 12/2021	TS UAS UAS UAS	Yes	Mass wasting of GT in right VBM (moraine).

OCC-02	450	07/2017 04/2021 12/2021	TS UAS UAS	Yes	Mass wasting of AL/LS/GT in left VBM (glacial terrace); Channel incision in LS
HTB-01	2,300	04/2021 02/2022	UAS UAS	Yes	Mass wasting of AL/LS and extensive reach scale incision into LS with multiple headcuts

<sup>1</sup> Survey methods included traditional ground-based topographic surveys with total station (TS) and unmanned aerial system (UAS) technology in combination with traditional ground survey.

<sup>2</sup> Sediment grain-size distribution analyses were completed for several sites to get representative ranges of fine sediment content (clay-silt) in the sampled sedimentologic units.

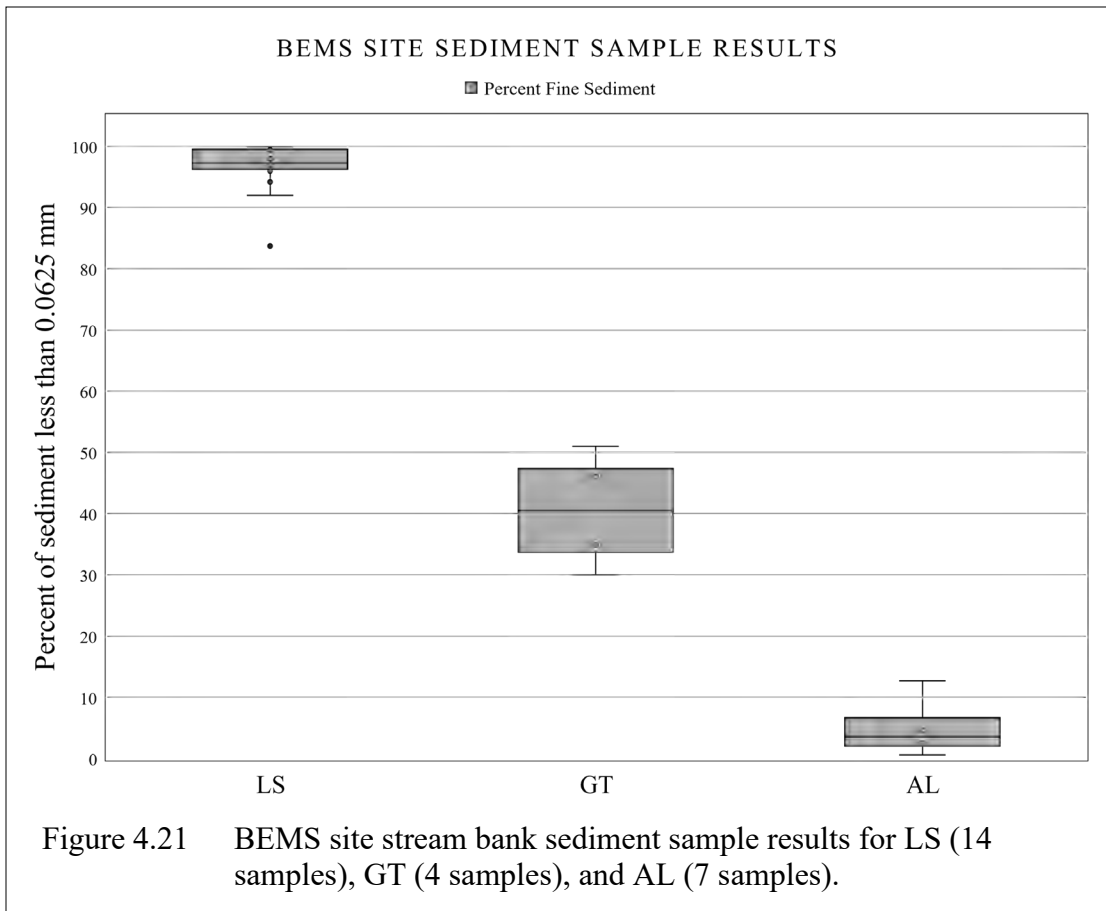
<sup>3</sup> Symbol key: AL = alluvium; GT = glacial till; LS = lacustrine sediment; VM = valley margin; VBM = valley bottom feature margin; ACM = active channel margin.

<sup>4</sup> WC-01 and WC-02 were surveyed following STRP construction in fall 2021 and once again after a bankfull streamflow event in spring 2021.

### Stream bank sediment sampling

Multiple bulk samples were taken at each BEMS location to document the grain size distribution of the SS source units exposed within the study area. The primary objective for the analysis was to obtain estimates of the percentage of fine-grained sediment (silts and clays) in each source that contributes to suspended sediment. The samples were submitted to Independent Material Testing Labs in Plainville, Connecticut, or to Atlantic Testing Labs in Highland, New York, for gradation and hydrometer analyses. The stream bank sediment sample fine sediment content results for AL, LS and GT are presented in Figure 4.21. The boxplots show the substantial difference in fine sediment content among the three primary SS sources – LS, GT, and AL.

The 14 LS samples have the highest percent fines, ranging from an outlier low of 83.7 % up to 99.9% and a mean of 96%. The four GT samples range from moderate to high (30-51%) with a mean of 50.5%. The seven AL samples represent the low-end with a range of 0.6-12.7% and a mean of 5.3%. It takes very little erosion of LS to exceed the SS contributions of GT and AL. This data supports the assumption that LS is the primary target for STRP sediment dis-connectivity.



DEP and SLR Consulting will continue to collect more stream bank samples and extend sediment sampling to active stream channel alluvium to obtain estimates of fine sediment storage that can be re-suspended during bed mobilizing flows. An initial round of streambed sediment sampling was conducted at BEMS site WC-02 during STRP construction in 2021. Four samples were collected by trackhoe excavation. Each sample was sub-sampled down to a 30-gallon sample size and partially processed on site to measure, weigh and remove all clasts greater than 2.5 inches. The diminished samples were then sent to a certified laboratory for further processing to obtain estimates of fine sediment content for the 30-gallon samples. The percent of fines for all the samples was relatively consistent at approximately 1%. A set of four samples was similarly collected and processed at the SCC-03 BEMS site during its conversion to an STRP site in 2022. The results were not ready for inclusion in this report. DEP and SLR Consulting will review the two BEMS sites sample results and plan to develop a field protocol for collecting smaller samples without trackhoe at all BEMS sites and other locations to develop a more robust estimate of the fine sediment stored in alluvium that can be re-suspended.

### GIS Analyses

Since DEP submitted its last FAD status report (DEP 2021), the biggest update is that all Stony Clove monitored sub-basin streams have ACM delineations completed and reviewed for 2009 and 2016. The recently available 2021 orthoimagery will be used to delineate 2021 ACMs,

providing the necessary spatial data to evaluate lateral adjustments in channel morphology associated with the December 2020 flood and any management practices or other disturbances that occurred during the study period. Assuming the SFI field component of the study has mostly been completed (two rounds of SFI for each Stony Clove sub-basin stream, except for Hollow Tree brook), DEP will resume work on the remote-sensed data analyses to further explore potential explanatory metrics for turbidity production.

## **4.6 Sediment and Turbidity Reduction Projects Monitoring**

A primary goal of the study is to evaluate STRP efficacy on measurably reducing Tn and SS at a range of spatial, temporal and hydrologic scales. STRPs disconnect a stream channel from primary turbidity production sources exposed in eroding streambeds, banks and adjacent hillslopes, at a reach scale. Individually and collectively, they test the role of reach scale processes on sub-basin to basin scale turbidity production and SS flux. A set of the USGS stream monitoring stations is used in the study to monitor and evaluate the performance of the STRPs in mitigating turbidity.

DEP funds STRPs through design contracts with engineering consultants and stream management contracts with county soil and water conservation districts. Additional federal funding for several of the STRPs was provided by the USDA Natural Resource Conservation Service and one project was supported by the Federal Emergency Management Agency.

The study focuses STRP evaluation on the Stony Clove sub-basin. Though not part of this study scope, STRP evaluation in other sub-basins is also performed by USGS, DEP and Cornell University in journal publications and conference proceedings. To date, one peer-reviewed journal publication authored by Cornell University and DEP researchers documents the STRP evaluation (of all UEC STRPs) using the first four years of monitoring data and novel statistical and physically-based modeling techniques to examine the role of STRPs in reducing turbidity during the period of low hydrologic forcing and geomorphic recovery through water year 2020 (Wang et al., 2021). USGS and DEP have written a second journal manuscript using a different set of statistical approaches to evaluate STRP efficacy through water year 2020 in the UEC and Stony Clove sub-basin that is currently under journal peer review. In both papers, the evaluated data does not include water year 2021 and the impact of the December 2020 flood on the STRP-influenced Tn-Q and SSC-Q relationship. This section of the report includes content from the two manuscripts for the Stony Clove sub-basin with a separate sub-section updating the analysis to evaluate the impact of the December 2020 flood on turbidity reduction achieved by STRPs.

### **4.6.1 STRP Implementation**

Table 4.25 lists the STRPs constructed through 2021, linking a number designation used hereafter to the project name used in prior FAD reports. The roman numeral designations are used for consistency with the published scientific journal articles usage. Table 4.26 provides details on the treated stream lengths, SS source conditions, STRP practices and costs. Figure 4.22 shows the locations of the Stony Clove sub-basin STRPs evaluated in this report.

All STRP treated stream reaches were either selected based on ranking the magnitude of mapped erosional connectivity with turbidity source sediment or in coordination with the USDA Emergency Watershed Protection Program following the 2011 Tropical Storm Irene flood. The most extensive work was conducted in the Stony Clove Creek sub-basin where eight STRPs were implemented along 8,930 feet of channel between 2012 and 2016. Two additional Warner Creek STRPs constructed in 2021 were selected as part of the study using upstream/downstream turbidity monitoring data, and geomorphic mapping and monitoring data (DEP, 2019b). Two nearly contiguous STRPs totaling 1,300 feet were completed in the Beaver Kill sub-basin in 2017 and one 1,350-foot long STRP was constructed in the Woodland Creek sub-basin in 2018. One additional Stony Clove Creek STRP and one Woodland Creek sub-basin STRP were constructed in 2022. Once sufficient post-construction data has been collected and analyzed for the 2021-2022 Stony Clove sub-basin STRPs, these projects will be used for evaluating reach scale turbidity reduction efficacy, since each project has upstream and downstream monitoring stations that can be used for analysis.

All STRPs disrupted some version of channel-hillslope connectivity and sediment input from glacial legacy sources, yet each treated reach had unique connectivity configurations and sediment composition (Table 4.26). The practices used included channel realignment where feasible, grade and planform control to limit erosional adjustment, in-stream structures to influence hydraulics, stabilization of hillslopes, enhancing floodplain connectivity and riparian zone revegetation.

Table 4.25. STRPs completed in the UEC sub-basins between 2012 - 2021 and associated study ID designation.

Stream project ID	Stream Project Name
STRP I	Stony Clove Creek at Chichester Site 1
STRP II	Warner Creek Site 5
STRP III	Stony Clove Creek at Chichester sites 2&3
STRP IV	Stony Clove Creek at Lanesville
STRP V	Stony Clove Creek at Stony Clove Lane
STRP VI	Stony Clove Creek-Warner Creek Confluence
STRP VII	Stony Clove Creek at Wright Road (channel)
STRP VIII	Stony Clove Creek at Wright Road (hillslope)
STRP IX	Beaver Kill at Van Hoagland Road 1
STRP X	Beaver Kill at Van Hoagland Road 2
STRP XI	Woodland Creek at Wilmot Way
STRP XII	Warner Creek Site 1
STRP XIII	Warner Creek Site 2

Table 4.26 STRPs completed in the UEC sub-basins. [GT = glacial till; LS = lacustrine sediment; STRP practices: 1 = channel realignment; 2 = grade control; 3 = planform control with revetment or bioengineering; 4 = in-stream hydraulic structures; 5 = restoring floodplain connectivity/disconnecting from hillslope; 6 = hillslope stabilization through regrading/improving drainage/restoring vegetation cover; 7 = riparian planting]

Stream project	Stream length (ft)	Year	Problem/SS source	Practices implemented	Total Cost
Stony Clove Creek (STRP I)	650	2012	Channel-hillslope erosion / LS	1, 2, 3, 4, 5, 6, 7	\$1,020,369
Warner Creek (STRP II)	800	2013	Channel-hillslope erosion / LS	1, 2, 3, 4, 5, 6, 7	\$495,465
Stony Clove Creek (STRP III)	1350	2013	Channel-hillslope erosion / LS+GT	1, 2, 3, 4, 5, 6, 7	\$1,415,113
Stony Clove Creek (STRP IV)	1700	2014-2015	Channel-hillslope erosion / GT	1, 2, 3, 4, 5, 7	\$301,789
Stony Clove Creek (STRP V)	455	2014	Channel-hillslope erosion / LS+GT	2, 3, 4, 5	\$540,146
Stony Clove-Warner Creeks confluence (STRP VI)	1300	2014-2015	Channel-hillslope erosion / LS+GT	2, 3, 4	\$1,585,454
Stony Clove Creek (STRP VII, VIII)	2675	2015-2016	Channel-hillslope erosion / LS+GT	1, 2, 3, 4, 5, 6	\$1,802,985
Beaver Kill (STRP IX, X)	1300	2017	Channel-hillslope erosion / GT	1, 2, 3, 4, 5, 6, 7	\$1,383,408
Woodland Creek (STRP XI)	1350	2018	Channel-terrace erosion / LS	1, 2, 3, 4, 5	\$1,075,795
Warner Creek (STRP XII)	540	2021	Channel-terrace erosion/LS	1, 2, 3, 4, 5, 6, 7	\$373,342
Warner Creek (STRP XIII)	560	2021	Channel-terrace erosion/LS	1, 2, 3, 4, 5, 6, 7	\$373,342

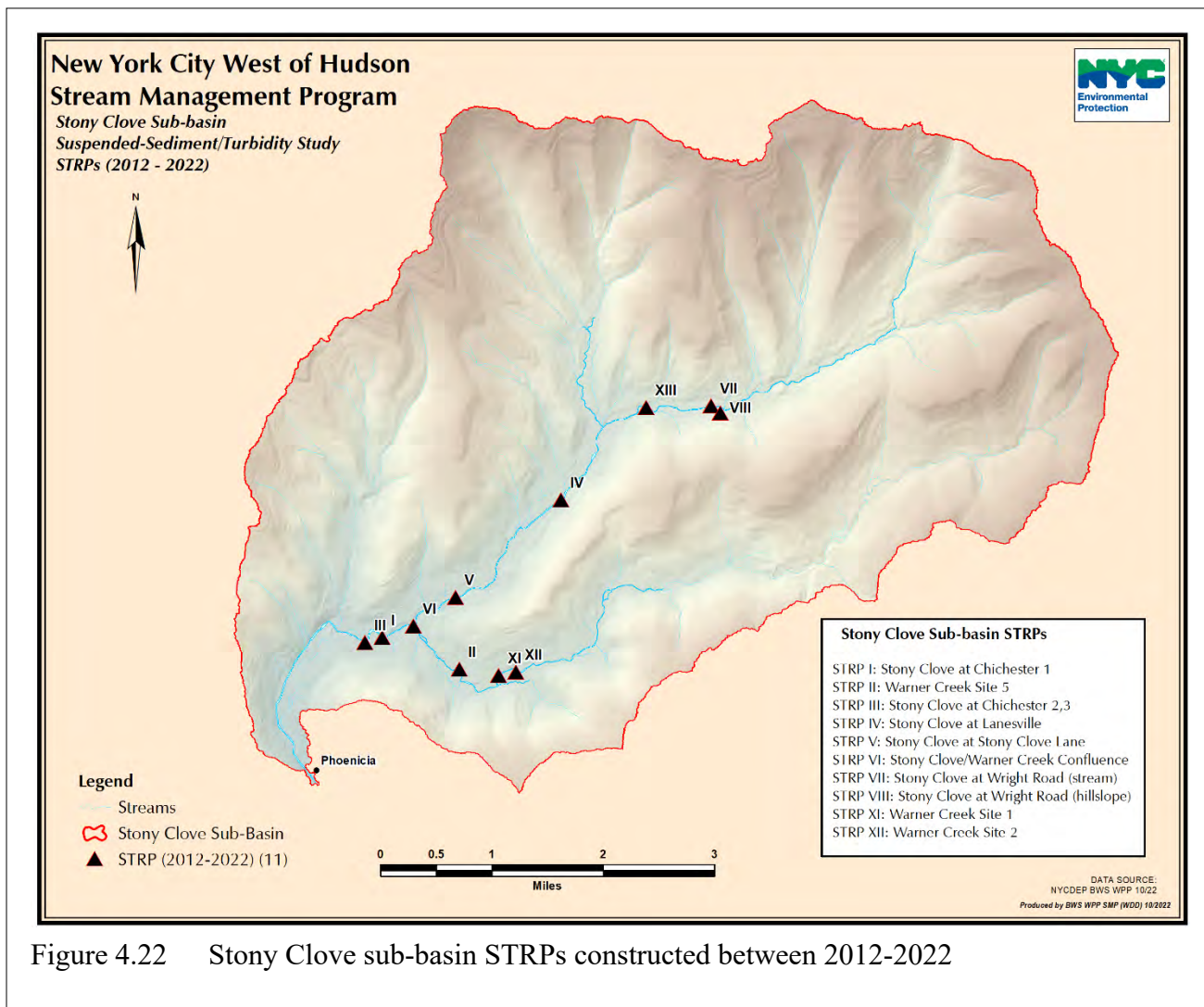


Figure 4.22 Stony Clove sub-basin STRPs constructed between 2012-2022

#### 4.6.2 STRP Turbidity and SS Monitoring: Water Years 2017-2020

Past research by USGS and DEP concluded that cumulative STRPs in the Stony Clove sub-basin reduce turbidity and SS flux and yield for a limited range of streamflow for a short monitoring period following implementation (Siemion et al., 2016). Using monitoring data from the Stony Clove Creek station #01362370, Warner Creek station #01362357, Little Beaver Kill station #0136497, and Esopus Creek monitoring station #01362500, USGS performed a series of statistical analyses in 2021 to estimate the influence of STRPs on reducing turbidity at the sub-basin to basin scale. The following content is largely derived from the USGS-DEP authored journal manuscript that is currently under peer review prior to publication. A portion of the analytical results from the work by Wang et al. (2021) is also incorporated to substantiate the presentation of evaluation results. In each case, only results are presented in this report. The

Wang et al. (2021) paper is included in Appendix A to provide a more substantial accounting of methodology and results not presented in the main body of the report.

### **Streamflow Conditions**

Streamflow is a principal driver of the geomorphic processes that produce turbidity in the study streams. The period before STRP construction in the Stony Clove sub-basin was more hydrologically active, and thus geomorphically active, than the period through water year 2020 after STRPs were constructed (Figure 4.23). Peak streamflows with RI >1.5 years occurred more frequently in the six years prior to construction of the initial STRP than after Stony Clove sub-basin STRP construction concluded in 2016. Three of the peaks during 2010 and 2011 exceeded a 10-year RI. The implication of these different streamflow conditions in the pre- and post-STRP period is that turbidity SS production was subject to different hydrological forcing conditions. The period prior to STRP implementation was subject to more disturbance that could elevate turbidity production and SSC across a range of flows. The prolonged period of lower hydrologic forcing following 2011 allowed the fluvial system to recover some geomorphic stability through re-vegetation in the stream corridor, re-sorting of in-stream sediment to a more stable channel configuration, and reduced connectivity with glacial legacy sediment. The work by Wang et al. (2021) investigated the potential role of differences in hydrologic forcing on the observed differences in turbidity production and SS flux. The analysis found that even though the lower disturbance hydrology influenced the observed decrease in turbidity and SS production in the Stony Clove sub-basin, there was a clear signal of faster reduction coincident with the STRP implementation.

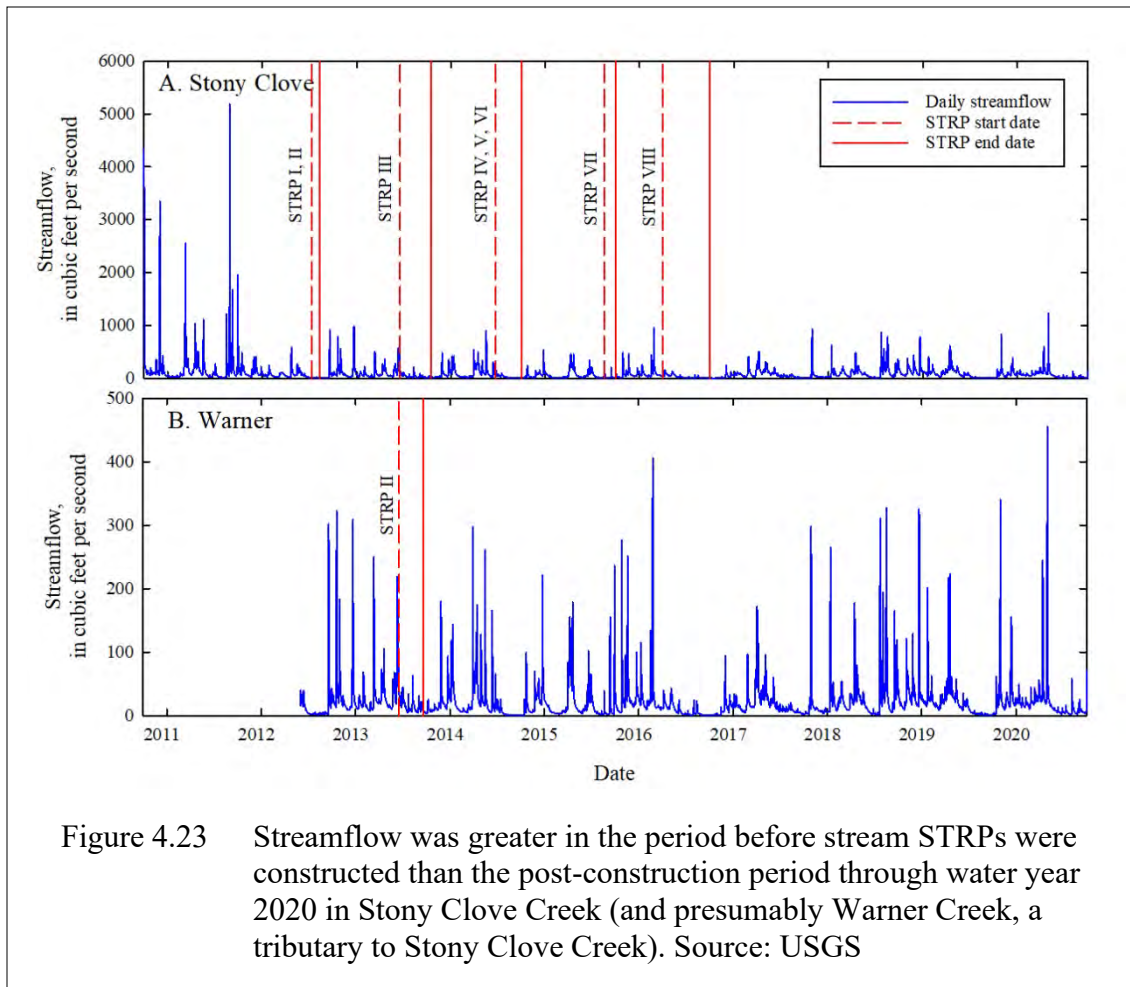


Figure 4.23 Streamflow was greater in the period before stream STRPs were constructed than the post-construction period through water year 2020 in Stony Clove Creek (and presumably Warner Creek, a tributary to Stony Clove Creek). Source: USGS

## USGS Statistical Analyses

### Changes in the streamflow – SSC relations

Changes in the slope and/or intercept of the streamflow-SSC regression line can be indicative of changes in the sediment transport regime (Asselman, 2000; Ahn et al., 2017; Wang et al., 2021), and consequently turbidity production. The relation between streamflow and SSC was analyzed using an Analysis of Covariance (ANCOVA) on  $\log_{10}$  transformed data to control for the effects of streamflow between the before and after STRP periods. Levene’s test was used to test the assumption of similar variance between experimental conditions (Levene, 1960). An Analysis of Variance (ANOVA) was used to check that the covariate did not vary significantly across levels of the predictor variable. The ANCOVA was run using daily mean SSC as the dependent variable, daily mean streamflow as the covariate, and a project factor that separated the dataset into periods before and after construction of the STRPs. The ANCOVA was re-run to test the assumption of homogeneity of regression slopes by including the interaction of the project factor and the covariate. The assumptions were not met in any of the ANCOVA analyses, so a robust ANCOVA (Wilcox, 2005) was used.

Stony Clove Creek and Warner Creek exhibited a significant ( $p < 0.01$ ) reduction in daily mean SSC after implementation of the STRPs through the range in streamflow monitored through water year 2020 (Figure 4.24). Decreases in SSC for a given streamflow from before to after STRP implementation can be indicative of reduction in SS transport (turbidity production) because of the STRP. The slope and intercept of the regression lines declined for the study sites after STRP implementation.

Regression equations of daily mean streamflow and SSC, before and after the STRP implementation period (2012 – 2016), were used to estimate changes in SSC potentially attributable to the STRPs at the monitoring sites. The largest decreases were measured at Stony Clove Creek through the range in streamflow (Table 4.27). The results indicate that the eight STRPs constructed between 2012 to 2016 were successful in decreasing SSC during “high” streamflows ( $Q_1$ ) generated by storms and from chronic sources that generated elevated SSC during lower streamflows ( $Q_{90}$ ). It is important to state that the high streamflows for the first four years did not exceed the range proximal to bankfull streamflow (Figure 4.23) and thus these results do not include the role of STRPs in turbidity production during much higher magnitude flows. The previous biennial research status reports (DEP, 2019a; DEP, 2021) presented temporally stratified regression results that showed most of the observed SSC reduction in Stony Clove Creek occurred following construction of the two 2013 STRPs on Stony Clove Creek and Warner Creek (STRPs II and III). These treated reaches had the largest erosional connectivity with LS in each stream and were actively producing turbidity at low flows associated with hillslope mass wasting processes.

Table 4.27 Slope and intercept for daily mean streamflow-SSC regression equations; and estimated declines in daily mean SSC in mg/L for high ( $Q_1$ ), moderately high ( $Q_{10}$ ), median ( $Q_{50}$ ), and low ( $Q_{90}$ ) streamflows after STRP implementation. Slope and intercept are  $\log_{10}$ .

USGS Station ID	Before or after STRP	STRPs	Slope	Intercept	Decrease in SSC at $Q_1$	Decrease in SSC at $Q_{10}$	Decrease in SSC at $Q_{50}$	Decrease in SSC at $Q_{90}$
01362370	Before	I-VIII	0.63	0.73				
01362370	After	I-VIII	0.61	-0.44	-431	-212	-96	-37
01362357	Before	II	0.80	0.21				
01362357	After	II	0.79	-0.22	-76	-24	-9	-2

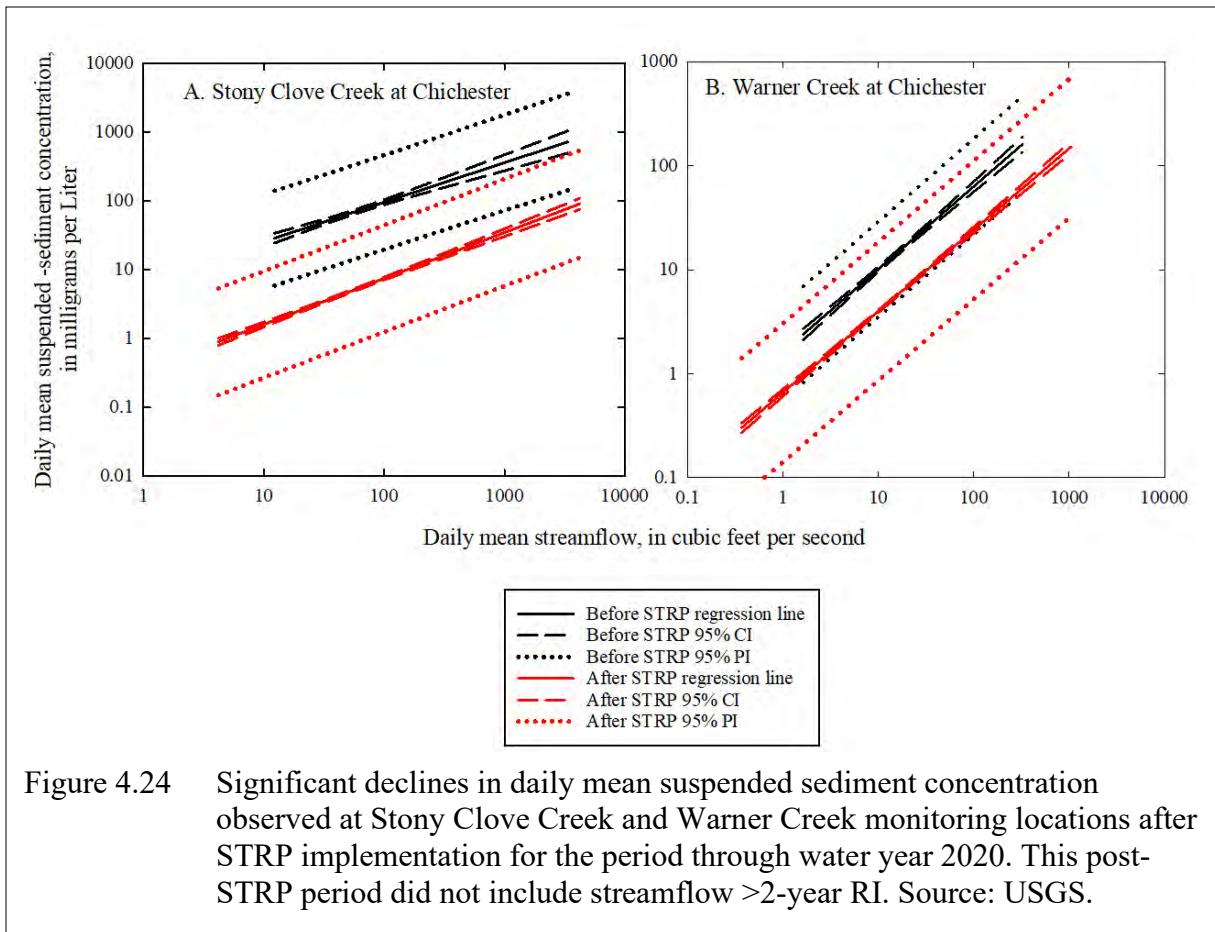


Figure 4.24 Significant declines in daily mean suspended sediment concentration observed at Stony Clove Creek and Warner Creek monitoring locations after STRP implementation for the period through water year 2020. This post-STRP period did not include streamflow >2-year RI. Source: USGS.

### Paired watershed analysis

A paired watershed analysis was conducted to determine if there were changes in turbidity in the study watersheds after implementation of the STRPs. The Little Beaver Kill was used as a control watershed. No STRPs were implemented in the Little Beaver Kill during the study period. The Little Beaver Kill has relatively low SSC and turbidity (McHale and Siemion 2014; Tables 4.8 and 4.13), and minimal erosional SS source connectivity (Table 4.18). Daily mean turbidity was used because daily mean SSC was not available from 01362497. ANCOVA was used on  $\log_{10}$  transformed data to determine if the relation in daily mean turbidity changed between the watersheds where STRPs were implemented and the Little Beaver Kill. The assumptions were not met in any of the ANCOVA analyses, so a robust ANCOVA (Wilcox 2005) was used.

Turbidity was significantly lower ( $p < 0.001$ ) at Stony Clove Creek and Warner Creek in relation to Little Beaver Kill, the control site, after implementation of the STRPs (Figure 4.25) except for the highest turbidity range at Warner Creek. The greatest decreases in turbidity at the study sites relative to the control site were measured at Stony Clove Creek (Table 4.8). The decrease in turbidity relative to the control watershed was much more pronounced at lower

turbidity at Stony Clove and Warner Creeks, indicative of successful disconnection from hillslope sources that supplied SS during low flow conditions.

Table 4.28. Slope and intercept for daily mean turbidity regression equations for study and control sites; and estimated declines in daily mean turbidity in FNU for high ( $T_{0.1}$ ), moderately high ( $T_1$ ), moderate ( $T_{10}$ ), and median ( $T_{50}$ ) turbidity after STRP implementation. Slope and intercept are  $\log_{10}$ . Source: USGS

USGS Station ID	Before or after STRP	STRPs	Slope	Intercept	Decline in $T_{0.1}$	Decline in $T_1$	Decline in $T_{10}$	Decline in $T_{50}$
01362370	Before	I-VIII	0.17	1.87				
01362370	After	I-VIII	0.61	0.63	-112	-114	-99	-85
01362357	Before	II	0.43	1.31				
01362357	After	II	0.67	0.81	-8	-26	-24	-18

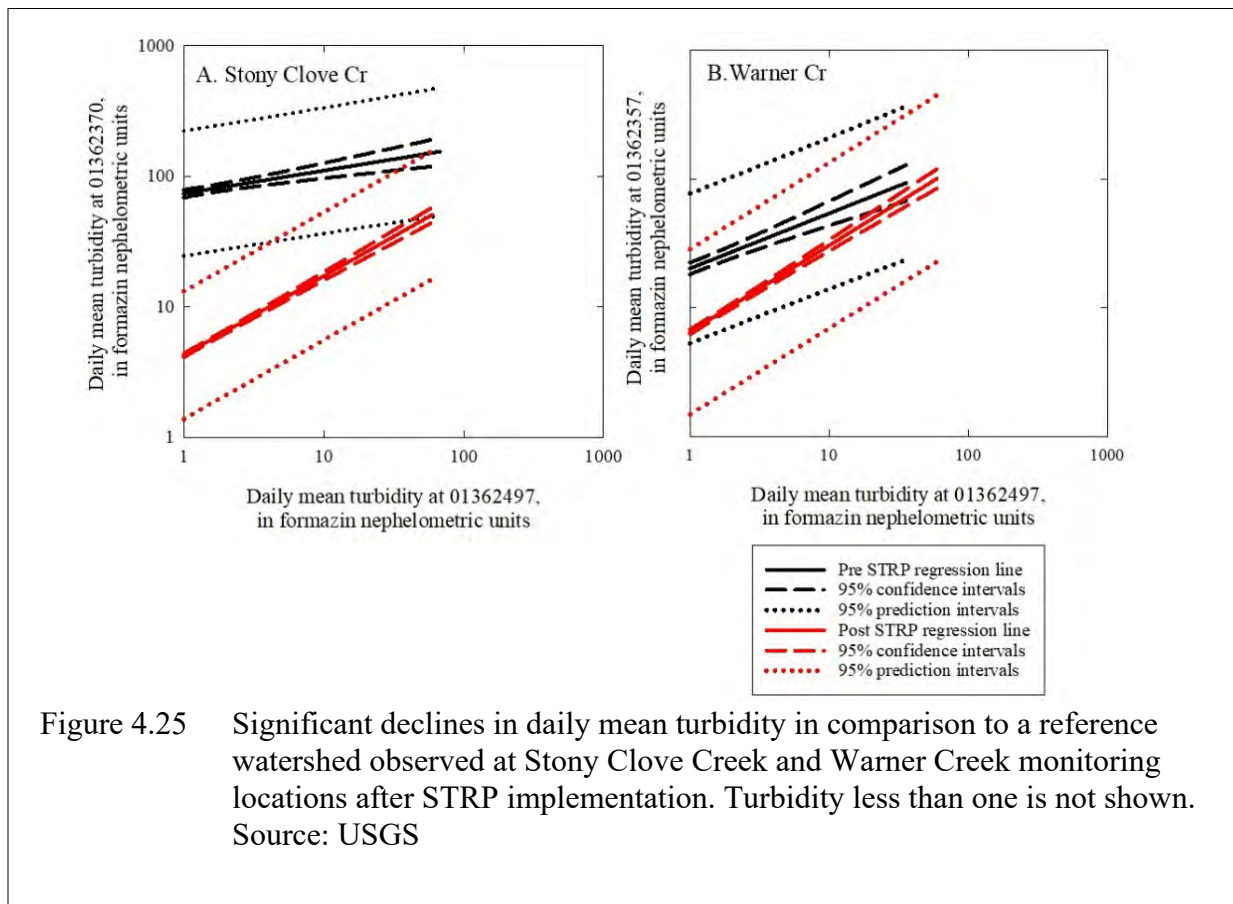


Figure 4.25 Significant declines in daily mean turbidity in comparison to a reference watershed observed at Stony Clove Creek and Warner Creek monitoring locations after STRP implementation. Turbidity less than one is not shown. Source: USGS

## Discrete data analysis at the watershed scale

Discrete sample SSC from Esopus Creek at Coldbrook was used to investigate changes in SSC at the UEC watershed scale that could have resulted from the implementation of the STRPs in all the sub-basins, including Woodland Creek and Beaver Kill. Daily mean values were not used because of gaps in monitoring data and changes in monitoring equipment through time at the monitoring site. The non-parametric Mann-Whitney test was used to test for significant differences in SSC in discrete samples collected at streamflows greater than  $Q_{10}$ . The relation between streamflow and discrete SSC was analyzed using an analysis of covariance (ANCOVA) on  $\log_{10}$  transformed data, like the methods described in section 2.3.1.

The SSC in samples collected at streamflows greater than  $Q_{10}$  before and after all STRPs were tested to investigate differences in SSC between the two time periods. There was a significant ( $p < 0.001$ ) decline in SSC in discrete samples at streamflows greater than  $Q_{10}$  after all STRPs were completed in the sub-basins (Figure 4.26). The median values decline from 660 to 200 mg/L.

There was a significant decrease ( $p < 0.05$ ) in discrete SSC per unit streamflow after completion of the STRPs in the UEC watershed (Figure 4.26). Small decreases in the slope and intercept of the streamflow-SSC regression lines were measured, 1.02 to 0.99 and -1.24 to -1.39, respectively.

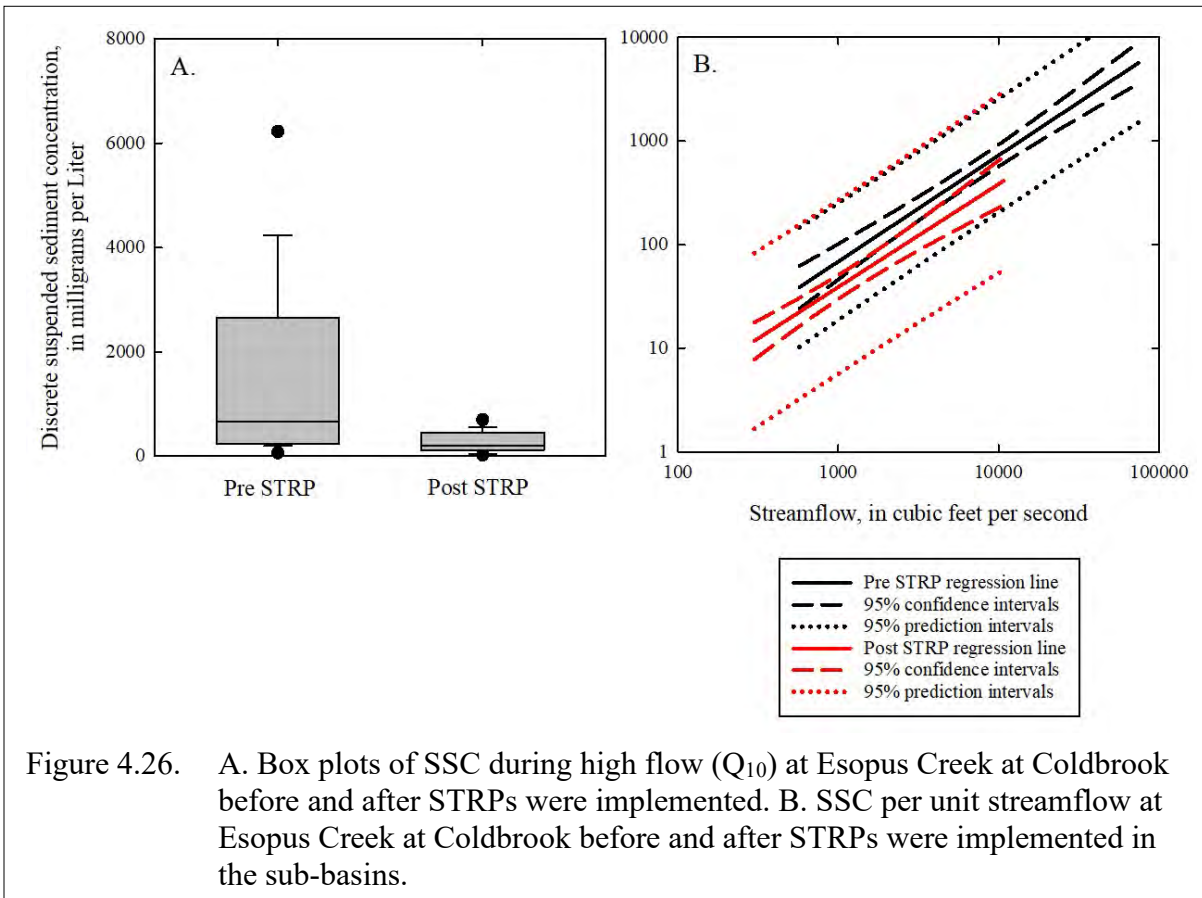


Figure 4.26. A. Box plots of SSC during high flow ( $Q_{10}$ ) at Esopus Creek at Coldbrook before and after STRPs were implemented. B. SSC per unit streamflow at Esopus Creek at Coldbrook before and after STRPs were implemented in the sub-basins.

## Cornell University Analysis

### Dynamic linear modeling (DLM) analysis

DEP collaborated with Cornell University researchers in 2019 and 2020 to investigate use of the time-varying regression approach, referred to as a dynamic linear model (DLM), to quantify how SS flow-yield changes over time in the Stony Clove sub-basin and to distinguish changes potentially attributable to STRPs versus hydrologic forcing conditions. SS flow-yield is a term defined in this research as changes in SSC per unit flow. The research included a more expansive investigation using a process-based model (the River Erosion Model (REM); Lammers and Bledsoe, 2018) to simulate natural fluvial processes in the Stony Clove sub-basin in the absence of STRPs to generate simulated SS flow-yield used to compare with observed SS flow-yield data which reflected both natural and STRP influences.

The DLM regression method is detailed in Wang et al. (2021). The regression parameters in the DLM are related to fluvial system processes. The magnitude of the intercept parameter represents the erodibility and sediment availability of a watershed and is associated with the erosive material composition, land cover, and geomorphology, while the slope parameter represents a stream's erosive capacity (Asselman, 2000; Ahn et al., 2017; Wang and Steinschneider, 2022). By allowing the intercept parameter to change at each time step, DLMs can characterize how erodibility of the watershed changes over time by quantifying shifts in SS flow-yield. The time-varying intercept is particularly helpful in quantifying the effectiveness of STRPs, since these projects are designed to stabilize the stream channels and reduce the active channel margins from erosional contact with non-alluvial SS sources. Comparing the intercept parameter progression before, during, and after STRP installation dates, allows for continuously monitoring the impact of STRPs on SS flow-yield over time.

Due to the complexity and breadth of the research performed, this section only presents the basic results of the analysis performed within the Stony Clove sub-basin that investigated the impacts of the timing of STRPs I, II, III and VI that were installed between 2012-2015 and between monitoring stations #01362350 (upstream) and #01362370 (downstream). By comparing the DLM intercept parameter at the downstream station (blue line) to the parameter at the upstream station (pink line) SS flow-yield declines shortly after the completion dates of the four STRPs at the downstream station (Figure 4.27). While there is a clear decline in the intercept parameter at #01362370, the intercept at the upstream station is relatively flat (Figure 4.27a). The intercept time series at the two stations exhibit similar intra-annual variations, except for the steeper downward slope at the downstream station during the overlapping period. These results provide evidence that appears to support the effectiveness of STRPs in reducing SS flow-yield. However, data at station #01362350 does not extend back prior to 2014, and so the analysis is unable to determine whether the downward trend in the intercept at #01362370 between 2011 and 2014 is unique to that station (and thus attributable to STRPs constructed in 2012 and 2013) or would have been seen at station #01362350 as well (and thus more indicative of natural recovery). Prior analyses by USGS suggest that the observed declines are coincident with the 2012 and 2013 STRPs.

On Warner Creek, only STRP II lies between the downstream (#01362357) and upstream (#01362367) stations (Figure 4.27b). There is a clear decline in the downstream intercept (blue line) immediately after the STRP completion date, suggesting some SS flow-yield reductions were achieved. However, the intercept at that site begins to trend upward starting in the middle of 2014. Without data available at the upstream location (pink line) near the STRP construction date, the difference in the intercept parameters between the two locations is unclear. During the overlapping period when both stations have data, the intercepts exhibit similar variability. The two intercepts have almost the same magnitude before 2017, and by the end of the instrumental period, the intercept at the downstream location has trended slightly higher than that at the upstream site. This suggests that, at least for STRP II, there may have been some benefits for reducing SS flow-yield early after construction, but this effect may have waned over time. This is also consistent with past USGS regression analyses for Warner Creek.

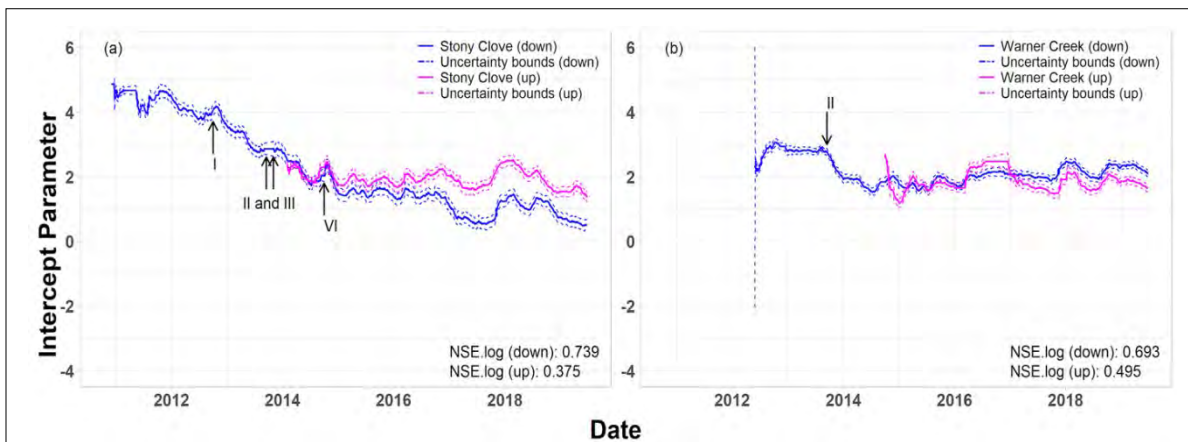


Figure 4.27. DLMs intercept parameters at (a) downstream of Stony Clove Creek and (b) downstream of Warner Creek. Black arrows indicate STRP construction dates. Figure from Wang, et al. 2021.

#### 4.6.3 STRP Turbidity and SS Monitoring: Impact of Water Year 2021

The significant rain-on-snow runoff event occurred in the Stony Clove sub-basin over a 24-hour period between December 24-25, 2020. The resulting flood ranged from a 10-year to 25-year recurrence interval event that produced substantial geomorphic adjustment in all monitored streams (Section 4.5) and transported the highest SS loads observed since STRP implementation began in 2012 (Section 4.4).

The flood accounted for 87% of the total measured SSL exported from Stony Clove sub-basin in water year 2021. The Stony Clove flood SSL accounted for 16% of the total SSL measured at the downstream Esopus Creek station (#01362500) for the flood (equivalent to the drainage area ratio) and 14% of the total SSL for water year 2021 (Table 4.13). With the exception of Esopus Creek at Allaben station (#01362200), all other monitored sub-basins contributed significantly less of the total load (ranging from near 0% to 6%) and much less than

the 1:1 drainage area ratio recorded for Stony Clove Creek. The storm event SSY for Stony Clove Creek was approximately equivalent to that for Esopus Creek at Coldbrook, providing further evidence of the role of SS export from Stony Clove Creek influencing the SS yield delivered to the Ashokan Reservoir during the storm event.

How did this one disturbance event effect the STRP-influenced turbidity production and SS load in Stony Clove sub-basin? Data from Stony Clove Creek station #01362370 suggest a 10-fold increase in the mass of sediment transported for a given flow relative to pre-storm conditions, and that increase persisted for months following the flood. Figure 4.28 is a combined hydrograph and turbidity graph for Stony Clove Creek at station #01362370 for the five-year study period. The increased turbidity for months following the flood is clearly depicted in this plot. Turbidity returned to near pre-storm levels at lower streamflows after 4-6 months but continued to remain above pre-storm levels at higher streamflows for more than a year (Figure 4.29).

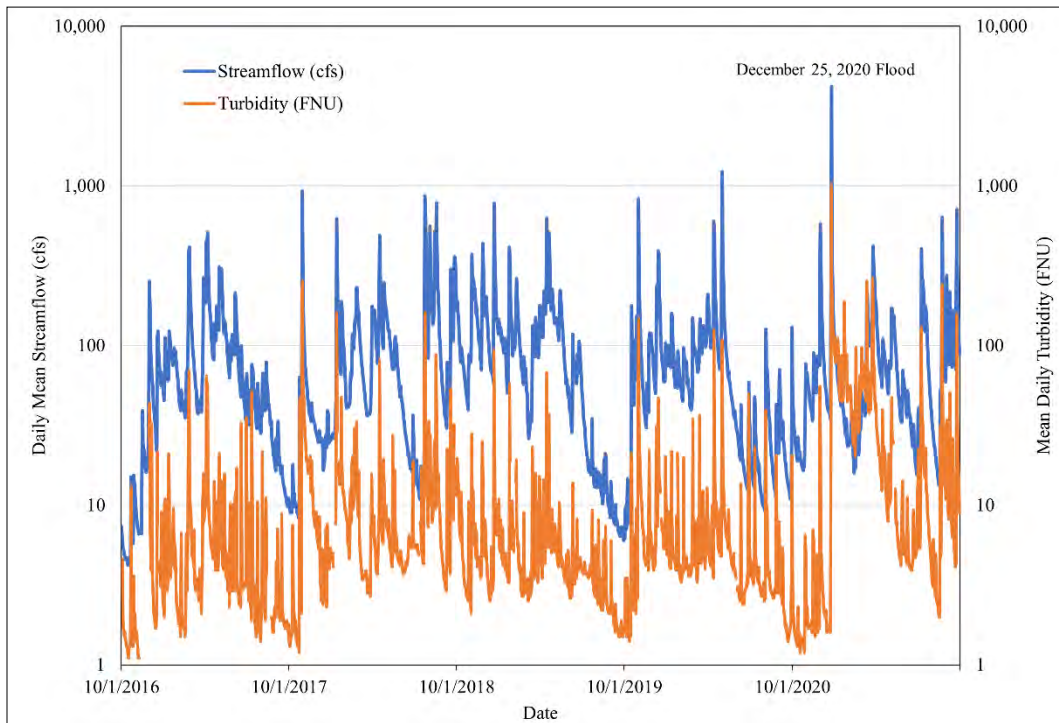


Figure 4.28 Hydrograph and turbidity graph for Stony Clove Creek at station #01362370 for water years 2017-2021 depicting elevated turbidity production response to the December 2020 flood for months following the event.

There was a range of observed geomorphic adjustment (erosion and deposition) that occurred at all STRPs; however, the resumed erosional connectivity with GLS was largely minimal for most STRP reaches. The exception was resumed connectivity with GLS at

streamflow less than bankfull at STRPs V (GT) and VI (GT and LS). Tributary sub-basin and reach-scale monitoring and SFI mapping results clearly show that the largest increases in post-flood sediment transport and turbidity production were due to the Stony Clove tributaries intersecting new GLS sources of sediment during and after the flood rather than failure of the STRPs.

Ongoing analysis of the Stony Clove sub-basin data through water year 2022 and beyond by USGS and DEP using linear regression methods, DLM methods, and turbidity-streamflow hysteresis will continue to investigate the extent and duration of changes in turbidity production and STRP-induced reduction that will be reported in future conference proceedings, peer-reviewed journal publications and FAD reporting.

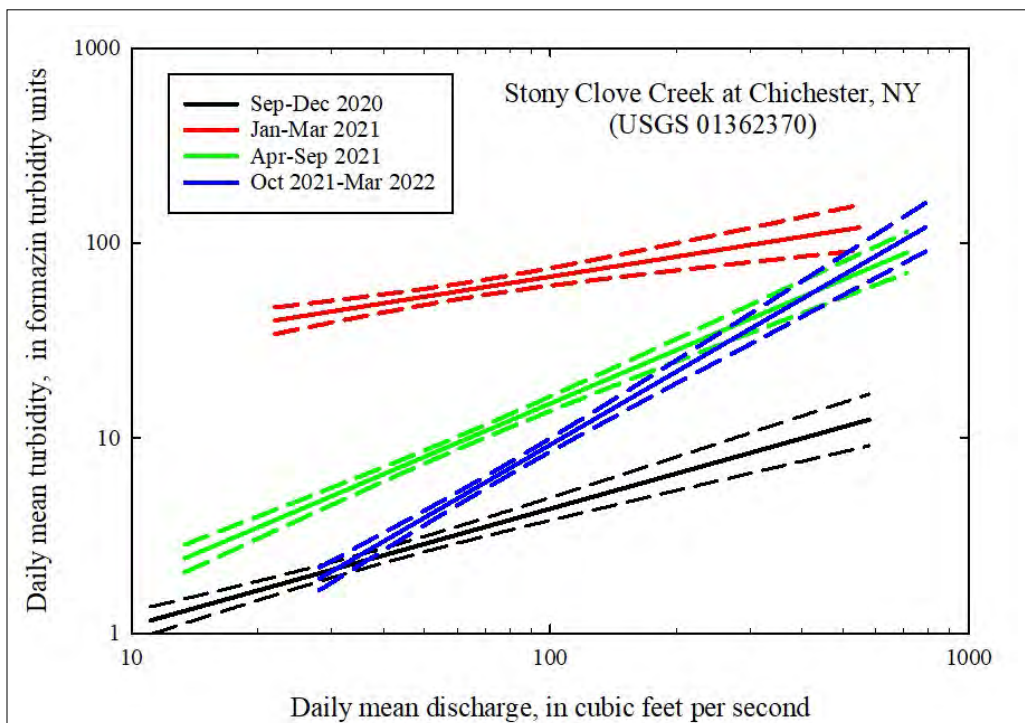


Figure 4.29 Progression of Q-Tn regression relationships from September 2020 to March 2022, depicting the impact of the December 2020 flood and the post-flood recovery conditions.

## 5. Discussion

At the mid-point in this 10-year study, DEP and USGS have collected and analyzed sufficient streamflow, turbidity, suspended sediment concentration and source data to reach some provisional findings that can offer preliminary answers to the New York City water supply resource management questions posed in Section 3.1:

- What are the primary sub-basin sources and causal factors influencing turbidity delivered to the Ashokan Reservoir?
- Can stream management practices reduce stream turbidity and suspended sediment delivered to the Ashokan Reservoir?

The following sections discuss the status of meeting the stated study goals and objectives with the first five years of data acquisition and preliminary analysis.

### 5.1 Turbidity and Suspended Sediment Production in the UEC

A prime objective of this study is to quantitatively characterize spatially and temporally variable turbidity and SS production in the UEC watershed that can be used to inform stream turbidity reduction management strategies through STRP implementation. The results presented in Section 4 can be used to provide a quantitative ranking of turbidity and SS production using a combination of the presented metrics: Q-Tn relations, turbidity exceedance values and annual SS load and yield.

Figure 4.4 and Table 4.7 presented the regression relationships and regression slopes and intercepts between streamflow and turbidity for the monitored UEC sub-basins and two mainstem Esopus Creek stations based on the first five years of data. This analysis lumps the inter-annual variability, and these relations change on a year-to-year basis, yet a multi-year composite allows for the analysis to minimize bias by a given year or event.

The regression slopes and intercepts can be related to fluvial system processes as described in Section 4.6 for the Cornell University DLM analysis. In the study area, the magnitude of the intercept is interpreted to represent the availability of turbidity source sediment as a function of stream corridor geologic composition and channel geomorphic condition. High magnitude intercepts are produced when turbidity source sediment is readily available at lower flows and are indicative in this study of the probable occurrence of elevated erosional sediment connectivity with GLS, especially LS. This interpretation is based on the source characterization results presented in Section 4.5. The slope parameter represents the erosive capacity of the stream to entrain and mobilize source sediment. High magnitude slopes can be indicative of streams having a higher hydrogeomorphic threshold to access stores of fine sediment, such as re-suspension of in-stream stored sediment.

Since STRPs have been demonstrated to be effective at modifying the regression intercept, e.g., reducing turbidity and SSC at streamflow below bankfull, it is helpful to start with a review of the data presented in Table 4.7. The monitored UEC sub-basin streams Q-Tn relations intercepts are in ranking order (excluding Esopus Creek at Allaben and Esopus Creek at

Coldbrook): Broadstreet Hollow Brook (0.6), Birch Creek (0.03), Woodland Creek (-0.02), Bushnellsville Creek (-0.21), Stony Clove Creek (-0.28), Little Beaver Kill (-0.56), Beaver Kill (-0.72), and Esopus Creek headwaters (-0.82).

The position of Stony Clove Creek in fifth place at generating turbidity at lower flows since 2016, when previous monitoring studies found it to be the highest producer at all flows (McHale and Siemion, 2014; Siemion et al., 2016) is further indication of how effective STRP implementation has been at modifying turbidity production in that sub-basin. Evaluating the Q-T<sub>n</sub> intercept information in combination with the annual streamflow and runoff data presented in Tables 4.1 and 4.2 reorders the ranking. While Birch Creek can produce elevated turbidity at lower streamflows, the relative contribution to the UEC watershed is relatively low. Though there is no monitored streamflow data for Broadstreet Hollow or Bushnellsville Creek, based on their drainage areas it is reasonable to assume that they are also relatively small contributors to the UEC watershed streamflow during these lower flow conditions. Given this, Woodland Creek and Stony Clove Creek are the likely highest contributors to Esopus Creek at lower to moderate streamflows.

A review of regression slopes finds that Beaver Kill (0.81) and Esopus Creek headwaters (0.67) have the greatest increase in turbidity as Q increases, followed by Birch Creek (0.62) and Stony Clove Creek (0.61). Interestingly, Beaver Kill transitions from a low turbidity producer at lower flows to a high turbidity producer at higher flows. Unfortunately, the available erosional sediment connectivity data for Beaver Kill is not coincident with the monitored conditions and it is not known at this time why this stream has this turbidity production dynamic, though it may be partially explained by the coarser grain size distribution of the sampled suspended sediment. The coarser the fine sediment the less effective it is at scattering light and influencing turbidity, thus it may take higher streamflow conditions to obtain SSC capable of producing very high turbidity values.

The turbidity exceedance data (Table 4.8; Figure 4.30) computed by USGS is also helpful in attempting to rank turbidity production in the UEC watershed. Woodland Creek and Stony Clove Creek generate the highest values for high flow conditions represented by T<sub>1</sub> and moderate flow conditions (T<sub>10</sub>). Broadstreet Hollow Brook, Beaver Kill and Birch Creek are all grouped together as a second tier of turbidity producing streams in the moderate to high flow category.

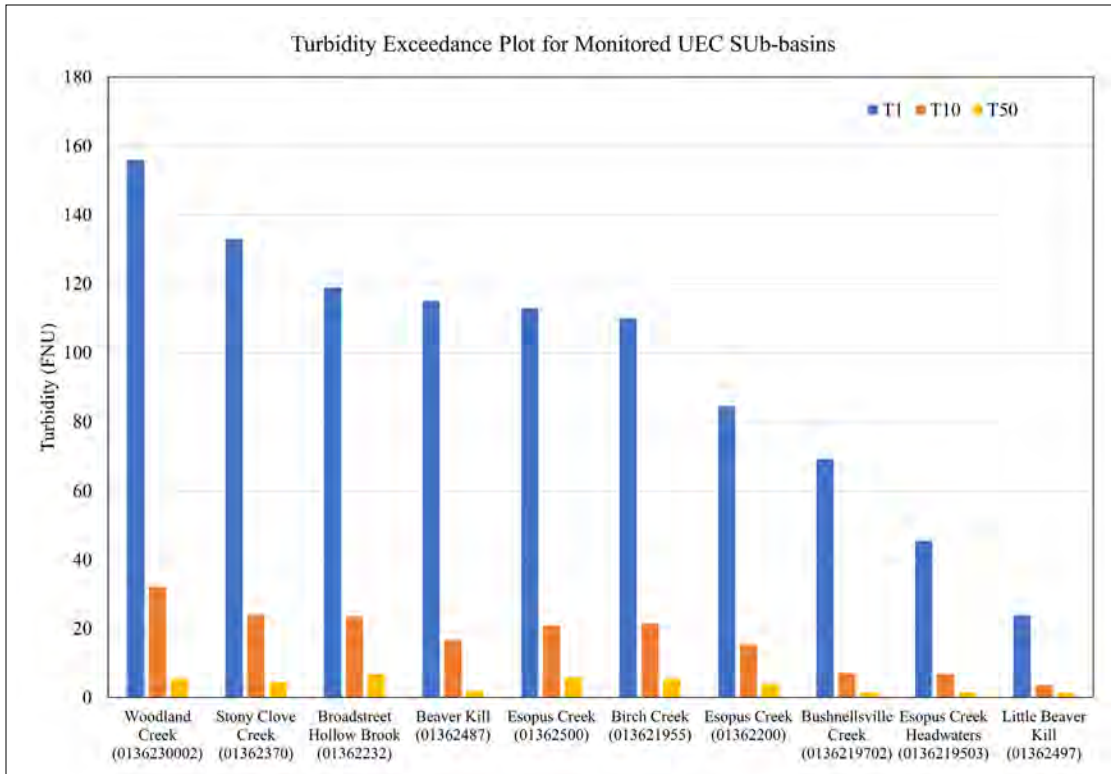


Figure 4.30 Turbidity exceedance chart for monitored UEC sub-basins for USGS water years 2016-2021.

Based on the turbidity and streamflow data so far, DEP concludes that Stony Clove Creek and Woodland Creek are still the top tier turbidity producers in the UEC watershed. They also have elevated turbidity at moderate flows that might be impacted by STRP implementation and therefore are recommended as sub-basins to continue intensive intra-sub-basin monitoring and geomorphic investigations that can inform a turbidity reduction strategy, especially if the strategy is to potentially have a measurable impact on the Ashokan Reservoir.

The smaller drainage area sub-basins with high turbidity production potential could also be suitable for STRP implementation if the reduction target is focused solely at the sub-basin scale. Broadstreet Hollow data suggests this can be a high turbidity production stream, especially at lower streamflow. The USGS monitoring station was converted from a secondary monitoring station to a primary station in 2022 which will allow more accurate estimate of streamflow-turbidity relations. Broadstreet Hollow has not had a geomorphic assessment since 2001 and current turbidity monitoring results suggest an assessment is merited. Beaver Kill and Birch Creek are also notable turbidity producers and have not had a geomorphic assessment in several years.

The review of the SS data presented in Section 4.4 finds a difference between turbidity production ranking and SS production ranking. Because SSC is a mass-based property, it can be

combined with streamflow to provide a more accurate comparison of relative loads and yields influencing the water delivered to the Ashokan Reservoir. It is complicated by the fact that SSC contains sediment ranging from the smallest clay minerals to sand. The complication is that a given stream sample may have a higher SSC but have a lower turbidity value, if the SSC includes coarser size fractions because turbidity is significantly more influenced by clay than silt and sand. Figure 4.9 depicting the grain size distribution of sampled suspended sediment for each UEC watershed primary station illustrates this variation. Beaver Kill and Esopus Creek headwaters have a relatively lower percentage of sediment less than 0.0625 mm while Stony Clove Creek and Woodland Creek have a higher percentage of silt and clay in suspension. Not surprisingly this influences differences between SSC values and Tn values among these streams. Beaver Kill and Esopus Creek headwaters can generate higher SSL and SSY for a given year, while Woodland Creek and Stony Clove Creek will still have higher turbidity levels.

Excluding the two Esopus Creek stations that include other monitored streams, Beaver Kill and Esopus Creek Headwaters have the highest mean SSL and SSY for the first four years through water year 2020 (Table 5.1). Stony Clove Creek has the third highest mean SSL for that period and Woodland Creek the fourth highest SSL. The latter two are reversed for SSY. The impact of the December 2020 flood in water year 2021 on the five-year mean is very evident, with Stony Clove Creek having the highest SSL and SSY mean values, highlighting both the importance of big floods on loads and yields and the importance of the study period extending to 10 years to help minimize the impact of a given year on the mean values, as well as to include a more representative range of flows across the study area. These SS results reveal that five years is an insufficient period to have a robust evaluation of turbidity and SS production in the study area.

Table 5.1 Annualized mean SS loads (t, short tons) and yields (t/mi<sup>2</sup>) for UEC sub-basins for two periods: 2017-2020 and 2017-2021. Water year 2021 data vary depending on last day of regression equation validation.

Stream	USGS Station ID	SSL 2017-2020 mean (t)	SSL 2017-2021 mean (t)	SSY 2017-2020 mean (t/mi <sup>2</sup> )	SSY 2017-2021 mean (t/mi <sup>2</sup> )
Esopus Creek Headwaters	0136219503	2,799	4,499	95	152
Birch Creek	013621955	985	1,182	79	95
Woodland Creek	0136230002	1,878	3,450	91	168
Stony Clove Creek	01362370	2,642	11,553	85	374
Beaver Kill	01362487	5,575	8,920	223	357
Little Beaver Kill	01362497	558	610	34	37

Based on the turbidity and SS data, it is clear that Stony Clove Creek and Woodland Creek still have a disproportionate contribution of turbid streamflow to the Ashokan Reservoir and merit the ongoing assessment and STRP implementation planned in these sub-basins.

## 5.2 Turbidity and SS Production in the Stony Clove Sub-basin

The monitoring and source characterization results for the Stony Clove sub-basin covering the first five years of the study can guide further assessment and turbidity reduction efforts in this sub-basin that still ranks as one of the highest contributors to turbid streamflow delivered to the Ashokan Reservoir. Using the same turbidity and SS metrics used for the UEC watershed characterization it is possible to provide a preliminary ranking of Stony Clove Creek and its monitored sub-basins. The current state of the study, however, has not adequately investigated the reach-scale production to rank the reaches within the Stony Clove sub-basin, though the mapped 2021 erosional sediment connectivity sources in Hollow Tree Brook and Ox Clove Creek are disproportionately significant turbidity production reaches. The monitoring and SFI data is available and will be investigated for a more thorough ranking prior to the next status report.

Using the streamflow-turbidity regression intercept and slope data presented in Figures 4.5 to 4.7 and Table 4.9, both Stony Clove Creek stations had lower intercept values than any of the tributary streams before the December 2020 flood, indicating that the majority of the chronic low flow turbidity sources originated in the tributary streams. The lower Stony Clove Creek station had an increased intercept after the flood but was still lower than the three main tributaries that supplied turbid streamflow to the main channel.

Ox Clove Creek, before the December 2020 flood is the most turbidity prone tributary at lower streamflows and is the second highest behind Warner Creek at higher streamflows. Before the December 2020 flood, Hollow Tree Brook and Myrtle Brook generally had low turbidity production capacity. Given the very low coefficient of determination for the Hollow Tree Brook regression, its regression and parameters are not considered reliable. However, the turbidity exceedance data (Table 4.10) demonstrates that Hollow Tree Brook was a very low turbidity production stream during the first four years of the study.

Following the December 2020 flood, all monitored streams had significantly elevated turbidity production across the range of monitored streamflow, except for Warner Creek which had lower turbidities in the higher range, which may be attributable to the two STRPs constructed during the monitoring period. Hollow Tree Brook and Ox Clove Creek became the highest turbidity contributing tributaries.

The evaluation of the study period mean SSL and SSY results for the Stony Clove streams is significantly limited by the missing values in 2020 and 2021 for Hollow Tree Brook and Myrtle Brook. In the first three years, the two Stony Clove Creek stations had the higher SSL values based on contributing loads from the other streams for the lower station and from the streamflow component in the upper station. The highest tributary load during that three-year period was from Warner Creek, followed by Ox Clove Creek, Hollow Tree Brook and Myrtle Brook. For the stations that had complete records through the five years, the mean load contributions were the same ranking.

The SSY ranking for the first three years is the upper Stony Clove Creek (influenced strongly by the 2018 data), followed by Ox Clove Creek, lower Stony Clove Creek, Warner

Creek, Myrtle Brook and Hollow Tree Brook. Following the flood, for the stations with complete records, the two Stony Clove Creek stations had the highest mean SSY followed by Warner Creek and Ox Clove Creek. Because the turbidity data is more continuous through the monitoring period, it is expected that Hollow Tree Brook would likely have the highest SSL and SSY for the period following the December 2020 flood.

Based on these turbidity and SS monitoring results and the impact of the December 2020 flood, it is evident that Hollow Tree Brook, Ox Clove Creek and Warner Creek are the current highest contributing sources of turbidity to Stony Clove Creek and thus have some influence on the turbidity measured at the Esopus Creek at Coldbrook station. Continued monitoring will be examined to evaluate the legacy impact of the December 2020 flood, in the absence of other similar magnitude events. Similarly, DEP is currently investigating use of turbidity-streamflow hysteresis patterns to evaluate the current legacy impact of the flood on subsequent turbidity generating streamflow events.

The extensive field-based geomorphic investigations in the Stony Clove sub-basin have demonstrated the role of erosional sediment connectivity as a major factor in explaining turbidity production in the study area. The measured channel adjustment in erosional connectivity with GLS in the banks and streambed is proportional to the measured increase in turbidity and SS production. Geomorphic connectivity to GLS is heterogeneously distributed in the sub-basin and is a primary intrinsic landscape property that determines spatial and temporal distribution of turbidity production at flows below floods capable of resuspending sediment stored in streambed alluvium. More specifically, connectivity to LS is a disproportionate loading source in the Stony Clove sub-basin, and presumably in the UEC watershed. Based on these findings, DEP recommends that the AWSMP and/or other researchers consider adoption of a streamlined SFI methodology focused on mapping erosional connectivity with GLS in some of the other high turbidity production sub-basins, coincident with the study monitoring period to help improve understanding of monitored turbidity production in the UEC watershed. This improved understanding and awareness of reaches with disproportionate connectivity with LS could better inform UEC turbidity reduction efforts.

### **5.3 Turbidity Reduction Through STRPs**

Provisional results show that STRPs concentrated within a single high turbidity producing sub-basin can be very effective in turbidity reduction for flows below the assumed hydrogeomorphic threshold that resuspends stored fine sediment. Thus far, the study supports a management strategy that concentrates turbidity reduction efforts in a select set of high turbidity producing sub-basins to get an optimally scaled impact that can potentially be measured at the reservoir basin scale.

With the occurrence of the December 2020 flood during the reporting period, it is clear that big floods export the most fine sediment and produce the biggest turbidity impacts that could affect reservoir management. This is not a surprising finding based on past research (Mukundan et al., 2013) but it is useful to have continued supporting evidence that floods that impact reservoir management exceed the capacity for existing STRPs to effectively reduce turbidity

during widely sourced flow events. However, preliminary analysis presented in Section 4.6 also finds that the STRPs in the Stony Clove sub-basin generally withstood the driving force of the flood's stream power, which in turn may have contributed to the measured recovery of the lower streamflow end of the streamflow-turbidity relationship. Certainly, more monitoring is needed to robustly analyze this supposition. The potential management significance is that the legacy impact of a large SS loading/turbidity production event can be diminished. The December 2020 flood focused primarily on the Stony Clove sub-basin, thus limiting the reach and applicability of the provisional findings.

STRPs are constructed to be resistant to erosion and prevent channel adjustment back into GLS. They are however susceptible to being breached and becoming turbidity production hotspots again. This did happen with the Woodland Creek at Wilmot Way STRP constructed in 2018. Following the 5-year RI scale flood in Woodland Creek, the STRP reach incised and laterally eroded into LS impacting turbidity production for an uncertain period. There was no active monitoring upstream or immediately downstream following the flood to measure the impact. This has not happened in the Stony Clove sub-basin yet, though several STRPs did adjust and are more prone to resumed connectivity. This suggests there is a limit on the sustainability of STRPs and that future designs, monitoring and/or maintenance planning may need to factor this into the turbidity reduction effort.

## **5.4 Conceptual Framework Suitability**

The geomorphic connectivity framework used to develop a simplified conceptual model of turbidity production drivers and controlling factors has thus far proven to be sufficient for capturing driving (hydrology) and controlling (sediment connectivity) variable data and response data (turbidity and SS load and yield). Although the simple model ignores a lot of contributing factors and nuances within the investigated drivers and controls that influence turbidity production, it is sufficient to show how big floods can drive immediate and lasting changes in turbidity productivity; it accounts for spatial variability in sediment supply via connectivity with GLS; it uses the monitoring network to account for the spatial and temporal variations in turbidity and SS production delivered to an observation point; and it is useful in relating STRPs to measured reductions in turbidity, SS load and yield.

The December 2020 flood and preceding bankfull floods in the Stony Clove sub-basin provided an excellent opportunity to test the value of the conceptual model and assumptions on turbidity production related to the hypothetical hydrogeomorphic thresholds. The flood RI range computed by USGS and presented in Table 4.6 was 10 to 25 years for the study area basin "integration" station at Esopus Creek at Coldbrook (#01362500) and a similar range for the Stony Clove sub-basin "integration" station at Stony Clove Creek at Chichester (#01362370). In the case of Stony Clove Creek, it is clear in the data presented in Sections 4.3 to 4.6 that the flood did produce a geomorphic response that increased turbidity and SS production by an order of magnitude and increased sediment connectivity by up to a factor of approximately six. As predicted by the stated hypothesis, the sediment connectivity in the sub-basin increased throughout the stream system and had a legacy impact on turbidity production that lasted through the reporting period.

While the model has proven useful, the analysis of existing data is not yet sufficient to fully test the veracity of some of the assumptions in the model. There is also a lack of data to fully evaluate those assumptions throughout the entire study area. For example, the hydrogeomorphic thresholds assumption of a 10-year RI scale event causing an acute and chronic adjustment to streamflow-turbidity dynamics through system scale geomorphic adjustment is too simple for what occurred in the Woodland Creek sub-basin. This same event was a 5-year RI event for Woodland Creek yet the increase in turbidity production was high and prolonged. The measured impact of the flood was not examined like it was for Stony Clove Creek, where the study focused the turbidity source characterization investigations and STRP evaluation.

Based on field observations by the AWSMP and DEP, much of the Woodland Creek turbidity production originated in a few locations that increased turbidity through increased connectivity with LS in the Woodland Creek tributary Panther Kill and at some previously mapped locations in Woodland Creek, including the STRP constructed in 2018. Without the before-after erosional sediment connectivity mapping it is not possible to quantify the scale of the geomorphic response and relate that to the turbidity production response. In this scenario a lower hydrologic threshold generated a substantial increase in turbidity production but seems to have had a less widely distributed geomorphic adjustment. This may highlight the importance of the heterogeneity in spatial distribution of source material in each sub-basin and that some reaches may be very susceptible to adjustment into GLS. Given the evident importance of source sediment heterogeneity and the complexities of network scale geomorphic process sequences, turbidity production and suspended sediment supply are influenced by stochastic spatial and temporal patterns that are impractical to predict. This does not mean the study conceptual model needs to be revised but it does suggest that, not surprisingly, turbidity production in the study area is far more complex than a simple model, and even an ambitious field investigation can account for.

## **5.5 Next Steps**

DEP and USGS will continue monitoring and source characterization through water year 2026. In the near term, USGS will continue the side-by-side different turbidity probe monitoring evaluation at two monitoring stations and detail any changes and impacts of equipment on the study future findings. As explained earlier, the change was deemed necessary to improve the range of measured turbidity values and increase efficiency in keeping the equipment calibrated.

BEMS monitoring is still undergoing data and analysis review. This component has served well in selecting STRPs and getting a time-series of channel adjustment through hydrology that can inform STRP design. There is the potential for reach-scale sediment budget estimates/simulations but this will not likely advance in this study and will be promoted as potential research for other researchers that may use the data. DEP plans to continue working with SLR Consulting to monitor, model and sample the BEMS sites through 2023.

The previous successful testing of sediment fingerprinting by USGS researchers as a tool for further quantitative evidence of the role of the various turbidity source sediments (AL, LS, GT) will be a primary component in advancing geomorphic source investigations.

In late 2022, DEP met with University of Vermont and other USGS researchers to optimize use of the study data for developing machine learning based turbidity forecasting in the UEC watershed. The researchers obtained National Oceanic and Atmospheric Agency and National Science Foundation funding for two related efforts to use the UEC streamflow, turbidity, SS and source characterization data to advance machine learning application in stream turbidity forecasting. This is well beyond the scope of this DEP-USGS study, yet it serves as an excellent example of DEP following up on recommendations of the National Academies of Science, Engineering and Medicine Expert Panel to partner with other researchers to advance analysis of the data.

## **6. Study Mid-Term Conclusions**

The geomorphic connectivity conceptual framework guiding data acquisition and analysis is proving to be useful for explaining turbidity production at a range of spatial, temporal and hydrologic scales. USGS has successfully completed the first five water years of monitoring streamflow, turbidity and SS while DEP continued to quantitatively characterize geomorphic connectivity to turbidity/SS sources in the Stony Clove sub-basin. Multiple analytical methods were successfully employed to demonstrate the turbidity reduction efficacy of the STRPs constructed in the Stony Clove sub-basin between 2012-2016. Stony Clove sub-basin STRPs constructed in 2021 and 2022 will provide the first chance to conduct an upstream/downstream, before/after evaluation of turbidity reduction efficacy at the reach scale to help meet the study objective of evaluating STRP efficacy from reach to reservoir basin scale.

One of the big questions this study intends to answer, as feasible, is the impact of big floods on diminishing STRP efficacy. Preliminary results of STRP monitoring indicate that for the observed range of streamflow conditions through water year 2021, the Stony Clove sub-basin STRPs are still effective in reducing turbidity and SSC even after a 10-25 year recurrence interval flow in late December, 2020, though their reduction impact has diminished in the context of new connectivity sources significantly controlling spatial and temporal turbidity production.

DEP expects that the next five years of monitoring, source characterization and STRP implementation and evaluation will complete a robust data set that can be used by USGS, DEP, partners and other researchers to investigate and analyze turbidity production and reduction potential through management in a glacially conditioned mountain stream system.

## 7. References

- Ahn, K. H., Yellen, B., & Steinschneider, S. 2017. Dynamic linear models to explore time-varying suspended sediment-discharge rating curves. *Water Resources Research*, 53, 4802–4820. <https://doi.org/10.1002/2016WR019804>.
- Asselman, N. E. M. 2000. Fitting and interpretation of sediment rating curves. *Journal of Hydrology*, 234, 228–248. [https://doi.org/10.1016/S0022-1694\(00\)00253-5](https://doi.org/10.1016/S0022-1694(00)00253-5)
- Baldigo, B.P., Ernst, A.G., Warren, D.R. and Miller, S.J., 2010. Variable responses of fish assemblages, habitat, and stability to natural-channel-design restoration in Catskill Mountain streams. *Transactions of the American Fisheries society*, 139 (2), 449-467. <https://doi.org/10.1577/T08-152.1>
- Cadwell, D. H. 1986. Late Wisconsin Stratigraphy of the Catskill Mountains. In D.H. Cadwell, ed., *The Wisconsinan Stage of the First Geological District, Eastern New York*. NYS Museum Bulletin 455.
- Castro, J.M., and Thorne, C.R. 2019. The stream evolution triangle triangle: integrating geology, hydrology, and biology. *River Research Applications*. 2019:1-2. <https://doi.org/10.1002/rra.3421>
- Cienciala, P., Nelson, A.D., Haas, A.D., Xu, Z. 2020. Lateral geomorphic connectivity in a fluvial landscape system: Unraveling the role of confinement, biogeomorphic interactions, and glacial legacies. *Geomorphology*. 354: 1-20. <https://doi.org/10.1016/j.geomorph.2020.107036>
- Cornell Cooperative Extension Ulster County, NYC DEP, and U.S. Army Engineer Research Development Center. 2007. Upper Esopus Creek Management Plan, Volume 3. P 121-129.
- Davis, D., Kneupfer, P., Miller, N. and Vian, M. 2009. Fluvial geomorphology of the upper Esopus Creek watershed and implications for stream management. In *New York State Geological Association 81<sup>st</sup> Annual Meeting Field Trip Guidebook*. New York State Geological Society; 8.1-8.20.
- DEP. 2008. Evaluation of Turbidity Reduction Potential through Watershed Management in the Ashokan Basin. Valhalla, NY.
- DEP. 2017. Upper Esopus Creek Watershed turbidity/Suspended Sediment Monitoring Study: Project Design Report. Valhalla, NY.
- DEP. 2019a. Upper Esopus Creek Watershed Turbidity/Suspended-Sediment Monitoring Study: Biennial Status Report. Valhalla, NY.

- DEP. 2019b. Stony Clove Watershed Suspended-Sediment and Turbidity Study: Turbidity Reduction Project Nomination Report. Valhalla, NY.
- DEP. 2021. Upper Esopus Creek Watershed Turbidity/Suspended-Sediment Monitoring Study: Biennial Status Report. Valhalla, NY.
- Dethier, E., Magilligan F.J., Renshaw, C.E., Noslow, K.H. 2016. The role of chronic and episodic disturbances on channel-hillslope coupling: the persistence and legacy of extreme floods. *Earth Surface Processes and Landforms* 41: 1437-1447.  
<https://doi.org/10.1002/esp.3958>
- Dewberry. 2015. Ulster, Dutchess, and Orange Counties, New York – Sandy LIDAR. U.S. Geological Survey: Rolla, MO.
- Edwards, T.K., and Glysson, G.D. 1999. Field methods for measurement of fluvial sediment: U.S. Geological Survey Techniques of Water-Resources Investigations, book 3, chap. C2, 89 pp. <https://pubs.usgs.gov/twri/twri3-c2/>
- Effler, S., Perkins, M., Ohrazda, N., Brooks, C., Wagner, B., Johnson, D., Peng, F., Bennet, A. 1998. Turbidity and particle signatures imparted by runoff events in Ashokan Reservoir, NY. *Lake and Reservoir Management* 14, 254-265.
- Frei, A., and Kelly-Voicu, P. 2017. Hurricane Irene and Tropical Storm Lee: how unusual were they in the Catskill mountains? *J Extreme Events*, 4(2).  
<https://doi.org/10.1142/S2345737617500099>
- Fryirs, K.A., and Brierley, G.J. 2013. *Geomorphic analysis of river systems: an approach to reading the landscape* Wiley & Sons. 345pp.
- Fryirs, K.A., Wheaton, J.M. and Brierley, G.J. 2015. An approach for measuring confinement and assessing the influence of valley setting on river forms and processes. *East Surface Processes and Landforms* 41, 701-710.
- Gazoorian, C.L., 2015, Estimation of unaltered daily mean streamflow at ungaged streams of New York, excluding Long Island, water years 1961–2010: U.S. Geological Survey Scientific Investigations Report 2014–5220, 29 p. <http://pubs.usgs.gov/sir/2014/5220/>
- Gellis, A.C., and Walling, D.E, 2011, Sediment-source fingerprinting (tracing) and sediment budgets as tools in targeting river and watershed restoration programs: Simon, A., Bennett, S., Castro, J.M., eds., *Stream Restoration in Dynamic Fluvial Systems: Scientific Approaches, Analyses, and Tools*, American Geophysical Union Monograph Series 194, p. 263-291
- Graziano, A. P., and Siemion, J., 2022, Flood-frequency data for select sites in the Esopus Creek Watershed, New York: U.S. Geological Survey data release,  
<https://doi.org/10.5066/P9O6GJCP>.

- Guy, R.P. 1969. Laboratory theory and methods for sediment analysis: U.S. Geological Survey Techniques of Water-Resources Investigations, book 5, chap. C1, 59 pp.  
<https://pubs.usgs.gov/twri/twri5c1/>
- Haskins, M.N., Vollmer, F.W., Rayburn, J.A. and Gurdak, J.J., 2010. Structural and Hydrologic Implications of Joint Orientations in the Warner Creek and Stony Clove Drainage Basins, Catskill Mountains, Eastern New York. In AGU Fall Meeting Abstracts (Vol. 2010, T33D-2295).
- Heckmann, T., Cavalli, M., Cerdan, O., Foerster, S., Javaux, M., Lode, E., Smetanová, A., Vericat, D., Brardinoni, F., 2018. Indices of sediment connectivity: opportunities, challenges and limitations. *Earth Sci. Rev.* 187, 77–108.  
<https://doi.org/10.1016/j.earscirev.2018.08.004>.
- Hinshaw, S., Wohl, E., Davis, D. 2020. The effects of longitudinal variations in valley geometry and wood load on flood response. *Earth Surface Processes and Landforms*.  
<https://doi.org/10.1002/esp.4940>
- Lammers, R.W. and Bledsoe, B.P. 2018. A network scale, intermediate complexity model for simulating channel evolution over years to decades. *Journal of Hydrology* 566: 886-900.  
<https://doi.org/10.1016/j.jhydrol.2018.09.036>
- Levene, H., 1961. Robust tests for equality of variances. *Contributions to probability and statistics. Essays in honor of Harold Hotelling*, 279-292.
- Lumia, Richard, Freehafer, D.A., and Smith, M.J., 2006, Magnitude and frequency of floods in New York: U.S. Geological Survey Scientific Investigations Report 2006–5112, 152 p
- Magilligan FJ, Buraas EM, Renshaw CE. 2015. The efficacy of stream power and flow duration on geomorphic responses to catastrophic flooding. *Geomorphology* **228**: 175–188.
- Matonse, A and Frei, A. 2013. A seasonal shift in the frequency of extreme hydrological events in southern New York State. *Journal of Climate*, 26(23): 9577–9593.  
<https://doi.org/10.1175/jcli-d-12-00810.1>
- McHale, M. R., and Siemion, J. 2014. Turbidity and suspended-sediment in the upper Esopus Creek watershed, Ulster County, New York: U.S. Geological Survey Scientific Investigations Report 2014-5200.
- Miller, S. J., & Davis, D. (2003). Optimizing Catskill Mountain Regional Bankfull Discharge and Hydraulic Geometry Relationships. *Watershed Management for Water Supply Systems: Proceedings of the American Water Resources Association 2003 International Congress*. New York City, NY
- Mukundan, R., D. Pierson, E. Schneiderman, D. O'Donnell, S. Pradhanang, M. Zion, et al. 2013. Factors affecting storm event turbidity in a New York City water supply stream. *Catena* 107:80–88. doi:10.1016/j.catena.2013.02.002

- Nagle, G. N., Fahey, T. J., Ritchie, J. C., and Woodbury, P.B. 2007. Variations in sediment sources and yields in the Finger Lakes and Catskills regions, of New York. *Hydrological Processes* 21, 828-838.
- RACNE. 2012. Terrain Surface Standards, project report, CAT-393 Airborne Lidar Quality Assurance and GIS Terrain Data Development, Phase 2, New York City Department of Environmental Protection.
- Rayburn, J. A., Desimone, D., Staley, A., Mahan, S. and Stone, Byron. 2015. Age of an ice dammed lake on the lee side of the Catskill Mountains, New York, and rough estimates for the rate of ice advance to the last glacial maximum. In *GSA Northeastern Sectional Meeting Abstracts*.
- Rich, J.L. 1934. *Glacial Geology of the Catskills*. New York State Museum Bulletin 299.
- Siemion, J., 2022, Estimated streamflow data and suspended sediment loads for select sites in the Esopus Creek watershed, New York: U.S. Geological Survey.
- Siemion, J., McHale, M.R., and Davis, W.D. 2016. Suspended-sediment and turbidity responses to sediment and turbidity reduction projects in the Beaver Kill, Stony Clove Creek, and Warner Creek, Watersheds, New York, 2010–14: U.S. Geological Survey Scientific Investigations Report 2016–5157, 28 pp.
- Siemion, J., Bonville, D.B., McHale, M.R., and Antidormi, M.R., 2021, Turbidity–suspended-sediment concentration regression equations for monitoring stations in the upper Esopus Creek watershed, Ulster County, New York, 2016–19: U.S. Geological Survey Open-File Report 2021–1065, 27 p., <https://doi.org/10.3133/ofr20211065>.
- Sauer, V.B., and Turnipseed, D.P., 2010, Stage measurement at gaging stations: U.S. Geological Survey Techniques and Methods, book 3, chap. A7, 45 p.
- Staub, L.E., Cashman, M.J., and Gellis, A.C., 2022, Sediment sample data for identifying and monitoring source sediment fingerprints within Stony Clove Creek, Catskills, NY from 2017 to 2020: U.S. Geological Survey data release, <https://doi.org/10.5066/P9YFWCN4>.
- Turnipseed, D.P., and Sauer, V.B., 2010, Discharge measurements at gaging stations: U.S. Geological Survey Techniques and Methods, book 3, chap. A8, 87 p..
- Ver Straeten, C. A. 2013. Beneath it all: bedrock geology of the Catskill Mountains and implications of its weathering. *Annals of the New York Academy of Sciences*. 1298(1), 1–29.
- Wagner, R.J., Boulger, R.W., Jr., Oblinger, C.J., and Smith, B.A. 2006. Guidelines and standard procedures for continuous water-quality monitors—Station operation, record computation, and data reporting: U.S. Geological Survey Techniques and Methods, book 1, chap. D3, 51 pp. <https://pubs.usgs.gov/tm/2006/tm1D3/>
- Wang, K., Davis, D., Steinschneider, S., 2021. Evaluating suspended sediment and turbidity reduction projects in a glacially conditioned catchment through dynamic regression and

- fluvial process-based modelling. *Hydrological Processes*, 35 (9): e14351.  
<https://doi.org/10.1002/hyp.14351>
- Wang, K., Steinschneider, S., 2022. Characterization of multi-scale fluvial suspended sediment transport dynamics across the United States using turbidity and dynamic regression. *Water Resources Research*, 58, e2021WR031863.  
<https://doi.org/10.1029/2021WR031863>
- Wheaton, J.M., Brasington, J., Darby, S.E., and Sear, D.A. 2010. Accounting for uncertainty in DEMs from repeat topographic surveys: improved sediment budgets. *Earth Surface Processes and Landforms* 35: 136–156.
- Wohl, E. 2019. Forgotten legacies: Understanding and mitigating historical human alterations of river corridors. *Water Resources Research* 55: 5181-5201.  
<https://doi.org/10.1029/2018WR024433>
- Wohl, E., Brierley, G., Cadol, D., Coulthard, T.J., Covino, T., Fryirs, K.A. et al. 2019. Connectivity as an emergent property of geomorphic systems. *Earth Surface Processes and Landforms*, 44(1) 4-26. <https://doi.org/10.1002/esp.4434>
- Yellen, B., Woodruff, J.D., Kratz L.N., Mabee, S.B., Morrison, J., and Martini, A.M. 2014. Source, conveyance and fate of suspended sediments following Hurricane Irene, New England USA. *Geomorphology* 226: 124-134.  
<https://doi.org/10.1016/j.geomorph.2014.07.028>

## **Appendix A**

Hydrological Processes journal manuscript documenting modeling analysis of STRP turbidity reduction efficacy conducted by Kezhen Wang (Cornell University), Scott Steinschneider (Cornell University) and Dany Davis (DEP):

## RESEARCH ARTICLE

# Evaluating suspended sediment and turbidity reduction projects in a glacially conditioned catchment through dynamic regression and fluvial process-based modelling

Kezhen Wang<sup>1</sup>  | Dany Davis<sup>2</sup> | Scott Steinschneider<sup>1</sup>

<sup>1</sup>Department of Biological and Environmental Engineering, Cornell University, Ithaca, New York, USA

<sup>2</sup>New York City Department of Environmental Protection, Kingston, New York, USA

**Correspondence**

Kezhen Wang, Department of Biological and Environmental Engineering, Cornell University, 111 Wing Drive, Riley-Robb Hall, Ithaca, NY 14853, USA.

Email: kw577@cornell.edu

**Funding information**

New York State Department of Environmental Conservation, Grant/Award Number: DEC-01-C01205GG-3350000

**Abstract**

Elevated turbidity ( $T_n$ ) and suspended sediment concentrations (SSC) during and following flood events can degrade water supply quality and aquatic ecosystem integrity. Streams draining glacially conditioned mountainous terrain, such as those in the Catskill Mountains of New York State, are particularly susceptible to high levels of  $T_n$  and SSC sourced from erosional contact with glacial-related sediment. This study forwards a novel approach to evaluate the effectiveness of stream restoration best management practices (BMPs) meant to reduce stream  $T_n$  and SSC, and demonstrates the approach within the Stony Clove sub-basin of the Catskills, a water supply source for New York City. The proposed approach is designed to isolate BMP effects from natural trends in  $T_n$  and SSC caused by trends in discharge and shifts in average  $T_n$  or SSC per unit discharge ( $Q$ ) following large flood events. We develop Dynamic Linear Models (DLMs) to quantify how  $T_n$ - $Q$  and SSC- $Q$  relationships change over time at monitoring stations upstream and downstream of BMPs within the Stony Clove and in three other sub-basins without BMPs, providing observational evidence of BMP effectiveness. A process-based model, the River Erosion Model, is then developed to simulate natural, hydrology-driven SSC- $Q$  dynamics in the Stony Clove sub-basin (absent of BMP effects). We use DLMs to compare the modelled and observed SSC- $Q$  dynamics and isolate the influence of the BMPs. Results suggest that observed reductions in SSC and  $T_n$  in the Stony Clove sub-basin have been driven by a combination of declining streamflow and the installed BMPs, confirming the utility of the BMPs for the monitored hydrologic conditions.

**KEYWORDS**

best management practices, extreme events, rating curves, stream restoration, suspended sediment, turbidity, water resources management

## 1 | INTRODUCTION

Suspended sediment (SS) and turbidity ( $T_n$ )-related water resource impairments can cause significant environmental damage and economic costs. These impairments include transporting other pollutants sorbed onto sediment, degrading aquatic habitat, and reducing water supply quality and light transmission through water (Bishop

et al., 2005; Davis-Colley & Smith, 2001; Holtan et al., 1988; Mukundan et al., 2018). These impacts motivate water resources and land use managers to employ fluvial sediment management strategies, but the implementation of these strategies can be difficult. Challenges related to effective management include identifying source conditions of impairments (Giri et al., 2012; Hanief & Laursen, 2019), siting best management practices (BMPs) in the watershed (Himanshu

et al., 2019; Qiu et al., 2018; Steinman et al., 2018; Strauch et al., 2013), quantifying the effectiveness of existing BMPs (Bishop et al., 2005; Engebretsen et al., 2019), and evaluating new BMPs for future climate scenarios (Jeon et al., 2018). BMP selection also needs to be tailored to the physiographic properties of the system under consideration.

The majority of BMP evaluations in the literature are related to agricultural management practices (Giri et al., 2012; Hanief & Laursen, 2019; Strauch et al., 2013). These BMPs include both structural and non-structural management practices that aim to reduce nonpoint source pollutants by controlling runoff, sediment, and nutrient losses from agricultural areas (Jeon et al., 2018). Models containing both process-based and empirical science are often used to evaluate BMP effectiveness. Some models (e.g., the Revised Universal Soil Loss Equation 2 [RUSLE2]; Agricultural Policy Environmental Extender) are designed for field-scale analysis, while others (e.g., the Soil and Water Assessment Tool) have been widely used to evaluate BMPs at the watershed scale (Du et al., 2019; Giri et al., 2012; Hanief & Laursen, 2019; Hoang et al., 2019; Sommerlot et al., 2013). The application of purely statistical models that utilize monitored water quality constituent data to evaluate BMPs is less common, often due to limited observational data. Nevertheless, these statistical models are more computationally efficient and rely on fewer assumptions (Bishop et al., 2005).

In geologic settings that contain significant amounts of fine sediment (silt and clay), stream channel and terrestrial erosion are the primary sources of SS in the fluvial system (Lammers & Bledsoe, 2019; Nagle et al., 2007). These conditions are common in mountainous regions of the northern United States and southern Canada, which experienced repeated glaciation during the Pleistocene, leaving a glacially conditioned landscape enriched in SS source sediment (e.g., glacial till and glacial lacustrine sediment) (Cadwell, 1986; Church & Slaymaker, 1989; Rich, 1934; Yellen et al., 2014). Flood induced mass-wasting in eroding channel margins linked to hillslopes composed of glacial sediment can lead to elevated SS yield for months to years (Dethier et al., 2016; Yellen et al., 2014). In these non-agricultural forested land settings,  $T_n$  induced by high SS linked to stream conditions and processes is a main water quality concern. At reaches that exhibit channel-hillslope coupling and glacially sourced SS, stream restoration projects such as bank stabilization are effective at removing the active channel margins (ACMs) from chronic erosional connectivity with fine sediments (Wohl et al., 2005). However, it is difficult to characterize the relationship between control variables (i.e., channel complexity) and response variables (i.e., water quality) (Wohl et al., 2015). Continuous monitoring of  $T_n$  or suspended sediment concentrations (SSC) upstream and downstream of restoration projects can be very useful to assess project effectiveness (i.e.,  $T_n$  or SSC reductions), although other strategies are possible (e.g., post-construction morphometric monitoring; Siemion et al., 2016; NYC DEP, 2019b).

A unique challenge when assessing BMP effectiveness arises when projects are installed immediately after (and in response to) major disturbance events (e.g., floods), especially when previous water

quality measurements are limited prior to the event. Resource managers are often motivated and have the opportunity to pursue adaptation actions during narrow windows of time following crises, such as extreme events (Young, 2010). However, the installation of BMPs following watershed disturbance events can greatly interfere with the ability to assess BMP effectiveness. First, large floods often occur during or near the end of periods of wet weather, which is then followed by milder hydrologic conditions. This may cause streamflow to trend downward. There is a strong relationship between SS and discharge (Tananaev, 2013), so downward trends in flow could drive declines in SSC and  $T_n$  that are unrelated to BMPs.

In addition, large floods or other such disturbances can significantly elevate levels of SSC and  $T_n$  for extended periods after a disturbance (Ahn et al., 2017; Dethier et al., 2016; Yellen et al., 2014). This long-term hysteresis is driven by degraded channels, mass wasting events and bank failures following the disturbance that continue to add sediments into the fluvial system. These geomorphological responses manifest as a significant increase in the observed SSC or  $T_n$  per unit discharge (hereafter defined as the “SS flow-yield”). The increase in SS flow-yield can persist for months or years after the original disturbance. The natural recovery of the system (i.e., decreases in the SS flow-yield) can co-occur with the BMPs implemented in response to the disturbance, thus obscuring the effectiveness of those BMPs.

BMP evaluation is further complicated by a frequent lack of  $T_n$  or SSC monitoring data, some of which can be related to declines in the number of SS monitoring programs in the United States (Warrick & Milliman, 2018). Often, BMPs are installed in reaction to disturbance events and not as part of a long-term turbidity reduction strategy. Therefore, long series of monitoring data are often unavailable prior to BMP installation. Similarly, monitoring systems are not always located both directly upstream and downstream of the BMP (due to budgetary constraints), making it difficult to isolate the effects of BMPs from other natural fluctuations in SS flow-yield.

Given the challenges above, this study forwards a novel approach to determine the degree to which observed reductions in  $T_n$  or SSC are attributable to stream restoration projects rather than natural geomorphologic and hydrologic conditions. We demonstrate our approach in a case study of the Stony Clove sub-basin in the upper Esopus Creek (UEC) basin of the Catskill Mountains, which is part of the New York City (NYC) water supply system. The Ashokan Watershed Stream Management Program (AWSMP) funded by NYC Department of Environmental Protection (NYC DEP) invested in a set of eight stream sediment and turbidity reduction projects (STRPs; a type of BMP) following Hurricane Irene in 2011. NYC DEP and USGS have also invested in a multi-year  $T_n$  and SSC monitoring program in the UEC basin (McHale & Siemion, 2014; NYC DEP, 2019a; Siemion et al., 2016). We use three evaluation methods to identify the signals of SS flow-yield reduction that are attributable to the STRPs, including an inter-watershed comparison, a within-watershed comparison, and a series of physics-based scenarios. We apply two separate modelling efforts, one statistical and another process-based, to support these three different evaluations.

## 2 | STUDY AREA AND DATA

### 2.1 | UEC basin, Stony Clove sub-basin, and STRP installation

The UEC is the primary source water for the Ashokan Reservoir in the south-central Catskill Mountains. The basin defines the southern section of the Catskill watershed, which is one of the three watersheds (Catskill, Delaware, and Croton) in the NYC water supply system (Figure 1). This system supplies drinking water to about half of the population of New York State, including over 8.5 million people in NYC and one million people in upstate counties. The Catskill/Delaware system is one of the largest unfiltered surface water supplies in the world (NYC DEP, 2018). The UEC is around 42 km long and drains about 497 km<sup>2</sup> from the headwaters at Winnisook Lake on Slide Mountain to the Ashokan Reservoir. The basin is greater than 90% forested, with a maximum elevation of 1274 m above sea level at Slide Mountain that falls to 178 m above sea level at the inlet to the Ashokan Reservoir. Catskill geology comprising Devonian-aged fluvial sedimentary bedrock and Pleistocene glacial and pro-glacial sedimentary deposits mantle much of the terrain. The fluvial network

is a mountain stream system characterized by high energy conveying a coarse and fine sediment load. Stream channel and adjacent hillslope erosion in the network is the dominant source of fluvial SSC and  $T_n$ , with very little contribution from the predominantly forested upland area (NYC DEP, 2019b). The connectivity of the stream channels in the UEC with glacial legacy sediment, particularly glacial lacustrine silt and clay deposits, makes the system prone to elevated  $T_n$  and SSC following high energy flow events (Mukundan et al., 2018).

The UEC basin includes multiple sub-basins (Figure 2a). Stony Clove Creek (Figure 2b) is the largest, draining around 17% of the UEC basin area above the Ashokan Reservoir, and serves as an experimental sub-basin system to study SS and  $T_n$  source dynamics at the reach and sub-basin scale (NYC DEP, 2019b). Stony Clove Creek was identified as the primary tributary source of SS and  $T_n$  to UEC during a monitoring study between October 1, 2009 and September 30, 2012; the Beaver Kill, Woodland Creek and Birch Creek sub-basins were the second, third, fourth largest tributary sources (McHale & Siemion, 2014).

The streams of the eastern Catskills are prone to acute and chronic levels of turbidity from SS flux during and following floods (NYC DEP, 2019b). Stream channel erosion and adjacent hillslope

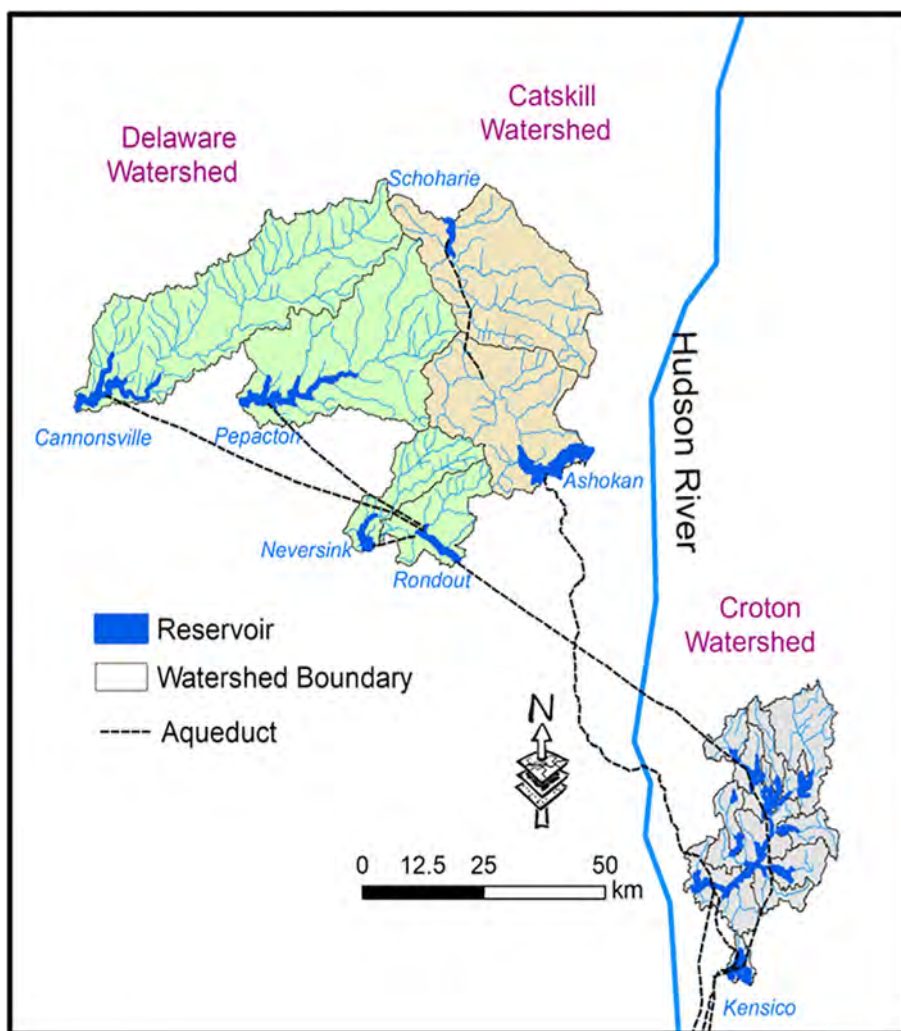


**FIGURE 1** Locations of the three watersheds in the NYC water supply system, where the reservoirs are linked by aqueducts across watersheds (NYC DEP)

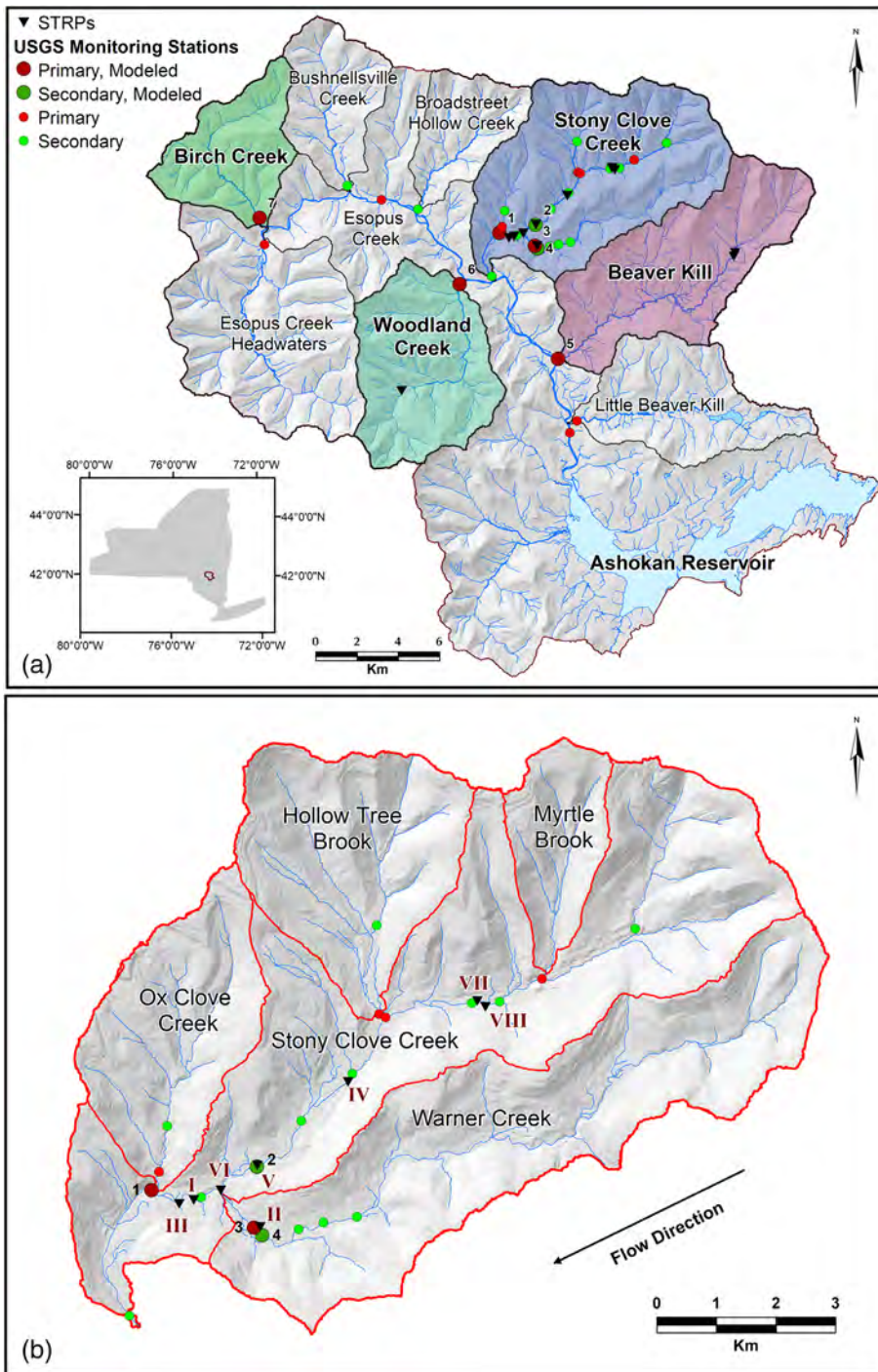


**FIGURE 2** Maps of the (a) UEC basin and (b) Stony Clove sub-basin

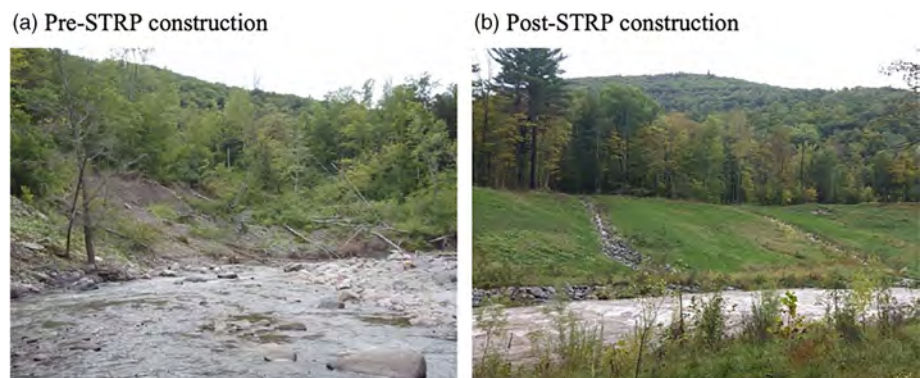
mass-wasting dominate lateral inputs of SS into the UEC basin (Figure 3). Sustained elevated levels of SSC and  $T_n$  originate where the stream erosional process connects with glacial legacy sediment. Following an 8-month period in 2010 and 2011 that contained three floods exceeding a 10-year recurrence interval threshold, SSC and  $T_n$  levels were elevated for months in Esopus Creek upstream of the Ashokan Reservoir. Chronic sources of elevated SSC and  $T_n$  from bank erosion, head-cuts and hillslope mass-wasting were mapped throughout the Esopus Creek basin, with many identified within the Stony Clove sub-basin (Siemion et al., 2016).

Between 2012 and 2014, AWSMP constructed four STRPs in the Stony Clove sub-basin (see Figure 2b for locations). The STRPs included stream channel stabilization practices through realignment, in-stream hydraulic structures and bank protection, restoring flood plain connectivity, and de-coupling stream channels from direct erosional contact with valley bottom margin hillslopes. Hillslope stabilization included reducing slope steepness, installing surface and subsurface drainage systems, and restoring stabilizing vegetation (Siemion et al., 2016). Restorations resulted in a more stable stream and channel bank connectivity (see Figure 4). In essence, STRPs

**FIGURE 3** Examples of the types of erosion in the Stony Clove sub-basin (NYC DEP, 2019a)



**FIGURE 4** An STRP installed in fall 2013 in Stony Clove Creek near Chichester, NY



enhance reach scale sediment dis-connectivity to reduce SS flow-yield at the sub-basin scale. No STRPs were constructed in the other UEC sub-basins during the 2012–2014 period. SS loads in Stony Clove Creek were generally greater than those in Beaver Kill by a factor between 6 and 10 during water years 2010–2013 (October 1 through September 30). During water year 2014, the difference was reduced to a factor of 2 (Siemion et al., 2016). Between 2014 and 2016, four more STRPs were installed in the Stony Clove sub-basin to further disconnect the stream channel from SS sources.

After the construction of the eight STRPs, continuous monitoring between 2017 and 2020 showed that acute  $T_n$  levels in the Stony Clove sub-basin were exceeded by Beaver Kill, Woodland Creek, and Birch Creek sub-basins (Figure 5). The acute levels are represented by the 1% exceedance percentile, or the  $T_n$  value that is exceeded only 1% of the time and is associated with flood conditions. Chronic  $T_n$  levels (represented by the 10% exceedance percentile) are more

similar across the four sub-basins, as well as Broadstreet Hollow Creek. Geomorphic mapping shows that chronic  $T_n$  levels in these sub-basins are related to erosive connectivity with glaciolacustrine sediment.

## 2.2 | Monitoring station data

USGS operates 29 stream monitoring stations in the UEC as part of a decadal  $T_n$  and SSC monitoring research program (Figure 2a) (NYC DEP, 2019b). There are 13 SS flux sub-basin monitoring stations recording daily discharge ( $Q$ ) and  $T_n$  as well as SSC sampling; these stations are referred to as primary stations. There are 16  $T_n$ -only monitoring stations, referred to as secondary stations. Six of the primary and 14 of the secondary stations are located within the Stony Clove sub-basin. These stations are used to delineate water quality

monitoring reaches for five streams: Stony Clove Creek, Ox Clove Creek, Warner Creek, Hollow Tree Brook, and Myrtle Brook (see Figure 2b). Though  $T_n$  is an optical property it is a good proxy measurement of SSC in the Catskill region (McHale & Siemion, 2014) that is easier to measure continuously over long period of time (Rymaszewicz et al., 2017), and it is used extensively in the NYC water supply system to measure water quality.

Data from the upstream/downstream monitoring stations used in this project to evaluate STRP impact on  $T_n$  or SSC reduction are listed in Table 1. The Stony Clove Creek upstream station (Station 2) is a secondary station; Q was estimated by drainage area weighting the Q data at the Stony Clove downstream primary station (Station 1). The Warner Creek upstream station (Station 4) is a secondary station as well. However, Station 4 is very close to Station 3 which is a primary

station where Q is available. This Q data are used for both Warner Creek stations. At Station 1,  $T_n$  data are missing between February 6, 2012 and October 29, 2013, however SSC data are available during this period. Therefore, we combined the two datasets to fill the gap by converting the  $T_n$  data to SSC data (see Figure S1) using the regression relationship  $SSC = 0.3 \times T_n^{1.29}$  derived for Station 1 during the period of record from December 1, 2010 to September 30, 2014 (Siemion et al., 2016). No regression relationship was available that covered the whole study period. Hereafter, this combined data is simply referred to as SSC data for Station 1.

The SSC data at the station nearest the outlet of the Stony Clove sub-basin (Station 1) show a downward trend during the study period (Figure 6). However, flow conditions after Hurricane Irene have also trended downward over the same period, which may have initiated a

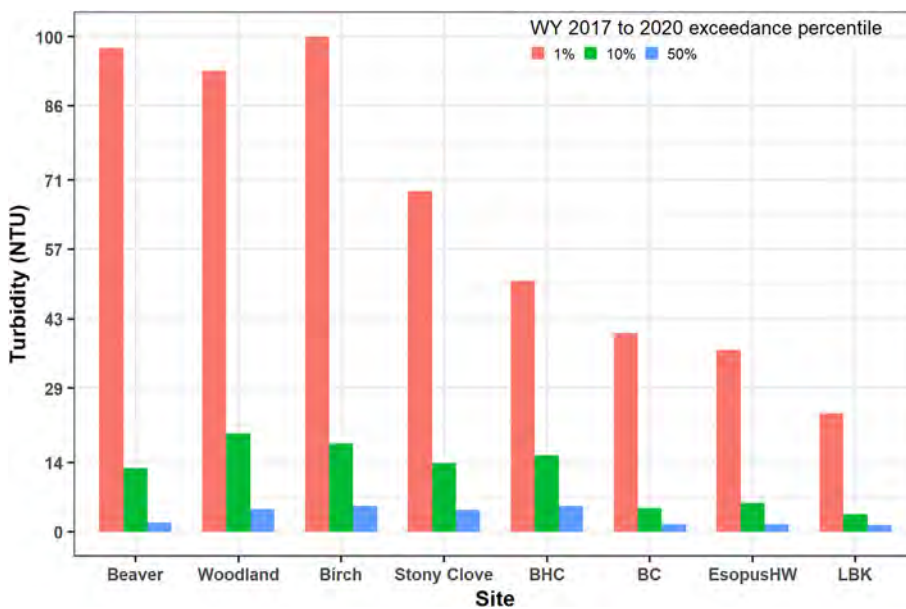


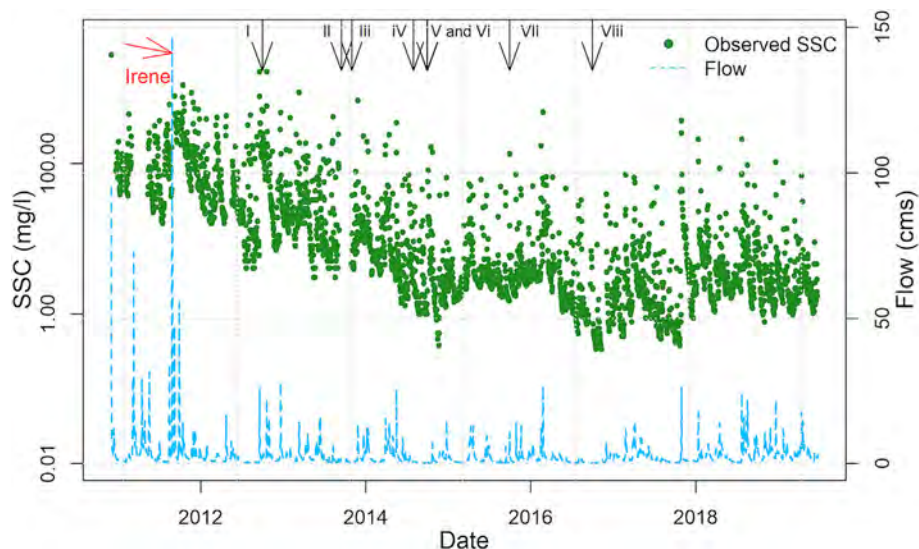
**FIGURE 5** Turbidity exceedance percentiles among the sub-basins of the UEC basin between 2017 and 2020. BC, Bushnellville Creek; BHC, Broadstreet Hollow Creek; EsopusHW, Esopus head water; LBK, little Beaver Kill

**TABLE 1** Data from the monitoring stations

Name	Station	USGS gage	Location	Discharge (code 00060) period	Turbidity (code 63680) period
Stony Clove downstream <sup>a</sup>	1	#01362370	Stony Clove Creek blw Ox Clove at Chichester	1 December 2010–26 June 2019	1 December 2010–26 June 2019
Stony Clove upstream	2	#01362350	Stony Clove Creek at Chichester, NY		1 February 2014–26 June 2019
Warner Creek downstream	3	#01362357	Warner Creek near Chichester, NY	29 May 2012–26 June 2019	29 May 2012–26 June 2019
Warner Creek upstream	4	#01362356	Warner Creek at Silver Hollow Rd near Chichester		30 September 2014–26 June 2019
Beaver Kill	5	#01362487	Beaver Kill at Mount Tremper	17 November 2010–26 June 2019	17 November 2010–26 June 2019
Woodland Creek	6	#0136230002	Woodland Creek above mouth at Phoenicia	23 November 2011–26 June 2019	23 November 2011–26 June 2019
Birch Creek	7	#013621955	Birch Creek at Big Indian	24 May 2012–26 June 2019	24 May 2012–26 June 2019

<sup>a</sup>Daily SSC (code 99409) data was also taken at the stony clove downstream location between 1 December 2010 and 29 September 2014.

**FIGURE 6** SSC data and Q data near Stony Clove Creek outlet (USGS #01362370). The black arrows indicate the completion dates of the eight STRPs



natural decline of SSC in the Stony Clove sub-basin. The eight STRPs were constructed during the period when streamflow transitioned from wet conditions around the time of Hurricane Irene to milder hydrologic conditions in the years following the 2011 flooding. Thus, it is not clear the degree to which the STRPs or the declining streamflow drove the observed reductions in SSC.

### 3 | METHODS

We forward three methods to evaluate the effectiveness of the STRP installations. In all three methods, we ultimately focus on trends in SS flow-yield, that is, changes in SSC or  $T_n$  per unit flow, which quantifies changes in SS after controlling for variations in discharge (more detail provided in Section 3.1). In our first assessment, we conduct an inter-sub-basin comparison of SS flow-yield at the four primary  $T_n$  sourcing tributaries in the UEC basin: Stony Clove Creek, Beaver Kill, Woodland Creek, and Birch Creek. Second, we compare SS flow-yield upstream and downstream of the STRPs in the Stony Clove sub-basin, both on the mainstem and the Warner Creek tributary. Lastly, we apply a process-based model (the River Erosion Model [REM]; Lammers & Bledsoe, 2018b) to simulate natural fluvial processes in the Stony Clove sub-basin in the absence of STRPs. The model-simulated SS flow-yield is compared to the SS flow-yield from observed data, which reflects both natural and STRP influences. The three methods above make use of a time-varying regression approach, known as a DLM, to quantify how SS flow-yield changes over time. We describe this regression model next (Section 3.1), and then provide more detail on the inter- and intra-basin comparisons (Section 3.2) and the REM-based modelling (Section 3.3).

#### 3.1 | Dynamic linear models

In this study, DLMs are used as time-varying regression models that can characterize the temporal dynamics of the SSC (or  $T_n$ )-Q

relationship (Ahn et al., 2017; Ahn & Steinschneider, 2019). These regression models can be written as:

$$y_t = \beta_{0,t} + \beta_1 \log(Q_t) + \varepsilon_t, \varepsilon_t \sim N(0, \sigma_t^2) \quad (1)$$

$$\beta_{0,t} = \beta_{0,t-1} + \omega_t, \omega_t \sim N(0, w_t) \quad (2)$$

$$\beta_{0,t=0} \sim \text{MVN}(m_0, c_0) \quad (3)$$

Here,  $y_t = \log(\text{SSC}_t)$  or  $\log(T_{n,t})$ ,  $\varepsilon_t$  is the observation error, and  $\sigma_t^2$  is the observation error variance. The regression intercept ( $\beta_{0,t}$ ) is considered a state parameter that varies through time via a random walk, where the state evolution error ( $\omega_t$ ) is assumed to follow a normal distribution with 0 mean and state evolution variance  $w_t$ . In our application, we only allow the intercept to change over time, that is, the slope parameter is kept constant. The state evolution error ( $\omega_t$ ) is assumed independent of  $\varepsilon_t$ , and the parameters  $m_0$  and  $c_0$  are the prior mean and state evolution variance for the initial parameter  $\beta_{0,t=0}$ . Discharge ( $Q_t$ ) in Equation (1) is normalized (i.e., divided) by its median value, as this normalization has been shown to effectively remove the dependence between the intercept and slope parameters of the rating curve (Warrick, 2015).

In Equations (1)–(3), SSC (or  $T_n$ ) is modelled based on a regression against Q, and the regression intercept is a state variable that is updated at each time step. The updating is achieved through a recursive Bayesian design and one-step Markov evolution (West & Harrison, 1997). Adjustments are made such that large prediction errors will cause the mean of the rating curve intercept to shift towards values that reduce those errors a posteriori. However, the magnitude of this adjustment is modulated if the observational error variance ( $\sigma_t^2$ ) is large compared to the prior variance of the regression coefficient ( $w_t$ ). Effectively, a larger observational error and smaller state evolution error will result in slower changes to the regression intercept over time.

The regression parameters in the DLM are related to fluvial system processes. Changes to these parameters over time reflect

changes in erosion severity, erodibility, sediment source availability, the emergence of new sediment sources, and the erosive power and transport capacity of the river (Asselman, 2000; East et al., 2018; Gray, 2018). Because in this study we only allow the intercept to change over time, and because discharge is normalized by its median value, several of these changes (e.g., erodibility, sediment source availability and supply) are reflected in the time-varying behaviour of  $\beta_{0,t}$  (Warrick, 2015). That is, changes to the intercept reflect shifts in SS flow-yield, and the magnitude of  $\exp(\beta_{0,t})$  is equivalent to the value of SSC (or  $T_n$ ) at the median flow, when the logarithm of normalized  $Q_t$  equals zero (Ahn et al., 2017). The time-varying intercept  $\beta_{0,t}$  is particularly helpful in quantifying the effectiveness of STRPs, since these projects are designed to stabilize the stream channels and reduce the ACMs from erosional contact with non-alluvial SS sources. By comparing the intercept parameter progression before, during, and after STRP installation dates, we can continuously monitor the impact of STRPs on SS flow-yield over time.

### 3.2 | Inter-and within-watershed comparison

In the inter-watershed analysis, we fit DLMs to the SSC (or  $T_n$ )-Q relationships in the four primary UEC sub-basins near their outlets (Table 1): Stony Clove Creek (Station 1), Beaver Kill (Station 5), Woodland Creek (Station 6), and Birch Creek (Station 7). SSC,  $T_n$  and Q data were obtained from these locations for the period with available data from each monitoring station. No STRPs were installed in the sub-basins besides Stony Clove during 2012 and 2016. The time series of inferred intercept values, with their uncertainty, are compared across the sub-basins to determine whether they exhibit differences in SS flow-yield. Particular focus is given to how SS flow-yield varies across the sub-basins during and shortly after the construction period for the eight STRPs in the Stony Clove sub-basin between September 2012 and September 2016. A similar approach is taken in the within-watershed analysis, except DLMs are fit to the SSC (or  $T_n$ )-Q relationships at two pairs of upstream and downstream stations that straddle STRP locations. The data were obtained from Stations 1, 2, 3, 4 in the Stony Clove sub-basin (see Table 1).

### 3.3 | River erosion model (REM)

To complement the observation-based approaches above, we used the REM to simulate daily SSC data using observed Q and geomorphic data in the Stony Clove sub-basin. The REM simulations represent fundamental natural fluvial processes in the sub-basin that would occur in the absence of the STRPs.

REM is a stream-power based morphodynamic model, which is designed for modelling channel evolution at reach to watershed scales by integrating a bank stability model—the Bank Stability and Toe Erosion Model (Lammers et al., 2017; Simon et al., 2011)—with novel stream-power based sediment transport equations (Lammers & Bledsoe, 2018a, 2018b). REM simulates bed erosion and aggradation in non-cohesive materials using a sediment mass balance approach and calculates bedload and total load sediment transport capacity based on specific stream power in excess of a critical specific stream power and modulated for grain size. The model simulates bed erosion into cohesive bed material using an excess shear stress approach. Stream channel width changes are simulated and account for two bank erosion mechanisms: fluvial erosion (e.g. excess shear) and mass-wasting (Figure 7a,b).

We use REM to represent how reach-scale stream processes of bed and channel erosion drive fundamental natural changes in SS flow-yield. The REM model is specified to primarily simulate channel bank erosional processes, which is one of the main sources of SS flow-yield in the Stony Clove sub-basin. REM simulates bed elevation changes as well, however, the simulated SSC input from the bed is very low, though bed incision into SS source sediment does occur in the Stony Clove sub-basin. While the REM is a useful tool to analyse channel bed and bank erosional processes in a natural system, some model limitations should be recognized up front. First, knickpoint migration followed by a head-cut event at the channel bed can produce fine sediment in the streams from the cohesive materials below the active channel bed sediments, but this process was not simulated in our REM application due to a lack of data to calibrate this process. In addition, any erosional contact with the glacial legacy sediment in the study area can produce SS in the streams. REM is not able to capture persistent fine sediment inputs from hillslope drainage through

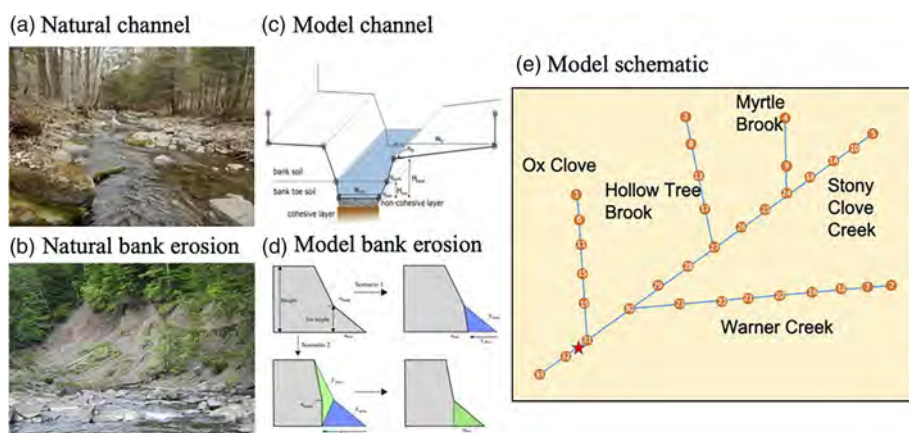


**FIGURE 7** REM model representations ((c) Lammers, 2018; (d) Lammers & Bledsoe, 2018b) of the Stony Clove sub-basin. (a) Natural channel and (b) model channel geometry; (c) natural bank erosion and (d) model representation of the bank erosional processes; (e) model schematic of the sub-basin including the mainstem, tributaries and reach numbers (in circles). Red star in (e) represents the USGS station at Stony Clove Creek below ox clove at Chichester, NY (#01362370)

mass-wasted colluvial/glacial sediment, nor can it account for fine sediment input driven by freeze–thaw processes, which can reduce the cohesive strength in bank sediments followed by their detachment and transportation in the stream (Inamdar et al., 2018). Freeze–thaw induced mass-wasting and slope hydrology can produce SS flux even during low flow conditions and the lack of this process in the REM simulation can further lower the SS flow-yield estimation. These limitations are expected to reduce REM-based sediment load estimates, particularly during low flow conditions.

### 3.3.1 | Input data and parameters

The REM model requires several parameter specifications and input data fields. The data can be classified into three broad categories: (1) channel geometry and connectivity; (2) channel bed and bank material properties; and (3) daily discharge values. Details on the model input data requirements can be found in the REM User Guide (Lammers, 2018).

REM assumes a prismatic channel, based on user-supplied bottom width, bank and toe height and angles, and floodplain width and slope (Figure 7c,d). All channel geometry specifications are unique for the right and left banks in each reach unit delineated in the basin. The channel geometry in Stony Clove Creek and its tributaries were derived from a 1-m resolution bare earth Digital Elevation Model (DEM) derived from an April 2009 airborne LiDAR dataset (RACNE, 2012) by using the profile tool in ArcGIS. Each reach unit can have several cross-section inputs that contain the variables that define cohesive layers located below the channel bed and define local longitudinal profile slope. In this study, we specified 33 reaches and 127 cross-sections to represent the channels in the Stony Clove sub-basin, including the mainstem and four main tributaries (Figure 7e).

Grain size distributions in the channel bed material, which are required for each reach unit, were derived from data collected under the NYC DEP Stream Management Program (SMP) using the modified Wolman pebble count sampling method (Wolman, 1954) at 199 cross-sectional locations along Stony Clove Creek. The SMP grain sizes were divided into six classes: slit/clay, sand, small gravels, large gravels, cobbles, and boulders. Grain size class distributions included in the model were selected from the SMP locations matching REM cross-section locations. Individual regression relationships for each grain size class distribution against bed slope were developed for Stony Clove Creek (see Supplementary Material). The regressions were then used to obtain the grain size class distribution for the remaining REM cross-sections not located at SMP sampling locations. Grain size class distributions were averaged across cross-sections within each reach and then interpolated to obtain 11 grain size distributions used in REM.

The REM model was calibrated by comparing simulated SSC at the beginning of Reach 31 to observed SSC at Station 1, which is located near the confluence of Stony Clove Creek and Ox Clove Creek (Table 1; Figure 7e). Channel bank material data for each reach unit were among the most difficult data to acquire for the model,

including bank toe critical shear stress, soil erodibility coefficient, bank/toe soil cohesion, bank/toe friction angle, bank/toe saturated unit weight, and the fraction of the bank and cohesive bed soil that are bed material load (i.e., sand and coarser). The soil erodibility coefficient and bank/toe soil cohesion can be calculated by the model (Lammers & Bledsoe, 2018b, 2019). However, the bank toe critical shear stress, bank/toe friction angle, bank/toe saturated unit weight, and the fraction of the bank that are bed material load need to be calibrated due to lack of observed data in the study area. The model calculates sediment transport capacity using two additional input parameters that required calibration: reference dimensionless specific stream power of the median grain size ( $\omega_{r50}^*$ ) and a hiding function empirical exponent ( $b$ ) (Lammers & Bledsoe, 2018b). More detail on model calibration is provided in the Supplementary Material.

### 3.3.2 | Outputs

REM was used to simulate fine sediment loading (kg) for each reach at each time step, including loading from bank erosion and cohesive bed erosion, from October 1, 2000 to June 26, 2019. While the observed data started on December 1, 2010, an extra 10 years of simulation was used to spin up the model and remove the effects of initial conditions. We calculated model estimated SSC at the beginning of Reach 31 (modelled catchment outlet reach) by the summation of all fine sediment loading from Reach 1 to Reach 30 divided by the Q data at the beginning of Reach 31. We calculated the percent loading from each reach to represent the distribution of the amount of fine sediment exported to the stream system in the Stony Clove sub-basin upstream of Station 1. This loading distribution helped to validate the model's ability to simulate known erosional hotspots within the Stony Clove sub-basin.

The discretization of the modelled fluvial network was a balance of capturing some longitudinal parameter heterogeneity while also keeping the model computation and data processing reasonable. The calibrated model is a coarse representation of the sub-basin due to the high level of longitudinal and lateral heterogeneity within the glacially conditioned fluvial network and limited sub-basin material property data. Therefore, the uncertainties associated with the model parameters are high, and selecting one optimal set of parameters and specifications was challenging. To address this problem, we used an ensemble of REM simulations with different parameter sets and specifications to represent a range of probable fluvial process SSC production scenarios in this mountain catchment (channel adjustment through widening, planform change, and degradation/aggradation). Recognizing that REM could not represent a full set of fluvial geomorphic adjustment factors such as riparian vegetation, large wood dynamics, antecedent saturation, hillslope processes and stream management practices, the modelling objective was to adequately simulate the “behavioural” adjustment response of the fluvial system to the driving hydrology. That is, the objective was to reasonably match the distribution and relative magnitude of variable adjustment through the fluvial network. We selected an optimized ensemble of REM

parameter sets by comparing REM SSC simulations with observed data and selecting those simulations that met a series of satisficing performance criteria: Spearman's rank correlation coefficient ( $\text{cor.S}$ )  $> 0.3$ ; Nash–Sutcliffe efficiency (NSE) in the original scale of the data  $> 0.3$ ; and NSE using data in log scale  $> 0$ .

In addition, the best performing simulation from the ensemble set was compared with the channel erosional patterns observed between spring 2009 and spring 2013. Comparison of the simulated versus observed fluvial geomorphic behavioural response focused on the period before and after the extreme hydrologic conditions of 2010–2011 in the study area. This was achieved using three available geospatial datasets: (1) high resolution (1-ft) aerial orthoimagery of the Stony Clove sub-basin for spring 2009 and spring 2013; (2) the April 2009 1-m DEM; and (3) field-mapped stream channel conditions in summer 2013. These data were used to develop digitized ACMs for 2009 and 2013. The digitized ACM polygons for 2009 and 2013 were developed iteratively using the aerial imagery, DEMs and field data to enclose a probable active channel comprising the bankfull channel, multi-threaded channels/avulsions, sediment features such as gravel/cobble bars and bounded by armoured channel margins and woody riparian vegetation. The uncertainty in the ACM accuracy was not ascertained for this investigation and thus the ACMs were used to identify stream reaches with clear changes in channel width and plan-form alignment (lateral migration and avulsions), rather than actual quantitative metrics of changes in channel width. Where such adjustments were observed and associated with confirmed post-flood stream stabilization projects, these locations were noted as adjustment reaches but the relative change was not used in the evaluation of the REM simulations. In this comparison, the observed data were used to inspect the model's ability to reasonably match longitudinal distribution and variation in simulating erosional “hotspots” that could account for heterogeneous SSC loading in the actual and simulated fluvial network.

### 3.3.3 | SSC-Q relationship dynamics with and without STRPs

The observed SSC-Q relationship in the Stony Clove sub-basin is a function of hydrology and geomorphic connectivity with sediment sources. The STRPs evaluated in this research intend to influence the SSC-Q relationship through disrupting the geomorphic connectivity. The REM simulations represent only the hydrology and fundamental fluvial processes, which serves as a base scenario for the SSC-Q dynamics without management impacts. We fit DLMs to both the observed and the REM-simulated SSC-Q relationships and obtained the time varying intercept parameter from all models to quantify changes in SS flow-yield. We compared these time series between the REM-modelled and observed cases to determine if the reduction in SS flow-yield in the observations outpaced that of the REM simulations. This would be an indication that the STRPs were driving additional SS flow-yield reductions beyond that which would be expected

due to the natural recovery of the system following disturbance hydrology during 2010–2011.

We also calculated cumulated sediment loads for both the observed and REM-simulated SSC to approximate the sediment reduction achieved by the STRPs. Given the uncertainty in the REM-simulated SSC and the wide range of DLM intercepts across the ensemble of REM simulations, we designed this comparison to isolate how the slope of the DLM intercept under the observed and simulated series influences cumulative sediment loads. Sediment loads were calculated as the product of Q and rating curve estimated SSC. The slope parameter of all rating curves was kept constant and set to the value from the observed DLM. The intercept parameter of each rating curve was approximated by fitting a linear regression to each of the intercept series against time. Therefore, the final estimated intercepts vary smoothly and only capture a linear trend in SS flow-yield over the study period. This procedure was repeated separately for both REM simulations and the observed data. The smoothed intercept parameters for all rating curves were adjusted to the same initial value at the beginning of the time series so that cumulative sediment loads all start on equal footing.

## 4 | RESULTS

### 4.1 | Inter-watershed analysis

Before comparing the DLM-estimated changes in SS flow-yield across the four sub-basins considered in the inter-watershed analysis, we first show the goodness of fit of the DLM to the flow and SSC data. Figure 8 provides an example of this fit for Station 1 near the outlet of the Stony Clove sub-basin. At this location, the DLM-estimated SSC performs well against the observed SSC, with a NSE in log-space of 0.74. While the dynamic rating curve generally underestimates the magnitude of peak SSC events, it is able to capture the timing of events. At the stations in the other three sub-watersheds, we fit the DLM to  $T_n$  and Q data. These DLM fits exhibit log-NSE values ranging from 0.41 to 0.59 and perform equal or better than static rating curve regressions. Overall, the DLM goodness of fit is sufficient to compare changes in SS flow-yield across sites.

Figure 9 shows the time-varying intercepts (with uncertainty) of the DLMs fit to the SSC (or  $T_n$ )-Q relationships in the Stony Clove, Woodland Creek, Beaver Kill, and Birch Creek sub-basins. There is a clear downward trend in the intercept parameter in the Stony Clove sub-basin that far exceeds the width of the 95% confidence intervals (Figure 9a). The bulk of this downward trend occurs between September 2012 and September 2016, during the time of installation for the eight STRPs. No STRPs were installed in the Woodland Creek, Beaver Kill, and Birch Creek sub-basins during the period when the eight STRPs were installed in the Stony Clove sub-basin, and there are no downward trends in the time-varying intercepts for these other three sub-basins (Figure 9b–d). We temper this claim slightly in Woodland Creek and Birch Creek because the confidence intervals

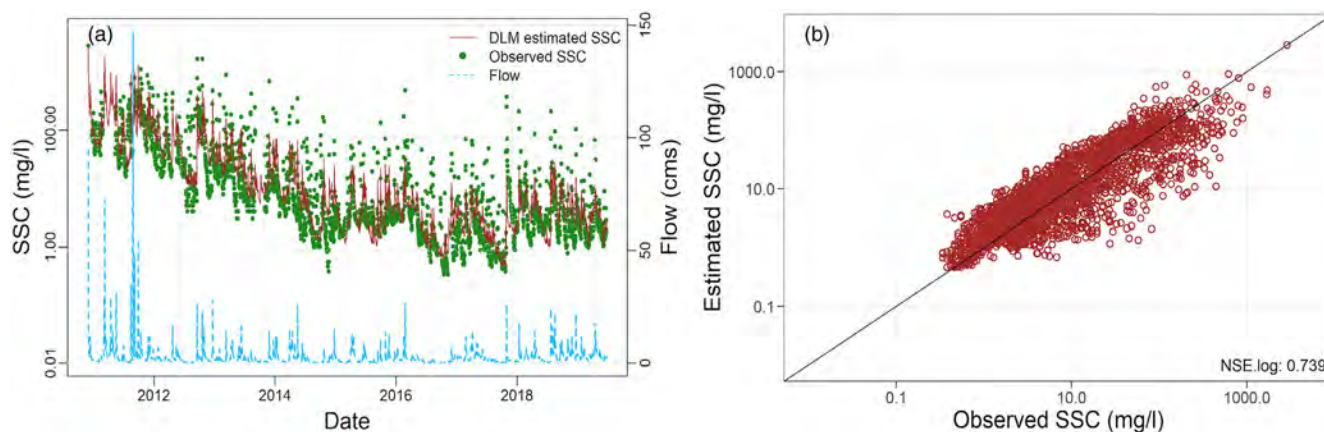


**FIGURE 8** DLM-estimated SSC compared to observed SSC at Stony Clove Creek below ox clove at Chichester (USGS #01362370), shown as (a) time series and (b) a scatterplot

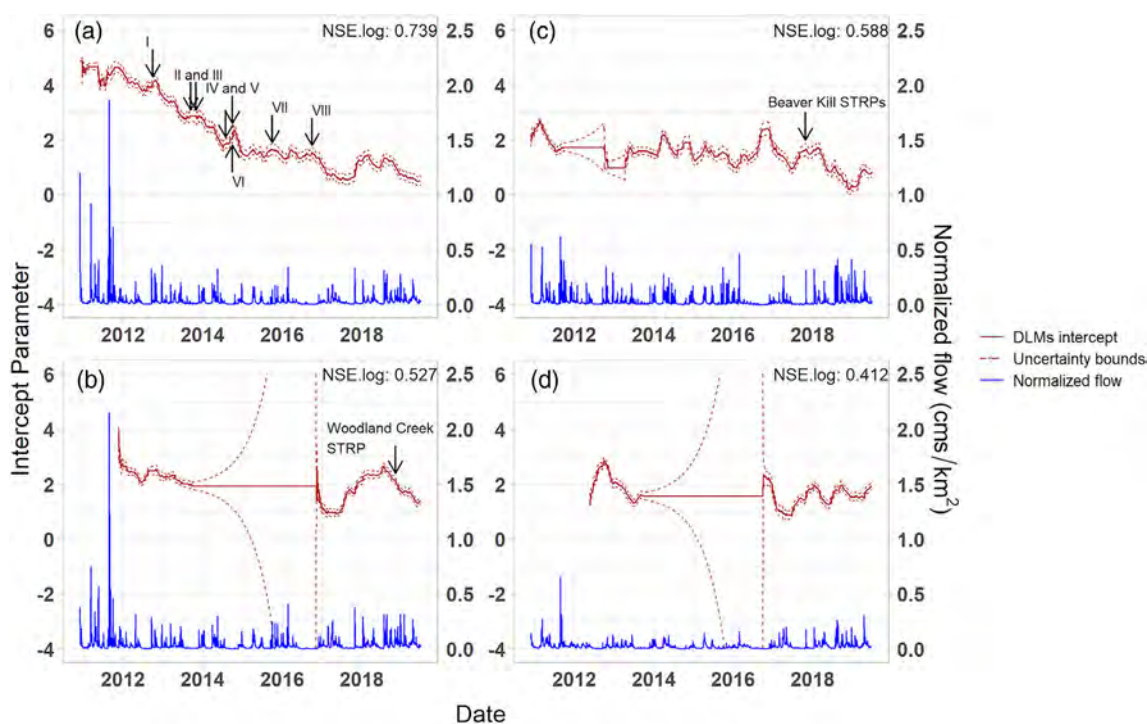


**FIGURE 9** DLM intercept parameters at the UEC sub-basins: (a) Stony Clove sub-basin (the eight STRP constructions are indicated by the black arrows); (b) Woodland Creek sub-basin (an STRP was constructed in November 2018); (c) Beaver Kill sub-basin (two STRPs were constructed in October 2017); (d) Birch Creek sub-basin. The log-NSE of the DLM is also shown for each sub-basin. When there is missing data, DLM intercepts remain constant, and the uncertainty bounds increase with increasing number of missing data

for the intercept widen considerably when there are missing  $T_n$  data. In addition, the three other sub-basins do exhibit long-term variations in the dynamic intercept, suggesting geomorphic response over seasonal-to-interannual timescales. Yet despite these fluctuations and some periods of large uncertainty, there are no clear and persistent downward trends in the dynamic intercept across the periods when data are available in Figure 9b–d.

The flow conditions in the Beaver Kill and Birch Creek sub-basins (presented in Figure 9 as normalized flow,  $Q/\text{drainage area}$ ) were not

as extreme during Hurricane Irene as they were in the Stony Clove sub-basin, and runoff in Birch Creek was much lower than the other three sub-basins after the end of 2011. The lack of downward trends in the intercepts of these two sub-basins may be due to the absence of either STRPs or the natural recovery because of the less disturbed sub-basin conditions. Flow conditions in the Woodland Creek sub-basin were high during Irene and the intercept parameters show a steep drop after the disturbance hydrology in August and September 2011 (Figure 9b). However, there is no turbidity data available

immediately after the disturbance events, which obscures the interpretation of the intercept decline. As a result, the inter-watershed analysis may provide some evidence in support of STRP effectiveness but is not conclusive.

## 4.2 | Within-watershed analysis

We now compare the intercept parameters at locations downstream and upstream of STRPs within the Stony Clove. For the stations on the mainstem of Stony Clove Creek, there are four STRPs (I, II, III and VI) installed between the upstream and downstream stations (see Figure 2b). We note that STRP II is located on Warner Creek and sediment yield at Station 1 has contributions from Stony Clove Creek, Warner Creek, and Ox Clove Creek. SS flow-yield appears to decline shortly after the completion dates of STRP I, II, III and VI at the downstream Station 1 location (Figure 10a). We compare the DLM intercept parameter at Station 1 to that at Station 2, which is located upstream of the aforementioned STRPs. While there is a clear decline in the intercept parameter at Station 1, the intercept at the upstream Station 2 is relatively flat. We note that the intercept time series at Stations 1 and 2 exhibit similar intra-annual variations, with the exception of the steeper downward slope at Station 1 during the overlapping period. These results provide evidence that supports the effectiveness of STRPs in reducing SS flow-yield. However, data at Station 2 do not extend back prior to 2014, and so we are unable to determine whether the downward trend in the intercept at Station 1 between 2011 and 2014 is unique to that station (and thus attributable to STRPs) or would have been seen at Station 2 as well (and thus more indicative of natural recovery).

On Warner Creek, only STRP II lies between the downstream (Station 3) and upstream (Station 4) stations (Figure 10b). There is a clear decline in the downstream intercept (Station 3) immediately after the STRP completion date, suggesting some SS flow-yield reductions were achieved. However, the intercept at that site begins to trend upward starting in the middle of 2014. Further, with no data

available at the upstream location (Station 4) near the STRP construction date, the difference in the intercept parameters between the two locations is unclear. During the overlapping period when both stations have data, the intercepts exhibit similar variability. The two intercepts have almost the same magnitude before 2017, and by the end of the instrumental period, the intercept at the downstream location has trended slightly higher than that at the upstream site. This suggests that, at least for STRP II, there may have been some benefits for reducing SS flow-yield early after STRP construction, but this effect may have weakened over time.

## 4.3 | Physics-based model scenario analysis

We selected one REM simulation to show the performance of the model in terms of its simulated SSC conditions (Figure 11a). For this particular simulation, performance metrics suggest a reasonable fit, with a NSE of 0.40, a log-NSE of 0.53, a Spearman correlation of 0.42, and a mean bias of  $-7.33$  tons per day. The model estimates are similar to observations at flow conditions above  $1 \text{ m}^3/\text{s}$ , while at lower flow conditions, estimated SSC are mostly zero or much lower than the observed data. This is expected given the limitations of the model in simulating non-hydraulic conditions that can drive SS loading at non-erosive flows. The span of estimated SSC at around  $10 \text{ m}^3/\text{s}$  is narrower and the peak value is lower than the observations. The bottom of the REM estimated rating curve has a distinct two-fold curvature, which is an artefact of the model. While there are limits to the fidelity of the model simulation (see Section 3.3), the results provide a reasonable representation of SSC dynamics in Stony Clove Creek sufficient for the objectives of this analysis, especially at moderate and high flow conditions that are the primary drivers of sediment flux.

Since the REM model was calibrated at Reach 31, percent sediment loadings were simulated for reaches upstream of Reach 31 (i.e., Reaches 1–30) (Figure 11b). Tributaries in the headwaters to the north of Stony Clove Creek have minimal sediment inputs, with cumulative inputs that are less than 10% of the total seen at Reach 31 in

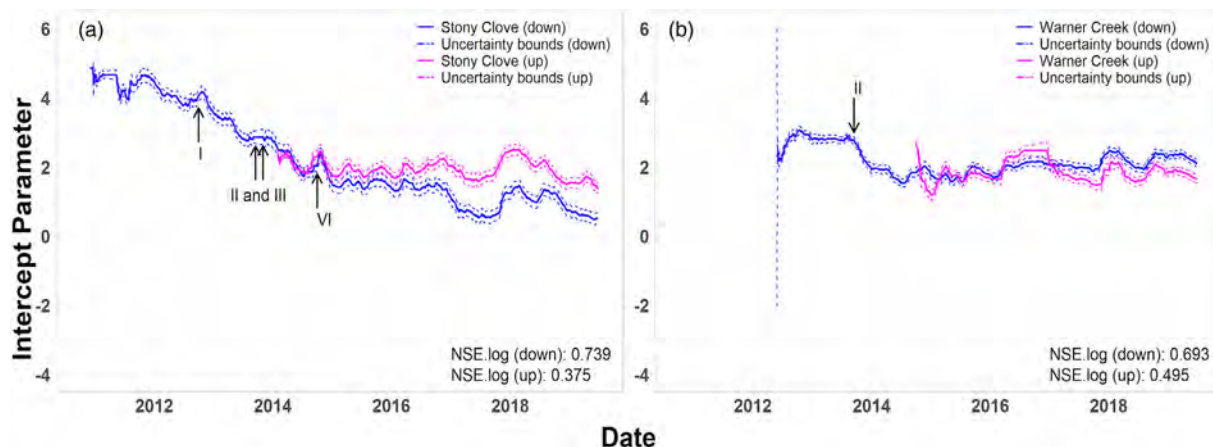


**FIGURE 10** DLM intercept parameters at (a) downstream of Stony Clove Creek and (b) downstream of Warner Creek. Black arrows indicate STRP construction dates

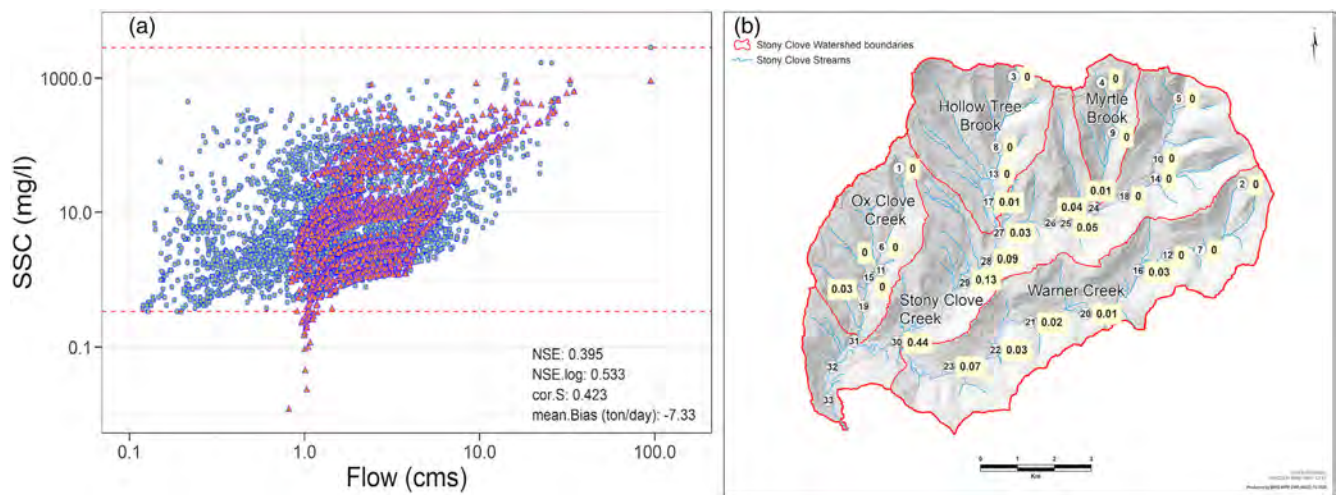


**FIGURE 11** (a) SSC-Q rating curve relationship simulated by the REM model (triangles) and from the observed data (circles) and (b) spatial distribution of the percent sediment loadings for Reaches 1–30 (numbers in circles are reach numbers and values in rectangle are percent sediment load)

the simulation results. In the model, Warner Creek contributes 16% of the total sediment loading at Reach 31, with most of the loading sourced in the lower modelled reach. Most of the sediment load simulated at Reach 31 is sourced downstream of Warner Creek, especially in Reach 30 and to a lesser extent 29. This is generally consistent with known sources of sediment loading prior to STRP implementation within the basin, as evidenced by the high concentration of STRPs that were located in this area. However, observations do indicate that Warner Creek serves as a larger SS source than estimated by the model (particularly around Reaches 22 and 23), suggesting some limitations of the REM model when estimating tributary SS contributions (NYC DEP, 2019a, 2019b).

For additional model validation, REM-simulated channel width changes were compared with the observed channel erosional patterns represented by the ACMs (Figure 12). Most of the REM-simulated channel widening is concentrated between Reaches 27 and 31 (Figure 12a). We examine in more detail four sections based on clusters of erosion intensity (Figure 12b–e). The simulated erosional hotspots are shown in Figure 12b,c. In Figure 12b, the cross-section marked by an arrow in the centre of the river section shows large simulated channel widening by REM, which is consistent with observed ACM widening at this location. In Figure 12c, two areas of observed ACM widening are visible, one of which is the largest in the ACM dataset. A third area shows stream channel migration. Throughout this entire stretch of stream, REM simulates cross-sections with considerable channel changes. Although the cross-sections with the most simulated widening do not always align with the specific areas of observed widening, REM is able to capture the general pattern of notable observed erosion seen along this section of the river, as compared to the other sections. In Figure 12d, there is only one area of Stony Clove Creek with notable differences in the 2009 and 2013 ACMs (marked by an arrow), and these differences suggest significant channel migration. The REM simulated moderate erosion upstream of

this area, but also significant channel narrowing (as indicated by the blue points) at cross-sections that straddle the observed channel migration. This is comparable with deposition of sediment entrained upstream that could lead to the observed channel migration. Figure 12e shows the comparison between simulated channel width change and observed ACMs towards the headwaters of Stony Clove Creek. The REM simulated cross-sections show no significant changes in channel width, which is consistent with the lack of change between the 2009 and 2013 ACMs. Overall, results in Figure 12 suggest that REM is able to simulate major spatial patterns of erosion along Stony Clove Creek sufficient to produce episodic SS loads, similar to the observed patterns of erosion and sediment load.

There are nine REM simulations that meet the satisficing performance criteria (see Section 3.3.2), and their DLM intercept time series are shown in Figure 13a. The REM simulation intercepts show a wide range of values, but all intercepts associated with these simulations exhibit a gradual downward trend starting after Hurricane Irene. Since the REM model does not model the effect of the installed STRPs, this suggests that natural recovery in the absence of further hydrologic disturbance after the extreme flood is contributing to the downward trend in the REM simulations. We also emphasize that there is a 10-year spin up in the simulations, so initial conditions are not driving this downward trend. The DLM fit to the observed data also exhibits a time-varying intercept with downward trend. Importantly though, the observed trend is steeper than those exhibited under the ensemble of REM simulations. The observation-based intercept was very high until 2013, before declining rapidly and ending towards the bottom of the REM-based ensemble of intercepts starting in 2015. The rapid decline in the observation-based intercept, as compared to the REM-based intercepts, coincides roughly with the construction date of the 2013 set of STRPs in the Stony Clove sub-basin. These STRPs specifically targeted channels linked to large hillslope mass failures in glacial lacustrine

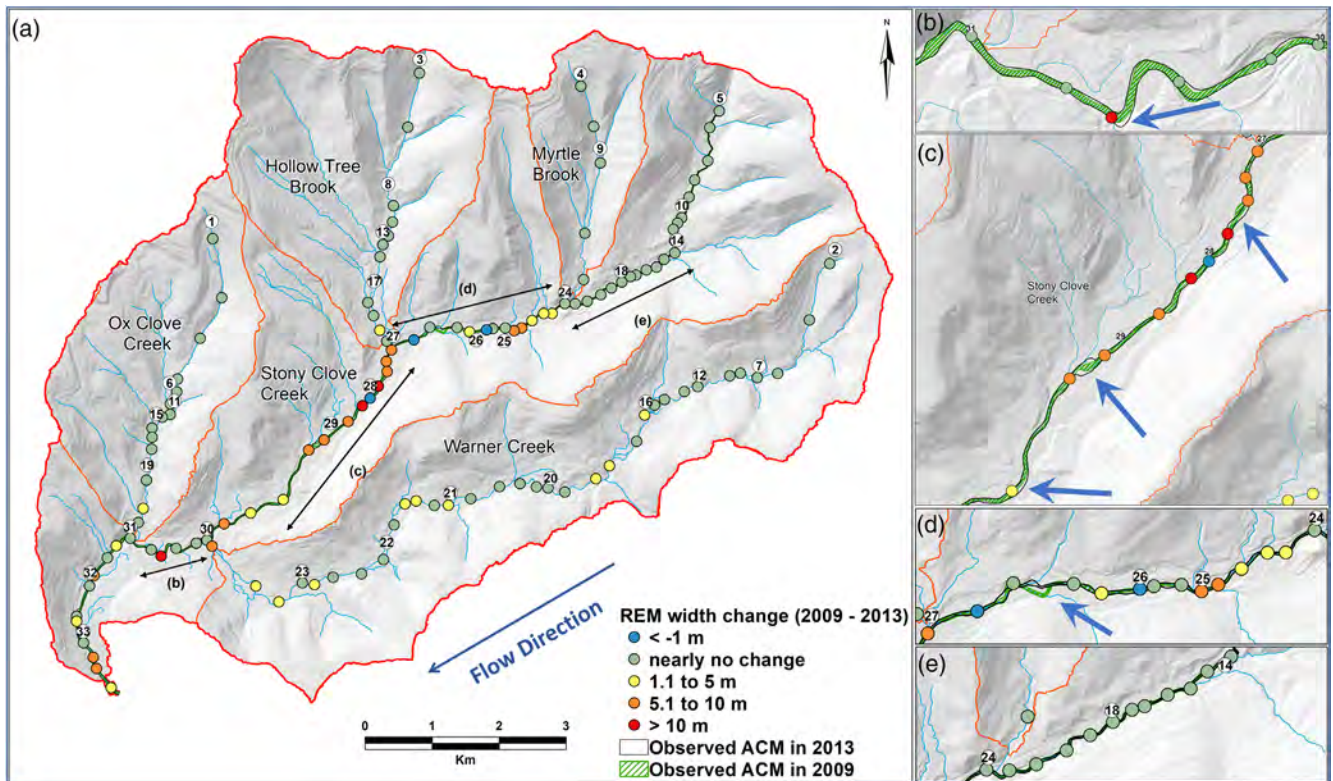


**FIGURE 12** REM simulated channel width changes at specified cross-sections (colour-filled circles) compared to ACM differences on the Stony Clove mainstem between 2009 and 2013. The mainstem is divided into four sections (a), which are enlarged in (b–e). Blue arrows show major changes in the observed ACMs

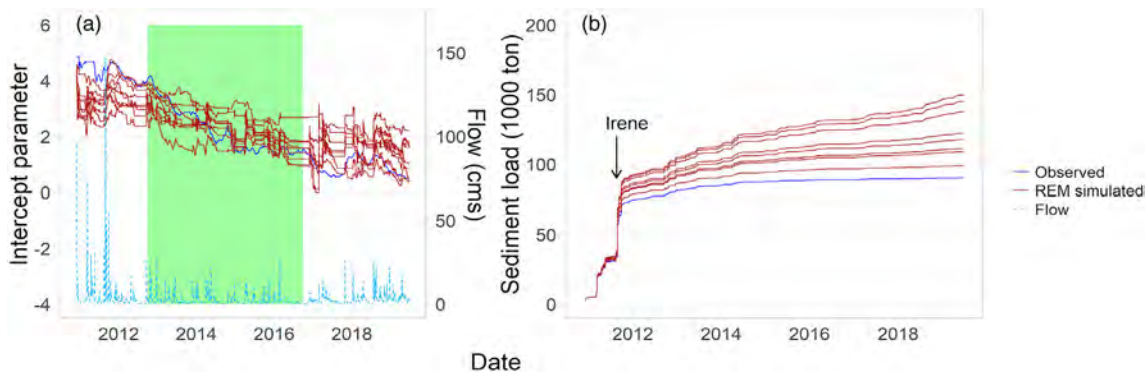


**FIGURE 13** (a) Intercept parameters of DLMs fit to the observed data and the REM simulations. Shaded area indicates the period of construction dates of the eight STRPs. (b) Cumulated sediment loads based on DLMs fit to the observed data and the REM simulations

sediment, conditions known to produce elevated SSC for long periods and during low Q conditions.

The cumulative sediment loads from all REM simulations are higher than that suggested by the observed data, based on rating curve estimated SSC (Figure 13b). The observed and average REM-simulated cumulated sediment loads during the study period were  $87.79 (\times 10^3 \text{ ton})$  and  $120.12 (\times 10^3 \text{ ton})$ , respectively, and during the post-September 2011 period (after Irene and Tropical Storm Lee) they were  $29.12 (\times 10^3 \text{ ton})$  and  $57.10 (\times 10^3 \text{ ton})$ . Both the total and post-

event cumulated sediment loads were significantly higher in the average, REM-simulated SSC compared to the observed SSC.

## 5 | DISCUSSION

The results from the three methods in this study, when taken together, suggest that the evaluated BMPs have contributed to SS flow-yield decline, beyond that which would be expected due to

natural recovery of the fluvial system following major flood events. The specific points of evidence that support this claim are as follows:

- The inter-watershed analysis showed that the Stony Clove sub-basin exhibited a prominent decline in SS flow-yield during the time of STRP installation, compared to three nearby sub-basins without STRPs that did not show a similar decline during the same period.
- The within-watershed analysis showed that locations downstream of STRP installations on Stony Clove Creek exhibited declines in SS flow-yield, as compared to locations directly upstream of the STRPs. On Warner Creek, SS flow-yield downstream of an STRP declined immediately after installation, although project effectiveness appeared to weaken over time.
- REM simulations showed that the rate of SS flow-yield decline in the modelled environment (without STRPs) was slower than that observed (with STRPs), especially during the period of STRP installation.

Any one of these lines evidence in isolation would only provide weak evidence in support of BMP effectiveness. However, when viewed together, these three lines of evidence provide a moderate degree of evidence that the STRPs had an effect on SS flow-yield declines.

However, we are careful not to indicate that the results provide strong evidence of STRP effectiveness because of unresolved uncertainties in all three methods. In the inter-watershed analysis, flooding was most intense on Stony Clove and Woodland Creeks, but missing data on Woodland Creek precluded a clear analysis of whether significant SS flow-yield declines also occurred in that sub-basin (in the absence of STRPs). In the within-watershed analysis, missing data at upstream sites on both the Stony Clove mainstem and Warner Creek precluded an unambiguous assessment of changes in SS flow-yield upstream and downstream of the STRP locations. The REM analysis was limited by uncertainties in model fit, lack of sufficient pre-STRP monitoring data for calibration, and insufficient field measurements to constrain model parameterization (e.g., particle size distribution in tributaries; see Figure S2). In addition, the erosion simulated by the REM was primarily driven by bank erosion, with relatively small contributions from erosion into cohesive bed material below the active layer. There are other natural supplies of SS, such as knickpoint migration followed by a head-cut event, remobilization of deposited material, and freeze-thaw processes, all of which are not accounted for by the specified REM model. During milder hydrologic conditions following flood events (like the time period when STRPs were installed), these processes can exhibit declining trends as well, which could explain the faster downward trend in observed SS flow-yield compared to the REM simulations.

The unresolved uncertainties described above highlight the need for greater investments in continuous SSC/ $T_n$  monitoring, especially at locations both upstream and downstream of proposed BMPs, so that sufficient pre- and post-project data can be used to unambiguously assess project performance. Current downward trends in SS

monitoring programs across the United States (Warrick & Milliman, 2018) are in direct conflict with this need, and reflect poor planning when considering the cost of BMP installation and the utility of assessing project efficiency before committing to further restoration using the same technologies. NYC DEP and USGS have invested in such monitoring but unfortunately the extensive longitudinal inter-basin monitoring in the study area started in 2016, after many of the STRPs were constructed. This monitoring network will be very useful for continued SSC and  $T_n$  reduction investigations.

In the absence of continuous, pre- and post- upstream and downstream monitoring, process-based modelling like the REM can help to resolve some uncertainties around BMP effectiveness, and more broadly, around changes in fluvial sediment dynamics. However, these modelling efforts require a significant amount of data to calibrate and validate. The case study presented in this work boasted a significant observational set of SSC and turbidity data, DEMs, and other field measurements to support REM parameterization. Yet additional data collection could still help to better constrain model calibration, for example, better representation of channel properties by including in-situ measurements of critical shear stress using novel instruments (Dunne et al., 2019). Potential model improvements may also be possible by incorporating more physical complexity and heterogeneity in the modelled system, such as decreased reach lengths and an increased number of cross-sections, although this would require even more data for effective calibration. In general, a significant amount of uncertainty is likely to accompany most physical modelling applications like REM, even for well-monitored watersheds such as the Stony Clove sub-basin.

Given issues of data scarcity that are likely to persist, our results highlight the utility of mixed methods as a means to help mitigate significant uncertainty when examining fluvial sediment dynamics. This study highlights these benefits in the context of evaluating water quality BMPs, where DLMs provided a computationally cheap assessment of streambank stabilization projects, while the REM supplied a baseline scenario of sediment dynamics with no BMPs against which to compare observed changes. However, similar benefits are likely achievable in other applications. Modelling fluvial sediment transport dynamics has been an enduring challenge, in part because of multi-scale (event-based to decadal) variations in the sediment-flow relationship that are not well-monitored (Aguilera & Melack, 2018; Gray, 2018; Gray et al., 2015; Hirsch et al., 2010). These challenges are likely to grow with more intense and frequent extreme events under climate change (USGCRP, 2017). DLMs are a reliable tool to investigate observed changes in these dynamics across time scales (Ahn et al., 2017), and they can be applied rapidly to basins with sufficient SS and flow data to detect emerging trends or diagnose other aperiodic oscillations. When coupled with physical models of fluvial sediment dynamics, any observed trends can then be contextualized by ensembles of simulations under different climate scenarios. For instance, the REM model developed in this work has the potential to predict how changes in future hydrology could impact stream morphology and sediment flux in the Catskills fluvial system, which is still adjusting to the Pleistocene glacial legacy. These results could then be

compared to recent observational changes, as highlighted by the DLMs, to understand the magnitude of potential future change as compared to those recently observed. This effort will be the focus of future work, and should be extended to locations outside the Catskill Range.

## 6 | CONCLUSION

This study presents three methods to evaluate the effectiveness of BMPs to reduce SS flow-yield, particularly in the presence of natural geomorphological and hydrologic trends in the aftermath of extreme flood events. These methods are demonstrated in a case study of STRPs installed in a formerly glaciated mountainous watershed in the northeastern U.S. The first two analyses leverage inter- and intra-watershed comparisons of temporal dynamics in SS flow-yield, as inferred by the dynamic intercept parameter of a DLM. Results suggest that the evaluated STRPs lead to reductions in SS flow-yield, although these reductions can weaken over time in some instances. While the observational-based analyses in these first two methods are relatively straightforward, they are limited by a lack of continuously measured daily data at all sites. We supplemented these methods with a third analysis that compared observed trends in SS flow-yield in the Stony Clove sub-basin with REM simulations that do not represent the effects of STRPs. The combined results of the three methods provide a moderate degree of evidence that the STRPs installed by AWSMP within the Stony Clove sub-basin have contributed to observed SS flow-yield reductions. Overall, the methods presented in this work serve as a basis for continuous assessment of changes in SS flow-yield and attribution to watershed management.

### ACKNOWLEDGEMENTS

This work was supported by the Cary Institute of Ecosystem Studies with funds from the New York State Department of Environmental Conservation (Contract No. DEC-01-C01205GG-3350000).

### DATA AVAILABILITY STATEMENT

The discharge, suspended sediment concentration and turbidity data that support the findings of this study are from the National Water Information System data available on the World Wide Web (USGS Water Data for the Nation) at URL <https://waterdata.usgs.gov/nwis/>. The rest of the data used in this study are available in the supplementary material of this article.

### ORCID

Kezhen Wang  <https://orcid.org/0000-0002-0033-4161>

### REFERENCES

- Aguilera, R., & Melack, J. M. (2018). Concentration-discharge responses to storm events in coastal California watersheds. *Water Resources Research*, 54(1), 407–424. <https://doi.org/10.1002/2017WR021578>
- Ahn, K. H., & Steinschneider, S. (2019). Time-varying, nonlinear suspended sediment rating curves to characterize trends in water quality: An application to the upper Hudson and Mohawk Rivers, New York. *Hydrological Processes*, 33(13), 1865–1882. <https://doi.org/10.1002/hyp.13443>
- Ahn, K. H., Yellen, B., & Steinschneider, S. (2017). Dynamic linear models to explore time-varying suspended sediment-discharge rating curves. *Water Resources Research*, 53, 4802–4820. <https://doi.org/10.1002/2016WR019804>. Received
- Asselman, N. E. M. (2000). Fitting and interpretation of sediment rating curves. *Journal of Hydrology*, 234, 228–248. [https://doi.org/10.1016/S0022-1694\(00\)00253-5](https://doi.org/10.1016/S0022-1694(00)00253-5)
- Bishop, P. L., Hively, W. D., Stedinger, J. R., Rafferty, M. R., Lojpersberger, J. L., & Bloomfield, J. A. (2005). Multivariate analysis of paired watershed data to evaluate agricultural best management practice effects on stream water phosphorus. *Journal of Environmental Quality*, 34, 1087–1101. <https://doi.org/10.2134/jeq2004.0194>
- Cadwell, D. (1986). Late Wisconsinan stratigraphy of the Catskill Mountains, New York. In D. Cadwell (Ed.), *The Wisconsinan stage of the first Geological District, eastern New York* (pp. 73–88). The University of the State of New York.
- Church, M., & Slaymaker, O. (1989). Disequilibrium of Holocene sediment yield in glaciated British Columbia. *Nature*, 337, 452–454.
- Davis-Colley, R. J., & Smith, D. G. (2001). Turbidity, suspended sediment, and water clarity: A review. *Journal of the American Water Resources Association*, 37(5), 1085–1101.
- Dethier, E., Magilligan, F. J., Renshaw, C. E., & Nislow, K. H. (2016). The role of chronic and episodic disturbances on channel-hillslope coupling: The persistence and legacy of extreme floods. *Earth Surface Processes and Landforms*, 41, 1437–1447. <https://doi.org/10.1002/esp.3958>
- Du, X., Zhang, X., Mukundan, R., Hoang, L., & Owens, E. M. (2019). Integrating terrestrial and aquatic processes toward watershed scale modeling of dissolved organic carbon fluxes. *Environmental Pollution*, 249, 125–135. <https://doi.org/10.1016/j.envpol.2019.03.014>
- Dunne, K., Arratia, P., & Jerolmack, D. (2019). A new method for in-situ measurement of the erosion threshold of river channels, 1–14. <https://doi.org/10.31223/OSF.IO/RQCEP>
- East, A. E., Stevens, A. W., Ritchie, A. C., Barnard, P. L., Campbell-Swarzenski, P., Collins, B. D., & Conaway, C. H. (2018). A regime shift in sediment export from a coastal watershed during a record wet winter, California: Implications for landscape response to hydroclimatic extremes. *Earth Surface Processes and Landforms*, 43(12), 2562–2577. <https://doi.org/10.1002/esp.4415>
- Engelbrechtsen, A., Vogt, R. D., & Bechmann, M. (2019). SWAT model uncertainties and cumulative probability for decreased phosphorus loading by agricultural best management practices. *Catena*, 175, 154–166. <https://doi.org/10.1016/j.catena.2018.12.004>
- Giri, S., Nejadhashemi, A. P., & Woznicki, S. A. (2012). Evaluation of targeting methods for implementation of best management practices in the Saginaw River watershed. *Journal of Environmental Management*, 103, 24–40. <https://doi.org/10.1016/j.jenvman.2012.02.033>
- Gray, A. B. (2018). The impact of persistent dynamics on suspended sediment load estimation. *Geomorphology*, 322, 132–147. <https://doi.org/10.1016/j.geomorph.2018.09.001>
- Gray, A. B., Pasternack, G. B., Watson, E. B., Warrick, J. A., & Gofii, M. A. (2015). Effects of antecedent hydrologic conditions, time dependence, and climate cycles on the suspended sediment load of the Salinas River, California. *Journal of Hydrology*, 525, 632–649. <https://doi.org/10.1016/j.jhydrol.2015.04.025>
- Hanief, A., & Laursen, A. E. (2019). Meeting updated phosphorus reduction goals by applying best management practices in the Grand River watershed, southern Ontario. *Ecological Engineering*, 130, 169–175. <https://doi.org/10.1016/j.ecoleng.2019.02.007>
- Himanshu, S. K., Pandey, A., Yadav, B., & Gupta, A. (2019). Evaluation of best management practices for sediment and nutrient loss control using SWAT model. *Soil and Tillage Research*, 192, 42–58. <https://doi.org/10.1016/j.still.2019.04.016>

- Hirsch, R. M., Moyer, D. L., & Archfield, S. A. (2010). Weighted regressions on time, discharge, and season (WRTDS), with an application to Chesapeake bay river inputs. *Journal of the American Water Resources Association*, 46(5), 857–880. <https://doi.org/10.1111/j.1752-1688.2010.00482.x>
- Hoang, L., Mukundan, R., Moore, K. E. B., Owens, E. M., & Steenhuis, T. S. (2019). Phosphorus reduction in the New York City water supply system: A water-quality success story confirmed with data and modeling. *Ecological Engineering*, 135, 75–88. <https://doi.org/10.1016/j.ecoleng.2019.04.029>
- Holtan, H., Kamp-Nielsen, L., & Stuanes, A. O. (1988). Phosphorus in soil, water and sediment: An overview. *Hydrobiologia*, 170, 19–34. <https://doi.org/10.1007/BF00024896>
- Inamdar, S., Johnson, E., Rowland, R., Warner, D., Walter, R., & Merritts, D. (2018). Freeze–thaw processes and intense rainfall: The one-two punch for high sediment and nutrient loads from mid-Atlantic watersheds. *Biogeochemistry*, 141, 333–349. <https://doi.org/10.1007/s10533-017-0417-7>
- Jeon, D. J., Ki, S. J., Cha, Y. K., Park, Y., & Kim, J. H. (2018). New methodology of evaluation of best management practices performances for an agricultural watershed according to the climate change scenarios: A hybrid use of deterministic and decision support models. *Ecological Engineering*, 119, 73–83. <https://doi.org/10.1016/j.ecoleng.2018.05.006>
- Lammers, R. (2018). *REM User Guide*.
- Lammers, R. W., & Bledsoe, B. P. (2018a). Parsimonious sediment transport equations based on Bagnold's stream power approach. *Earth Surface Processes and Landforms*, 43, 242–258. <https://doi.org/10.1002/esp.4237>
- Lammers, R. W., & Bledsoe, B. P. (2018b). A network scale, intermediate complexity model for simulating channel evolution over years to decades. *Journal of Hydrology*, 566, 886–900. <https://doi.org/10.1016/j.jhydrol.2018.09.036>
- Lammers, R. W., & Bledsoe, B. P. (2019). Quantifying pollutant loading from channel sources: Watershed-scale application of the river erosion model. *Journal of Environmental Management*, 234, 104–114. <https://doi.org/10.1016/j.jenvman.2018.12.074>
- Lammers, R. W., Bledsoe, B. P., & Langendoen, E. J. (2017). Uncertainty and sensitivity in a bank stability model: Implications for estimating phosphorus loading. *Earth Surface Processes and Landforms*, 42, 612–623. <https://doi.org/10.1002/esp.4004>
- McHale, M. R., & Siemion, J. (2014). *Turbidity and suspended sediment in the upper Esopus Creek watershed*. New York: U.S. Geological Survey Scientific.
- Mukundan, R., Scheerer, M., Gelda, R. K., & Owens, E. M. (2018). Probabilistic estimation of stream turbidity and application under climate change scenarios. *Journal of Environment Quality*, 47, 1522–1529. <https://doi.org/10.2134/jeq2018.06.0229>
- Nagle, G. N., Fahey, T. J., Ritchie, J. C., & Woodbury P. B. (2007). Variations in sediment sources and yields in the Finger Lakes and Catskills regions of New York. *Hydrological Processes*, 21, 828–838.
- NYC DEP. (2018). *2017 Watershed water quality annual report*. <http://medcontent.metapress.com/index/A65RM03P4874243N.pdf>
- NYC DEP. (2019a). *Stony Clove Watershed suspended sediment and turbidity study: Turbidity Reduction Project Nomination Report*.
- NYC DEP. (2019b). *Upper Esopus Creek watershed turbidity/suspended-sediment monitoring study: Biennial Status Report*.
- Qiu, J., Shen, Z., Huang, M., & Zhang, X. (2018). Exploring effective best management practices in the Miyun reservoir watershed, China. *Ecological Engineering*, 123, 30–42. <https://doi.org/10.1016/j.ecoleng.2018.08.020>
- RACNE. (2012). *Terrain surface standards, project report, CAT-393 airborne Lidar quality assurance and GIS terrain data development, phase 2*. New York City Department of Environmental Protection.
- Rich, J. (1934). *Glacial geology of the Catskills*. The University of the State of New York.
- Rymaszewicz, A., O'Sullivan, J. J., Bruen, M., Turner, J. N., Lawler, D. M., Conroy, E., & Kelly-Quinn, M. (2017). Measurement differences between turbidity instruments, and their implications for suspended sediment concentration and load calculations: A sensor inter-comparison study. *Journal of Environmental Management*, 199, 99–108. <https://doi.org/10.1016/j.jenvman.2017.05.017>
- Siemion, J., McHale, M. R., & Davis, W. D. (2016). *Suspended-sediment and turbidity responses to sediment and turbidity reduction projects in the Beaver Kill, Stony Clove Creek, and Warner Creek, Watersheds*. New York: U.S. Geological Survey Scientific. pp. 2010–2014
- Simon, A., Pollen-bankhead, N., & Thomas, R. E. (2011). Development and application of a deterministic Bank stability and toe erosion model for stream restoration. In *Stream Restoration in Dynamic Fluvial Systems* (Vol. 194).
- Sommerlot, A. R., Pouyan Nejadhashemi, A., Woznicki, S. A., & Prohaska, M. D. (2013). Evaluating the impact of field-scale management strategies on sediment transport to the watershed outlet. *Journal of Environmental Management*, 128, 735–748. <https://doi.org/10.1016/j.jenvman.2013.06.019>
- Steinman, A. D., Hassett, M., & Oudsema, M. (2018). Effectiveness of best management practices to reduce phosphorus loading to a highly eutrophic lake. *International Journal of Environmental Research and Public Health*, 15(10), 2111. <https://doi.org/10.3390/ijerph15102111>
- Strauch, M., Lima, J. E. F. W., Volk, M., Lorz, C., & Makeschin, F. (2013). The impact of best management practices on simulated streamflow and sediment load in a central Brazilian catchment. *Journal of Environmental Management*, 127, S24–S36. <https://doi.org/10.1016/j.jenvman.2013.01.014>
- Tananaev, N. I. (2013). Applying regression analysis to calculating suspended sediment runoff: Specific features of the method. *Water Resources*, 40(6), 585–592. <https://doi.org/10.1134/S0097807813060110>
- USGCRP (2017). In D. J. Wuebbles, D. W. Fahey, K. A. Hibbard, D. J. Dokken, B. C. Stewart, & T. K. Maycock (Eds.), *Climate science special report: Fourth National Climate Assessment* (Vol. 1, p. 470). U.S. Global Change Research Program.
- Warrick, J. A. (2015). Trend analyses with river sediment rating curves. *Hydrological Processes*, 29(6), 936–949. <https://doi.org/10.1002/hyp.10198>
- Warrick, J. A., & Milliman, J. D. (2018). Do we know how much fluvial sediment reaches the sea? Decreased river monitoring of U.S. coastal rivers. *Hydrological Processes*, 32(23), 3561–3567. <https://doi.org/10.1002/hyp.13276>
- West, M., & Harrison, J. (1997). *Bayesian forecasting and dynamic models* (2nd ed.). Springer.
- Wohl, E., Angermeier, P. L., Bledsoe, B., Kondolf, G. M., MacDonnell, L., Merritt, D. M., Palmer, M. A., Poff, N. L. R., & Tarboton, D. (2005). River restoration. *Water Resources Research*, 41(10), 1–12. <https://doi.org/10.1029/2005WR003985>
- Wohl, E., Lane, S. N., & Wilcox, A. C. (2015). The science and practice of river restoration. *Water Resources Research*, 51, 5974–5997. <https://doi.org/10.1002/2014WR016874>. Received
- Wolman, M. G. (1954). A method of sampling coarse river-bed material. *Transactions American Geophysical Union*, 35(6), 951–956.
- Yellen, B., Woodruff, J. D., Kratz, L. N., Mabee, S. B., Morrison, J., & Martini, A. M. (2014). Source, conveyance and fate of suspended sediments following hurricane Irene. New England, USA. *Geomorphology*, 226, 124–134. <https://doi.org/10.1016/j.geomorph.2014.07.028>
- Young, O. R. (2010). Institutional dynamics: Resilience, vulnerability and adaptation in environmental and resource regimes. *Global Environmental Change*, 20(3), 378–385. <https://doi.org/10.1016/j.gloenvcha.2009.10.001>

## SUPPORTING INFORMATION

Additional supporting information may be found in the online version of the article at the publisher's website.

**How to cite this article:** Wang, K., Davis, D., & Steinschneider, S. (2021). Evaluating suspended sediment and turbidity reduction projects in a glacially conditioned catchment through dynamic regression and fluvial process-based modelling. *Hydrological Processes*, 35(9), e14351. <https://doi.org/10.1002/hyp.14351>